Lincoln University
Te Whare Wānaka o Aoraki
CHRISTCHURCH•NEW ZEALAND

Lincoln University Digital Thesis

Copyright Statement

The digital copy of this thesis is protected by the Copyright Act 1994 (New Zealand).

This thesis may be consulted by you, provided you comply with the provisions of the Act and the following conditions of use:

- you will use the copy only for the purposes of research or private study
- you will recognise the author's right to be identified as the author of the thesis and due acknowledgement will be made to the author where appropriate
- you will obtain the author's permission before publishing any material from the thesis.

Understanding protoplast technology as a tool to enhance biocontrol

---

A thesis

submitted in partial fulfilment

of the requirements for the Degree of

Doctor of Philosophy

at

Lincoln University

by

Jessica A. Yardley

Lincoln University

2018

Abstract of a thesis submitted in partial fulfilment of the requirements for the Degree of Doctor of Philosophy.

Understanding protoplast technology as a tool for to enhance biocontrol

by

Jessica A. Yardley

Biocontrol of plant pathogens is an integral part of modern pest and disease management. Issues of pesticide residues/resistance and a drive towards sustainability within crop protection systems have created an opportunity for sustainable alternatives to synthetic agro-chemicals. One approach within integrated pest management programmes is the use of biocontrol agents, such as fungi. The development of novel biocontrol strains using protoplast technology provides the opportunity to re-combine or introduce desired features, in particular fungicide tolerance, without the need for sexual reproduction. This present study employed protoplast regeneration to produce novel *Trichoderma* strains with attributes such as pesticide tolerance for the control of the bacterium causing kiwifruit canker, *Pseudomonas syringae* pv*. actinidae* (Psa). To achieve this, leading *Trichoderma* strains were selected from within current research programmes targeted at kiwifruit health. Using protoplast regeneration, numerous strains were produced that were tolerant separately to copper sulphate and Chief® (a.i. carbendazim). Further bioactivity trials showed that biocontrol potential of the protoplast progeny was not reduced as a consequence of this strain enhancement. However, despite the use of fungal protoplast technology for strain improvement very little is known of the underlying genetic changes responsible for the modified phenotypes. The overall hypothesis was that cytosine methylation may be responsible for the phenotypic plasticity that was observed in these protoplast progeny, with this study being the first to examine the consequences of protoplast regeneration through a multi-layered, integrative 'omics approach. The differential cytosine mapping through whole genome bisulphite sequencing showed sparse differential methylation between a protoplast regenerant (copper tolerant FCC237/R5 *T.* sp. *"atroviride* B") and its parent (FCC237 *T.* sp. *"atroviride* B"). This cytosine methylation did not appear to modulate corresponding gene expression levels to differentially methylated associated genes, as it had been reported in other fungal species. The transcriptome analysis indicated differential gene expression between the parent and regenerant in both sub-lethal levels of copper sulphate (1 mM) (88 DEGs) and also in the control PDB (281 DEGs). The changes in DEGs profiles, especially regarding proteins involved in oxidative stress, secondary

metabolites and transporters could suggest that the regenerant may induce a general stress response as opposed to a specific pathway for copper tolerance that has arisen as a putative result of protoplast regeneration. Other epigenetic factors, including histone and chromatin modifications and RNA interference, are likely to play an important in both regulating gene expression states and the phenotypic plasticity observed in the protoplast regenerant. Although other epigenetic modifications have not been tested here, they would be expected to be present due to the interconnectedness of the epigenome and further elucidation is required. This work has contributed to a better understanding of the basic genetic events that occur during protoplasting in *Trichoderma*, which may allow for greater advances in not only strain enhancement, but also in genetic modification experiments, in both *Trichoderma* but other filamentous fungi.

Keywords: *Trichoderma, Trichoderma* sp. *"atroviride* B", biological control, protoplast technology, protoplast regeneration, cytosine methylation, whole genome bisulphate sequencing, transcriptomics.

Acknowledgements

First of all, I would like to express my thanks and huge appreciation to my supervisory team, Johanna Steyaert, Artemio Mendoza-Mendoza, Travis Glare, Mark Braithwaite and Robert Hill. Jo, your continued encouragement, passion for science and feedback has been instrumental to me both in starting and finishing this project. Artemio, Travis and Mark, your varying areas of expertise, support and critiques (in the best way) has enabled me to complete this work and learn so many things along the way. Also, thank you to Robert, who without him, this project would never have the strains or working model to begin with. To Darrell Lizamore, who although wasn't a supervisor, I could never have completed this project with him. His knowledge and passion about epigenetics is evident and has made learning a whole new topic very enjoyable.

I would also like to thank the Ministry of Business, Innovation and Employment (through the Next-Generation Bio-pesticide project) for funding this PhD project. To the team at New Zealand Genomics Limited (NZGL) in Dunedin, who helped and advised me with part of the methylation experiment and data analysis.

Special thanks to those people in particular who helped out with varying aspects on some of the chapters, namely, Christine Stark, Janaki Kandula, Stu Larson (at the Biotron), Dave Saville (for his amazing help with the contrast tables), Brent Richards and Leona Meachen down at the nursery. In addition to all the staff and students here at the Bio-Protection Research Centre who helped along the way. To my fellow past and present PhD students who have continued to inspire me and remind me why I started this in the first place, Federico (for being such a great office mate), Priscila, Aimee, Abi, Anish, Laura, Damian, Ben, Claudia, Francesco, Kooki, Bryony, Mariona, Memo and Fabiola, you guys are all so great!

To my friends and family, who have been there for both my ups and downs over the past few years and always putting up with my science stories. Thank you for all the food, gelato, walks and talks, and patience, in particular to my flatmates over the years (Cat, Rose and Alice), Anisha, Lisa, Emily, Kate, Jose and Laura. To my Aunty Ruth, whose academic perspective from another field, along with your advice about how to get a PhD done has been truly wonderful. To my Mum, Dad and brother, Alex, you guys have made this possible, your continued encouragement and belief in my abilities have made the world of difference.

And finally, to Kiran (Clam). Your own work ethic and drive, along with your enthusiasm and support for my project all from afar have inspired/helped me beyond words. Thank you, thank you, thank you. GLC.

Table of Contents

Abstract ii

Acknowledgements iv

Table of Contents v

List of Tables viii

List of Figures x

List of Abbreviations xii

Chapter 1 Introduction 1

1.1 Biological control 1

1.2 The genus *Trichoderma* 1

1.3 *Trichoderma* as biocontrol agents 2

1.4 *Pseudomonas syringae* pv. *actinidiae* 3

1.4.1 Psa in New Zealand 3

1.4.2 Control of Psa 3

1.5 Protoplast technology 4

1.5.1 Protoplast regeneration as a tool 5

1.5.2 Protoplast fusion as a tool 6

1.5.3 Mechanisms behind protoplasting 7

1.6 Research aims and objectives 12

Chapter 2 Induction of pesticide tolerance via protoplast technology and characterisation of the resulting progeny 13

2.1 Introduction 13

2.2 Materials and methods 14

2.2.1 Fungal strain selection and identificaion 14

2.2.2 Pre-screening for naturally occurring sensitivity to pesticides 15

2.2.3 Preparation of protoplasts and optimisation 16

2.2.4 Production of protoplast fusants 18

2.2.5 Interactive toxicity effects of pesticides in agar 18

2.2.6 Phenotypic characterisation- growth rate and conidiation 19

2.2.7 Basic molecular characterisation 20

2.3 Results 21

2.3.1 Fungal identification 21

2.3.2 Pre-screening for naturally occurring sensitivity to pesticides 21

2.3.3 Preparation of protoplasts and optimisation 23

2.3.4 Production of protoplast fusants 25

2.3.5 Phenotypic characterisation- growth rate, conidiation quantity and conidial germination 26

2.3.6 Basic molecular characterisation: UP-PCR profiles (Universally Primed-PCR) 28

2.4 Discussion 29

2.5 Conclusion 32

Chapter 3 Bioactivity of selected *Trichoderma* sp. "*atroviride* B" parental and protoplast regenerant strains against *Pseudomonas syringae* pv. *actinidae* 33

3.1 Introduction 33

3.2 Materials and Methods 34
3.2.2 Trial 1 (June-August 2016) 34
3.2.3 Trial 2 (March-July 2017) 38
3.2.4 Trial 3 (April-August 2017) 40
3.3 Results 41
3.3.1 Trial 1 41
3.3.2 Trial 2 44
3.3.3 Trial 3 47
3.3.4 Combined Trials 2 and 3 50
3.4 Discussion 53
3.5 Conclusion 55

Chapter 4 Genome-wide analysis of cytosine methylation between a *Trichoderma* sp. "*atroviride* B" parental and protoplast regenerant strains 56
4.1 Introduction 56
4.2 Materials and methods 60
4.2.1 Fungal strain management and DNA extraction 60
4.2.2 WGBS library construction and sequencing 61
4.2.3 WGBS analysis 61
4.3 Results 65
4.3.1 Differentially methylated regions 65
4.3.2 Differentially methylated cytosines 69
4.3.3 SNP analysis 79
4.3.4 Comparison between the two different methods for calling differential cytosine methylation 79
4.4 Discussion 79
4.4.1 Differential methylation levels are low in *Trichoderma* between the parent and regenerant 80
4.4.2 Differential methylation occurs mainly in gene bodies 80
4.4.3 Functional annotation of differentially methylated associated genes 82
4.4.4 Differences between the two analysis types (DMR vs DMC) 82
4.4.5 Limitations of this methylome data 83
4.5 Conclusion 85

Chapter 5 The impact of cytosine methylation on the transcriptional activity of a *Trichoderma* sp. "*atroviride* B" parental and protoplast regenerant strains 87
5.1 Introduction 87
5.2 Materials and methods 88
5.2.1 Fungal growth for RNA extraction and RNA extraction 88
5.2.2 RNA-seq library construction and sequencing 89
5.2.3 RNA-seq analysis 89
5.2.4 Analysis of Read Data 90
5.3 Results 92
5.3.1 Data quality control, transcript assembly and RNA-seq QC 92
5.3.2 Differential gene expression and gene ontology analysis 93
5.3.3 SNPs 105
5.4 Discussion 105
5.4.1 Effects of differential methylation on transcriptional levels 105
5.4.2 Biological function of differentially expressed genes 108
5.5 Conclusion 116

Chapter 6 General discussion 118

Appendix A Access to Raw Data from Bioactivity Trials.....124

Appendix B Access to Methylation Reports and Data.....124

B.1 WGBS differentially methylated regions (Peter Stockwell).....124

B.2 WGBS differentially methylated cytosines (Darrell Lizamore).....124

B.3 Full list of differentially methylated cytosines (DMCs).....124

Appendix C Access to RNA-seq Reports and full DEGs lists 125

C.1 Novogene RNA-seq report, QC data and read counts.....125

C.2 Complete list of all upregulated genes of the regenerant strain compared to the parent of *Trichoderma* sp. *"atroviride* B" in the control (plain PDB).....125

C.3 Complete list of all downregulated genes of the regenerant strain compared to the parent of *Trichoderma* sp. *"atroviride* B" in the control (plain PDB).....129

References..... 134

List of Tables

Table 2.1 Identification of *Trichoderma* strains selected for this study based on *tef1α* sequences. 15
Table 2.2 UP-PCR primers and their respective annealing temperatures (Lubeck et al., 1996). .20
Table 2.3 Absolute kill points for the *Trichoderma* strains against copper sulphate ($CuSO_4.5H_2O$) and Chief® (500 g/L carbendazim) for both mycelial plugs and conidial suspensions on recovery medium. 23
Table 2.4 Effect of different osmotic stabilisers and methodologies on yield of protoplasts for a selection of *Trichoderma* strains (both parent [WT] and regenerants). 25
Table 2.5 Rate of protoplast regeneration from selected *Trichoderma* strains on pesticide amended media: copper sulphate ($CuSO_4.5H_2O$) and Chief® (500 g/L carbendazim)..25
Table 2.6 Average growth rate (mm/d) of *Trichoderma* sp. "*atroviride* B" FCC237 (parent) and *Trichoderma* sp. "*atroviride* B" FCC237/R5 (copper tolerant regenerant) on either PDA or MEA. 26
Table 2.7 Average growth rate (mm/d) of *Trichoderma hamatum* FCC207 (parent) and *Trichoderma hamatum* FCC207/R9 (carbendazim tolerant regenerant) on either PDA or MEA. 27
Table 2.8 Conidia quantity (measured as conidia/mL) of *Trichoderma* sp. "*atroviride* B" FCC237 (parent) and *Trichoderma* sp. "*atroviride* B" FCC237/R5 (copper tolerant regenerant). There was no statistical difference and the data represents the average of two experiments. 27
Table 2.9 Conidia germination percentage of *Trichoderma* sp. "*atroviride* B" FCC237 (parent) and *Trichoderma* sp. "*atroviride* B" FCC237/R5 (copper tolerant regenerant). 27
Table 3.1 Selected *Trichoderma* strains used as treatments over the three Psa bioactivity trials. Species listed in the table as follows: LU753: *Trichoderma* sp. novel LU753, FCC207: *Trichoderma hamatum,* FCC237, FCC456: *Trichoderma* sp. *"atroviride* B". /R# indicates regenerant. 35
Table 3.2 Disease scoring assessment for Psa symptoms on kiwifruit seedlings after four weeks growth post inoculation with Psa used in Trial 1. 37
Table 3.3 Updated disease scoring assessment for Psa symptoms on kiwifruit seedlings after four weeks growth post inoculation with Psa used for trials 2 and 3.....39
Table 3.4 Disease parameter scores of Hayward kiwifruit seedlings after four weeks post inoculation with Psa for Trial 1.....42
Table 3.5 Disease parameter scores of Hort 16a kiwifruit seedlings after four weeks post inoculation with Psa for Trial 2.....45
Table 3.6 Disease parameter scores of Hort 16a kiwifruit seedlings after four weeks post inoculation with Psa for Trial 3.....48
Table 3.7 Combined disease parameter scores of Hort 16a kiwifruit seedlings after four weeks post inoculation with Psa for trials 2 and 3. 51
Table 4.1 Differentially methylated regions (DMRs) between the parent and regenerant strains through DMAP analysis completed by Peter Stockwell. Difference in methylation is from the [av. par meth – av. reg meth]. A blank space in the GO ID or KOG class and function category means there is no assigned class or ID. 66
Table 4.2 Summary of 5mC sites mapped. 69
Table 4.3 Differentially methylated cytosines (DMRs) between the parent and regenerant strains, through methylKit analysis completed by Darrell Lizamore, with more than 25% differential methylation. Difference in methylation is from the [parental methylation – regenerant methylation]. A full list can be seen in Table A.1. 74
Table 4.4 The distribution of DMCs in the parent versus regenerant across the genic regions. .76
Table 4.5 Genes with multiple differentially methylated cyotsines (DMCs) between the parent and regenerant strains following methylKit analysis. 78
Table 5.1 Databases used by Novogene Ltd for the gene functional annotation analysis. 91

Table 5.2 Differentially expressed and differentially methylated cytosine's (DMCs)-associated genes in the parent and regenerant strains of *Trichoderma* sp. *"atroviride* B" in sub-lethal levels of copper sulphate (1 mM) amended PBD and the control (plain PDB). .97
Table 5.3 Significantly upregulated genes in the regenerant strain compared to the parent of *Trichoderma* sp. *"atroviride* B" in sub-lethal levels of copper sulphate (1 mM) amended PDB. Bold entries are also present in the upregulated control dataset. 98
Table 5.4 Significantly downregulated genes in the regenerant strain compared to the parent of *Trichoderma* sp. *"atroviride* B" in sub-lethal levels of copper sulphate (1 mM) amended PDB. Bold entries are also present in the upregulated control dataset. 100
Table 5.5 Top 50 most upregulated genes of the regenerant strain compared to the parent of *Trichoderma* sp. *"atroviride* B" in the control (plain PDB). Bold entries are also present in the upregulated sub-lethal levels of copper sulphate dataset. 101
Table 5.6 Top 50 most downregulated genes of the regenerant strain compared to the parent of *Trichoderma* sp. *"atroviride* B" in the control (plain PDB). Bold entries are also present in the downregulated sub-lethal levels of copper sulphate dataset. 103

List of Figures

Figure 2.1 Inhibitory effect on growth of *Trichoderma* sp. "*atroviride* B" (FCC237) on varying concentrations of copper sulphate ($CuSO_4.5H_2O$) amended recovery media agar after 7 d growth. 22

Figure 2.2 A selection of protolast regenerants that were produced tolerant to copper sulphate ($CuSO_4.5H_2O$). The tolerance is shown on 3 mM of copper sulphate compared to their respective parental strain. 24

Figure 2.3 UP-PCR, using primer L15/AS19, of selected *Trichoderma* parental strains (P) and the respective regenerants (R) separated on a 2% agarose gel electrophoresis in borate/NaOH. (1) LU297 *T. trixiae,* (2) LU297/R2 *T. trixiae,* (3) LU668 *T.* sp. *"atroviride* B", (4) LU668/R *T.* sp. *"atroviride* B", (5) LU753 *T.* sp. novel LU753, (6) LU753/R19 *T.* sp. novel LU753, (7) FCC207 *T. hamatum,* (8) FCC207/R9 *T. hamatum,* (9) FCC237 *T.* sp. *"atroviride* B", (10) FCC237/R5 *T.* sp. *"atroviride* B", (11) negative control (12) FCC261 *T. harzianum,* (13) FCC261/R16 *T. harzianum,* (14) FCC270 *T.* sp. novel FCC270, (15) FCC270/R7 *T.* sp. novel FCC270, (16) FCC273 *T.* sp. *"atroviride* B" (17) FCC273/R13 *T.* sp. *"atroviride* B" (18) FCC456 *T.* sp. *"atroviride* B", (19) FCC456/R3 *T.* sp. *"atroviride* B". P= parent, R=regenerant. 28

Figure 3.1 Updated disease scoring assessment of Psa on Hort16A kiwifruit seedlings after four weeks growth post inoculation with Psa. (A) 0-no symptoms or discolouration; (B) 1-light discolouration around wound; (C) 2-darker discolouration around wound/stem blackening starting; (D) 3-further discolouration around the wound, beginning to constrict around wound; (E) 4-completely constricted, brown; (F) 5-disease has moved systemically (past the stem and into the leaves); (G) 6-death/girdled (collapsed entirely)....40

Figure 4.1 Principal component analysis (PCA) between the parental (red) and regenerant (blue) strains after differential methylation analysis using methylKit. (A) CpG methylation with no overlap filtering. (B) CpG methylation with overlap filter (at least one mC in at least two replicates of the treatment). Figure produced by Darrell Lizamore. 70

Figure 4.2 Hierarchical cluster analysis between the parental (red) and regenerant (blue) strains after differential methylation analysis using methylKit. (A) CpG methylation with no overlap filtering. (B) CpG methylation with overlap filter (at least one 5mC in at least two replicates of the treatment). Figure produced by Darrell Lizamore....70

Figure 4.3 Histogram of the percentage of methylation per base generated from methylKit. The X axis shows percent methylation for each individual CpG. The numbers on the bars in A denote the percentage of CpGs contained in each bar. The Y axis is the frequency that this methylation occurs. (A) CpG methylation distribution of parent1_forward. (B) A more typical methylation pattern from other species- CpG methylation distribution in zebrafish brain- ranging from 0-100% (4.3B histogram modified from Chatterjee et al. (2013)). 71

Figure 4.4 Density of 5mCs in and around all genes over the genome. (A) CpG, (B) CHG, (C) CHH. Blue= parental strain, red=regenerant strain. Figure produced by Darrell Lizamore. .72

Figure 4.5 Variation of methylation differences of the significantly different methylated cytosines (DMCs) based on the methylKit analysis between the three cytosine methylation contexts. Y axis: [parent average methylation] – [regenerant average methylation]. X axis is the individual DMCs. (A) CpG, (B) CHG, (C) CHH. 73

Figure 5.1 A simplified diagrammatic outline of the workflow used in this transcriptomic analysis without a reference sequence by Novogene. Fastq files are the Illumina sequencing output file. Functional analysis used a variety of programs including Diamond, KAAS, NCBI blast among others (see section 5.2.4.3 for full list of the seven databases). 89

Figure 5.2 The R^2 of the Peason correlation coefficient of the samples for RNA-seq. R^2 is the square of the Pearson coefficient. Figure produced by Novogene. 93

Figure 5.3 Volcano plots of the differentially expressed genes between the four different comparisons. (A) Regenerant versus parent in plain PDB (control), (B) regenerant versus parent in copper amended PDB, (C) parent in plain PDB (control) versus copper amended PDB, (D) regenerant in plain PDB (control) versus copper amended PDB. Volcano plots show the log_2(fold change) vs the log_{10}(padj), points with more fold change and higher log_{10}(padj) are more reliable. Log counts are the log of the read counts mapping to each gene. Log_2(fold change) indicates the log of the change in expression of the regenerant compared to the parent. The log_2(fold change) [x-axis] represents the gene expression change of the different transcripts. The -log_{10}(padj) [y-axis] is the p-value after normalisation. The greater the -log_{10}(padj) is, the more significant the difference is. The significant differential up regulated genes were represented by red dots, the green dots represented the significant differential down regulated genes and the blue dots were no difference. Figure produced by Novogene. 94

Figure 5.4 Hierarchical cluster analysis of differentially expressed genes. The overall result of the FPKM (fragments per kilobase of transcript sequence per millions of base pairs sequenced) cluster analysis, clustered using the log_{10} (FPKM+1) value. Red denotes upregulated genes ad blue denotes downregulated genes. The colour range from red to blue represents the log_{10} (FPKM+1) value from large to small. Figure produced by Novogene. 95

List of Abbreviations

Système International abbreviations were used for chemicals, elements and formulae. Other abbreviations used in the text are listed below.

4mC	4-methylcytosine
5-AC	5-azacytidine
5hmC	5-hydroxymethycytosine methylation
5mC	5-methylcytosine methylation
6mA	6-adenine methylation
A	Adenine
a.i.	Active ingredient
AFLP	Amplified fragment length polymorphism
ANOVA	Analysis of variance
ATMT	*Agrobacterium tumefaciens*-mediated transformation
BCA	Biocontrol agent
blast	Basic local alignment search tool
bp	Base pairs
C	Cytosine
cDNA	Complementary deoxyribonucleic acid
CGH	Cytosine-guanine-H
CHH	Cytosine-H-H
CpG/CG	Cytosine-phosphate-guanine
DMCs	Differentially methylated cytosines
DMRs	Differentially methylated regions
DNA	Deoxyribonucleic acid
DNMTases	DNA methyltransferases
ETDA	Ethylenediaminetetra-acetate
FCC	Forestry Culture Collection
G	Guanine
gDNA	Genomic deoxyribonucleic acid
GO	Gene ontology
GYEC	Glucose Yeast Extract Casein
H	Corresponds to A, T or C in relation to a methylation context
ICEs	Integrative conjugative elements
IGV	Integrative Genomics Viewer
IPM	Integrated Pest Management
JGI	Joint Genome Institute
kb	Kilobase
KOG	Eukaryotic orthologous group
LBA	Luria Bertani agar
l.s.d.	Least significant difference
LUMCC	Lincoln University Microbial Culture Collection
Mb	Megabase
MEA	Malt extract agar
mRNA	Messenger ribonucleic acid
MT	Metallothionein
MSAP	Methylation sensitive amplified polymorphism
ncRNAs	Non-coding RNAs
NGS	Next generation sequencing
OD	Optimal density (absorbance)

PEG	Polyethylene glycol
PCR	Polymerase chain reaction
PDA	Potato dextrose agar
PDB	Potato dextrose broth
pers. comm.	Personal communication
Psa	*Pseudomonas syringae* pv. *actinidiae*
RAPD	Randomly amplified polymorphic DNA
ROS	Reactive oxygen species
RM	Recovery media
RNA	Ribonucleotide acid
RT-qPCR	Reverse transcriptase quantitative polymerase chain reaction
SD	Standard deviation
SDW	Sterile distilled water
SNP	Single nucleotide polymorphism
SMRT	Single-molecule real-time sequencing
sRNAs	Small RNA species
T	Thymine
Tris	Tris (hydroxymethyl) aminomethane
TTS	Transcriptional termination sites
U	Uracil
UTR	Untranslated region
UP-PCR	Universally primed polymerase chain reaction
WGBS	Whole genome bisulphite sequencing
WT	Wild type

Chapter 1

Introduction

1.1 Biological control

Biological control (biocontrol) of plant pathogens is an integral part of modern pest and disease management. Issues of pesticide residues, development of pesticide resistant organisms and the drive towards sustainability within traditional crop protection systems have created an opportunity for beneficial/sustainable options and alternatives. The use of chemicals in traditional farming systems has increased dramatically over the last 70 years (Pradhan et al., 2015; Woo et al., 2014), raising serious environmental concerns that have prompted governing bodies to implement legislation to either ban or decrease the dependence on pesticides in agriculture (Clarke et al., 2011; Woo et al., 2014). This has forced farmers to use other approaches such as implementing integrated pest management (IPM) programmes that use lower pesticide inputs as a necessity rather than by choice. One approach within these IPM programmes is the use of biocontrol agents as an alternative to synthetic agro-chemicals (Woo et al., 2014). Biocontrol is the application of a living organism (predator, insect pathogen, antagonist or competitor) or products derived or extracted from a living organism to control harmful microorganisms or pests that cause plant disease, including host resistance (constitutive and elicited) (Wilson, 1997). The main purpose of biocontrol of plant diseases is to reduce the disease damage threshold below an economically significant level (Sumeet and Mukerji, 2000). Plant disease biocontrol agents are traditionally fungi and bacteria and can be both foliar and rhizosphere competent (Sumeet and Mukerji, 2000; Sundh and Goettel, 2013; Woo et al., 2014). Currently, these beneficial microorganisms are increasingly being used as an effective tool within IPM programmes (Hyakumachi et al., 2014).

1.2 The genus *Trichoderma*

Trichoderma species are primarily asexual, free-living saprophytic fungi present in the soil, roots, and leaves of plants in nearly all ecosystems (Harman et al., 2004b; Samuels, 1996; Woo et al., 2014). They have been found to comprise as much as 3% of the total fungal populations in forests and 1.5% of the total fungal population in other soils (Tripathi et al., 2010). This genus includes more than 200 species (Atanasova et al., 2013), of which many tend to be opportunistic plant endophytes. This close relationship that *Trichoderma* forms with plants can promote growth and activate induced systemic resistance to pests. In addition, they can parasitise plant pathogens and produce bioactive secondary metabolites and enzymes (Harman, 2006). These characteristics make *Trichoderma* invaluable in

various industries such as: agriculture, biotechnology, paper and pulp treatment and also for use in bioremediation (Harman et al., 2004a; Harman et al., 2012).

1.3 *Trichoderma* as biocontrol agents

The biocontrol ability of *Trichoderma* species against plant pathogens have been extensively studied over the past 80 years. They have long been recognised as potential biocontrol agents and for their ability to increase plant growth and development (Harman et al., 2004b). Various *Trichoderma* species are currently marketed as active ingredients of biopesticides, biofertilisers, growth enhancers and stimulants of natural resistance; together they represent the most common fungal biocontrol genera commercially available for the control of plant diseases (Sharma and Gothalwal, 2017; Woo et al., 2014).

Trichoderma have varying antagonistic properties based on the activation of multiple mechanisms. These modes of action include antibiosis, mycoparasitism, biofertilisation, inducing plant defence systems and competition with the pathogen for nutrients. These mechanisms are complex, and the biocontrol potential of *Trichoderma* spp. is often the result of different mechanisms acting synergistically to achieve disease control (Howell, 2003; Mendoza-Mendoza et al., 2017; Sharma et al., 2014). These modes of action depend greatly on the individual strain along with external factors such as the antagonised pathogen, the (crop) plant and environmental conditions including nutrient availability, pH and temperature (Sharma and Gothalwal, 2017). The range of bioactivity of individual *Trichoderma* strains is comprehensive. For example, commercial products containing *Trichoderma* have been developed for *Sclerotium cepivorum* (McLean and Stewart, 2000), *Botrytis cinerea* (Card et al., 2009; De Meyer et al., 1998), *Rhizoctonia solani* (Sarrocco et al., 2009), *Pythium* (Howell, 2002), *Fusarium oxysporum* (Sivan and Chet, 1986), nematodes (Sharon et al., 2007) and wood-rot fungi (Monte, 2010). The majority of these products are fungicidal (65%), being used for biocontrol of root diseases caused by soil-borne pathogens (Woo et al., 2014).

On a commercial production scale, the success of *Trichoderma* can be credited to the large volume of viable spores that can be produced rapidly and inexpensively on numerous substrates. These low-cost substrates include rice, wheat bran/peat and recycled materials from food manufacturing. This approach has enabled the production of *Trichoderma* worldwide without the need for expensive high-tech fermentation methods making *Trichoderma* based products more accessible (Kumar and Ashraf, 2017; Woo et al., 2014). In addition, *Trichoderma* spores can be incorporated into various formulations including pure spores, liquid culture, granules or as a seed treatment and be stored for months without losing efficacy. Between the production capability and the biocontrol potential, the number of *Trichoderma* containing products found on the international market has grown extensively (Woo et al., 2014).

Work within our research group has identified and commercialised a biocontrol product based on a combination of three *Trichoderma* strains (identified by Robert Hill and Christine Stark, Bio-Protection Research Centre, Lincoln University [BPRC]) called Kiwivax™ (Agrimm Technology, New Zealand). It has a limited label claim to reduce the symptoms of the canker-causing bacterium *Pseudomonas syringae* pv. *actinidiae* (Psa) and to increase the survivability of kiwifruit seedlings.

1.4 *Pseudomonas syringae* pv. *actinidiae*

Pseudomonas syringae pv. *actinidiae* (Psa) is a gram-negative bacterium that causes bacterial canker on a variety of kiwifruit species, including the economically important *Actinidia chinensis* (gold fleshed kiwifruit, cv. Hort16A) and *A. deliciosa* (green fleshed kiwifruit, cv. Hayward) (Scortichini et al., 2012; Vanneste, 2017). The symptoms of this disease include brown-black leaf spots with chlorotic halos, extensive twig die-back, blossom necrosis and bleeding cankers along the main trunk which produce red coloured exudates, eventually leading to vine decline and death (Scortichini et al., 2012; Vanneste, 2017).

1.4.1 Psa in New Zealand

In 2008, a virulent form of Psa was identified in Italy. It subsequently spread throughout other kiwifruit growing regions of the world eventually reaching New Zealand in November 2010. The disease symptoms were initially found on the cultivar 'Hort16A' in Te Puke, Bay of Plenty. Symptoms were soon found on the 'Hayward' cultivar, which overseas had been more tolerant than other cultivars, and spread beyond the primary region (Everett et al., 2011). As of May 2018, 2949 orchards had been identified with Psa and 92% of New Zealand's kiwifruit hectares are on orchards identified with the disease (http://www.kvh.org.nz/maps_stats; last accessed 22.5.2018). The only kiwifruit growing region free from the disease is the South Island (Nelson/Takaka). Te Puke and Waihi are the most severely affected region with 100% of orchards confirmed as infected with Psa disease (http://www.kvh.org.nz/maps_stats; last accessed 22.5.2018). Despite a swift response from the kiwifruit industry, the Ministry of Primary Industries (MPI) and scientists to minimise the impacts, the financial impact of this Psa outbreak was severe (Vanneste, 2017). In 2012, a report by Lincoln University's Agribusiness and Economics Research unit projected that Psa would cost the kiwifruit industry between NZ$310-410 million over the next five years (Greer and Saunders, 2012). However, by 2014 the cost of lost exports alone was estimated to be as high as NZ$930 million (Vanneste, 2017).

1.4.2 Control of Psa

Research has focused on developing efficient strategies for understanding the epidemiology of the disease and controlling the economic loss to the kiwifruit industry. Potential chemical and biocontrol options, alongside strict orchard management practices and breeding resistant varieties are all being

used in this effort (Cameron and Sarojini, 2014). Currently chemical control of Psa in the field is highly dependent on the multiple sprayings of two main bactericides, copper compounds and streptomycin (Colombi et al., 2017), although resistance to both of these bactericides can occur (Colombi et al., 2017; Goto et al., 1994). Strains isolated from Japan throughout the 1980s had a single plasmid that contained both streptomycin and copper resistance genes (Nakajima and Tadaaki, 2002). This raises a very serious concern of bacterial resistance developing to the only current preventative measures. At the beginning of the New Zealand outbreak the single clone responsible was sensitive to copper and lacked genes encoding copper resistance (Colombi et al., 2017; McCann et al., 2013). However, in 2014 copper resistant strains started to appear with a quarter of isolated strains showing resistance. These strains are able to grow in the laboratory in excess of 0.8 mM (~200 ppm) of copper sulphate. A recent study of seven copper resistant strains of Psa led to the identification of three new integrative conjugative elements (ICEs) and two large plasmids carrying genes encoding copper resistance (Colombi et al., 2017).

Fortunately, the kiwifruit industry in New Zealand has recovered and is producing more kiwifruit than before the Psa outbreak. This is mainly due to the replacement of 'Hort16A' with another yellow-fleshed cultivar *A. chinensis* var. *chinensis* 'Zesy002' (Gold3; which is marketed as Zespri® SunGold Kiwifruit). This new cultivar is less susceptible to Psa than 'Hort16A' (Vanneste, 2017). However, the industry still relies mostly on copper-based products to limit the impact of the disease. Although there has been no loss of control using copper products yet, new control options for Psa are still needed in case this does occur. One potential option is the integration of these current control approaches with biocontrol (IPM) at key growing times during the season. This strategy can reduce the use of these chemical control options and potentially prolong their effective lifespan.

1.5 Protoplast technology

In order to integrate Kiwivax™ into an IPM programme, it would be desirable if the *Trichoderma* strains were tolerant to chemical treatments such as copper and other fungicides routinely applied in kiwifruit orchards. One approach of enhancing *Trichoderma* is the use of protoplast technology (Hanson and Howell, 2002; Harman, 2000; Hassan et al., 2013; Hatvani et al., 2006).

Protoplast technology is a powerful tool which provides a mechanism both to screen for rare genetic traits and recombine desired traits without the need for sexual reproduction (Hanson and Howell, 2002; Harman and Stasz, 1991; Narayanasamy, 2013). This is particularly helpful as reproducing sexually is rarely seen in *Trichoderma*, especially in laboratory situations. Therefore other methods must be explored rather than sexual crossing. Protoplasts are cells where the cell wall has been removed so the cytoplasmic membrane is the outermost cell layer (Balasubramanian and Lalithakumari, 2008; Paszkowski et al., 1992; Rodriguez-Iglesias and Schmoll, 2015). Protoplasts are

able to readily adapt to environmental changes as well as being able to fuse, in turn recombining genetic material. The production of protoplasts is an effective technique which has been applied in both plant and fungal systems to enhance strains (Eeckhaut et al., 2013; Paszkowski et al., 1992; Savitha et al., 2010).

There are two primary applications for protoplasting. The first one is the production of protoplast regenerants (one parent) which allows cell regeneration for screening and selection of naturally occurring rare genetic alterations (Braithwaite et al., 2013; Kandula et al., 2012; Paszkowski et al., 1992). In the literature some researchers have described these progenies as arising from self-fusion (intra-strain). However, when only one parental strain is present, it is not possible to definitively state that the selected progeny was the result of any fusion event. For the purpose of this thesis reports of self- or intra-strain fusion will be referred to as regenerants. The second application for protoplasting is protoplast fusion (inter-strain fusion). This occurs between two parental strains and is when cell fusion and mixing of genetic material takes place (Balasubramanian and Lalithakumari, 2008; Harman et al., 1998). Since genetic mixing takes place, this technique can be used to combine desirable characteristics into one strain. This process of mixing genetic material can also occur in nature not only through sexual reproduction but via vegetative hyphal fusion or anastomosis in filamentous fungi (Daskalov et al., 2017). Additionally, producing novel strains via protoplast fusion is beneficial from a regulatory standpoint as they do not involve genetic engineering so there are no restrictions on using this technology within New Zealand and elsewhere around the world.

1.5.1 Protoplast regeneration as a tool

Exposure of protoplasts to extreme conditions is a proven technique to select for regenerants with specific environmental tolerances (Paszkowski et al., 1992). Fungi grown from these regenerated protoplasts appear to be more vigorous and are readily able to adapt to stresses through an unknown mechanism/s. This technique has the ability to select for rare genetic traits and stimulate spontaneous mutations (Paszkowski et al., 1992) without the need for mutagenesis, or reset the cell's gene expression program (Avivi et al., 2004). Within our research group, protoplast regeneration has been successfully used to develop *T*. sp. "*atroviride* B" variants that are tolerant to the fungicide Switch® (active ingredients cyprodinil and fludioxonil) and others that are more biologically active at cooler temperatures than the parental strain (Braithwaite et al., 2013; Kandula et al., 2012). Protoplast regeneration is therefore a very effective tool to screen and select for desired traits such as tolerance to chemical treatments within already successful biocontrol *Trichoderma* strains.

1.5.2 Protoplast fusion as a tool

Desirable characteristics can also be combined from two strains or species using protoplast fusion (Hanson and Howell, 2002; Mohamed and Haggag, 2010). Protoplast fusion has been shown to be a successful technique for the improvement of biocontrol *Trichoderma* strains. This was first shown in the 1980s, with *T. reesi* strains, where protoplast fusion resulted in new genetic progeny (Manczinger and Ferenczy, 1985). Since then it has been applied to numerous other *Trichoderma* and other filamentous fungi (Ahmed and Fatma, 2007; Couteaudier et al., 1996; Harman, 2000). The most commonly cited example is *T. harzianum* T-22 (Harman, 2000). This novel strain was produced using protoplast fusion from two *T. harzianum* strains in an attempt to obtain a strain that was highly rhizosphere competent with the ability to suppress spermosphere bacteria (Harman, 2000). Various other research groups have also achieved success in the fusion of protoplasts within the genus *Trichoderma* to enhance biological attributes. One such example is a fusant that was produced between *T. koningii* (good storage qualities, but poor biocontrol efficacy) and *T. virens* (good biocontrol activity against *Rhizoctonia solani*). This newly created fusant had significantly better biocontrol activity and an increase in storage potential for up to a year compared to their respective parents (Hanson and Howell, 2002).

There are various applications of progeny resulting from fungal protoplast fusions, not just in *Trichoderma* species. These include genetic analyses where progeny from protoplast fusion have been used in gene mapping and complementation tests (Strom and Bushley, 2016), fermentation and enzyme production (Ahmed and Fatma, 2007; Dillon et al., 2008; Hassan, 2014; Ushijima et al., 1990), pharmaceutical production (Anné, 1982; Tahoun, 1993; Zhou et al., 2008), bioremediation (Patil et al., 2015) and biocontrol. Protoplast fusion has also been used in the development of an effective biocontrol agent between two strains of *Beauveria bassiana*. This fusant exhibited greater virulence against their insect host (Couteaudier et al., 1996). In another study fusant strains of *B. bassiana* with enhanced thermotolerance were produced from fusing two strains (Kim et al., 2011). Another research group produced a fusant between the entomopathogenic fungi *Lecanicillium muscarium* and *L. longisporum* that had higher virulence than each parental strain and had an enhanced ability to withstand humidity extremes (Aiuchi et al., 2008).

It is important to note that not all fusion events between different fungal species and strains are successful (Daskalov et al., 2017; Stasz et al., 1989). A potential outcome is the formation of unstable heterokaryons. Heterokaryosis is unique to fungi and refers to the presence of two or more genetically distant nuclei within the same cell (Strom and Bushley, 2016). Although there are many stable examples of heterokaryons across the fungal kingdom, there are numerous molecular mechanisms in place that regulate this cellular fusion and potential heterokaryon formation. The production of

unstable heterokaryons can lead to programmed cell death, with heterokaryon or vegetative incompatibility occurring commonly. This mechanism has been further hypothesised that it can act as a defence against mycoparasitism and genome exploitation from other fungi. This potentially occurs by inducing programmed cell death via incompatible alleles and other non-self recognition mechanisms (Daskalov et al., 2017).

1.5.3 Mechanisms behind protoplasting

Protoplast regenerants

Although both uses of protoplast technology (regeneration and fusion) are commonly used to produce improved fungal strains, little is known about the underlying genetic consequences of protoplasting. Even less is known about the processes underlying phenotypic change in regenerants with altered characteristics. The genetic basis for fungicide resistance (Switch®) within the regenerants produced by our group was explored (Johanna Steyaert, pers. comm.). Universally primed PCR (UP-PCR) and Amplified Fragment Length Polymorphism (AFLP) profiles were identical in the parent and Switch® resistant regenerant suggesting that the phenotypic changes were due to either subtle DNA arrangements or involved non-genomic changes. Five key genes that are known to be associated with Switch® resistance were sequenced revealing no change between parent and regenerant. However, Methylation Sensitive Amplified Polymorphism (MSAP) analysis detected multiple methylation changes which strongly suggests that methylation may play an important role in determining the phenotype plasticity of regenerants.

Causes of changes in phenotype

Phenotypic differences are typically induced in three main ways: changes of the DNA sequence, extra-chromosomal DNA elements and by epigenetic modifications that can influence gene expression. These genomic and gene expression differences can lead to altered protein compositions or function in the cells which in turn causes phenotypic changes (Williams et al., 2007). For phenotypic alterations to be maintained over subsequent generations the changes need to be heritable. Major DNA differences between strains stem from events such as deletions, insertions, transposable elements, translocations, chromosomal polymorphisms, different gene copy number and different intron positions (Kistler and Miao, 1992). However, these large genomic differences normally would have been picked up via the DNA fingerprinting methods mentioned above suggesting a more subtle change may be more likely. Single nucleotide polymorphisms (SNPs) are responsible for most of the genetic variation between individuals. They can arise from spontaneous mutations and cause major phenotypic changes or remain silent (Lange et al., 2016a; Porciuncula et al., 2013). For example, Porciuncula et al. (2013) tested a hyper-cellulolytic mutant strain of *T. reesei* produced by UV-

irradiation. A single SNP in the DNA-binding domain of *cre1* (a carbon catabolite repressor gene) was found to solely be responsible for the increased cellulase production.

Extra-chromosomal DNA elements are defined as changes that occur in non-chromosomal elements. Examples of extra-chromosomal changes in fungi are changes within the DNA resulting from mitochondrial genome, mycovirsuses and plasmids (Ghabrial et al., 2015; Kistler and Miao, 1992; Nuss and Koltin, 1990; Samac and Leong, 1989). Lange (2015) showed that there were single stranded RNA (ssRNA) bands detected in a strain of *T.* sp "*atroviride* B" (LU660). This is significant as viruses can induce hypovirulence in plant pathogenic fungi and also secrete different secondary metabolites (Ghabrial et al., 2015; Nuss, 2005), which could have an effect on phenotype. These mycoviruses are commonly found in endophytic fungi, with research postulating that there is potentially a mutualistic role within this already complex interaction (between the fungus and plant) (Ghabrial et al., 2015; Herrero et al., 2009).

Finally, epigenetic modifications can also alter the phenotype of an organism. These are heritable alterations that are not due to changes in the DNA sequence. There are different types of modifications that can lead to epigenetic effects that include: DNA methylation, histone modifications and deacetylation and RNA-based mechanisms such as microRNAs and small RNAs (sRNAs) (Jaenisch and Bird, 2003; Martienssen and Colot, 2001). These can alter DNA accessibility and chromatin structure that in turn change patterns of gene expression, either causing gene activation or silencing (Martienssen and Colot, 2001). All of these modifications have the potential to alter the biology of a strain and, in this case, potentially the phenotype between a parent and the protoplast regenerant.

Cytosine DNA methylation is thought to be a major contributor in epigenetic regulation as it can lead to other epigenetic modifications such as modified histones and chromatin structures. Cytosine methylation is a well-established epigenetic mark within eukaryotes that involves the addition of a methyl group to the C5 carbon residue (5mC) of cytosines by DNA methyltransferases (Krueger et al., 2012). It plays a crucial role in numerous cellular processes including genome regulation and development, gene imprinting and transposon silencing (Feng et al., 2010; Zemach et al., 2010). Cytosine methylation is not present in all eukaryotes and higher methylation levels have been found in mammals and plants compared to lower (or non-detectable) levels in insects, yeast and fungi. A consensus view of DNA methylation in fungi was primarily as a genome maintenance mechanism that controls the genome stability against transposable elements and repeat sequences, chromatin condensation and regulation of non-coding RNAs (ncRNAs) (Li et al., 2017b; Zemach et al., 2010). However, it is becoming more common to see methylation in gene bodies in fungi than previously thought with numerous papers recently reporting this phenomenon (Jeon et al., 2015; Li et al., 2017b; Wang et al., 2015; Zemach et al., 2010). This is notable as previous studies showed methylation

primarily of intergenic regions which was thought to play a role in the maintenance of genome stability. Methylation found in genic regions can control gene transcription (Bird, 2002; Li et al., 2017b), theoretically having a more direct influence over the phenotype of an organism.

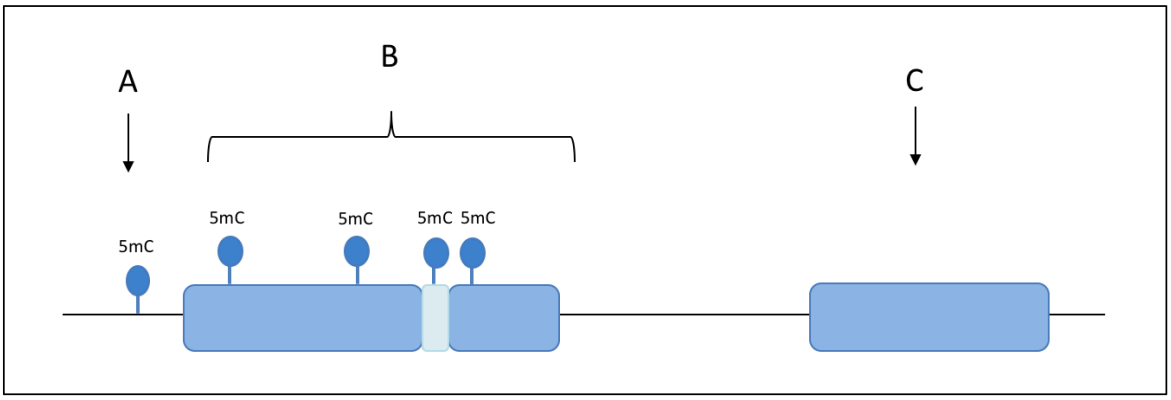

Figure 1.1 The effect that cytosine DNA methylation or mutation may have on gene expression following the production of a protoplast regenerant. (A) Methylation in promoters can cause repression of gene expression. (B) Methylation of introns and exons is associated with alternative splicing, transcriptional elongation etc. (C) Other factors that could cause phenotypic plasticity include changes in DNA sequence (SNPs), extrachromosomal DNA elements or other epigenetic modifications.

Protoplast fusants

Researchers have examined the basis of the changes resulting from fusion where genome rearrangement was observed. However, the exact nature, mechanism and frequency of rearrangements occurring is unknown. Traditionally fungi have a variety of mechanisms whereby they undergo interspecific hybridisation; either by a partial or complete sexual cycle or via a parasexual process (Schardl and Craven, 2003). Fused protoplasts initially form heterokaryons and may progress partway or completely through the parasexual cycle, resulting in diploid or recombined haploid hybrids (Strom and Bushley, 2016). Genome reshuffling can occur with the acquisition and/or loss of multiple traits and is often documented through DNA profiling and fragmenting such as UP-PCR, Random Amplified Polymorphic DNA (RAPD) and Inter-simple Sequence Repeat PCR (ISSR-PCR) (Hassan et al., 2011; Lakhani et al., 2016; Xu et al., 2012). Fungal fusants often exhibit faster growth than either of the two parental strains and have desirable characteristics of both parents (Strom and Bushley, 2016). For example, protoplast fusants were produced from *T. koningii* and *T. viride* resulting in a two-fold increase in enzyme activity of β-glucanase within the fusants compared to the parental strains (Hassan et al., 2013). Additionally, for this fusant the protein pattern of the extracellular cellulase enzymes was acquired through Sodium Dodecyl Sulphate Polyacrylamide Gel Electrophoresis (SDS-PAGE) that further revealed a new recombinant protein. It was hypothesised that the presence of this protein

resulted from a partial or incomplete genetic recombination during nuclear and cytoplasmic protoplast fusion (Hassan et al., 2013).

However, there is much debate over genome recombination and to the extent and frequency this occurs with different studies suggesting different mechanisms. Harman et al. (1998) examined the mitochondrial and genomic RFLP and RAPD patterns of the parental strains and fusion progeny of two *T. harzianum* strains (T95 lys^- ben^+ and T12 his^-). In only one case out of fifteen did the genomic RFLP or the RAPD pattern differ from one or the other parental strain. Moreover, in all progeny the mitochondrial genotype matched the same pattern of the nuclear genotype with similarities to a single parent opposed to a combination. These results posed a paradox as they suggested that classical parasexuality that includes recombination of large sections of the parental genome did not occur during protoplast fusion at detectable levels. Instead they proposed a mechanism called inter-strain gene transfer to explain these changes in phenotype (Harman and Hayes, 1993; Harman et al., 1998). They suggested that within inter-strain fusions many nuclei of the non-prevalent parent are degraded and that DNA fragments are produced. These very small fragments are subsequently inserted into the genome of the prevalent strain and give rise to novel genotypes. In addition, the unusual phenotype of many progeny strains might be explained by the insertion of sequences at sites that disrupt key genes or regulatory sequences. To test this hypothesis they used a dominant selectable marker that could be identified using Southern blot analyses with a transformed *T. harzianum* strain containing a gene for hygromycin B resistance (*hygB*). The progeny were screened and Southern blot analyses confirmed that *hygB* (from the non-prevalent parent) was incorporated into the genome. RFLP and RAPD analyses were performed on this strain and all gave the same genotype as the prevalent parent (Harman and Hayes, 1993; Harman et al., 1998). This mechanism is cited from a chapter within the book *Trichoderma* and *Gliocaldium* Volume 1: Basic biology, taxonomy and genetics (1998), with the original papers being reported as submitted in 1998. However, after an extensive literature search, these original papers were not found suggesting that they were never published, which raises some doubt regarding these hypotheses.

As previously mentioned, fusion of protoplasts may result in a transitional heterokaryotic phase without nuclear fusion. Early research into protoplast fusion suggested that the recombination of the nuclei between two fused parental strains may be due to either heterokaryosis or karyogamy. Pe'er and Chet (1990) showed heterokaryotic colonies were produced by the fusion of two auxotrophic *T. harzianum* mutants. However, after several rounds of single spore selection the heterokaryotic colonies segregated into the two parental types. This indicated that nuclei from both parental strains were in a transitional heterokaryotic phase (Pe'er and Chet, 1990). Interestingly, protoplasts of *Candida tropicalis* were also shown to produce heterokaryons after a fusion event which were unstable and quickly reverted into their two respective nuclear components (Fournier et al., 1977). Genetic

instability of intra-specific and inter-specific fusants is a commonly reported problem (Anné, 1982; Stasz et al., 1989; Wang et al., 2010). Industrial strains of *Penicillium chrysogenum*, which can synthesise higher levels of penicillin due to alloploidy, often reverted back to wild-type antibiotic production levels due to chromosome loss over repeated rounds of sub-culturing (Künkel et al., 1992). It has been suggested that this instability is a natural progression of the parasexual cycle in which diploids formed from heterokaryons undergo haploidisation through gradual chromosome loss (Strom and Bushley, 2016). This genetic instability is noted in wild-type fungi even when undergoing sexual reproduction as offspring can have different sized chromosomes over numerous generations (Davière et al., 2001). This highlights how sporadic and potentially unstable fungal fusion can be, whether occurring naturally through anastomosis or *in vivo* via protoplast fusion.

Although heterkaryosis is not strictly protoplast fusion some of the mechanisms behind the improved qualities of these stable fungal heterokaryons may still be of interest. Several genetic mechanisms have been proposed (Couteaudier et al., 1996; Strom and Bushley, 2016). It has been suggested that deleterious alleles in one genome are masked by dominant or complementary alleles in the second genome. Another possibility is that new gene interactions arise in heterokaryons due to distinct allele combinations. Finally, hybrids between these genotypically divergent parents may express novel combinations of genes or a greater diversity of transcripts. This would result in an increased variety of proteins that may confer a faster growth rate or increased production of secondary metabolites (Strom and Bushley, 2016). It was postulated that all of these mechanisms likely play a part in enhancing the phenotypes of these fungal heterokaryons.

Another similar system involving combining of different chromosomes is that of plant and fungal polyploids. The resulting polyploids are often ecologically competitive. The improved qualities relative to parental strains are similar to fungal heterokaryons and are thought to arise from masking of deleterious alleles, fixed hybrid vigour and/or greater evolutionary plasticity resulting from the duplicated gene copies (Chen, 2007; Cox et al., 2014; Madlung, 2013; Yoo et al., 2013). One example is that of the asexual fungal grass-endophyte *Epichloë* that is a diploid hybrid between *Epichloë typhina* and *Neotyphodium loli* (Cox et al., 2014; Shoji et al., 2015). The exact mechanism of allopolyploidy that translates to phenotype is also unknown, but it is presumed to be similar to normal fungal mating where cells fuse to create a dikaryon (a cell containing two nuclei) followed by nuclear fusion. Cox et al. (2014) found that the transcriptional response involves both copies of most genes being retained with over half of the genes inheriting parental gene expression patterns. Additionally, in plants it has been shown that reprogramming of gene expression patterns in allopolyploids is due to chromatin modifications and RNA-mediated pathways. These alterations may cause changes in adaptive traits such as flowering-time variation, self-incompatibility and hybrid vigour (Chen, 2007). This shows that this hybridisation has an obvious large effect on both gene expression and phenotypic variation.

In summary, despite the long history and frequent usage of fungal protoplast technology for strain improvement very little is known of the underlying genetic changes which results in modified phenotypes. An understanding of the basic genetic events that occur during protoplasting in *Trichoderma* may allow for greater advances in the production of superior strains of not only *Trichoderma* but various other fungi of interest.

1.6 Research aims and objectives

The overall aims of this project were to i) produce better fungal biocontrol agents and ii) to develop an understanding of the process that led to these changes. Both protoplast regeneration and fusion strategies were used to produce desirable attributes such as pesticide tolerance and increased bioactivity against Psa to develop novel biocontrol agents. To achieve this leading *Trichoderma* candidates were selected from current BPRC research programmes targeted at kiwifruit health. To develop an understanding of the underlying molecular consequences of using protoplast technology the pesticide tolerant biocontrol agents were used as a model system to examine this issue. An 'omics approach was used to characterise the chosen protoplast progeny based on the hypothesis from previous work within our lab group that cytosine methylation may be responsible for the phenotypic plasticity induced by protoplasting.

Accordingly, Chapters 2-5 had the following research objectives:

i) To develop and characterise protoplast regenerants and/or fusants which are either copper or fungicide tolerant.

ii) To screen for increased bioactivity against Psa.

iii) Explore the molecular consequences of either protoplast regeneration or fusion through an integrative 'omics.

The findings from these objectives will result in novel enhanced biocontrol agents against Psa for kiwifruit and will reveal fundamental insight into this poorly understood phenomenon of protoplast technology.

Chapter 2

Induction of pesticide tolerance via protoplast technology and characterisation of the resulting progeny

2.1 Introduction

The biocontrol ability of *Trichoderma* strains to reduce plant pathogens has been extensively studied over the past 80 years, and many have been selected from naturally occurring populations for their ability as biocontrol agents. Others, however, have had their biocontrol ability enhanced through chemical or UV mutation. Tolerance of *T. harzianum* to benomyl was induced by ultraviolet irradiation and subsequent selection (Papavizas et al., 1982). There are numerous further examples of UV-mutagenesis being used to produce *Trichoderma* mutants such as Hatvani et al. (2006) who used this method to produce two mutants resistant to carbendazim (*T. harzianum*) and tebuconazole (*T. atroviride*). An alternate method for strain enhancement is the use of protoplast technology. It has been shown to be a powerful tool for the improvement of filamentous fungi, not solely used for improving biocontrol potential but also in the biotechnology industry. The development of novel strains using this technology provides the opportunity to re-combine or select for desired features, such as fungicide tolerance, increased bioactivity or increased enzyme production, without the need for sexual reproduction. This is particularly helpful as the ability to reproduce sexually is rarely seen in many *Trichoderma* species in the laboratory, therefore other methods must be explored rather than sexual crossing.

There are two primary strategies for the production of protoplasts for downstream work. The first is the production of protoplast regenerants (one parent) which allows for direct manipulation through cell regeneration for the screening and selection of naturally occurring rare genetic alterations. The second is protoplast fusion. This occurs between two parental strains and is when cells fuse, thereby allowing the mixing of genetic material takes (Balasubramanian and Lalithakumari, 2008; Harman et al., 1998). This technique can be used to combine desired characteristics into one strain. Both of these techniques have been used for strain improvement within *Trichoderma* and other filamentous fungi species. Protoplast regeneration has also been used to produce fungicide resistant and cold tolerant varieties of the biocontrol *T*. sp. "*atroviride* B" strain LU132 (Braithwaite et al., 2013; Kandula et al., 2012). Protoplast fusion has been applied to numerous other *Trichoderma* and it has been shown that it is possible to combine desirable traits from various parental strains to improve biocontrol ability (Harman, 2000; Hatvani et al., 2006). This was shown as early as 1985, where the use of protoplast fusion of *T. reesei* strains resulted in new genetic recombinations that improved cellulose production

(Manczinger and Ferenczy, 1985). Further examples include *T. harzianum* (T-22), this novel strain was produced from protoplast fusion of two *Trichoderma* strains to obtain a strain that was highly rhizosphere competent with the ability to suppress various spermosphere bacteria (Harman, 2000). In addition protoplast fusion has been used to produce fusants for intraspecific, interspecific and even intergeneric crosses and also for the improvement of industrial strains, with traits such as increased chitinase production (Ahmed and Fatma, 2007; Patil et al., 2015; Prabavathy et al., 2006b).

Work within our research group has identified a mix of *Trichoderma* strains able to reduce the symptoms of Psa. This aims of this chapter were to i) develop copper resistant strains as copper could be a major limitation in the field as it is extensively applied to Psa, and to ii) produce another variant tolerant to alternative pesticide used within kiwifruit orchards. Having two pesticide tolerant strains would allow for confirmation of a fusion event through the use of double pesticide amended media. The resulting protoplast progeny are to be further characterised in the later chapters which aims to explore the molecular consequences of using protoplast technology.

2.2 Materials and methods

2.2.1 Fungal strain selection and identificaion

Various *Trichoderma* strains that have shown *in planta* biological activity against Psa were chosen for this project. Strains were obtained from the Lincoln University Microbial Culture Collection (LUMCC, Bio-Protection Research Centre, Lincoln) and the Forestry Culture Collection (FCC, Bio-Protection Research Centre, Lincoln) and maintained on Potato Dextrose Agar (PDA) (Difco Laboratories Inc, USA) and as spore suspensions at 10^8 conidia/mL in 25% glycerol at -80°C (Table 2.1).

To generate biomass for DNA extraction, 20 µL aliquots of the spore suspension stocks of the selected strains were inoculated into 30 mL of Potato Dextrose Broth (PDB) (Difco) in a 50 mL centrifuge tube (ThermoFisher, USA). Each tube was sealed, wrapped in foil and incubated at 23°C for 3 d. The mycelium was filtered through a double layer of Miracloth (Merck Millipore, Germany) and snap frozen in liquid nitrogen. Genomic DNA (gDNA) was extracted from the frozen mycelia using the Gentra Puregene TissueKit (Qiagen, Germany) according to the manufacturer's instructions and recommendations for extraction of fungal DNA. All strains listed in Table 2.1 were identified by sequencing a standard *Trichoderma* identification marker, translation elongation factor 1*α* (*tef1α*), using primers and amplification conditions described in Braithwaite et al. (2017).

Table 2.1 Identification of *Trichoderma* strains selected for this study based on *tef1α* sequences.

Strain	*Trichoderma* species	Origin	GenBank
LU297	*Trichoderma trixiae*	Roots of a grape, Auckland	KJ871256
LU668	*Trichoderma* sp. *"atroviride* B"[1]	Soil, unknown location, New Zealand	KJ871103
LU753	*Trichoderma* sp. novel LU753	Soil under grass, Lincoln University	KJ871147
FCC207	*Trichoderma hamatum*	Roots of Hort16A, Te Puke	KJ871162
FCC237	*Trichoderma* sp. *"atroviride* B" [1]	Roots of N3, Te Puke	KJ871103
FCC261	*Trichoderma harzianum sensu stricto*	Cane of Hayward, Te Puke	KJ871171
FCC270	*Trichoderma* sp. novel FCC270	Leaves from Hayward, Te Puke	N/A
FCC273	*Trichoderma* sp. *"atroviride* B" [1]	Flower from Hayward, Te Puke	KJ871103
FCC456	*Trichoderma* sp. *"atroviride* B" [1]	Cane of Hayward, Te Puke	KJ871103

[1] *Trichoderma* sp. "*atroviride* B" is a newly described *Trichoderma* species closely related to *T. atroviride*, but found predominantly in the southern hemisphere (Braithwaite et al., 2017).

2.2.2 Pre-screening for naturally occurring sensitivity to pesticides

A variety of chemicals were tested on the selected *Trichoderma* strains to determine what would be suitable to use as unique selection markers for confirmation of a fusion event. Copper was selected as it is currently used as a bactericide against Psa in kiwifruit orchards (Cameron and Sarojini, 2014), alongside the fungicide Flint® (active ingredient [a.i.] 500 g/kg trifloxystrobin) (Bayer, Germany) and the fungicide Chief® (a.i. 500 g/L carbendazim) (Adama Agricultural Solutions, Israel) which are both used on kiwifruit against *Sclerotinia sclerotiorum*.

To determine the absolute kill point, being the lowest concentration of pesticide where no mycelial growth could be observed, all strains were exposed to differing amounts of copper II sulphate ($CuSO_4.5H_2O$) and Flint®. Copper sulphate was selected over commercially available copper products (such as Nordox 75 WG™ [Nordox, Norway] or Kocide® Opti™ [DuPont, USA]) as it releases a known amount of Cu++ ions in solution, the active ingredient against bacteria and fungi. Commercial formulations need time, moisture and acidity for the copper to degrade and release the Cu++ ions. Therefore, traditional methods such as incorporation into agar are not suitable for commercially available copper products. Balasubramanian and Lalithakumari (2008) previously used copper sulphate as an alternative and successfully produced protoplasts using this source of copper.

Trichoderma conidia (2 µL aliquot) from the -80°C stock of all the strains listed in Table 2.1 were inoculated centrally onto PDA and incubated for 3 d at 23°C in the dark. After 3 d, a mycelial disk (0.7 cm) was cut from the colony margin and placed centrally onto the amended PDA in 90 mm Petri dishes prepared as follows: PDA was prepared with nanopure water and sterilised in a pressure cooker (All

American pressure cooker model no. 921, USA). All amendments (chemical fungicides or copper sulphate) were dissolved in nanopure water, filter sterilised and added to the prepared PDA at the following rates: copper sulphate at 2.5 mM, 2 mM, 1 mM and 0.5 mM and Flint® at 10 µg/mL, 1 µg/mL, 0.1 µg/mL and 0.01 µg/mL. Strains were plated to non-amended PDA for comparison. Three plates were inoculated per treatment. The plates were incubated at 23°C in the dark for 7 d. The experiment was repeated twice.

Due to the *Trichoderma* strains showing high tolerance to the trifloxystrobin fungicide Flint®, another fungicide also used in kiwifruit orchards, Chief®, was chosen as the secondary selective marker to confirm a fusion event had occurred. Conidial suspensions were used from this point onwards instead of mycelial agar plugs as they provide more consistent and reliable growth on pesticide amended agar compared to mycelial plugs. The mycelial plugs can provide additional nutrients and potentially false positive growth. Furthermore, instead of using PDA as the selection agar, recovery medium (RM) (yeast extract 0.5 g/L, 0.8 M sucrose, 15 g agar/L, cooled to 45°C) was used, as this is the agar the protoplasts are plated onto to recover their cell walls. The RM was amended at the following rates based on the previous experiment: copper at 4 mM, 3 mM, 2 mM and 1 mM and Chief® at 10 µg/mL, 1 µg/mL, 0.1 µg/mL and 0.01 µg/mL. A 2 µL aliquot of the respective conidial suspensions (at 1x 10^8 conidia/mL) were inoculated centrally onto the amended media. Three plates were inoculated per treatment. The plates were incubated at 23°C in the dark for 7 d. The experiment was repeated twice.

2.2.3 Preparation of protoplasts and optimisation

2.2.3.1 Production of protoplasts- Method 1

The isolation of protoplasts was based on a method described by Prabavathy et al. (2006a) and modified by Janaki Kandula (pers. comm.). Conidia were generated as follows: 10 µL of the conidial suspension (1 x 10^8/mL) was mixed with 100 µL sterile distilled water (SDW) and spread over a PDA plate. Plates were incubated at 23°C under a 12/12 h light/dark cycle for 7 d. Conidia were harvested by flooding the plates with 5 mL SDW, scrapped into suspension using a bent glass rod and were filtered through a sterile double layer of Miracloth to remove mycelial fragments. The conidial concentration was adjusted and added to 100 mL of Glucose Yeast Extract Casein broth for a final concentration of 1 X 10^5 conidia/mL (GYEC broth; Glucose 15 g/L, Yeast Extract 3 g/L, Bacto tryptone 5 g/L) in a 250 mL flask and incubated on a rotary shaker (Orbitron, Infors HT, Switzerland) (120 rpm) at 23°C under 12/12 h light/dark cycle, for a predetermined amount of time from the optimisation step (section 2.2.3.5). The freshly germinated conidia were collected on Miracloth and washed with SDW, followed by two washes with an osmotic stabiliser (OM buffer; 1.2 M $MgSO_4.7H_2O$, 10 mM Na_2HPO_4, pH 5.8). The mycelium was incubated in 1% Glucanex (Novozymes®, Denmark), prepared in OM buffer, on an orbital

shaker (120 rpm) at 25°C for 4 h. The lysis of mycelia and the release of the protoplasts were monitored at 30 min intervals under a microscope.

Protoplasts released from the mycelium-enzyme mixture were filtered through Miracloth. An overlay of 2 mL ST buffer (0.6 M Sorbitol, 100 mM Tris–HCl, pH 8.0) was added to every 5 mL of protoplasts obtained and the solution separated at 3000 x*g* for 5 min. This produced a white foggy layer of pure protoplasts which was collected from the interphase between the two buffers and then pelleted at 3000 x*g* for 5 min. The supernatant was discarded and the pellet purified by washing twice in STC buffer (1.2 M Sorbitol, 10 mM $CaCl_2$, 10 mM Tris–HCl, pH 7.5) and centrifuged after each addition. The pellet was re-suspended in STC buffer and diluted to 10^6/mL.

2.2.3.2 Production of protoplasts- Method 2

Based upon advice from other members of our lab group, another protoplast isolation method was trialled as it was thought to produce a higher number of protoplasts. The isolation of protoplasts was based on a method described by Gruber et al. (1990) using a cellophane disk, modified by Lawry (2016). Conidia were harvested from 7 d *Trichoderma* cultures as described in section 2.2.3.1. A 100 µL aliquot of conidia was plated onto the centre of a large (150 mm x 150 mm) petri plate containing PDA with a piece of sterile cellophane (Bio-Rad, Cat No. 1650963, USA) placed upon the agar and spread over the surface. Plates were incubated (22°C; 12/12 h light/dark cycle) for 15 h, the cellophane was removed and immersed in 10 mL of an enzymatic solution consisting of 48 mg cellulase (Sigma-Aldrich, USA) and 0.1 g Glucanex in mannitol osmoticum (50 mM $CaCl_2$, 0.7 M mannitol, 50 mM MES, pH 5.5). The digestion mix was incubated for 4 h at 25°C with shaking at 150 rpm. Protoplasts were recovered by filtration through Miracloth, followed by a second filtration through a sterile 40 µm nylon mesh supported in a Swinnex holder. The protoplast suspension was centrifuged at 4000 x*g* for 10 min. The supernatant was discarded and the pellet was re-suspended in 500 µL of mannitol osmoticum.

2.2.3.3 Regeneration of protoplasts

One mL of the protoplast solution (1 x 10^6 protoplasts/mL) was mixed with 5 mL RM, which was cooled to 45°C, and poured as an overlay onto amended media at the absolute kill point values from section 2.2.2 (4 mM copper sulphate and 1 µg/mL Chief® respectively). Plates were incubated in the dark at 23°C for 10 d. Regenerants were selected on the basis of their growth on the amended media.

2.2.3.4 Purification of protoplast regenerants

Selected regenerants were purified to ensure strains were homokaryons by three rounds of single spore isolation. The conidia were generated in the absence of selection, then germinated in the presence of selection on PDA. These purified selected regenerants were tested for phenotypic stability by repeated sub-culturing on non-amended PDA. The cultures were grown until they reached the edge of the plate and then a mycelial plug transferred to a fresh PDA plate. This process was repeated seven

times and after the seventh sub-culture, a mycelial plug was transferred to media containing the selection to ensure the selection tolerance was still present.

2.2.3.5 Optimisation of protocol for each strain

For both methods, the optimal conditions for generating protoplasts for each strain were determined. The length of incubation time required for germlings to form was tested. For Method 1, 7 d conidia from all the strains in Table 2.1 were inoculated in the GYEC broth and samples taken at 14, 16, 18, 20, 22 and 24 h, diluted and examined under the microscope for germination of the conidia. For Method 2, 7 d conidia were inoculated on the cellophane disks for 12, 14, 15 and 16 h. The length of enzymatic digestion time for the first method was also determined: the mycelium was placed in a flask with 35 mL OM buffer/Glucanex and incubated on an orbital shaker (120 rpm) for either i) 2 h; ii) 4 h; or iii) 2 h at room temperature, then placed in the cold room (4°C) overnight and placed again on the shaker for a further 2 h the following day.

2.2.4 Production of protoplast fusants

Fusion of the protoplast regenerants was based on a method described by Stasz et al. (1988) modified by Janaki Kandula (pers. comm.). Forty percent polyethylene glycol solution (PEG, molecular weight 3350) (Sigma-Aldrich) solution containing 50 mM Tris-HCl (pH 7.5) and 50 mM $CaCl_2$ was used as the fusogen. An aliquot of equal portions of two selected protoplast regenerants (1 x 10^6/mL) was centrifuged at 2500 x*g* for 10 min and the supernatant removed. The pellet was resuspended in 1 mL 40% PEG solution and incubated at 30°C for 30 min. The mixture was added directly to RM (cooled to 45°C) and plated as an overlay on double amended RM (4 mM copper sulphate and 1 µg/mL Chief®). Plates without any additives were inoculated with protoplasts (1 x 10^2/mL) to establish the protoplast regeneration rate in the absence of pesticides and on single pesticide amended plates. Plates were incubated in the dark at 22°C for 10 d. Fusants were selected based on their survivability and purified to eliminate heterokaryons as described in section 2.2.3.4.

2.2.5 Interactive toxicity effects of pesticides in agar

The results from 2.2.4 suggested a potential interactive toxicity effect of the pesticides in agar (between the copper sulphate and the carbendazim of Chief®). To test this hypothesis, sub-lethal amounts of copper sulphate (1 mM) and Chief® (0.01 µg/mL) were added to PDA and RM. A 2 µL aliquot of the respective *Trichoderma* parental strains conidial suspension (10^8 conidia/mL) was inoculated centrally onto the double amended pesticide plates. The plates were incubated at 23°C under a 12/12 h light/dark cycle for 10 d. They were scored for the ability to grow on the amended media. This experiment was repeated twice. This experiment was also repeated with the pure chemical

carbendazim (Sigma-Aldrich), opposed to the commercial product, at the same rate of active ingredient.

2.2.6 Phenotypic characterisation- growth rate and conidiation

2.2.6.1 Experimental setup

Two regenerants, one tolerant to copper (*T*. sp. "*atroviride* B" FCC237/R5) and one tolerant to carbendazim (Chief®) (*T. hamatum* FCC207/R9) respectively, were chosen for further phenotypic characterisation as they were the most morphologically similar to their respective parents and genome resources for these species are publically available.

Radial mycelial growth rates and conidiation rates of the chosen regenerants (and their parental strains) were determined on PDA and malt extract agar (MEA; Difco). Agar plates were inoculated centrally with a 2 µL conidial suspension (10^8 conidia/mL) and plates were then incubated in the dark at 23°C for 4 d, with radial growth measured daily. Positions of the colony margins were marked on the reverse of the plates every 24 h until the colony reached the edge of the plate. The morphology of the colonies was also recorded. Conidial yield was determined by mixing 10 µL of the conidial suspension (1 x 10^8/mL) with 100 µL SDW and spreading evenly across the surface of a PDA plate. Plates were incubated at 23°C under a 12/12 h light/dark cycle for 14 d, with conidial measurements taken on days 3, 5, 7, 10 and 14. Ten plates per treatment were included. Conidia were harvested by flooding the plates with 5 mL of SDW and the conidia were scrapped into suspension and filtered through a double layer of Miracloth. The suspensions were diluted 10^2-fold and 10^3-fold with water and counted using a haemocytometer, the results were expressed as conidia/plate. The experiment was repeated once.

The germination percentage was determined as follows: each aliquot of conidia was serially diluted to 5 X 10^5 conidia/mL with SDW and then 500 µl aliquots were transferred to fresh 1.7 mL centrifuge tubes and 500 µL of PDB added. Samples were kept on ice until they were attached to the rotating wheel in a hybridisation oven (Stuart, John Morris Scientific Ltd., Australia) and slowly rotated (7 rpm) at 23°C. After 16 h, all samples were placed on ice, checked for germination and those not germinating were placed back into the incubator until germinated. The time taken for good germination (~80%) was noted. Germination was recorded for 100 conidia from four samples per tube on days 3, 5, 7, 10 and 14.

2.2.6.2 Statistical analysis

The growth rate, conidiation quantity and germination were analysed using Analysis of Variance (ANOVA) within GenStat 16 (VSN International Ltd.). The Least Significant Differences of Means (LSD) at a significance level of 5% (p<0.05) were determined for each experiment and Multiple Comparisons

of the treatments of each experiment were carried out using Fisher's Unprotected LSD algorithm (using $p<0.05$).

2.2.7 Basic molecular characterisation

2.2.7.1 UP-PCR profiles (Universally Primed-PCR)

UP-PCR is a PCR fingerprinting technique similar to the randomly amplified polymorphic DNA (RAPD) method (Bulat et al., 1998). This technique can amplify DNA without previous knowledge of the organisms DNA sequence and generate multiple banding profiles following gel electrophoresis. These primers are short, random sequences known to be highly repetitive in fungi, which allows for a strain specific "fingerprint" to be created (Lubeck et al., 1996) to see if any large scale genetic changes are present between different strains.

Genomic DNA was extracted from all of the selected strains listed in Table 2.1 and the respective regenerants produced from each parent as described in section 2.1. Single primer amplifications were performed using 11 UP-PCR primers (Table 2.2) and PCR conditions as described in Lubeck et al. (1996) except that the denaturation temperature of 95°C was used instead of 94°C. PCR products for each primer were separated in a 2% agarose gel electrophoresis in borate/NaOH buffer (0.4 g NaOH, 3.09 g Boric acid per litre of H_2O, adjusted to pH 8.5 with 1 M Boric acid or 5 M NaOH). Each gel was run at 200 v for 1 h. The entire experiment was repeated once.

Table 2.2 UP-PCR primers and their respective annealing temperatures (Lubeck et al., 1996).

Primer	Sequence 5'-3'	Annealing temperature (°C)
Fok1	GGATGACCCACCTCCTAC	52
AS4	TGTGGGCGCTCGACAC	50
L21	GGATCCGAGGGTGGCGGTTCT	55
0.3-1	CGAGAACGACGGTTCT	50
AA2M2	GAGCGACCCAGAGCGG	50
3-2	TAAGGGCGGTGCCAGT	50
L15	GAGGGTGGCGGTTCT	52
AS15	GGCTAAGCGGTCGTTAC	52
AS15/inv	CATTGCTGGCGAATCGG	52
L15/AS19	GAGGGTGGCGGCTAG	52
L45	GTAAAACGACGGCCAGT	51

2.3 Results

2.3.1 Fungal identification

Trichoderma strains were identified based on their tef1*α* sequences and their relationship to previously identified *Trichoderma* species within a phylogenetic tree generated by MAFFT (version 7.309) (Katoh and Standley, 2016). *Trichoderma tef1*α sequences (approximately 500 sequences) were obtained from within our research group.

2.3.2 Pre-screening for naturally occurring sensitivity to pesticides

The sensitivity to the selected pesticides were determined for all strains. Growth of the colonies in the presence of the pesticides on RM was observed after 5-7 d.

2.3.2.1 Copper sulphate ($CuSO_4.5H_2O$)

The *Trichoderma* strains had slightly varying absolute kill points against copper. They ranged from 2 mM to 4 mM (Table 2.3). The concentration used for the conidial suspensions was the amount of copper that was added to amended pesticide media for protoplast regeneration/fusion. Figure 2.1 is an example of the inhibitory effects of copper against a selected *Trichoderma* strain (FCC237 [*T.* sp. "*atroviride* B"]). The concentration used for the amended plates for the selection of protoplast was 4 mM $CuSO_4.5H_2O$.

2.3.2.2 Flint® (500 g/kg trifloxystrobin)

The selected *Trichoderma* strains showed high tolerance to the trifloxystrobin fungicide, Flint® across all concentrations that were tested. Therefore, another fungicide (Chief®) was chosen for the second selective marker for the protoplast fusion experiments.

2.3.2.3 Chief® (500 g/L carbendazim)

All nine of the *Trichoderma* strains had the same absolute kill point of 1 µg/mL for the fungicide Chief® (Table 2.3). As above, this concentration for conidial suspensions was used in the amended pesticide media for the selection and screening of the protoplasts (Table 2.3).

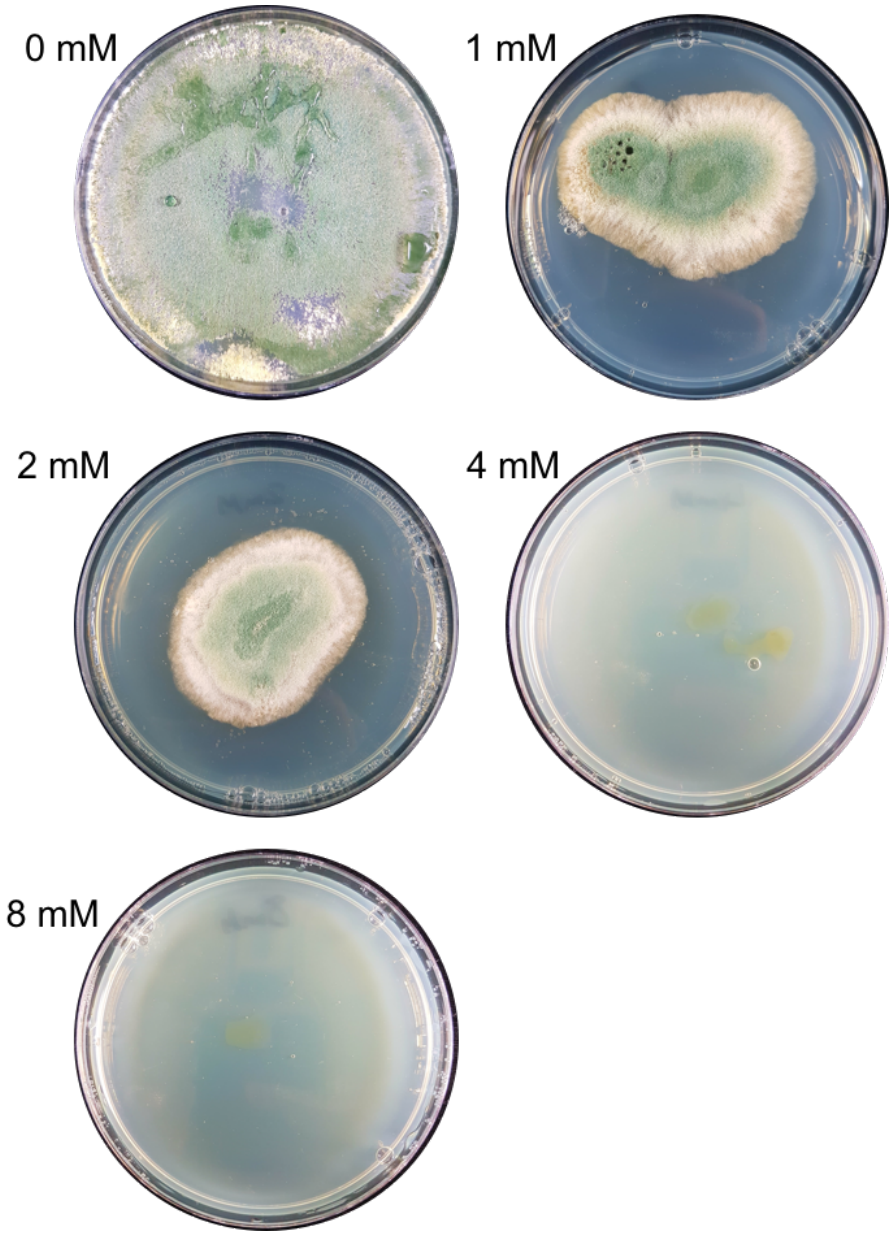

Figure 2.1 **Inhibitory effect on growth of *Trichoderma* sp. "*atroviride* B" (FCC237) on varying concentrations of copper sulphate ($CuSO_4.5H_2O$) amended recovery media agar after 7 d growth.**

Table 2.3 Absolute kill points for the *Trichoderma* strains against copper sulphate ($CuSO_4.5H_2O$) and Chief® (500 g/L carbendazim) for both mycelial plugs and conidial suspensions on recovery medium.

Strain	*Trichoderma* species	Copper (mycelial plug)	Copper (conidia)	Chief® (mycelial plug)	Chief® (conidia)
LU297	*T. trixiae*	4 mM	4 mM	1 µg/mL	1 µg/mL
LU668	*T.* sp. *"atroviride* B"	3 mM	4 mM	1 µg/mL	1 µg/mL
LU753	*T.* sp. novel LU753	2 mM	4 mM	1 µg/mL	1 µg/mL
FCC207	*T. hamatum*	2 mM	3 mM	1 µg/mL	1 µg/mL
FCC237	*T.* sp. *"atroviride* B"	4 mM	4 mM	1 µg/mL	1 µg/mL
FCC261	*T. harzianum sensu stricto*	2 mM	4 mM	1 µg/mL	1 µg/mL
FCC270	*T.* sp. novel FCC270	3 mM	4 mM	1 µg/mL	1 µg/mL
FCC273	*T.* sp. *"atroviride* B"	4 mM	4 mM	1 µg/mL	1 µg/mL
FCC456	*T.* sp. *"atroviride* B"	4 mM	4 mM	1 µg/mL	1 µg/mL

2.3.3 Preparation of protoplasts and optimisation

The optimal conditions for generating protoplasts from each strain were determined in a series of pilot experiments which determined the length of incubation time required for germlings to form and the length of time that the mycelium was left in the enzymatic lysing buffer for the digestion step. It varied between each strain, with the incubation time required for the germlings to form being the more important step out of the two. The different osmotic stabilisers also had an effect on the protoplast yield (Table 2.4) with the mannitol osmoticum/cellophane method producing a higher yield of protoplasts suitable for downstream applications.

Protoplast regenerants separately tolerant to copper (eleven) and Chief® (nine) at the absolute kill point values were produced from the selected *Trichoderma* strains. Figure 2.2 shows a selection of the protoplast regenerants that were produced. There were differences in the numbers of protoplasts produced for each. The recovery rates varied from 0.09% to 1% on copper and 0.1% to 0.7% on Chief® (Table 2.5). In contrast, exposing non-protoplast (parent) conidia to amended agar plates only yielded a colony recovery rate of 0.00041% for copper and the colonies either grew abnormally or did not sporulate, and no colonies appeared on the Chief® amended plates. Mycelium was also exposed to the amended agar plates and did not grow on both pesticides (data not shown).

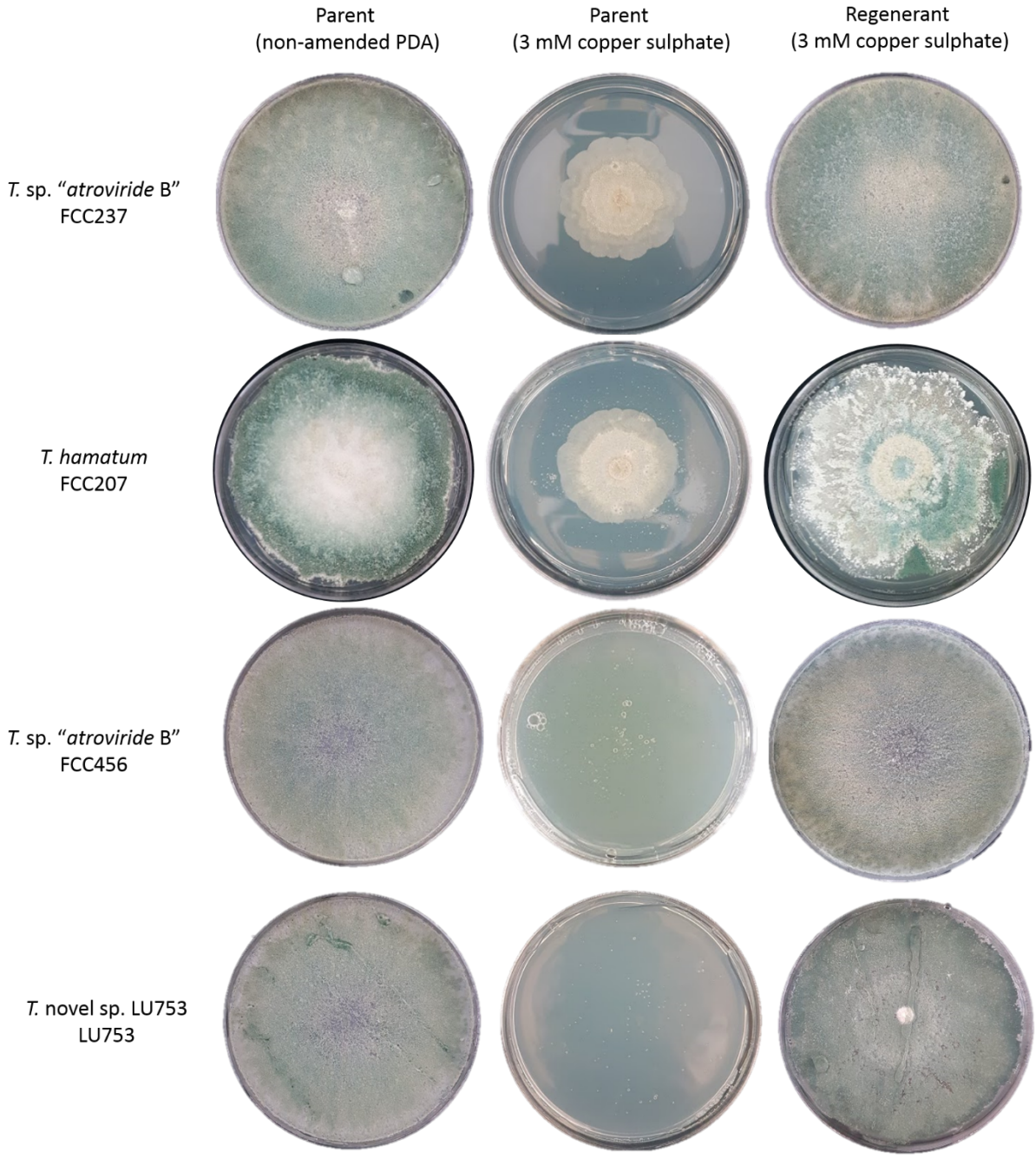

Figure 2.2 **A selection of protolast regenerants that were produced tolerant to copper sulphate ($CuSO_4.5H_2O$). The tolerance is shown on 3 mM of copper sulphate compared to their respective parental strain.**

Table 2.4 Effect of different osmotic stabilisers and methodologies on yield of protoplasts for a selection of *Trichoderma* strains (both parent [WT] and regenerants).

Strain	*Trichoderma* species	Protoplast yield/mL	
		OM buffer[1]	Mannitol osmoticum[2]
LU753 (WT)	*T.* novel sp. LU753	4.87×10^8	3.22×10^9
FCC207 (WT)	*T. hamatum*	7.54×10^7	8.19×10^9
FCC237 (WT)	*T.* sp. "*atroviride* B"	8.19×10^8	8.21×10^9
FCC273 (WT)	*T.* sp. "*atroviride* B"	4.0×10^8	1.63×10^9
FCC456 (WT)	*T.* sp. "*atroviride* B"	6.68×10^8	7.12×10^8
FCC456/R3 (Cu)[3]	*T.* sp. "*atroviride* B"	5.1×10^7	3.98×10^8
FCC273/R13 (Cu) [3]	*T.* sp. "*atroviride* B"	4.97×10^8	6.34×10^8
FCC207/R9 (Chief®)[4]	*T. hamatum*	8.2×10^7	1.2×10^8
FCC237/R5 (Cu) [3]	*T.* sp. "*atroviride* B"	9.15×10^7	4.15×10^8
LU753/R19 (Chief®)[4]	*T.* novel sp. LU753	6.0×10^8	5.87×10^8
LU297/R2 (Chief®)[4]	*T.* sp. "*atroviride* B"	4.32×10^7	7.26×10^7

[1] based on the protoplast isolation method 1 (section 2.2.3.1)
[2] based on the protoplast isolation method 2 (section 2.2.3.2)
[3] regenerant tolerant to copper
[4] regenerant tolerant to Chief®

Table 2.5 Rate of protoplast regeneration from selected *Trichoderma* strains on pesticide amended media: copper sulphate ($CuSO_4.5H_2O$) and Chief® (500 g/L carbendazim).

Strain	*Trichoderma* species	Rate of regeneration on copper	Rate of regeneration on Chief®
LU297	*T. trixiae*	0.41%	0.1%
LU668	*T.* sp. "*atroviride* B"	0.75%	0.68%
LU753	*T.* sp. novel LU753	0.17%	0.74%
FCC207	*T. hamatum*	1%	0.7%
FCC237	*T.* sp. "*atroviride* B"	0.09%	0.25%
FCC261	*T. harzianum sensu stricto*	0.24%	0.3%
FCC270	*T.* sp. novel FCC270	0.45%	0.41%
FCC273	*T.* sp. "*atroviride* B"	0.36%	0.12%
FCC456	*T.* sp. "*atroviride* B"	0.72%	0.35%

2.3.4 Production of protoplast fusants

After multiple protoplast fusion rounds, no stable fusants could be produced. The rate of putative fusants being produced between the various regenerants varied between 0.0002% and 0.009% which is significantly lower than previous reports. This rate of fusion was based on colonies appearing on the double amended media (copper and carbendazim). Any fusants produced lost their stability on the

double amended media after three rounds of single spore selection suggesting that they were unstable heterokaryons and that no nuclear fusion had occurred.

Based upon the low fusant rate, it was hypothesised that there may have been an interactive toxicity effect of having both copper and carbendazim present in the agar medium. Using sub-lethal concentrations of copper and Chief®, it was demonstrated that the combination in agar was toxic to both the parental strains and the regenerants that were produced. They were able to tolerate these pesticide concentrations as a single pesticide amendment (data not shown) but not together.

2.3.5 Phenotypic characterisation- growth rate, conidiation quantity and conidial germination

Comparisons were done to assess the extent of phenotypic differences between the selected parent and regenerant strains. Across both regenerants, there were no statistically significant differences in growth rate compared with the parental strain (Table 2.6 and Table 2.7). For the conidia parameters, only the strain selected for the 'omics characterisation was selected (*T*. sp. "*atroviride* B" FCC237/R5). Again there were no significant differences in either conidial quantity or germination rates between the parent and regenerant (Table 2.8 and Table 2.9). In the beginning of the conidial germination experiment there was a significant difference between the two strains, with the regenerant showing a higher level of conidial germination (p<0.05). However, this only occurred in the first two days of measurements (d 3 and d 5) and the increase in germination percentage did not correlate with the amount of conidia that was produced or the growth rate.

Table 2.6 Average growth rate (mm/d) of *Trichoderma* sp. "*atroviride* B" FCC237 (parent) and *Trichoderma* sp. "*atroviride* B" FCC237/R5 (copper tolerant regenerant) on either PDA or MEA.

Experiment number	Medium	Strain (mm/d)		LSD
		FCC237	FCC237/R5	
1	PDA	18.08	18.14	0.37
2	PDA	17.23	17.48	0.39
3	MEA	17.32	17.51	0.5
4	MEA	17.55	17.7	0.51

Table 2.7 **Average growth rate (mm/d) of *Trichoderma hamatum* FCC207 (parent) and *Trichoderma hamatum* FCC207/R9 (carbendazim tolerant regenerant) on either PDA or MEA.**

Experiment number	Medium	Strain (mm/d)		LSD
		FCC207	FCC207/R9	
1	PDA	18.25	18.4	0.35
2	PDA	18.11	18.27	0.32
3	MEA	17.99	18.06	0.28
4	MEA	17.84	17.96	0.32

Table 2.8 **Conidia quantity (measured as conidia/mL) of *Trichoderma* sp. "*atroviride* B" FCC237 (parent) and *Trichoderma* sp. "*atroviride* B" FCC237/R5 (copper tolerant regenerant). There was no statistical difference and the data represents the average of two experiments.**

Strain	Day				
	3	5	7	10	14
FCC237	2.38×10^4	5.48×10^6	8.21×10^8	2.11×10^9	3.45×10^9
FCC237/R5	3.55×10^4	6.1×10^6	7.99×10^8	3.61×10^9	3.87×10^9

Table 2.9 **Conidia germination percentage of *Trichoderma* sp. "*atroviride* B" FCC237 (parent) and *Trichoderma* sp. "*atroviride* B" FCC237/R5 (copper tolerant regenerant).**

Experiment number	Strain	Day				
		3	5	7	10	14
1	FCC237	69.3*	77.4*	91.3	87.9	95.4
	FCC237/R5	77.6*	82.1*	94.5	93.6	95.1
LSD:		5.77	4.14	5.77	7.34	3.57
2	FCC237	67.1*	78.4	92.8	92.5	94.6
	FCC237/R5	80.3*	80.4	93.1	94	94.3
LSD:		6.87	5.79	4.55	3.65	3.45

* represents significantly different values (p<0.05) between the two strains on that particular day/experiment (as indicated).

2.3.6 Basic molecular characterisation: UP-PCR profiles (Universally Primed-PCR)

From the 11 UP-PCR primers that were trialled (Table 2.2), the L15/AS19 primer amplified a PCR product from all of the original strains and respective regenerants. The other primers would only amplify some strains, making them unsuitable as a tool to compare between the strains. The results from the UP-PCR using primer L15/AS19 showed that there was no large-scale genomic differences between any of the parental strains and their respective regenerants (Figure 2.3).

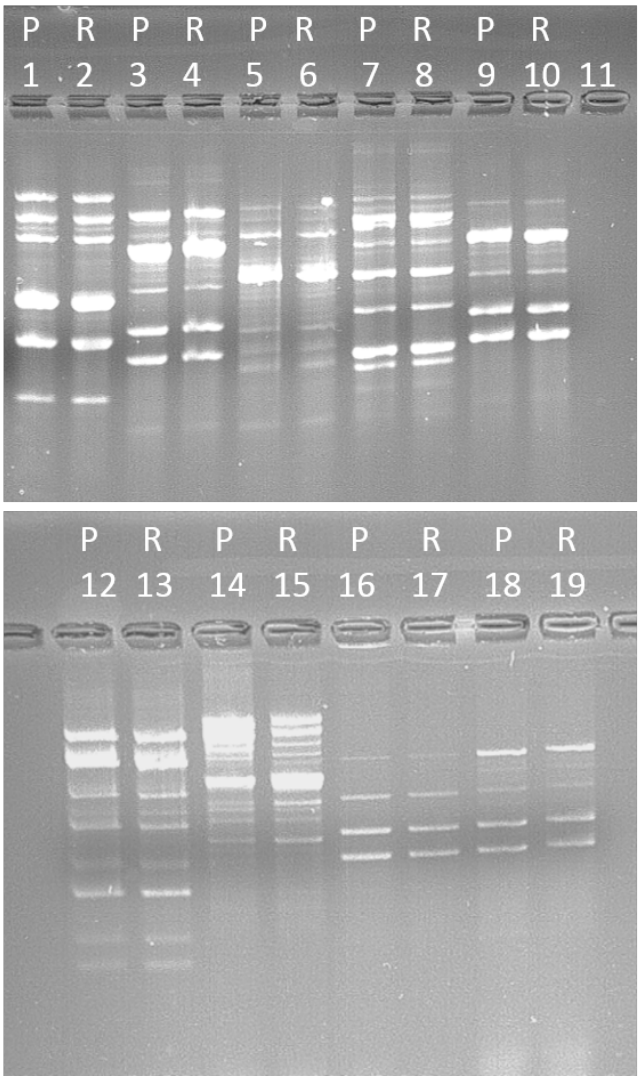

Figure 2.3 **UP-PCR, using primer L15/AS19, of selected *Trichoderma* parental strains (P) and the respective regenerants (R) separated on a 2% agarose gel electrophoresis in borate/NaOH. (1) LU297 *T. trixiae,* (2) LU297/R2 *T. trixiae,* (3) LU668 *T.* sp. *"atroviride* B", (4) LU668/R *T.* sp. *"atroviride* B", (5) LU753 *T.* sp. novel LU753, (6) LU753/R19 *T.* sp. novel LU753, (7) FCC207 *T. hamatum,* (8) FCC207/R9 *T. hamatum,* (9) FCC237 *T.* sp. *"atroviride* B", (10) FCC237/R5 *T.* sp. *"atroviride* B", (11) negative control (12) FCC261 *T. harzianum,* (13) FCC261/R16 *T. harzianum,* (14) FCC270 *T.* sp. novel FCC270, (15) FCC270/R7 *T.* sp. novel FCC270, (16) FCC273 *T.* sp. *"atroviride* B" (17) FCC273/R13 *T.* sp. *"atroviride* B" (18) FCC456 *T.* sp. *"atroviride* B", (19) FCC456/R3 *T.* sp. *"atroviride* B". P= parent, R=regenerant.**

2.4 Discussion

Protoplast regeneration is an effective tool that can be used for strain improvement. This can lead to strains with improved characteristics more suited to the incorporation into an IPM programme. In this study, various strains of *Trichoderma* that showed bioactivity potential against Psa in kiwifruit orchards were used to produce protoplast regenerants that were tolerant to pesticides used in these orchards. The use of protoplast fusion (both intra-strain and inter-strain) is a common technique used to enhance biocontrol agents, however it has been have found that regenerating protoplasts on selective media enables selection for rare genetic variants at a rate that far exceeds that within the parental population. This highlights the potential for the usage of protoplast regeneration in place of traditional mutant forming methods such as UV or chemical mutagenesis.

Previously some researchers have described such progeny as arising from self-fusion (intra-strain). However, when only one parental strain is present, it is not possible to definitively state that the selected progenies were the result of any fusion event. Previous studies where protoplast technologies have been used to select or modify varying *Trichoderma* strains have not always offered proof of these changes at a molecular level. Prabavathy et al. (2006a) reported that regenerated protoplasts from a single *T. reesei* strain were mixed with the PEG solution (for self-fusion) and pairs of protoplasts were subsequently observed. They then stated the nuclei of the pairing protoplasts had fused together from having observed the two cells near to one another (Prabavathy et al., 2006a). Another study used intra-strain fusion to develop progeny from a single strain of *T. harzianum* to enhance the level of production of chitinase and the antagonistic potential against *Rhizoctonia solani*. Fifteen of these progeny were selected for further testing, and both the chitinase and antagonistic activity against pathogens had substantially increased (Prabavathy et al., 2006b). The authors postulated that this was the result of self-fusion, however no evidence of self-fusion was provided for this strain so the exact mechanism has not yet been identified. However, Sharma et al. (2016) showed that there were novel fragments between the progeny in the RAPD profiles of self-fused *T. harzianum* fusants. This highlights the importance of some form of molecular characterisation to prove that intra-strain fusion has occurred.

After multiple protoplast fusion rounds, a stable fusant was unable to be produced. The putative fusion rate between the various regenerants varied between 0.0002% and 0.009% which is significantly lower than previously reported. For example, previous fusion rates with our research group on other *Trichoderma* strains were ~0.036% (unpublished data) and other studies have reported a fusion rate of up to 6.2% between *T. harzianum* and *T. viride* (Balasubramanian and Lalithakumari, 2008). Furthermore, any fusants produced lost their stability on the double amended media after three rounds of single spore selection. Previous studies producing protoplast fusants have encountered similar problems, in which some protoplast progeny form as the result of heterokaryosis or temporary

cytoplasmic fusion formation and lose their selection through successive cycles of mitotic division during mycelial growth (Hassan et al., 2011; Stasz et al., 1988; Stasz and Harman, 1990). Fungi are well known for having unstable genomes and even fungi undergoing purely asexual reproduction can produce offspring with different sized chromosomes over a few generations (Davière et al., 2001; Strom and Bushley, 2016). Genetic instability of intraspecific and interspecific hybrids formed through protoplast fusion is a commonly reported problem (Anné, 1982; Stasz and Harman, 1990; Wang et al., 2010).

Additionally stable heterokaryon formation can be rare due to the issues of heterokaryon or vegetative incompatibility, which is responsible for preventing the formation of these stable heterokaryons through expression of heterokaryon incompatibility genes (*het*) (Daskalov et al., 2017; Strom and Bushley, 2016). If two incompatible nuclei occupy the same cell, the expression of these *het* genes leads to the eventual death of the heterokaryotic cell. Hassan et al. (2011) also reported loss of double pesticide fungicide tolerance after successive subculturing in *Trichoderma* fusants. They determined the genetic stability of their double fungicide tolerant strains by their ability to maintain tolerance to both fungicides after subculturing three times in the absence of fungicide. Five out of the seven fusants they produced retained the double pesticide tolerance. This raises a notable difference in the production of fusants from other studies compared to this present one, that the parental strains used were either wild type fungi or mutants that were produced via UV-mutagenesis, not tolerant regenerated protoplasts. The unknown mechanism behind the phenotypic plasticity and remodelling that is observed from protoplast regeneration may be responsible for the incompatibility that was seen in the attempt to fuse these strains.

Due to the problems that were encountered with the low rate of fusion, it was postulated that there may be a potential interactive toxicity effect of the double amended pesticide media (between copper sulphate and the carbendazim of Chief®) on the strains tested. This was confirmed by the inability of parental strains to grow on combined media with sub-lethal amounts of the pesticides. The same result was obtained when pure carbendazim (rather than the commercial fungicide) was used. This is in contrast to a strain of *T. longibrachiatum* that was fused by Lalithakumari et al. (1996) which was found to be tolerant to 200 mmol/L copper sulphate and 10 µmol/L carbendazim. They used protoplast fusion to combine a *T. harzianum* strain that had a high biocontrol potential and the highly tolerant *T. longibrachiatum* that was mentioned above (Lalithakumari et al., 1996).

The results from this study raise some interesting questions with regards to the interactive effect of chemicals in nature, due to the fact that chemicals almost never occur in nature as a single solution, but as complex mixtures or part of a spray programme (Komárek et al., 2010; Kungolos et al., 2009). For kiwifruit alone, according to the 2018/2019 New Zealand NovaChem Agrichemical Manual

(https://www.novachem.co.nz/; last accessed 23.4.18) over 98 pesticide and herbicides are recommended for the protection of kiwifruit from pests (including fungi, bacteria and insects) and weeds. Numerous studies have shown that some interactions between pesticides influence both their behaviour in the soil and their toxicity (Kungolos et al., 2009; Schuster and Schroeder, 1990; Tsiridis et al., 2006; Zhang et al., 2003). Zhang et al. (2003) showed that the IC_{50} toxicity level (half minimal inhibitory concentration of a substance) of three agrochemicals that they tested (acetochlor, methamidophos and copper) under combinations were much lower that the individual IC_{50} values against overall indigenous microorganism populations in soil. Moreover, different toxicological tests on various bacterial species have shown that common environmental concentrations of copper based fungicides can pose a risk for other non-target organisms (Kungolos et al., 2009). Combining these chemicals may result in unexpected toxicity towards soil microbes, in particular beneficial ones.

Further studies within our lab group are underway investigating the impact of intensive spraying regimes on the microbial communities within kiwifruit orchards, focusing particularly on *Trichoderma* populations. Soil was collected from seven sites around the Nelson and Bay of Plenty kiwifruit growing regions and the copper levels within these soils were tested (Christine Stark, pers. comm.). While at elevated levels (over 500 ppm) copper can become toxic most of the tested orchards had copper levels around 100 ppm. In contrast, the base level of selection for protoplasting (being also the cessation level of growth of the parents) was approximately 1000 ppm (4 mM). Although the level of copper toxicity may not be an issue for soil fungal communities currently, the regenerants that are copper tolerant could be used alongside copper sprays in an IPM programme within the same time frame when the levels are temporarily high during copper application unlike Kiwivax™ which cannot be used within three days of applying foliar coppers.

The production and isolation of protoplasts is a crucial step in strain enhancement of *Trichoderma* and other filamentous fungi that do not have an obvious sexual stage. The results presented here show that a significant increase in protoplast recovery is possible with the optimisation of each strain. Numerous studies have shown the importance of optimisation for the formation and regeneration of protoplasts, each with different recommendations. Tschen and Li (1994) highlighted the significance between species with differences in both the isolation of protoplasts and the regeneration frequency from two *Trichoderma* (*T. koningii* and *T. harzianum*) varying greatly. This most likely is dependent on the structural properties of the fungal cell wall as this can vary between species. They looked at eight different factors affecting protoplast formation: lytic enzymes, concentration of Novozym 234, culture age, concentration of mycelium, temperature used for lytic digestion, pH, osmotic stabiliser and incubation time in osmotic stabiliser and consequently gave a general recommendation that they suggested for all *Trichoderma* strains. This current study has found the isolation of protoplasts to be highly strain specific, with previous work within our group showing substantial differences in the

resistance of various strains to protoplasting techniques. Of four *T*. sp. "*atroviride* B" strains, the number of protoplasts that were produced varied from 5.1 x 10^7 protoplasts/mL to 8.19 x 10^9 protoplasts/mL and the methodology needed to be slightly modified for each strain. Strain-specificity has also been observed for *T. viride* and *T. harzianum*, with research having shown different optimisation methods varyingly greatly for the same species. For example, the release in protoplasts from different culture ages for the same species (between studies) varied. For *T. viride*, the optimal time for mycelial formation is between 14-18 h, and for *T. harzianum* that same figure varies from 16-24 h (Balasubramanian and Lalithakumari, 2008; Mrinalini and Lalithakumari, 1998). Together these results highlight that significant optimisation of protoplast methodology for each strain is essential.

Despite the frequent use of protoplast technology for strain enhancement in both the biotechnology industry and for biocontrol agents, very little is known of the underlying genetic consequences and the potential effects downstream. Further research is needed to understand the full extent of these changes. The phenotypic plasticity and remodelling that is induced in the production of protoplasts is beneficial for potential strain enhancement as seen in this study. One possible explanation for the protoplast-induced phenotypic plasticity is methylation as previously mentioned. The UP-PCR patterns were identical between both the parental strains and the respective progeny suggesting no major DNA rearrangements had occurred. Previous work within our group on other protoplast progeny using Methylation-Sensitive-AFLPs (MSAP) analysis detected remodelling of the methylation profile, suggesting that gene expression through methylation changes could be the cause of the enhanced phenotypic plasticity observed in the regenerant variants produced. Further chapters within this thesis attempt to characterise the influence of methylation changes in protoplast-induced phenotypic plasticity.

2.5 Conclusion

These results show that the use of protoplast regeneration is a very effective tool to screen and select for rare desirable traits within an already successful biocontrol agent, with protoplast progeny tolerant to current control pesticides being effectively achieved. This has the potential to lead to the incorporation of these biocontrol agents into a commercial IPM programme. Additionally, these results using protoplast regeneration for strain improvement also raise the important question of what is the source of this variation during regeneration in the absence of fusion?

Chapter 3

Bioactivity of selected *Trichoderma* sp. "*atroviride* B" parental and protoplast regenerant strains against *Pseudomonas syringae* pv. *actinidae*

3.1 Introduction

Pseudomonas syringae pv. *actinidae* (Psa) is a gram negative bacterium that causes bacterial canker on a variety of kiwifruit species, including the economically important *Actinidia chinensis* (gold fleshed kiwifruit, cv. Hort16A) and *A. deliciosa* (green fleshed kiwifruit, cv. Hayward) (Scortichini et al., 2012; Vanneste, 2017). The symptoms of this disease include brown-black leaf spots with chlorotic halos, extensive twig die-back, blossom necrosis and bleeding cankers along the main trunk which produce red coloured exudates, eventually leading to vine decline and death (Scortichini et al., 2012; Vanneste, 2017).

Since the outbreak of the disease in New Zealand in November 2010, research has focused on developing efficient strategies for minimising both the spread of the pathogen and the economic loss to the kiwifruit industry and growers. Potential chemical and biocontrol options, alongside strict orchard management practices and breeding resistant varieties, are all being used in this effort (Cameron and Sarojini, 2014). Currently, chemical control of Psa in the field is highly dependent on the multiple spraying of two main bactericides: copper compounds and streptomycin (Vanneste, 2017). However resistance to both copper compounds and streptomycin can occur within this bacterium (Goto et al., 1994; Nakajima and Tadaaki, 2002). In 2014, Psa strains within New Zealand that were resistant to copper sulphate began to appear (Colombi et al., 2017). At the beginning of the New Zealand outbreak, the single strain responsible for the outbreak was sensitive to copper. However a recent study has shown that within a sample of isolates, taken in 2015 and 2016, a quarter were now copper resistant (Colombi et al., 2017). Alongside the bactericide resistance that is emerging, the primary strategy of streptomycin and copper compounds could potentially present further issues with phytotoxicity and residues in fruit (Cameron and Sarojini, 2014). One potential option is the integration of these traditional approaches with biocontrol at crucial growing times during the season.

The biocontrol ability of *Trichoderma* species against plant pathogens has been extensively studied over the past 80 years. They have long been recognised as potential biocontrol agents and for their ability to increase plant growth and development (Harman et al., 2004a) and for the control of a wide

range of plant pathogens such as *Botrytis* (Card et al., 2009), *Sclerotium* (McLean and Stewart, 2000), *Rhizoctonia* (Sarrocco et al., 2009) and *Pythium* (Monte, 2010).

Protoplast technology has been used to screen and select desirable traits from various parental strains to improve biocontrol ability within *Trichoderma* strains as well as other filamentous fungi (Braithwaite et al., 2013; Harman, 2000; Kandula et al., 2012). Based on the proven success of *Trichoderma* being used as a biocontrol agent, work within our group has identified a combination of *Trichoderma* strains that are active against Psa (Kiwivax™ (Agrimm Technology, New Zealand)). Building on this, pesticide tolerant variants of these same Psa active *Trichoderma* strains were able to be produced via protoplast regeneration which would be ready to be integrated into an IPM programme. However, the exact mechanism by which these modifications are induced is unknown and other changes not tested may have occurred. Therefore it is imperative to assess the biocontrol potential of these protoplast progeny to ensure there has been no reduction. This chapter aimed to test a selection of the protoplast regenerants that were produced in Chapter 2, to ensure the bioactivity against Psa has not been lost.

3.2 Materials and Methods

In planta bioactivity of the protoplast progeny

An in-house bioassay developed by Christine Stark and Robert Hill (Bio-Protection Research Centre, Lincoln) was used for this experiment (Hill et al., 2015), with modifications being made to the disease scoring methodology (Trials 2-3) after reviewing the data from Trial 1. Furthermore the statistical analysis from previous work was also changed.

3.2.2 Trial 1 (June- August 2016)

3.2.1.1 *Trichoderma* inoculum preparation

To generate *Trichoderma* inoculum for the bioactivity bioassay, three PDA plates per strain (see Table 3.1 for strains used) were inoculated separately with a 2 µL conidial suspension, spread over the plate with 100 µL sterile distilled water (SDW) and incubated at 23°C under a 12/12 h light/dark cycle for 10 d. Conidia were harvested by flooding the plates with 5 mL of SDW and the conidia were scrapped into suspension and filtered through a double layer of Miracloth. The conidial concentration was determined by haemocytometer counts and each *Trichoderma* treatment adjusted to a final concentration of 1 x 10^6 spores/mL for inoculation of the kiwifruit seedlings.

Table 3.1 Selected *Trichoderma* strains used as treatments over the three Psa bioactivity trials. Species listed in the table as follows: LU753: *Trichoderma* sp. novel LU753, FCC207: *Trichoderma hamatum,* FCC237, FCC456: *Trichoderma* sp. *"atroviride* B". /R# indicates regenerant.

Trial 1 (June- August 2016)	Trial 2 (March- July 2017)	Trial 3 (April- August 2017)
D13 (LU753 + FCC207)	FCC237	FCC237
FCC237	FCC237 + FCC207	FCC237 + FCC207
FCC237 + FCC207	FCC237/R5	FCC237/R5
FCC237/R5	FCC237/R5 + FCC207	FCC237/R5 + FCC207
FCC237/R5 + FCC207	FCC456	FCC456
FCC456	FCC456 + FCC207	FCC456 + FCC207
FCC207/R2	FCC456/R4	FCC456/R4
Kiwivax™	FCC456/R4 + FCC207	FCC456/R4 + FCC207
Positive control	FCC207	FCC207
Negative control	FCC207/R2	FCC207/R2
	Kiwivax™	Kiwivax™
	Positive control	Positive control
	Negative control	Negative control

3.2.1.2 Kiwifruit seedlings

Very young seedlings of *A. deliciosa* (green fleshed kiwifruit, cv. Hayward) (provided from Plant and Food Research, Motueka) (approximately 2 true leaf stage) were transplanted into Lincoln University special seed raising mix (50:50 peat: sterilised pumice, 200 g Osmocote extract mini (3-4 months) 16-3/5-9-1, 400 g Dolomite lime, 100 g Hydroflo) into four cell seed raising trays. The following day seedlings were treated with *Trichoderma* (including Kiwivax™) by pipetting 5 mL of the conidial suspension (containing 10^6 conidia/mL) around the stem base. This inoculation density had been chosen based on pot trials with *Pinus radiata* seedlings (Stark et al., 2018). Additionally this concentration has led to consistent results of disease reduction over the approximately 26 bioassay trials that Christine Stark has performed. Kiwivax™ is a commercialised biocontrol product based on a combination of three *Trichoderma* strains (developed by Robert Hill and Christine Stark, Bio-Protection Research Centre) that has a limited label claim to reduce Psa symptoms on kiwifruit. It is applied as root drench through springtime and post-harvest; has been re-isolated from treated kiwifruit vine roots at least 3-4 months after application. Control plants (with no *Trichoderma* treatment) were treated with 5 mL of SDW. The experiment was organised into a randomised block design to help reduce variability by strain treatment, with 10 replicates per treatment, each represented in 10 blocks (for treatment strains see Table 3.1). The plants were watered lightly and covered with a plastic sheet in the glasshouse (Nursery Greenhouse Centre, Lincoln University). The seedling raising trays were placed on heating pads and kept at 18-20°C, with 16 h of light. The average daily temperature fluctuated between 15.5 and 22.1°C, with an average temperature of 17.3°C. The seedlings were grown

in the glasshouse and moved into the Biotron (a PC2 plant growth containment facility, Lincoln University https://bioprotection.org.nz/Facilities/?sti=1) after approximately 10 weeks. The four cell seedling trays were also cut into individual seedling cells for the remainder of the experiment.

3.2.1.3 Psa inoculum preparation and inoculation of the kiwifruit

The Psa strain (*Pseudomonas syringae* pv. *atinidiae* strain 10627) was supplied by Plant and Food Research (Te Puke) and was stored at -80°C in 15% glycerol. This strain was used for all trials in this study. This strain belongs to the Psa biovar 3 (haplotype NZ-V; Psa-V) and is known to be pathogenic in potted kiwifruit seedling trials. Psa was plated onto Nutrient Sucrose Agar (NSA) (10 g sucrose, 10 g bacterial peptone, 14 g agar per L) and incubated at 25°C in complete darkness for 48 h. The colonies of Psa were harvested by flooding the plates with 10 mL of SDW and were scrapping into suspension with a sterile loop. The suspension was transferred into a sterile universal and the bacterial concentration was determined spectrophometrically (Genesys 10S UV-Vis, Thermo Scientific). Concentrations were adjusted to 6.1 x 10^8 CFU/mL with SDW (optical density at 600 nm=0.47 is equivalent; Tony Reglinski, pers. comm.) then diluted to the inoculation rate of 1 x 10^7 CFU/mL with SDW. In addition, dilution plates from the final concentration were plated on NSA and incubated at 25°C in complete darkness. After 3 d, the plates were counted to confirm the inoculum concentration (CFU/mL) (data not shown).

All kiwifruit plants (apart from the negative control group) were challenged with Psa via stem stab inoculation in a climate controlled growth room in the Biotron (18°C day/15°C night, 65% RH, 16 h photoperiod). The age that the kiwifruit seedlings were inoculated is based on the development of the seedlings. They need to have around four nodes as Psa is inoculated between the second and third node on the seedling. A sterile wooden toothpick was dipped into a 2 mL microcentrifuge tube containing the Psa inoculum and was angled at 45° in relation to the seedling stem between the nodes. The toothpick was pushed in just enough to penetrate the stem. The negative control group was inoculated with sterile water. Each large plastic container (82 L) held seven individual seedling tray cells that were standing on a petri dish lid to prevent cross contamination within the plastic containers. The same randomised block design was carried over from the greenhouse. Plants were watered as required and grown for four weeks in the Biotron.

3.2.1.4 Disease assessment

The disease development was assessed after four weeks based on a scoring system developed from Hill et al. (2015) and Hoyte et al. (2013). The symptoms/parameters that were assessed were: plant height (mm), stem lesion size (mm), stem lesion score (a severity scale of 0-3), petiole collapse, petiole blackening, stem tip death, stem collapse and death, with the different symptoms having different weighting to combine for a final disease severity score that was between 0 and 6 (Table 3.2).

Table 3.2 Disease scoring assessment for Psa symptoms on kiwifruit seedlings after four weeks growth post inoculation with Psa used in Trial 1.

Weight (%)[1]	Parameter	Scoring	Description
N/A	Plant height	Measured in mm	N/A
N/A	Stem lesion length	Measured in mm	Length of stem lesion wound measured in mm
40	Stem lesion length %	Length of the lesion/height of the plant	Represented as a percentage of the length of the lesion/height of the plant
30	Stem lesion score	Subjective score	(0) Lesion only, water soaking only; (1) lesion black/stem blackening starting; (2) severe blackening of most of the stem; (3) black stem all around and dry
N/A	Leaf wilt	Yes/no	Recorded but too variable on its own to include in weighting system
40	Petiole collapse or blackening	Subjective score (blackening only to severe)	None, some, all petioles collapsed; petiole blackening starting at base; petioles clearly black; leaf drop/black veins/severe wilting
40	Leaf spots	Yes/no	Yes/no (only if clearly caused by Psa; usually comes with ooze from leaves)
15	Ooze	Yes/no	N/A
80	Fungal growth on bacterial exudates	Yes/no	Secondary symptom; if yes: point of no return for the plant even if lack of other symptoms
50	Stem tip death	Yes/no	Yes/no
100	Total collapse	Yes/no	Yes/no
100	Death	Yes/no	Yes/no

N/A= not applicable

[1] weight expressed as a percentage (out of 100%), i.e. if a plant had both petiole blackening (40% weighting) and total collapse (100% weighting) it would be automatically scored as 100%.

3.2.1.5 Statistical analysis

The five main parameters (height [mm], stem lesion length [mm], stem lesion percentage [length of the lesion/height of the plant], stem lesion score and the disease severity score) were analysed using Analysis of Variance (ANOVA) within GenStat 16. Contrasts corresponding to questions of interest were specified and included in the ANOVA. The Least Significant Difference of Means (LSD) at a significance level of 5% (p<0.05) were determined for each parameter. Additionally, for this trial 18 plants that were dead or had stem collapse (both symptoms of full blown disease; automatic disease severity score of 6), the lesion length was not assessed and these data were estimated as "missing values" in the ANOVA.

3.2.3 Trial 2 (March- July 2017)

In the following two bioassays, sterile *A. chinensis* (gold fleshed kiwifruit, cv. Hort16A) tissue culture plantlets were used (Multiflora Laboratories Limited, Auckland) due a lack of kiwifruit seedlings available from Plant and Food Research. Although Hort16A is more susceptible to this biovar of Psa than Hayward in field situations, studies have shown that there is very little difference in the susceptibility to infection of young leaves of comparable age (Tyson et al., 2015), making the difference in cultivar used here still comparable.

3.2.2.1 *Trichoderma* inoculum preparation

The *Trichoderma* inoculum was prepared as described above (section 3.2.1.1) with the strains listed in Table 3.1 for Trial 2. Treatment D13 (LU753 and FCC207) was dropped due to space constraints.

3.2.2.2 Kiwifruit seedlings

Very young tissue culture plantlets of *A. chinensis* (Hort16A) (Multiflora Laboratories Limited, Auckland) (approximately one true leaf stage) were transplanted into Lincoln University special seed raising mix into four cell seed raising trays. The following day seedlings were treated with *Trichoderma* (including Kiwivax™) by pipetting 5 mL of the conidial suspension (containing 1 x 10^6 conidia/mL) around the stem base. Control plants (with no *Trichoderma* treatment) were treated with 5 mL of SDW. The experiment was organised into a randomised block design to help reduce variability, with two extra blocks to use in case of seedling death. This was expected as the tissue culture plantlets are less robust than the seedlings used in Trial 1. There were 10 replicates used per treatment, each represented in 12 blocks (10 for the trial with the additional 2 blocks). The plants were watered lightly and covered with a plastic sheet in the glasshouse. The seedling raising trays were placed on heating pads and kept at 18-20°C, with 16 h of light. The average daily temperature fluctuated between 10.3 and 30.3°C, with an average temperature of 17.6°C. The seedlings were grown in the glasshouse and moved into the Biotron after approximately 12 weeks, when they had four nodes. The plants chosen were selected from all 12 blocks based on the height of the kiwifruit seedlings to maintain as much homogeneity as possible in the plant size and growth stage. If a seedling was chosen from the extra two blocks, this seedling replaced the plant from the original block, so the main randomised block design with the orginal ten blocks could be continued into the Biotron.

3.2.2.3 Psa inoculum preparation and inoculation of the kiwifruit

The Psa inoculum preparation and inoculation of the kiwifruit seedlings was as described above (see section 3.2.1.3).

3.2.2.4 Disease assessment

The disease development was assessed after four weeks. After analysing the results from the first trial, the scoring system was changed to help maintain consistency with the reporting of the disease symptoms and the weighting was also removed. Some of the symptoms that contributed to the final disease score were not solely disease symptoms of Psa which could skew the final score. The symptoms/parameters that were assessed were: plant height (mm), stem lesion size (mm), stem lesion percentage and an updated disease scored that ranged from 0-6 (Table 3.3) (see Figure 3.1 for a more detailed explanation of the disease score scale).

Table 3.3 Updated disease scoring assessment for Psa symptoms on kiwifruit seedlings after four weeks growth post inoculation with Psa used for trials 2 and 3.

Parameter	Scoring	Description
Plant height	Measured in mm	N/A
Stem lesion length	Measured in mm	Length of stem lesion wound measured in mm
Stem lesion %	Length of the lesion/height of the plant	Represented as a percentage of the length of the lesion/height of the plant
Disease score	Subjective score (0-6)	(0) No symptoms or discolouration, just base water soaking wound only; (1) light discolouration around wound; (2) darker discolouration around wound/stem blackening starting; (3) further discolouration around the wound, beginning to constrict around wound; (4) completely constricted, brown; (5) disease has moved systemically (past the stem and into the leaves); (6) death/girdled (collapsed entirely)

N/A= not applicable

3.2.2.5 Statistical analysis

The four main parameters (height [mm], stem lesion length [mm], stem lesion percentage [length of the lesion/height of the plant] and the disease severity score) were analysed using ANOVA within GenStat 16. Various contrasts were specified and included in the ANOVA and the LSD at a significance level of 5% (p<0.05) was determined for each parameter.

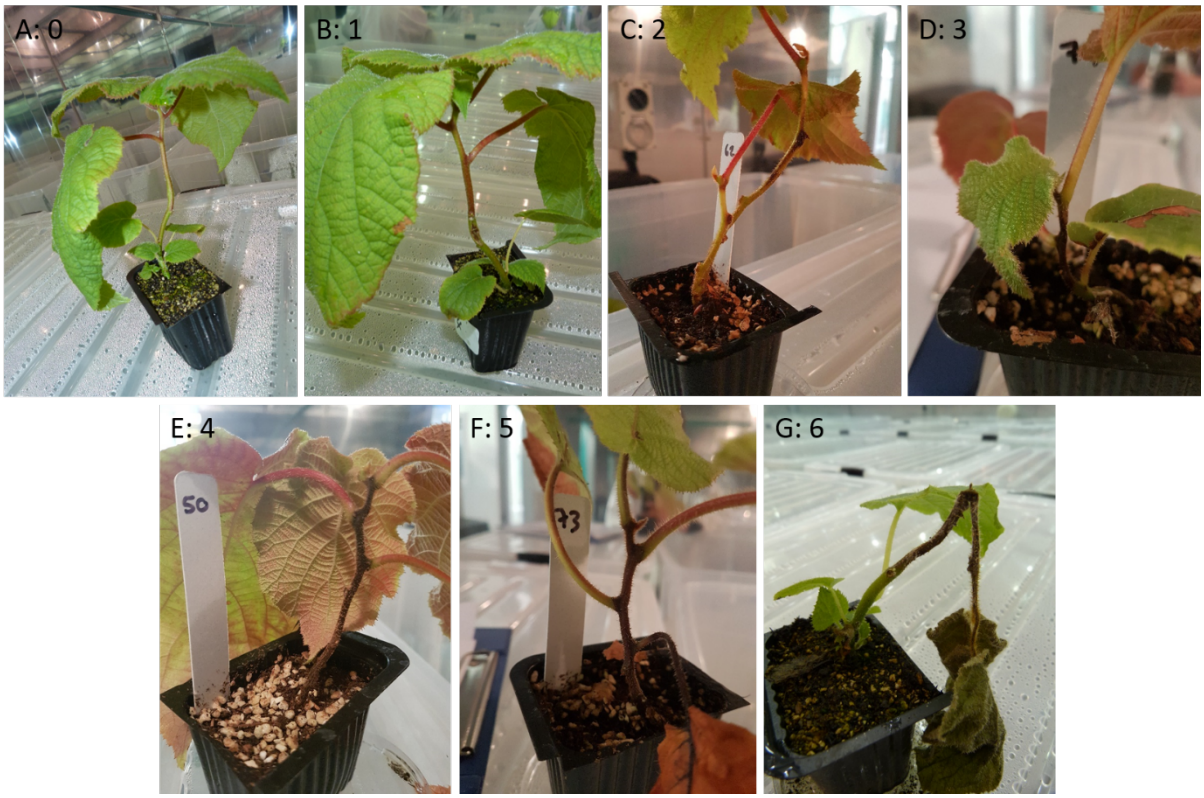

Figure 3.1 **Updated disease scoring assessment of Psa on Hort16A kiwifruit seedlings after four weeks growth post inoculation with Psa. (A) 0-no symptoms or discolouration; (B) 1-light discolouration around wound; (C) 2-darker discolouration around wound/stem blackening starting; (D) 3-further discolouration around the wound, beginning to constrict around wound; (E) 4-completely constricted, brown; (F) 5-disease has moved systemically (past the stem and into the leaves); (G) 6-death/girdled (collapsed entirely).**

3.2.4 Trial 3 (April- August 2017)

Trial 3 was set up as an exact repeat as Trial 2 (see section 3.2.2 for details) with the same treatments (Table 3.1). During this experiment, the average daily temperature fluctuated between 10.3 and 25.6°C, with an average temperature of 17.1°C in the glasshouse. With the only difference in set up being there were no extra lights or heating pads for the kiwifruit in the glasshouse due to space confinements, which led the kiwifruit seedlings to be in the glasshouse for an additional two weeks to ensure size homogeneity of the seedlings. However, even with the additional two weeks the seedlings were smaller than the previous two trials which was visible in the heights recorded. The Psa inoculum preparation, inoculation of the kiwifruit, disease assessment and statistical analysis were as described above.

3.3 Results

For all three trials, the raw measurements, statistics and tables can be viewed in Appendix A.

3.3.1 Trial 1

For Trial 1, the assessment of the biocontrol potential of the protoplast progeny showed three main results (Table 3.4). Firstly, the strains selected for 'omic's analysis (Chapter 4 and 5- FCC237 and FCC237/R5) showed no significant difference in any of the five parameters that were assessed meaning that the biocontrol ability of this strain was not reduced due to protoplasting. Furthermore, the most noticeable positive effect was the addition of FCC207 to both FCC237 and FCC237/R5. Interestingly, when FCC207 was used in combination with the above strains for three of the parameters (the stem lesion percentage, the stem lesion score and the disease severity score), there was a significant reduction in the severity of the scored Psa symptoms (all three parameters $p<0.05$). Due to this observed reduction it was decided that for the remaining trials, the treatment list would be changed to include FCC207 to be used in combination with the original treatments.

Additionally, the high scoring of the negative control in the disease severity score (2.02) was a point of concern. This scoring was likely due to the weighting and combination of the different parameters that were used which included: petiole collapse or blackening, leaf spots, ooze, fungal growth, stem tip death, stem death, stem lesion length and stem lesion score (see section 3.2.1.4/Table 3.2 for the percentages for the weighting). It was decided that some of the parameters that were being measured may not be solely restricted to the symptoms of Psa but more so due to abiotic factors such as water, soil type or nutrient quantity. Comparing the disease score parameter to a more quantitative one related solely to the inoculation such as the stem lesion length made this trend more apparent. The stem lesion length comes from the point of the stem stab inoculation with Psa and the distance from the wound that the blackening has spread, or the respective stem stab inoculation with water that was the case for the negative control. The negative control had a very low score (3 mm) exclusively from the stress that the stem stab inoculation method caused as opposed to the average of the other nine treatments that had been inoculated with Psa (32.2 mm).

Due to this observation from Trial 1, it was decided to change the scoring method to be more quantitative and to follow the spread of the disease within the plant. It is important to note that there is no pathogenicity assay and respective scoring that reflects the whole range of pathogenic capabilities of Psa, as the progression of the disease appears differently depending on the age of the plants and the inoculation method (Vanneste, 2017).

Table 3.4 Disease parameter scores of Hayward kiwifruit seedlings after four weeks post inoculation with Psa for Trial 1.

Treatment		Height (mm)	Stem lesion length (mm)	Stem lesion % (% of height)	Stem lesion score	Disease score (1-6)
1	D13[1]	109.3 ± 30.0	34.6 ± 21.7	30.9 ± 15.9	2.13 ± 0.37	4.73 ± 1.30
2	FCC237	76.3 ± 36.8	30.0 ± 20.7	35.8 ± 22.7	2.65 ± 0.78	4.75 ± 1.19
3	FCC237 + FCC207	91.0 ± 33.7	24.7 ± 17.7	30.2 ± 24.8	2.05 ± 0.35	3.93 ± 1.26
4	FCC237/R5	88.6 ± 39.3	32.7 ± 19.1	32.7 ± 15.2	2.65 ± 0.34	4.81 ± 0.87
5	FCC237/R5 + FCC207	109.7 ± 29.3	36.0 ± 35.5	32.4 ± 25.3	1.57 ± 0.41	3.73 ± 1.22
6	FCC456	94.4 ± 31.8	20.3 ± 11.5	21.2 ± 10.9	1.70 ± 0.72	3.31 ± 1.39
7	FCC207/2	85.4 ± 33.1	47.1 ± 44.8	45.4 ± 31.5	2.65 ± 0.41	5.40 ± 1.18
8	Kiwivax™	92.0 ± 44.2	35.9 ± 27.2	32.7 ± 19.6	2.80 ± 0.58	4.87 ± 1.05
9	Positive control	96.9 ± 26.1	29.4 ± 16.0	32.2 ± 16.3	2.36 ± 0.18	4.18 ± 1.11
10	Negative control	108.0 ± 31.0	3.0 ± 3.5	3.8 ± 5.6	0.05 ± 0.15	2.02 ± 1.25
	LSD (5%)	27.1	19.7	16.2	0.39	1.14
	P Value	0.234	0.007	0.001	<0.001	<0.001
Significance of contrasts						
All *Trichodermas* vs not inoculated (trts 1-8 vs 9)		ns	ns	ns	ns	ns
Kiwivax vs all other *Trichodermas* (trt 8 vs 1-7)		ns	ns	ns	ns	ns
Kiwivax vs FCC237 progeny (trt 8 vs 4, 5)		ns	ns	ns	ns	ns
2 x 2 factorial main effects (m.e.) & interaction for trts nos 2-5						
237 vs 237/R5 (parent vs progeny m.e.)		ns	ns	ns	ns	ns

Main effect of adding FCC207	ns	ns	*	*	*
Interaction (parent x FCC207)	ns	ns	ns	ns	ns

[1]D13 is a combination between LU753 and FCC207

* $p<0.05$

** $p<0.01$

3.3.2 Trial 2

For Trial 2, the majority of the points of significant difference were between the parents and progeny, with the protoplast regenerants performing better in all of these cases relating to the disease scoring (Table 3.5). There were five main effects where this effect was apparent: i) all parents vs all progeny main effect, ii) FCC237 vs FCC237/R5 main effect, iii) FCC456 vs FCC456/R4 main effect, iv) the 2x2x2 factorial main effect (all three parents vs three progeny including the addition of FCC207) and v) the 3x2 factorial main effect (all three parents vs three progeny excluding the addition of FCC207 used in combination). The only contrast that went against the general trend was the disease score in the 3x2 factorial between the interaction of the parent/progeny with FCC456 and FCC207. However this was due to the high disease score in the FCC207 regenerant when that was in contrast with FCC456. These results show that again within this bioassay there was no reduction in activity of the protoplast regenerants due to protoplasting. Interestingly, within this bioassay, the positive (Psa inoculated) control seedlings were significantly taller compared to any of the *Trichoderma* treated seedlings but they also had the highest stem lesion length as well. FCC207 did not have the same beneficial effect over any of the parameters when used in combination as it did in Trial 1. One reason for this could be the difference in cultivar between Trial 1 and Trial 2. Kiwivax™ performed substantially better this trial, suggesting that an incorrect application may have occurred in Trial 1 or another factor that could have impeded its performance.

Table 3.5 Disease parameter scores of Hort 16a kiwifruit seedlings after four weeks post inoculation with Psa for Trial 2.

Treatment		Height (mm)	Stem lesion length (mm)	Stem lesion % (% of height)	Disease score (0-6)
1	FCC237	118.1 ± 21.8	63.4 ± 25.7	55.45 ± 24.7	2.81 ± 0.97
2	FCC237 + FCC207	101.5 ± 18.2	62.5 ± 19.6	63.2 ± 22.1	2.90 ± 0.73
3	FCC237/R5	105.0 ± 23.4	30.5 ± 25.7	33.9 ± 33.8	2.00 ± 0.94
4	FCC237/R5 +FCC207	106.0 ± 14.3	34.0 ± 12.2	33.2 ± 12.1	2.40 ± 0.51
5	FCC456	96.0 ± 25.0	64.0 ± 22.3	68.1 ± 22.1	3.40 ± 1.50
6	FCC456 + FCC207	123.5 ± 61.0	52.5 ± 40.2	43.8 ± 31.4	2.20 ± 1.13
7	FCC456/R4	129.0 ± 36.7	53.2 ± 31.2	42.8 ± 21.9	2.13 ± 1.05
8	FCC456/R4 +FCC207	131.0 ± 44.8	53.0 ± 31.6	41.4 ± 23.3	2.10 ± 0.99
9	FCC207	119.0 ± 34.4	48.5 ± 28.1	50.0 ± 37.6	3.00 ± 1.88
10	FCC207/R2	117.4 ± 24.9	37.3 ± 27.3	32.1 ± 20.6	3.25 ± 1.39
11	Kiwivax	124.5 ± 60.8	39.5 ± 52.2	28.0 ± 27.8	2.10 ± 0.87
12	Positive control	147.0 ± 66.9	75.1 ± 58.1	49.0 ± 23.5	2.70 ± 1.41
13	Negative control	102.0 ± 27.4	1.5 ± 2.4	1.9 ± 3.2	0.10 ± 0.31
	LSD (5%)	33.5	27.9	37.7	1.01
	P value	0.157	<0.001	0.09	<0.001
Significance of contrasts					
All *Trichodermas* vs not inoculated (trts 1-11 vs 12)		*	*	ns	ns
All parents vs all progeny (trts 1, 2, 5, 6, 9 vs 3, 4, 7, 8, 10)		ns	**	**	*
Effect of 207 overall (trts 2, 4, 6, 8, 9 vs 1, 3, 5, 7, 12)		ns	ns	ns	ns
Kiwivax vs all other *Trichodermas* (trt 11 vs 1-10)		ns	ns	ns	ns

2 x 2 factorial main effects (m.e.) & interaction for trts nos 1-4				
237 vs 237/R5 (parent vs progeny m.e.)	ns	**	*	ns
Main effect of adding 207	ns	ns	ns	ns
Interaction (parent/progeny x 207)	ns	ns	ns	ns
2 x 2 factorial main effects (m.e.) & interaction for trts nos 5-8				
456 vs 456/R4 (parent vs progeny m.e.)	ns	ns	*	ns
Main effect of adding 207	ns	ns	ns	ns
Interaction (parent/progeny x 207)	ns	ns	ns	ns
2 x 2 x 2 factorial main effects (m.e) & interaction for trts 1-8				
Parent vs progeny m.e.	ns	*	**	**
Main effect of adding 207	ns	ns	ns	ns
237 vs 456 m.e.	ns	ns	ns	ns
Interaction (parent/progeny x 207)	ns	ns	ns	ns
Interaction (parent/progeny x 237/456)	ns	ns	ns	ns
Interaction (207 x 237/456)	ns	ns	ns	ns
Interaction (parent/progeny x 207 x 237/456)	ns	ns	ns	ns
3 x 2 factorial main effects (m.e.) & interactions for trts 1, 3, 5, 7, 9, 10				
Parent vs progeny m.e.	ns	*	*	*
237 vs (av. of 456, 207) m.e.	ns	ns	ns	ns
456 vs 207 m.e.	ns	ns	ns	ns
Interaction (parent/progeny x (237 vs av. of 456, 207)	ns	ns	ns	ns
Interaction (parent/progeny x (456 vs 207)	ns	ns	ns	*

* $p<0.05$
** $p<0.01$

3.3.3 Trial 3

The final trial had the same overall trend, with no significant reduction in the bioactivity of protoplast regenerants compared to their respective parental strains (as shown in Table 3.6). Unsurprisingly this trial had the lowest overall kiwifruit seedling heights of all three trials, mainly due to the set up in the nursery with no overhead lighting or heat pads because of the space confinements at the time. Here, the effect on growth seen from the various treatments was the most significant between the three trials. In particular, the contrasts focusing on all i) *Trichodermas* vs not inoculated, ii) all parents vs all progeny and iii) the effect of FCC207 overall were all significant (p<0.05). Furthermore, compared to the other two trials (see Table 3.4 and 3.5), the positive control height was very low, suggesting that in times of stress (with limited lighting, heat and disease pressure) *Trichoderma* mostly has a growth promoting effect on the kiwifruit seedlings. The negative control was not as low as the positive control, however, the measurement is taken at the end of the trial so it did not have the additional disease pressure (biotic stress) that the positive control did. Additionally, FCC237/R5 performed significantly better than the parent (FCC237) in the 2x2 factorial main effect in both stem lesion length and stem lesion percentage (p<0.05). The use of FCC207 in combination with the treatments also showed a positive impact on the two 2x2 factorials overall in relation to height, stem lesion length and stem lesion percentage respectively.

Table 3.6 Disease parameter scores of Hort 16a kiwifruit seedlings after four weeks post inoculation with Psa for Trial 3.

Treatment		Height (mm)	Stem lesion length (mm)	Stem lesion % (% of height)	Disease score (0-6)
1	FCC237	66.8 ± 15.0	59.2 ± 29.6	91.5 ± 44.1	2.56 ± 1.13
2	FCC237 + FCC207	65.6 ± 14.5	34.5 ± 14.6	53.4 ± 19.1	3.02 ± 1.22
3	FCC237/R5	66.5 ± 22.24	36.0 ± 22.1	58.4 ± 42.7	2.00 ± 0.94
4	FCC237/R5 +FCC207	65.5 ± 17.2	31.0 ± 20.2	47.3 ± 25.3	2.40 ± 0.51
5	FCC456	56.0 ± 18.4	38.0 ± 16.5	67.7 ± 19.4	2.80 ± 0.91
6	FCC456 + FCC207	61.5 ± 18.6	42.0 ± 18.6	73.5 ± 44.8	2.20 ± 0.63
7	FCC456/R4	62.7 ± 17.5	37.0 ± 11.0	60.4 ± 10.3	2.79 ± 0.88
8	FCC456/R4 +FCC207	86.5 ± 21.8	50.0 ± 29.1	57.6 ± 27.6	2.20 ± 1.03
9	FCC207	71.5 ± 16.5	34.5 ± 16.1	47.3 ± 16.1	2.80 ± 0.63
10	FCC207/R2	78.4 ± 22.9	41.1 ± 18.1	54.1 ± 20.9	2.78 ± 1.03
11	Kiwivax	66.0 ± 19.0	29.8 ± 16.7	43.7 ± 20.7	2.12 ± 1.05
12	Positive control	55.4 ± 14.2	29.8 ± 16.7	52.3 ± 22.9	2.46 ± 1.13
13	Negative control	67.5 ± 16.2	3.0 ± 4.2	4.8 ± 7.0	0.20 ± 0.42
	LSD (5%)	15.9	16.7	24.7	0.84
	P value	0.008	<0.001	<0.001	<0.001
Significance of contrasts					
All *Trichodermas* vs not inoculated (trts 1-11 vs 12)		*	ns	ns	ns
All parents vs all progeny (trts 1, 2, 5, 6, 9 vs 3, 4, 7, 8, 10)		*	ns	*	ns
Effect of 207 overall (trts 2, 4, 6, 8, 9 vs 1, 3, 5, 7, 12)		*	ns	ns	ns
Kiwivax vs all other *Trichodermas* (trt 11 vs 1-10)		ns	ns	ns	ns

2 x 2 factorial main effects (m.e.) & interaction for trts nos 1-4				
237 vs 237/R5 (parent vs progeny m.e.)	ns	*	*	ns
Main effect of adding 207	ns	*	**	ns
Interaction (parent/progeny x 207)	ns	ns	ns	ns
2 x 2 factorial main effects (m.e.) & interaction for trts nos 5-8				
456 vs 456/R4 (parent vs progeny m.e.)	**	ns	ns	ns
Main effect of adding 207	*	ns	ns	*
Interaction (parent/progeny x 207)	ns	ns	ns	ns
2 x 2 x 2 factorial main effects (m.e) & interaction for trts 1-8				
Parent vs progeny m.e.	ns	ns	*	ns
Main effect of adding 207	ns	ns	ns	ns
237 vs 456 m.e.	ns	ns	ns	ns
Interaction (parent/progeny x 207)	ns	ns	ns	ns
Interaction (parent/progeny x 237/456)	*	*	ns	ns
Interaction (207 x 237/456)	ns	*	*	*
Interaction (parent/progeny x 207 x 237/456)	ns	ns	ns	ns
3 x 2 factorial main effects (m.e.) & interactions for trts 1, 3, 5, 7, 9, 10				
Parent vs progeny m.e.	ns	ns	ns	ns
237 vs (av. of 456, 207) m.e.	ns	ns	*	*
456 vs 207 m.e.	**	ns	ns	ns
Interaction (parent/progeny x (237 vs av. of 456, 207))	ns	*	*	ns
Interaction (parent/progeny x (456 vs 207))	ns	ns	ns	ns

* $p<0.05$
** $p<0.01$

3.3.4 Combined Trials 2 and 3

When the results were combined from Trials 2 and 3, the main trend that was seen was the individual parent versus progeny main effects within each of the different factorial contrasts that were set up over the disease score and stem lesion percentage (as well as occasionally the stem lesion length), with all cases the progeny outperforming the parents (Table 3.7). Although the effect of adding FCC207 was not as prominent in Trial 2 and 3 compared to the first trial, when the results were pooled, the effect of using FCC207 in combination was positively significant for reducing the disease score parameter for FCC456 in particular. Finally, Kiwivax™ lessened the disease score as well as the stem lesion percentage compared to all of the other *Trichoderma* treatments.

Table 3.7 Combined disease parameter scores of Hort 16a kiwifruit seedlings after four weeks post inoculation with Psa for trials 2 and 3.

	Treatment	Height (mm)	Stem lesion length (mm)	Stem lesion % (% of height)	Disease score (0-6)
1	FCC237	92.4 ± 36.3	61.3 ± 3.0	75.2 ± 23.1	2.68 ± 0.20
2	FCC237 + FCC207	83.5 ± 25.4	48.5 ± 19.8	58.3 ± 6.9	2.96 ± 0.10
3	FCC237/R5	85.8 ± 27.2	33.2 ± 3.9	46.1 ± 17.3	2.00 ± 0.00
4	FCC237/R5 +FCC207	85.8 ± 28.6	32.5 ± 2.1	40.2 ± 10.0	2.40 ± 0.00
5	FCC456	76.0 ± 28.3	51.0 ± 18.4	67.9 ± 0.3	3.10 ± 0.40
6	FCC456 + FCC207	89.3 ± 39.4	47.2 ± 7.4	78.0 ± 6.3	2.20 ± 0.00
7	FCC456/R4	95.8 ± 46.9	45.4 ± 11.5	51.6 ± 12.4	2.46 ± 0.50
8	FCC456/R4 +FCC207	108.8 ± 31.5	51.5 ± 2.1	49.5 ± 11.5	2.15 ± 0.10
9	FCC207	95.2 ± 33.6	41.5 ± 9.9	48.6 ± 1.9	2.90 ± 0.10
10	FCC207/R2	97.9 ± 27.6	39.2 ± 2.7	41.1 ± 18.4	3.02 ± 0.30
11	Kiwivax	95.2 ± 41.4	34.6 ± 6.9	35.9 ± 11.1	2.11 ± 0.00
12	Positive control	101.2 ± 64.77	52.4 ± 32.1	50.6 ± 2.3	2.58 ± 0.17
13	Negative control	84.5 ± 17.3	2.2 ± 1.1	3.4 ± 2.1	0.15 ± 0.10
	LSD (5%)	26.0	22.5	21.1	0.48
	P value	0.499	0.012	<0.001	<0.001
Significance of contrasts					
All *Trichodermas* vs not inoculated (trts 1-11 vs 12)		ns	ns	ns	ns
All parents vs all progeny (trts 1, 2, 5, 6, 9 vs 3, 4, 7, 8, 10)		ns	ns	**	**
Effect of 207 overall (trts 2, 4, 6, 8, 9 vs 1, 3, 5, 7, 12)		ns	ns	ns	ns
Kiwivax vs all other *Trichodermas* (trt 11 vs 1-10)		ns	ns	*	*

2 x 2 factorial main effects (m.e.) & interaction for trts nos 1-4				
237 vs 237/R5 (parent vs progeny m.e.)	ns	*	**	**
Main effect of adding 207	ns	ns	ns	ns
Interaction (parent/progeny x 207)	ns	ns	ns	ns
2 x 2 factorial main effects (m.e.) & interaction for trts nos 5-8				
456 vs 456/R4 (parent vs progeny m.e.)	*	ns	**	*
Main effect of adding 207	ns	ns	ns	**
Interaction (parent/progeny x 207)	ns	ns	ns	ns
2 x 2 x 2 factorial main effects (m.e) & interaction for trts 1-8				
Parent vs progeny m.e.	ns	*	**	**
Main effect of adding 207	ns	ns	ns	**
237 vs 456 m.e.	ns	ns	ns	ns
Interaction (parent/progeny x 207)	ns	ns	ns	*
Interaction (parent/progeny x 237/456)	ns	ns	ns	ns
Interaction (207 x 237/456)	ns	ns	ns	**
Interaction (parent/progeny x 207 x 237/456)	ns	ns	ns	ns
3 x 2 factorial main effects (m.e.) & interactions for trts 1, 3, 5, 7, 9, 10				
Parent vs progeny m.e.	ns	ns	ns	**
237 vs (av. of 456, 207) m.e.	ns	ns	ns	*
456 vs 207 m.e.	ns	ns	*	ns
Interaction (parent/progeny x (237 vs av. of 456, 207))	ns	ns	ns	*
Interaction (parent/progeny x (456 vs 207))	ns	ns	ns	*

* $p<0.05$
** $p<0.01$

3.4 Discussion

Overall, the results from the three trials showed that there was no reduction in the bioactivity of these protoplast progeny, with the regenerants regularly outperforming their respective parental strains. Although there was a bias in the selection of the protoplast progeny with the pesticide amended plates (i.e. not selecting for bioactivity), the selected strains do not appear to have lost their biocontrol abilities. Both protoplast regeneration and protoplast fusion are regularly used to enhance the biocontrol potential of various *Trichoderma* and other filamentous fungi strains. This technology has been used to improve rhizosphere competency (Sivan and Harman, 1991), produce pesticide-polyresistance (Hatvani et al., 2006), enhanced antagonistic potential over *Rhizoctonia, Fusarium* and other pathogens (Lalithakumari et al., 1996) and numerous other biocontrol applications (see Chapter 1 and 2 for further examples regarding the use of protoplast technology for strain improvement in *Trichoderma* and other fungi). The ability to enhance desired traits, however, is not guaranteed as an outcome from producing protoplast progeny. Migheli et al. (1995) produced protoplast progeny from *T. harzianum* and an unknown strain of *Trichoderma*. These fusant progeny showed a high degree of variability in both their biocontrol and mycoparasitic ability, moreover, the fusants were generally less active than their parental strains against *Botrytis, Sclerotinia* and *Pythium*.

Another trend observed during these trials was the reduction in the disease-related parameters with the addition of FCC207 (*T. hamatum*) to the selected strains, particularly in Trial 1 and in the combined data from Trials 2 and 3. It appears that using the selected *Trichoderma* strains in combination has resulted in synergy. This ability for strains to enhance the biocontrol capabilities of one another has been documented in numerous studies. Using multiple strains of biocontrol agents has been suggested as a method of reducing the variability while increasing the reliability of biocontrol provided they have different requirements (Guetsky et al., 2001). *Trichoderma* have different modes of action that include: antibiosis, mycoparasitism, inducing host resistance and competition with the pathogen (Harman et al., 2004a; Harman, 2006; Sharma et al., 2014). Research suggests that some *Trichoderma* biocontrol strains have multiple modes of action against their target organism (Sharma et al., 2014). FCC207 may have differing modes of action to the selected other strains which potentially caused the reduction in the disease parameters. Hill et al. (2015) elaborated on this further suggesting that there is no single approach that is likely to provide complete control of Psa, with biocontrol organisms needing to be used in combination or as part of a comprehensive IPM strategy to combat this disease. Kiwivax™ is a combination of three different *Trichoderma* strains that may have different modes of action resulting in its biocontrol potential against Psa. The exact mode of action of the Kiwivax™ strains is unknown, and this is beyond the scope of this project, however, sites treated with Kiwivax™ have shown an increase in microbial diversity (Stark et al., 2018).

Furthermore, the results from Trial 3 show the beneficial effect that *Trichoderma* can have on plants against abiotic stress. The height of the kiwifruit seedlings that were inoculated with *Trichoderma* were significantly higher than the non-*Trichoderma* inoculated control in Trial 3. It is well documented that certain *Trichoderma* species have positive effects on plant growth and enhance resistance to both biotic and abiotic stresses (Brotman et al., 2013; Harman, 2000; Hermosa et al., 2012; Nicolás et al., 2014). The results were similar to those reported by Mastouri et al. (2010) in which they examined the effects of seed treatment with *T. harzaianum* strain T-22 on germination of seeds exposed to both biotic (seed and seedling disease caused by *Pythium ultimum*) and abiotic stresses (osmotic, salinity and temperature stress). They showed that if the seedlings were not under any of the above stresses, the *Trichoderma* strain had little effect on seedling performance. However, under the conditions tested, treated seed performed significantly better. In Trials 1 and 2 this did not occur, but with limited lighting and heat combined with disease pressure, these biotic and abiotic factors caused a positive growth response in the *Trichoderma* treated samples. This demonstrates that the *Trichoderma* enhances tolerance to a wide range of stresses (Mastouri et al., 2010).

However, growth promotion is not a universal trait for all *Trichoderma* species and strains. Research by Nieto-Jacobo et al. (2017) tested various strains for growth effects in *Arabidopsis* and observed varying degrees of success. The growth effects observed ranged from an increase in plant biomass, a decrease in plant biomass to no effect at all, which is similar to previous work reported by Lee et al. (2016). Additionally, Nieto-Jacobo et al. attributed this variability in plant growth enhancing potential as the result of environmental parameters rather than the choice of the plant host. This highlights the importance of further research into the environmental control of potential biocontrol strains, again as seen with the differences in plant growth under the abiotic stresses.

Building on this biocontrol/growth promotion variability seen within *Trichoderma* strains and species, differences have also been observed within different trial *Trichoderma* combinations for Psa on kiwifruit seedlings. Different combinations of *Trichoderma*, when developing Kiwivax™ performed better with certain cultivar seedlings, with the combination that led to Kiwivax™ continuously performed better on the Hort16A cultivar (Hill et al., 2015). They further highlighted the potential that each *Trichoderma* strain-*Actinidia* cultivar combination may make use of a different specific mechanism to protect the plant itself.

One final point of note is the lack of overall significance in the bioactivity scores compared to the Psa positive control. However, as previously mentioned, Kiwivax™ does have a limited label claim within the Agricultural Compounds and Veterinary Medicines (ACVM) register through the Ministry for Primary Industries (MPI) based solely on seedling assays because there is no field efficacy data available yet. Over the 26 Biotron trials used for registration, Kiwivax™ performed consistently better

than the Psa positive control. Anecdotally, growers, packhouse and nursery managers who have used Kiwivax™ have responded positively (Christine Stark, pers. comm.). As mentioned above, it does increase *Trichoderma* numbers in kiwifruit orchard soils for up to six months after application (Stark et al., 2018). There are numerous limiting factors of this trial design that may be the cause this lack of significance in protection against Psa. One potential is that the mode of action is not expressed in the window of this trials time frame. Additionally, dealing with the pathogen in containment is an artificial situation and its developmental behaviour would be different from the stem stab inoculation used here. Christine Stark did try a different inoculation method of Psa via the leaf but did not find the bioactivity scores varied. For example, for Kiwivax™ the disease score (based on the initial scoring methodology [Table 3.2]) was 3.0 ± 0.85 (n=10), compared to the Psa positive control of 3.3 ± 1.37 (n=22). Moreover, the Biotron compared to the field are contrasting environments. The space of a pot is limited, which leads to nutrient and space competition for both the plant and microorganism. These factors, among numerous others in this artificial environment influences the plant growth and the developmental stage, as well as the diversity of soil microorganisms compared to a field situation (Stark et al., 2018). However, the disease scoring system for the bioassay was improved upon over the course of this study with the negative control score reducing, thereby becoming more quantitative.

3.5 Conclusion

Due to the change in phenotype of the protoplast regenerants that were produced, the biocontrol potential of these regenerants were assessed to ensure there was no reduction. Across the three trials, there was no decrease in the biocontrol potential with the progeny regularly out performing their respective parental strains. Furthermore, these trials have shown two beneficial characteristics of *Trichoderma* that have been previously reported, these being the synergistic potential of *Trichoderma* when used in combination and the growth promoting effect that *Trichoderma* can have on plants against abiotic stress.

Chapter 4

Genome-wide analysis of cytosine methylation between a *Trichoderma* sp. "*atroviride* B" parental and protoplast regenerant strains

4.1 Introduction

DNA methylation is a common and stable epigenetic modification of DNA found in most eukaryotes. It plays a crucial role in numerous cellular processes including, but not limited to, genome regulation and development, gene transcription and transposon silencing (Bird, 2002; Feng et al., 2010; Zemach et al., 2010). The most commonly studied mechanism is that of 5-methylcytosine methylation, which involves the addition of a methyl group to the C5 carbon residue (5mC) of cytosines, typically by DNA methyltransferases (Krueger et al., 2012). Cytosine DNA methylation is found in three different sequence contexts: CG (or CpG =C- phosphate-G), CHG or CHH (in which H corresponds to A, T or C). The sequencing context, such as CpG, refers to methylation occurring on cytosines followed by guanine residues (Jang et al., 2017).

Cytosine methylation is widespread across the kingdoms. However, its patterns and roles vary significantly between the taxa. It occurs at high levels in mammals and plants compared to insects and fungi, where it is very low or non-existent. Even further, between these groups, methylation differs in genomic distribution, sequence specificity and heritability (Martienssen and Colot, 2001). Plants, invertebrates and fungi have been shown to have a 'mosiac' pattern of methylation because only specific genomic elements are targeted such as repetitive DNA and actively transcribed sequences. Cytosine methylation also commonly occurs in all three sequencing contexts within these groups. However, within mammals, methylation is found almost exclusively at CpG dinucleotides throughout entire genome (~70-80% of CpG nucleotides) which is typically involved in gene silencing, with non-CpG methylation being observed in the developmental process such as within embryonic stem cells (Bird, 2002; Schübeler, 2015).

Cytosine methylation patterns in eukaryotes are established by *de novo* and maintenance DNA methyltransferases (DNMTases) (Feng et al., 2010). Briefly, DNMTases catalyse the transfer of a methyl group to the strand of DNA. These *de novo* DNMTases induce methylation, then the methylation is maintained through cell division via other DNMTases, which acts on hemi-methylated DNA (where one strand is methylated) that is produced through cell division to ensure the methylation is present on the daughter strand of DNA. The number of DNMTases vary between mammals, plants and fungi (Feng

et al., 2010). Interestingly in plants, DNA methylation is maintained by three different pathways, that depend on the sequence context of the methylation (CpG, CHG or CHH) as methylation differs strand wise in replication between the different sequence contexts (Bewick et al., 2016; Law and Jacobsen, 2010). The methylation mechanisms of DNMTases in certain fungi, such as *Neurospora crassa*, *Magnoporthe oryzae* and *Metarhizium robertsii* have been well studied (Jeon et al., 2015; Kouzminova and Selker, 2001; Wang et al., 2017). Although the DNMT1 family of DNMTases have been found in these genomes, no DNMT3 homologues have been found in any fungi so far. Ascomycete fungi possess DNMT-related DNA methyltransferase, DIM-2, which methylates transposable elements and repeat sequences in a way that are dependent on methylation of lysine 9 of histone H31 (Kouzminova and Selker, 2001; Rountree and Selker, 2010). In these fungi, DIM-2 is responsible for all known cytosine methylation events and repeat-induced point (RIP) defective (RID) is responsible for the methylation specificity throughout the genome, which implies that there must an interaction between these two proteins for DNA methylation to occur (Jeon et al., 2015; Selker et al., 2003; Wang et al., 2017). As expected, within the *Trichoderma atroviride* v2.0 genome (https://genome.jgi.doe.gov/Triat2/Triat2.home.html), most of the proteins known to be involved in RIP and DNA methylation in *Neurospora crassa* were found, including rid-1 (TA_310388), dim-2 (TA_36027; DNA methyltranserase), dim-5 (TA_131894; H3K9 methyltranserase), dim-7 (TA_233240), dim-8 (TA_146031), dim-9 (TA_282963) and hpo (300583; HP1). This was identical for other *Trichodermas* such as *T. reesei* and *T. virens* (Kubicek et al., 2011; Li et al., 2018; Li et al., 2017a).

In fungi in particular, recent methylome studies have shown that DNA methylation varies significantly, which suggests that cytosine methylation may be involved in different mechanisms within this group (Jeon et al., 2015; Kim et al., 2018; Li et al., 2017b; Liu et al., 2012; Selker et al., 2003; Wang et al., 2015; Zemach et al., 2010). These studies show that DNA methylation of fungal genomes range, typically between 0.07% -1.5%, for both CpG and non-CpG methylation, suggesting that fungal cytosine methylation levels are low compared with other eukaryotes, or even negligible in the case of *Aspergillus flavus* (Liu et al., 2012). In black truffle, cytosine methylation is very high, between 10-30% of cytosine residues being methylated, however, this is very unusual and most likely due to the high proportion of repetitive sequences and large genome size of this fungus (Montanini et al., 2014). Traditionally, a consensus view of cytosine methylation in fungi was as a stable genome defence mechanism against transposable elements (TE) and repeat sequences, with active genes being unmethylated, and this pattern is seen in numerous fungi over different families such as *N. crassa* (Rountree and Selker, 2010), *Tuber melanosporum* (Montanini et al., 2014), *Phycomyces blakesleanus, Corpirnopsis cinerea, Laccaria bicolor* and *Postia placenta* (Zemach et al., 2010). However, methylation is found more commonly in gene bodies than previously thought, suggesting the role of cytosine methylation is not strictly conserved. Numerous papers have reported that DNA methylation is found

not only in the promoter regions of genes, transposable elements and repeat sequences but also in the transcribed regions of genes, which suggests that cytosine methylation may have a prominent role in the regulation of gene expression as well (Jeon et al., 2015). This poses a paradox in which cytosine methylation may have the dual and opposing ability to both repress transcription and also occur in the body of active genes in the same species of fungi (Zemach et al., 2010).

The function of cytosine methylation in genes is not well understood and gene body methylation has different effects on the transcript abundance of genes depending on the species. For example, in *Cordyceps militaris*, hypermethylated genes were found to be downregulated (Wang et al., 2015), whereas in *M. robertsii* (and in contrast to most other eukaryotes) transcription tended to be enhanced in genes with moderate promoter methylation, while gene expression was decreased in genes with high or low promoter methylation (Li et al., 2017b). Interestingly, this pattern of moderate or partial methylation showing an increase in transcript abundance within gene bodies is also shared with the diatom, *Phaeodactylum tricornutum* (Veluchamy et al., 2013). Additionally, within these gene bodies, methylation tends to occur in the exons (and be correlated to an increase in RNA levels), whereas introns tend to be unmethylated. This suggests that gene body DNA methylation may be directed by spliced mRNA (Maor et al., 2015; Zemach et al., 2010).

As previously mentioned, the genetic basis for fungicide resistance within the protoplast regenerants that were produced by our group was explored (Johanna Steyaert, pers. comm.). The UP-PCR and AFLP profiles were identical, which suggests that no major DNA rearrangements had occurred. Additional sequencing of key genes known to be associated with this fungicide's resistance revealed no change between the parent and regenerant. However, MSAP analysis detected multiple methylation changes which strongly suggest that methylation may play an important role in determining the phenotype of the protoplast regenerants. In the present study, UP-PCR profiles of the protoplast regenerants that were produced in Chapter 2 showed no major DNA rearrangements, which suggests another mechanism, such as methylation may be influencing the tolerance to copper.

Methylation within *Trichoderma* has only been observed using simple methods such as MSAP analysis (Lange, 2015), so it is unknown what role methylation has in *Trichoderma*, or even at what level it occurs. It is important to note that MSAP can only detect methylation at CpG sites, which most likely only represents a fraction of the total 5mCs in the genome. Furthermore *Trichoderma* species typically have low levels of transposable elements within the genome (only 0.49% in *T. atroviride* (Kubicek et al., 2011)), suggesting that it is unlikely to be involved as a genome defence mechanism compared to *N. crassa* and *Uncinocarpus reesii* where silent repeated loci are heavily methylated with little methylation elsewhere (Selker et al., 2003; Zemach et al., 2010).

It is well documented that changes in methylation help contribute as a stress adaptation to environmental changes in plants (Verhoeven et al., 2010; Yong-Villalobos et al., 2015). Some papers suggest that epigenetic regulation in plants could contribute to novel traits related to plant stress adaptation by the controlled generation and exploitation of transposon-induced genetic diversity, which could be used to broaden plant phenotypic and genetic variation (Chen, 2007). It has also been observed that major genomic events, such as hybridisation, and also environmental stresses can trigger cytosine methylation in plants and in particular, stress-induced methylation changes may be targeted to stress-related genes (Verhoeven et al., 2010). Within rice, CHG hypomethylation has been reported in plants treated with heavy metal compared to control plants, and that this CHG hypomethylation was heritable through the germlines, which resulted in enhanced tolerance for both the parental plant and subsequent generations (Ou et al., 2012). In fungi, biotic and abiotic stressors have been shown to induce epigenetic changes. The causal agent of chestnut blight*, Cryphonectria parasitica*, showed changes in its cytosine methylation pattern (which was determined both via MSAP analysis and whole genome bisulphite sequencing) after a mycovirus infection (Kim et al., 2018; Nuskern et al., 2017). The infection increased the number and diversity of methylated, hemimethylated (when only one of two strands is methylated) and total MSAP markers found in the infected fungal isolates compared to the virus-free controls (Nuskern et al., 2017). Additionally, cold treatment of the edible mushroom *Pleurotus eryngii* induced an increase in methylation (Hua et al., 2017).

Recent studies have further shown the influence of DNA methylation with morphology changes in fungi (Kim et al., 2018; Wang et al., 2017). Kim et al. (2018) showed that a mutation in the signalling pathway component (mitogen-activated protein kinase kinase kinase [MAPKKK]), in *C. parasitica* resulted in sporadic occurrences of sectors alongside hypomethylation compared to wild-type. This mitrogen-activitated protein kinase (MAPK) is manipulated by the presence of the mycovirus (Cryphonectria Hypovirus 1) as mentioned above. Additionally, Wang et al. (2017) produced mutants for two DNMTases (MrRID and MrDIM-2) in *M. robertsii* which resulted in a significant decrease in cytosine methylation (between 8-71% of sites remained depending on the specific mutant) compared to the wild type. This methylation decrease resulted in changes in the development, stress tolerance and virulence of *M. robertsii* (Wang et al., 2017). This pattern of changes of colony morphology, radial growth and sporulation has also been reported in a mutant with a deletion in the DIM-2 gene in *M. oryzae* (Jeon et al., 2015). This combination of both phenotypic consequences and heritability of cytosine methylation suggests that it could play a large role in adaptation, when changes in DNA sequence may not be as obvious (Verhoeven et al., 2010). A similar mechanism could also be involved in protoplast regeneration in fungi, as protoplasts are readily adapt to external stress factors.

As the exact mechanism that induces these phenotypic modifications remains unknown, it is essential to understand these underlying genetic events, not only for the mechanisms involved but also that to ensure that other, non-target changes have not occurred. The research in this chapter aimed to characterise these changes by exploring the methylome of a parental strain and the chosen regenerant via whole genome bisulphite sequencing (WGBS). WGBS provides the highest precision mapping of the methylome and measuring the state of cytosine methylation (Dolzhenko and Smith, 2014). Briefly, sodium bisulphite converts unmethylated cytosines to uracils (which after PCR are converted then to thymines) while leaving methylated cytosines unconverted. This chemical treatment of the DNA effectively turns an epigenetic difference into a genetic difference, therefore enabling cytosine methylation detection and analysis. By mapping bisulphite-treated DNA back to the reference genome, it is then possible to determine the methylation state of individual cytosines.

4.2 Materials and methods

4.2.1 Fungal strain management and DNA extraction

The two fungal strains used in this part of the study were the protoplast regenerant tolerant to copper (*T*. sp. "*atroviride* B" FCC237/R5) and its respective parental strain (*T*. sp. "*atroviride* B" FCC237) as selected in Chapter 2. This regenerant strain was chosen as it was the most morphologically similar to its parent and a very similar genome of *T. atroviride* was available and annotated on JGI. This was in contrast to others such as *T. hamatum* which although being morphologically similar, at the time of sequencing the genome was only available in scaffolds. Additionally, before gDNA extraction, conidia of the chosen regenerant was taken from the -80°C and sub-cultured onto a 4 mM $CuSO_4.5H_2O$ to ensure the copper tolerance of the stored conidia remained.

In other fungal methylome papers, 3 d mycelium was shown to have the highest number of 5mCs among the different tissue types (Jeon et al., 2015), therefore this time point and tissue type was used for the gDNA in this study. Additionally because the phenotypic changes (hypothesised to be induced by methylation) appeared to be stable and heritable over numerous generations, plain PDB was chosen for the growing medium and not amended with copper. Biomass was generated for gDNA extraction from 3 d old mycelium as described in Chapter 2 (2.1) in PDB using the Gentra® Puregene™ Tissue Kit (Qiagen). Three biological replicates for the regenerant and the parent respectively were used for the WGBS. For each replicate, three 50 mL Nunc tubes were used to ensure there was enough mycelial mass, and then combined per replicate. The DNA was further purified using a modification of the DNeasy® Plant Mini Kit (Qiagen), starting at step 2: 250 µL DNA of the sample was combined with 150 µL AP1 buffer and 4 µL RNase A stock solution (100 mg/mL), and continued from step 3 as per manufacturer's instructions. The DNA quality was checked by gel electrophoresis. DNA concentration

was measured on a NanoDrop™ machine (NanoDrop Technologies Inc, USA) and also on a Quibit™ 3.0 Fluorometer (ThermoFisher Scientific) as per manufacturer's instructions.

4.2.2 WGBS library construction and sequencing

The bisulphite conversion of the gDNA was performed by New Zealand Genomics Limited (NZGL), Dunedin, New Zealand using a EZ DNA Methylation-Gold kit (Zymo Research, USA), followed by the library preparation using TruSeq DNA Methylation Kit (Illumina®, USA). The bisulphite treated libraries were sequenced at the Otago Genomics Facility, University of Otago, Dunedin, New Zealand, using the Illumina HiSeq 2500 sequencing system (Illumina®). The samples were sequenced on a single sequencing lane with 125 paired-end reads being generated for the respective samples.

4.2.3 WGBS analysis

The Next Generation Sequencing (NGS) data was analysed by identifying differentially methylated cytosines between the two strains by two bioinformaticians using different methods. The following methods and subsequent results will be split into their respective sections according to the approach of the different bioinformaticians, whose main difference can be summarised by searching for the differentially methylated regions (DMRs) or differentially methylated cytosines (DMCs).

4.2.3.1 Read quality control

For both sets of data analysis, the same read quality control was performed by Peter Stockwell (Otago University). The raw paired-end reads were trimmed and quality checked by using cleanadapters v1.22 software (Chatterjee et al., 2012) with default parameters. This program scans the reads and identifies any sections which show 75% of higher matching with any adapter sequences (Chatterjee et al., 2012).

4.2.3.2 Differentially methylated region (DMR) analysis (Peter Stockwell)

The WGBS data was analysed by Peter Stockwell, bioinformatician at the Department of Biochemistry, Otago University, Dunedin, New Zealand. The following methods description is a summary based on his report with additional detail added (Appendices B.1). Anything in *italics* is verbatim from his report.

4.2.3.2.1 Mapping of WGBS reads

Reads from the WGBS of parental and regenerant strains were mapped against the Trichoderma atroviride *IMI206040 genome v2.0 assembly downloaded from JGI* (Genome build v2.0, May 2010, Joint Genome Institute, http://genome.jgi.doe.gov/Triat2/Triat2.home.html). *Mapping was performed using Bismark* (Krueger and Andrews, 2011) *using both bowtie1 and bowtie2 and also with BSMAP* (Xi and Li, 2009), *with the mapping being confined to the first of the paired end reads (forward reads) for both programs*. The BSMAP mapping was chosen to continue with as it gave consistently higher mapping percentages.

The two aligner programs work in different ways. Bismark, which is a Perl application, works alongside Bowtie fragment aligner (Langmead et al., 2009), this allows both the aligning of short DNA sequences reads to large genomes and determines the methylation state of each cytosine position in the read (being either in a CpG, CHG or CHH context) calling in a single step. The output contains genomic and read sequences for each match from which methylated cytosines can be visualised and explored further (Chatterjee et al., 2012). It uses a three-letter aligning approach, where by all Cs in the reference genome and both sequenced reads are converted to Ts prior to mapping, and mapping is performed using a seed and extend approach (Kunde-Ramamoorthy et al., 2014). Conversely, BSMAP (Bisulfite Sequence MAPping program) is a C++ application. It employs a wild card approach, this allows either Cs or Ts in the reads to map to Cs in the reference genome. One of the main processing differences between these two approaches, is that wild card algorithms can tolerate more mismatches than the three-letter approach (Kunde-Ramamoorthy et al., 2014).

4.2.3.2.2 Differential methylation analysis using DMAP

Differential Methylation Analysis Package (DMAP) (Stockwell et al., 2014) is a fragment-based approach for investigating cytosine methylation patterns (looking at a 1000 bp window of the WGBS data) and produces associated statistics and the proportion of methylation for each of these windows. The different components of this package can filter, and process aligned bisulphite sequenced data to generate reference methylomes. This pipeline directly imports output from any bisulphite aligner (e.g. Bismark or BSMAP) in Sequence Alignment/Map (SAM) format and identifies differential methylation, based on two additional programs, diffmeth and identgeneloc. As the data consisted of three replicates each of the parental and regenerant samples, ANOVA was run between the different samples. This allows for the determination of the significance of these potential methylation differences between the groups in relation to the variation within each replicate in these groups. Based on those results, significantly differentially methylated regions were filtered out, based on the low probability regions. Rather than just looking at CpG methylation, the script was changed to detect all three types of methylation (CpG, CHG, CHH).

4.2.3.2.3 Finding proximal genes

The low probability differentially methylated output from above was run with the DMAP program identgeneloc, which associates each of the differentially methylated regions (DMRs) to the nearest gene by comparing the genomic coordinates of the start and end of the DMR and gives relative distances from the transcription start site with an annotation file in the GenBank format (Stockwell et al., 2014). Identgeneloc also considers the sense of the gene (5' or 3') and relates the DMRs with respect to the upstream region of the gene. From the JGI protein ID's provided, the respective proteins were searched for manually on the JGI site (*T. atroviride* v2.0) and blasted using NCBI blastp for

conserved domains and similar protein alignments. A spreadsheet was generated that listed the contig, DMR, average parent and average regenerant methylation percentage, significance, proximal gene start and end as well as the protein ID from JGI.

4.2.3.3.4 Potential functional consequences of DNA methylation

To assess more generally a potential function of these DMRs, the proximal genes were functionally categorised into gene ontology (GO) terms. These JGI protein ID's from above were entered into two protein family domain databases, InterPro (Finn et al., 2016) and Pfam (Finn et al., 2015) to obtain a list of predicted protein domains and a list of GO ID's from the respective protein domains. It is important to note that it is only a predicted function as the majority of the genes are uncharacterised. Additionally these proximal genes were also annotated with the KOG (EuKaryotic Orthologous Groups) database (Tatusov et al., 2003) from the JGI website, which aids in the identification and phyletic classification of the orthologous proteins.

4.2.3.3 Differentially methylation cytosine (DMC) analysis (Darrell Lizamore)

The WGBS data was additionally analysed by Darrell Lizamore, Department of Wine, Food and Molecular Bio-Sciences, Lincoln University, Lincoln, New Zealand. The low amount of variability found in the DMR approach suggested that this may not be an appropriate method, as it was designed to analysis larger genomes such as the human genome, so a new method was sought. The following methods description is a summary based on Darrell's report with additional detail added (Appendices B.2). Anything in *italics* is verbatim from his report.

4.2.3.3.1 Mapping of WGBS reads

The resulting trimmed reads were aligned to the *T. atroviride* IMI206040 genome v2.0 assembly. Mapping was performed using BS-Seeker2 (Guo et al., 2013), which gave approximately 65% mapping efficiency using both pair-end reads (opposed to just the forward read in the previous method). The methylation ratios were also called with BS-Seeker2. BS-Seeker2 is a Python application, that is a bisulphite sequencing alignment tool that performs genome indexing, read alignment (via BAM, SAM or BS-Seeker format) and DNA methylation calling for each cytosine (Guo et al., 2013). BS-Seeker2, yields similar mapping results to those of Bismark, but it provides more detailed information post processing (Kunde-Ramamoorthy et al., 2014). BS-Seeker 2 also employs a three-letter approach, as does BSMAP.

4.2.3.3.2 Differential methylation analysis using methylKit and filtering out SNPs

The differentially methylated cytosine (DMC) sites were detected using a R package, methylKit (Akalin et al., 2012), which uses a single 5mC approach. Upon further investigation, an overlapping filter was included as there was variation between replicates within each strain. As the client of this

bioinformatics approach, I was worried that this could be as a result of incomplete bisulphite conversion. This incomplete conversion could lead to an increase in false positives, both with non-conversion and thymidine-to-cytosine sequencing errors. Other researchers investigating the methylome of the silkworm, *Bombyx mori* (Dazao) (Xiang et al., 2010) and *Aspergillus flavus* (Liu et al., 2012), which both had negligible rates of methylation, have used this approach when they were unsure of their low methylation levels, only to discover their methylation was, in fact, the result of false positives. For the silkworm, only 11.3% (65 of the initial 574 5mCs) were validated as actual 5mCs. As NZGL didn't include a positive control, such as unmethylated DNA for the bisulphite conversion, it was very important to include this step. After discussion of this issue with the bioinformatician (Darrell Lizamore), a script was written to ignore the 5mCs that were only present in one replicate of each treatment/strain.

However, after visualising the methylation differences on IGV v2.3.91 (Robinson et al., 2011; Thorvaldsdóttir et al., 2013) between IMI206040, LU132 (an unannotated *T*. sp. "*atroviride* B" strain) and the bisulphite treated sequences of the parent and regenerant strain, the majority of the assumed methylation points were actually SNPs between *T*. sp. "*atroviride* B" and *T. atroviride*. A variety of programs were employed to eliminate these SNPs from the DMC list including BS-Snper (Gao et al., 2015) and Biscuit (BISulfite-seq Comprehensive Utilisation and Integration Toolkit (Zhou, 2016)). Both of these programs had issues with the dependencies and were unable to be used. However, CGmap tools (Guo et al., 2017) was able to map as it used asymmetrical scoring to ensure that genomic sequence with T/A before bisulphite conversion did not match with C/G in the probe sequence; therefore it can discern SNPs from 5mCs. A spreadsheet was generated that listed the contig, methylation type, 5mC position, average parent and average regenerant methylation percentage and the significance of the 5mC.

4.2.3.3.3 Finding proximal genes

The resulting significantly different 5mC sites (CpG, CHG and CHH methylation) were joined with the respective gene features file (for *T. atroviride* v2.0). These files were opened within both Geneious (v10.2.4) (Kearse et al., 2012) and IGV; the individual DMCs (that were either 1 kb upstream of the gene or found within the gene body) were manually associated with the proximal genes. The DMCs were further grouped into patterns within gene regions: upstream (1 kb of gene body), gene body including introns and UTR (untranslated regions), downstream (1 kb of gene body) and intergenic regions (both upstream and downstream [1 kb each] of gene body was deleted).

4.2.3.3.4 Potential functional consequences of DNA methylation

To assess more generally a potential function of these DMCs in the genes of interest (defined as genes with a DMC located in their gene bodies or within 1 kb upstream), the methylated genes were

functionally categorised into gene ontology (GO) terms. These JGI protein ID's from above were entered into two protein family domain databases, InterPro (Finn et al., 2016) and Pfam (Finn et al., 2015) to obtain a list of predicted protein domains and a list of GO IDs from the respective protein domains. These lists were condensed through REVIGO (Supek et al., 2011), which summarises long lists of GO by removing redundant terms. It is important to note that it is only a predicted function as the majority of the genes are uncharacterised. These GO ID's were further separated into all DMCs, hypermethylated DMCs in the parent and hypermethylated DMCs in the regenerant. The DMCs that had associated genes with them were also annotated with the KOG (EuKaryotic Orthologous Groups) database (Tatusov et al., 2003) from the JGI website, which aids in the identification and phyletic classification of the orthologous proteins.

4.3 Results

4.3.1 Differentially methylated regions

4.3.1.1 Global mapping of differentially methylated regions

The mapping efficiency varied from bismark/bt1 ~40% to bsmap ~68% compared to the reference genome of *T. atroviride* IMI206040; therefore BSMAP was chosen to proceed with. There were a total of 33 DMRs identified following the analysis throughout the genome. From this, five of these DMRs were found to hypermethylated in the parent strain compared to 28 being hypermethylated in the regenerant (Table 4.1). This suggests that there are higher levels of (differential) cytosine methylation occurring in the regenerant, possibly due to the protoplasting process, with methylation being gained in these situations. However, the cytosine methylation percentages over the 1000 bp window were very low ranging from 0.64% to 2.24%, with the differences between the parent and regenerant ranging only from 0.05% to 0.57%. A total of 24 genes/proteins were annotated with either the InterPro or Pfam databases; 15 were assigned with at least one GO term. Four of these were assigned in the biological process category, one was assigned in the cellular component category, and ten were assigned to the molecular function category.

Table 4.1 Differentially methylated regions (DMRs) between the parent and regenerant strains through DMAP analysis completed by Peter Stockwell. Difference in methylation is from the [av. par meth – av. reg meth]. A blank space in the GO ID or KOG class and function category means there is no assigned class or ID.

Contig	DMR		Protein ID[1]	Av. par meth	Av. reg meth	Difference in methylation	GO ID	KOG class and function	Putative function
	Start	End							
contig_10	82001	83000	TA_55004	0.72	1.03	-0.31	Integral component of membrane		Glycogen synthase
contig_12	455001	456000	TA_314109	1.28	1.79	-0.051	RNA binding	Information storage and processing/RNA processing and modification	mRNA cleavage and polyadenylation factor I complex, subunit RNA15
contig_13	850001	851000	TA_52932	1.04	0.92	0.12	Metabolic process	Metabolism/secondary metabolites, transports and catabolism	Candidate NRPS-like enzyme
contig_14	507001	508000	TA_181620	0.73	1.3	-0.57			WD40 repeat-like protein
contig_15	164001	165000	TA_93057	1.64	2.09	-0.45			FOG: Low-complexity
contig_15	988001	989000	TA_181695	1.3	1.58	-0.28			SMC-N superfamily
contig_17	814001	815000	TA_156368	1.02	1.5	-0.48	Transcription, DNA-templated		Fungal transcription factor regulatory middle homology region
contig_17	190001	191000	TA_213474	1.05	1.24	-0.19			Bin/Amphiphysin/Rvs (BAR) domains- fungal Snf1p interacting proteins
contig_19	120001	121000	TA_173237	1.08	1.36	-0.28	Chromatin remodelling	Information Storage and Processing/ chromatin structure and dynamics	SWF-SNF chromatin remodelling complex, Snf5 subunit

contig_20	661001	662000	TA_238588	1.11	1.01	0.1	ATPase activity, coupled to transmembrane movement of substances	Metabolism/secondary metabolites, transports and catabolism	Multi drug resistance protein (MRP)
contig_21	36001	37000	TA_46319	0.83	1.22	-0.39	Catalytic activity	Cellular Processes and Signalling/defense mechanisms	Flavonon reductase/cinnamoyl-CoA reductast
contig_21	71001	72000	TA_263302	0.64	0.98	-0.34			Fatty acid hydroxylase superfamily
contig_22	1552001	1553000	TA_256549	1.28	1.79	-0.51	Oxidoreductase activity	General function prediction only	Aldo/keto reductase, related to diketogulonate reductase
contig_22	193001	194000	TA_218126	1.2	1.37	-0.17			Cytochrome domain of fungal cellobiose dehydrogenases
contig_23	249001	250000	TA_88971	1.06	1.57	-0.51			No conserved domains
contig_23	908001	909000	TA_317939	0.79	0.88	-0.09			No conserved domains
contig_23	1218001	1219000	TA_318025	1.77	1.31	0.46			Chromosomal replication initiation protein
contig_24	2221001	2222000	TA_39146	1.31	1.69	-0.38	Oxidoreductase activity	Metabolism/secondary metabolites, transports and catabolism	Iron/ascorbate family oxidoreductases
contig_25	2403001	2404000	TA_319665	0.98	1.26	-0.28			No conserved domains
contig_25	1285001	1286000	TA_87116	1.28	1.51	-0.23			No conserved domains
contig_26	1787001	1788000	TA_310473	0.9	1.46	-0.56	Glycerol-3-phosphate transmembrane transporter activity		Chromosomal replication initiation protein
contig_26	2587001	2588000	TA_301051	0.87	1.1	-0.23			No conserved domains
contig_26	2981001	2982000	TA_247582	1.03	1.22	-0.19	GTP binding	General function prediction only	GTPase involved in cell partitioning and DNA repair
contig_26	3470001	3471000	TA_179060	0.73	0.85	-0.12			No conserved domains
contig_26	3755001	3756000	TA_226045	0.96	1.08	-0.12	Metal ion binding	General function prediction only	Putative methyl transferase, based on outlier plant homologues. OR PHD-finger

contig_27	2150001	2151000	TA_295125	1	1.51	-0.51	Monooxygenase activity	Metabolism/secondary metabolites, transports and catabolism	Cytochrome P450 CYP3/CYP5/CYP6/CYP9 subfamilies
contig_27	4365001	4366000	TA_126941	1.33	1.76	-0.43			Mitochondrial carrier protein
contig_27	1278001	1279000	TA_130541	0.94	1.2	-0.26			Spliceosomal protein FBP22/Splicing factor PRP40
contig_27	2700001	2701000	TA_180523	1.09	1.32	-0.23			No conserved domains
contig_27	3181001	3182000	TA_228302	1.25	1.2	0.05	Transmembrane transport	Metabolism/energy production and conversion	Mitochondrial tricarboxylate/dicarboxylate carrier proteins
contig_28	601001	602000	TA_302544	1.69	2.24	-0.55	Oxidoreductase activity	General function prediction only	NAD (P)- dependent dehydrogenase
contig_28	833001	834000	TA_268651	1.53	1.01	0.52			Domain of unknown function
contig_29	426001	427000	TA_288239	0.68	1.01	-0.33			No conserved domains

[1] Origin of the protein ID numbers are from *Trichoderma atroviride* v2.0 https://genome.jgi.doe.gov/pages/search-for-genes.jsf?organism=Triat2

4.3.2 Differentially methylated cytosines

4.3.2.1 Global mapping of differential cytosine methylation

In total, between 24,578,536 and 31,301,618 reads were generated for the respective parent and regenerant samples after removing the adapter contaminants, unknown and low-quality reads. A total of 13 million cytosine's were mapped with BSseeker2, equating to a unique mapping efficiency of 65% compared to the reference genome of *T. atroviride* IMI206040 v.20. Although this mapping efficiency is on the lower side, namely because the strains sequenced were *T.* sp "*atroviride* B" opposed to *T. atroviride* which is the reference genome, it is still within what other papers have published. For example, the methylome of *Magnaporthe oryze* (Jeon et al., 2015) had a mapping efficiency for one of their samples at 62.75%, with their average being 72.65%. Additionally bisulphite sequencing does reduce the complexity of the genome and reduces the ability of mapping programs to align the sequences onto the reference genome. The alignment can only be as good as the reference genome (Yaish et al., 2018). As there are differences between *T. atroviride* and *T.* sp. "*atroviride* B", the gaps and undetermined regions do negatively affect the mapping efficiency. There were 35,000 regions that could not be uniquely mapped compared the reference genome, ~2,700 had a greater length than 100 bp, but none were over 1 kb. Despite having a lower mapping efficiency the genome coverage was high with over 12 million cytosines had above 10x coverage.

After applying the overlapping filter on the dataset, approximately 760,000 of 2.8 million reads remained (Table 4.2), which shows that most 5mCs were only found in one sample. This suggests that this may have been to bisulphite conversion inefficiencies since most 5mCs have <1% methylation. The DMCs were analysed using methylKit, with better clustering of replicates by treatment (after the overlapping filter was put in place, see Figure 4.1 and 4.2). A Principal Component Analysis (PCA) plots and Hierarchical Cluster Analysis were identical for CHG and CHH methylation as well (data not shown). The resulting 5mCs were filtered for significantly different methylation among treatments (p<0.001).

Table 4.2 Summary of 5mC sites mapped.

	CpG	CHG	CHH	Total
Sites mapped	3,064,618	2,710,741	7,226,297	13,001,696
Sites mapped >10x	2,874,174	2,707,972	6.619,754	12,201,900
5mCs (pass replicate overlap filtering[1])	762,854	1,143,115	1,694,184	3,520,153
Sig. diff 5mCs (p<0.01)	111	53	166	330
Sig. diff hypermethylated 5mCs in parent (p<0.01)	58	39	73	170
Sig. diff hypermethylated 5mCs in regenerant (p<0.01)	53	14	93	160

[1] at least one 5mC in at least two replicates of at least one condition
H=A, T or C

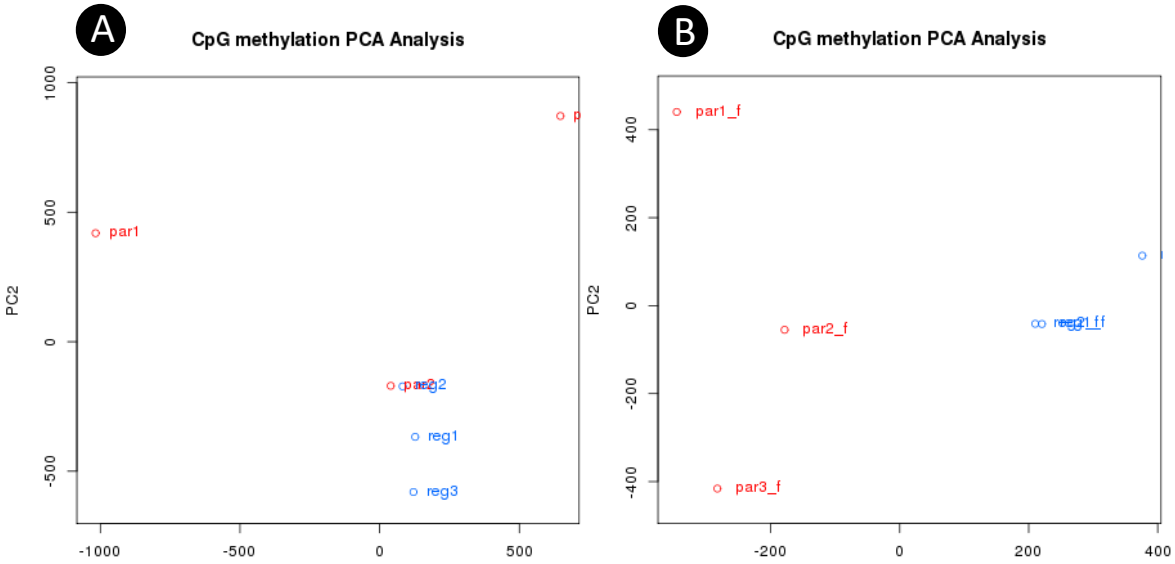

Figure 4.1 **Principal component analysis (PCA) between the parental (red) and regenerant (blue) strains after differential methylation analysis using methylKit. (A) CpG methylation with no overlap filtering. (B) CpG methylation with overlap filter (at least one mC in at least two replicates of the treatment). Figure produced by Darrell Lizamore.**

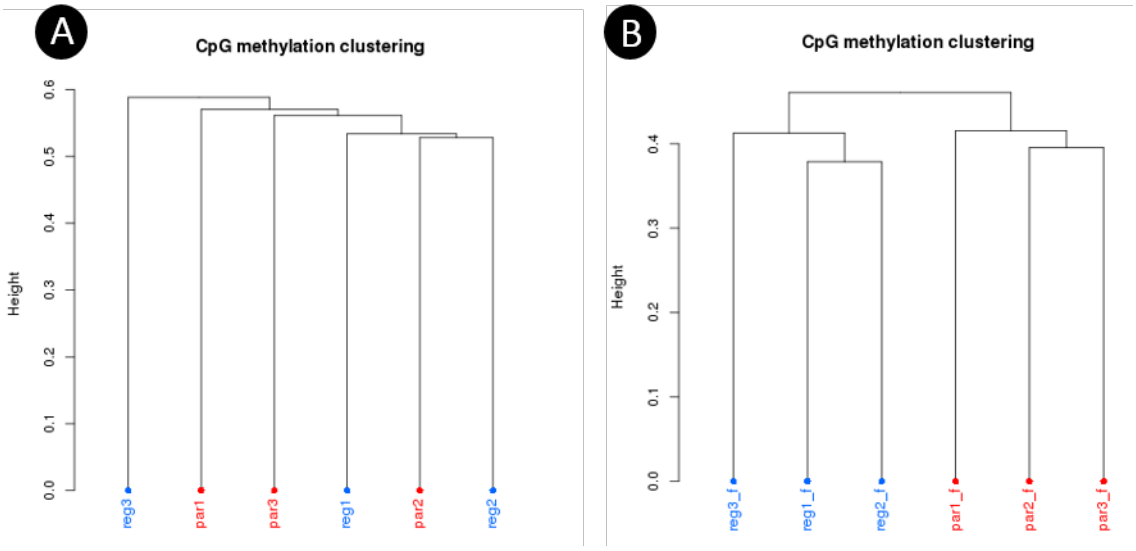

Figure 4.2 **Hierarchical cluster analysis between the parental (red) and regenerant (blue) strains after differential methylation analysis using methylKit. (A) CpG methylation with no overlap filtering. (B) CpG methylation with overlap filter (at least one 5mC in at least two replicates of the treatment). Figure produced by Darrell Lizamore.**

There were no significant differences in the percentage or densities of 5mCs of genomic cytosines between the parent and regenerant (Figure 4.4), but there were subtle variations in the distribution of differential 5mCs across the genome. Additionally, after filtering for SNPs the number of significantly different 5mCs among the two treatments decreased from 556 to 330 (data not shown). Both strains methylation patterns over the different sequence contexts were almost identical (Figures 4.4 and 4.5),

with no clustering of methylation sites in one that are absent from the other. More methylation was found in the parent in the CHG context than the regenerant, while the regenerant had higher levels of CHH methylation (Table 4.2).

In addition to having a very low occurrence (330) of significantly differentiated methylation sites across the genome the methylation percentage for each DMC was very low, which was similar to the DMR analysis. Almost all DMCs had less than 10% methylation (Figure 4.3). The average methylation levels in the parent in these DMCs was 5.69% (with the highest individual 5mC level being 39.45%), and in the regenerant it was 7.06% (with the highest individual 5mC level being 60.44%). This is in contrast with other methylation results from other eukaryotes such as plants and mammals, where the scale of methylation tends to be spread from 0 to 100% (Figure 4.3B). Another trend was within the DMCs that had a methylation difference greater than 25% (18 DMCs in total), the majority were found to be hypermethylated in the regenerant compared to the parent (fifteen vs three). Additionally, in sixteen of these sites, the methylation that occurred was in the CHH context, compared to CpG and CHG (one and one respectively) (Table 4.3).

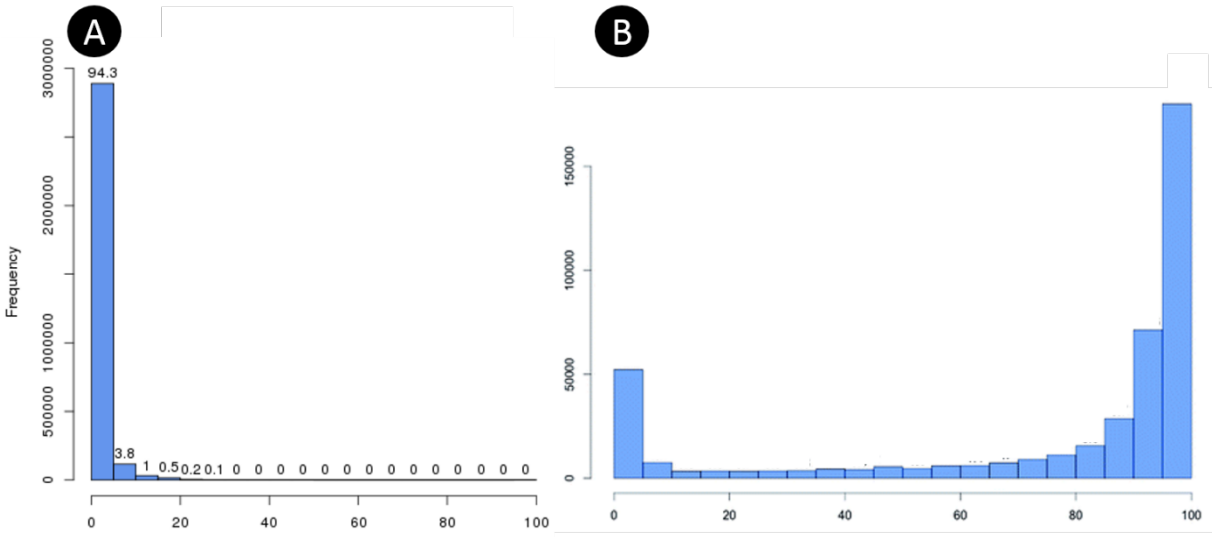

Figure 4.3 Histogram of the percentage of methylation per base generated from methylKit. The X axis shows percent methylation for each individual CpG. The numbers on the bars in A denote the percentage of CpGs contained in each bar. The Y axis is the frequency that this methylation occurs. (A) CpG methylation distribution of parent1_forward. (B) A more typical methylation pattern from other species- CpG methylation distribution in zebrafish brain- ranging from 0-100% (4.3B histogram modified from Chatterjee et al. (2013)).

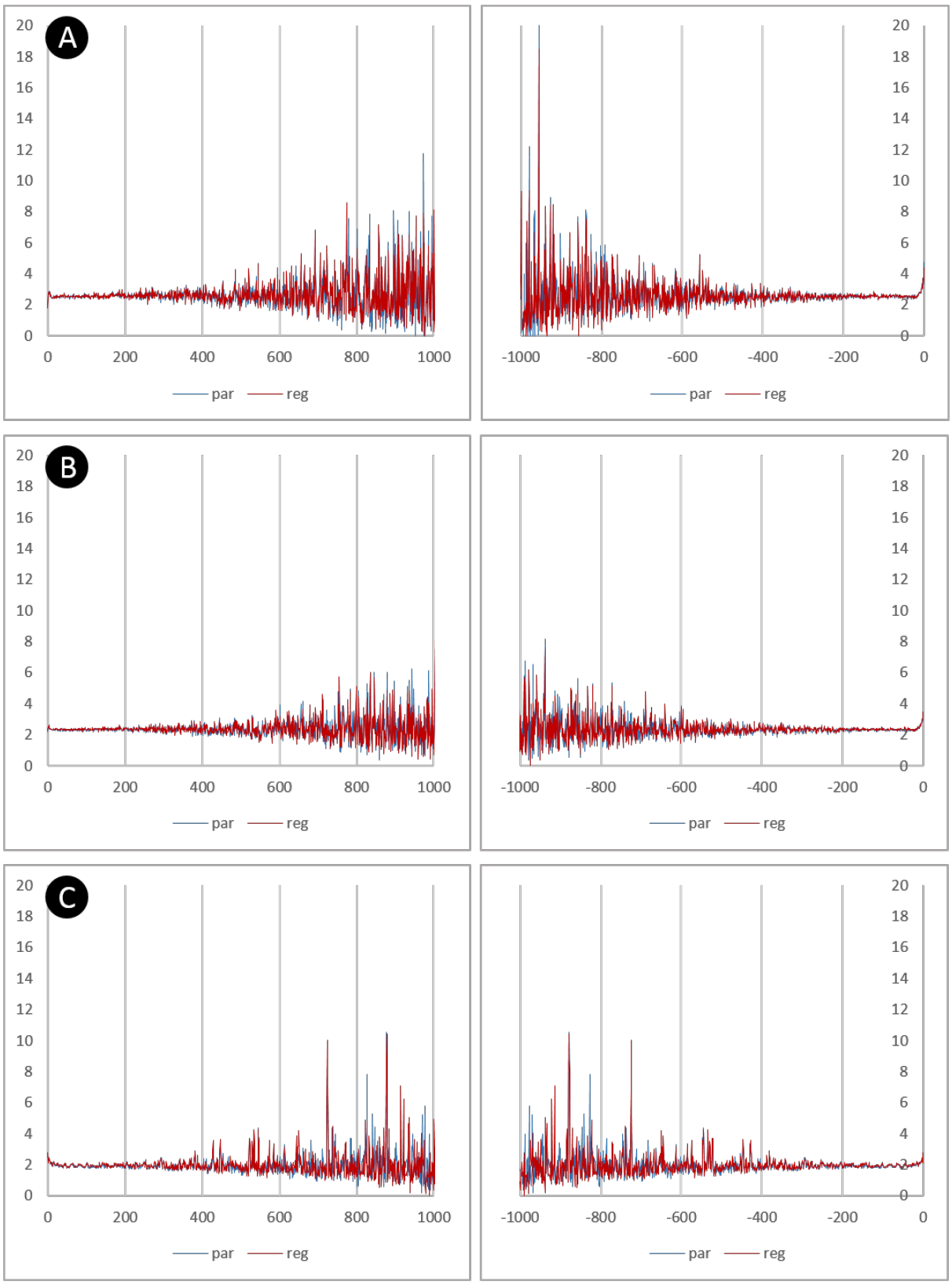

Figure 4.4 **Density of 5mCs in and around all genes over the genome. (A) CpG, (B) CHG, (C) CHH. Blue= parental strain, red=regenerant strain. Figure produced by Darrell Lizamore.**

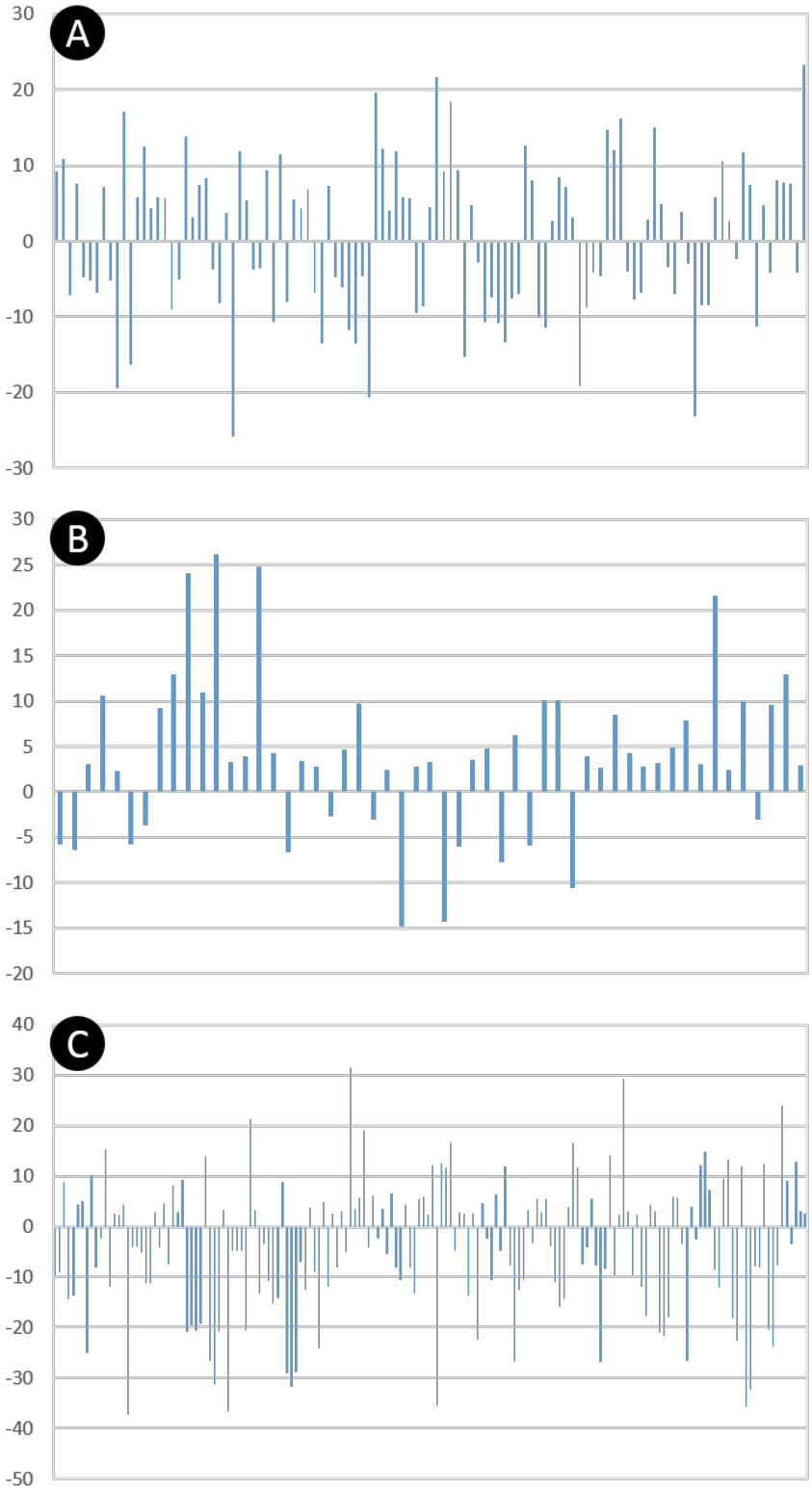

Figure 4.5 **Variation of methylation differences of the significantly different methylated cytosines (DMCs) based on the methylKit analysis between the three cytosine methylation contexts. Y axis: [parent average methylation] – [regenerant average methylation]. X axis is the individual DMCs. (A) CpG, (B) CHG, (C) CHH.**

Table 4.3 **Differentially methylated cytosines (DMRs) between the parent and regenerant strains, through methylKit analysis completed by Darrell Lizamore, with more than 25% differential methylation. Difference in methylation is from the [parental methylation – regenerant methylation]. A full list can be seen in Table B.1 (Appendices B.3).**

Contig	Methylation type	mC position	parMean	regMean	methDiff (parMean-regMean)[1]	Position (intron, exon etc)[2]	Protein ID (JGI)[3]	Putative function
contig_15	mCHH_s	848,390	3.92	41.16	-37.24		TA_133724	Pyridoxal kinase
contig_18	mCHH_s	669,329	0	36.64	-36.64		TA_53493	No putative conserved domains
contig_27	mCHH_s	4,286,465	0	35.79	-35.79	UTR	TA_302213	Nucleoside phosphatase
contig_24	mCHH_s	2,189,499	3.703	39.277	-35.574	UTR	TA_151377	NMT1/THI5 like domian containing protein
contig_27	mCHH_s	4,584,856	19.87	52.15	-32.28		TA_287340	Multidrug resistance-associated protein/mitoxantrone resistance protein, ABC superfamily
contig_20	mCHH_s	311,271	0	31.83	-31.83		TA_193414	Triglyceride lipase-cholesterol esterase
contig_22	mCHH_s	1,092,071	37.89	6.34	31.55	Intron	TA_317515	No putative conserved domains
contig_18	mCHH_s	176,261	0	31.3	-31.3		TA_93906	Predicted transporter (major facilitator superfamily)
contig_27	mCHH_s	277,841	37.13	7.85	29.28		TA_294677	Cell cycle control protein (crooked neck)
contig_20	mCHH_s	153,794	2.56	31.62	-29.06	120 bp up	TA_298543	Predicted membrane protein
contig_20	mCHH_s	513,507	0	28.78	-28.78	668 bp down	TA_255946	Transcription factor MEIS1 and related HOX domain proteins
contig_26	mCHH_s	889,625	25.08	51.84	-26.76	503 bp up	TA_224476	No putative conserved domains
contig_26	mCHH_s	3,415,713	0	26.73	-26.73		TA_225852	Large-conductance mecahnosensitive channel, MscL
contig_27	mCHH_s	2,288,364	0	26.67	-26.67	443 bp down	TA_227718	GTP-binding protein DRG1 (ODN superfamily)

contig_18	mCHH_s	176,246	0	26.65	-26.65		TA_93906	Predicted transporter (major facilitator superfamily)
contig_20	mCHG_s	144,316	32.28	6.18	26.1	459 bp up	TA_52415	Predicted transporter (major facilitator superfamily)
contig_21	mCpG_s	261,952	0	25.82	-25.82	534 bp down	TA_81632	Zinc-binding oxidoreductase
contig_13	mCHH_s	341,554	0	25	-25	316 bp up	TA_164398	Predicted telomere binding protein

[1] The methylation difference is the difference from the [parental methylation mean] - [regenerant methylation mean] at the individual 5mC. Any number that is a negative implies hypermethylation in the regenerant

[2] The position is where 5mC lies in relation to a gene. A blank space means it is within the exons of the genes. - means that is it was not within 1 kb of a gene body either upstream or downstream.

[3] Origin of the protein ID numbers are from Trichoderma atroviride v2.0 https://genome.jgi.doe.gov/pages/search-for-genes.jsf?organism=Triat2

H=A, T or C

UTR= untranslated regions

4.3.2.2 Cytosine methylation patterns in gene regions

To understand the very low level of differential DNA methylation found between the two strains, the methylation profiles of intragenic regions (including coding sequences and introns) and intergenic regions were further analysed. Of the total of 330 DMCs that were identified, 212 were located in gene bodies, with 39 DMCs were concentrated in 1 kb regions upstream of genes, 40 DMCs downstream and the rest in intergenic regions (Table 4.4). There were 170 hypermethylated DMCs in the parent and 160 hypermethylated DMCs in the regenerant which occurred in different regions, which suggests that cytosine methylation may occur at specific sites between the two strains.

Five of the individual 5mCs were within overlapping or overprinting genes and therefore had two genes associated with them (Appendices B.3). The five individual 5mCs are: contig 24: 1,840,368, contig 25: 929,609, contig 25: 1,428,802, contig 25: 2,397,592 and contig 26: 3,760,038. However, this did not change the number of 5mCs, there were still 330 individual 5mCs.

Table 4.4 The distribution of DMCs in the parent versus regenerant across the genic regions.

	Total	Upstream[1]	Gene body[2]	Downstream[3]	Intergenic regions[4]
Total	330	39	212	40	39
Hyper Par	170	23	103	19	25
Hyper Reg	160	16	109	21	14

[1] Upstream 1 kb of gene body
[2] Gene body including introns and untranslated regions (UTRs)
[3] Downstream 1 kb of gene body
[4] Both upstream and downstream (1 kb each) of gene body was deleted

Upon further analysis, twelve genes had more than one DMC located within their proximity: nine in the coding regions (exons), one in the downstream region, one in the untranslated region and one in the upstream region. The majority of these had a higher level of methylation in the regenerant (10 out of 12). Table 4.5 contains the protein names (if known), functional description based on KOG class, average differential methylation percentage (across the different DMCs in the gene), number of DMCs found within the gene and the position of the DMC in relation to the gene.

The genes that had the highest methylation differences averaged across the DMCs were typically hypermethylated in the regenerant opposed to the parent. Additionally, these differences in methylation were higher than the average over all DMCs of 9.8% between the parent and regenerant. This suggests that these genes, in particular, may be the most likely to have a functional consequence due to both having multiple DMCs and also a higher level of methylation occurring. Furthermore, the DMCs hypermethylated in the regenerant appear to be involved more so with transport; this could be how the regenerant can be more tolerant to copper compared to the parental strain. The two genes that had multiple DMCs in the parent were both involved in the transcription process. There were an

additional three genes (TA_161835 [uncharacterised protein], TA_243551 [RNA helicase BPR2, DEAD-box superfamily] and TA_256374 [aldehyde dehydrogenase]) that had a significantly DMC in both the parent and regenerant respectively.

4.3.2.3 Potential functional consequences of cytosine methylation

To investigate the potential functional consequences of cytosine methylation, the methylated genes (defined as genes with a DMC located in their gene bodies [intron, exon or UTR] or within 1 kb upstream) were functionally categorised into GO ID's. The results showed that the differentially methylated genes could be categorised into three main GO domains: biological processes (128), cellular components (14) and molecular function (62) (Appendices B.3). Among these three GO groups above, the greatest amount of differentially hypermethylated genes were located in the sub-categories of: i) lipid metabolism; ii) vesicle-mediated transport, iii) DNA metabolism and iv) response to stress for the parental strain. For the regenerant they were: i) intein-mediated protein splicing, ii) microtubule-based movement, iii) vesicle-mediated transport and iv) response to stress. The results of this GO functional annotation indicate that genes of multiple biological processes may be subjected to DNA methylation regulation.

The DMC associated genes were annotated further with the KOG database. The resulting annotations grouped the genes (169) into three functional categories: cellular processing and signalling (58; 34.3%); information storage and processing (38; 22.4%); and metabolism (49; 28.9%), and the others into poorly characterised genes (24; 4.2%) (Appendices B.3). The remaining genes (87) did not have a KOG classification associated with them. The groupings were similar in parent and regenerant, with two exceptions. The first being the regenerant did not have any hypermethylated DMC associated genes that fell into the following five categories: i) cell wall/ membrane/ envelope biogenesis; ii) defence mechanisms; iii) inorganic ion transport and metabolism; iv) nuclear structure or v) replication, recombination and repair. Secondly, the regenerant had more DMCs associated genes in the intracellular, trafficking, secretion and vesicular transport group (cellular processing and signalling) with 12 (16.4% of all hypermethylated regenerant DMCs associated genes) compared to only 7 in the parent (9%). This could be of interest as these DMC associated genes within this group can be involved in directing movements of proteins in a cell, from one side of a membrane to another, suggesting that there may be a higher frequency of protein transport occurring in either the parent or the regenerant. Additionally, the parent had more DMCs associated genes assigned to the KOG functional class of transcription (parent: 12 [14.1%], regenerant: 7 [9%]).

Table 4.5 Genes with multiple differentially methylated cyotsines (DMCs) between the parent and regenerant strains following methylKit analysis.

Protein ID[1]	Putative function	Av. differential methylation across the DMCs[2]	Number of DMCs	DMC position
TA_50107	Polyadenylate-binding protein (RRM superfamily)	19.95% R	4	Exon
TA_50845	Predicted transporter	3.98% R	2	Exon
TA_52775	Vesicle coat complex COPII, subunit SEC23	13.98% R	2	Exon
TA_93906	Predicted transporter	28.9% R	2	Exon
TA_149621	Vesicle coat complex COPI, gamma subunit	13.61% R	4	Exon
TA_163678	RNA-binding Ran Zn-finger protein	20.4% R	2	416 and 420 bp downstream
TA_229437	Hypothetical polyketide synthase	8.23% R	2	Exon
TA_249414	Phospholipase C, phosphatidylinositol-specific, X region	19.9% R	2	Exon
TA_281461	FOG: RRM domain protein	4.7% R	3	Exon
TA_297464	Putative G protein coupled receptors (PTH11-type)	11.2% R	2	UTR
TA_127707	Chromodomain-helicase DNA-binding protein	12.06% P	2	192 and 195 bp upstream
TA_137221	Transcription factor TCF20	6.9% P	2	Exon

[1] Origin of the protein ID numbers are from https://genome.jgi.doe.gov/pages/search-for-genes.jsf?organism=Triat2

[2] P= represts hypermethylation in the parental strain, R= represents hypermethylation in the regenerant strain

4.3.3 SNP analysis

There were numerous SNPs that appeared between the respective parent and regenerant compared to the *T. atroviride* v2.0 genome from using the cgmaptools SNP calling. There were 2633 SNPs in the parent and 3251 SNPs in the regenerant, again compared to the *T. atroviride* reference genome. There were only 587 SNPs that were similar between these two strains when they were analysed for duplicates. This suggests that there may be a large occurrence of SNPs between the two strains. However, this is unlikely as the SNP analysis was performed on the WGBS data. The RNA-seq SNP analysis will be used to confirm if these are true SNPs or an artefact from using the three bases from the WGBS data. Calling SNPs from WGBS is complicated and will be discussed in the following chapter.

4.3.4 Comparison between the two different methods for calling differential cytosine methylation

To explore the similarities between the two methods of looking for DMRs versus DMCs, the two lists that were generated were combined, and any duplicated protein IDs were noted. However, only three proximal genes were found in both: TA_ 126941 (mitochondrial carrier protein), TA_256549 (alcohol/keto reductase) and TA_319665 (hypothetical protein). In two of these genes, the hypermethylation is reversed between the two analysis types. For example in TA_126941, in the DMR analysis, the parent and regenerant proportions were 1.33% and 1.76% respectively. However, the DMC had 0% methylation in the parent and 3.44% in the regenerant. This also occurred in TA_256549 (DMR- 1.28% parent, 1.79% regenerant and DMC- 5.66% parent, 0% regenerant). None of the genes with the clusters of DMCs as mentioned in Table 4.5 were included in these three genes listed here.

4.4 Discussion

This work describes the first genome-wide cytosine methylation map at a single-base resolution with deep bisulphite sequencing of a *Trichoderma* species. Furthermore, it describes the methylation differences between protoplast regenerant and its parental strain from any organism. Overall there were no large-scale significant differences in either the global patterning or density of cytosine methylation between the parental strain and regenerant. However, several observations seen in both analyses types suggest that the regenerant may subtly differ from the parental strain, potentially being the cause of the phenotypic changes.

Within the DMR analysis, the regenerant was hypermethylated (higher level of methylation) in 28 out of the 33 regions, compared to the parent having only five hypermethylated differential regions. The function of these DMRs both in the parent or regenerant appear to be randomly distributed among the different contigs and within different functional groups (via GO ID's and KOG classes). A similar trend was seen within the DMC analysis. With the 18 individual mCs sites that had the highest level of

differential methylation (being greater than 25% in this dataset), 15 were found to be hypermethylated in the regenerant compared to only three in the parent, and they were found primarily in the CHH context. Additionally, within the genes that contained multiple individual DMCs, the majority of these were found to be hypermethylated in the regenerant compared to the parent (ten vs two). These trends of differential methylation observed highlight the importance of exploring the functional consequences through RNA sequencing, as the effect of intragenic methylation varies greatly between fungal species. This will be explored in the following chapter (Chapter 5).

4.4.1 Differential methylation levels are low in *Trichoderma* between the parent and regenerant

A point of note, from both analyses, is that the cytosine methylation proportion found in these differentially methylated sites or regions are very low, averaging around 1.2% in the DMRs and within the individual DMCs, the methylation level was only at 6.8% per individual 5mC. These observations call into question the actual role of DNA methylation within these strains and the biological significance of this change if it does not modulate gene expression. The level of methylation within mammals and plants tends to be a lot higher, therefore the change in gene expression can be correlated to the cytosine methylation differences (as seen in Figure 4.3B). In *A. flavus*, the individual 5mCs levels were very low, with only a small fraction of them being above 5%, and few being greater than 15%. Once an overlapping strategy was applied to the results, it showed that DNA methylation was negligible (Liu et al., 2012). Very few of the fungal methylome studies published state, however, the proportion of DNA methylation levels. For the methylome of *M. oryzae*, Jeon et al. (2015) showed the methylation level as a proportion of the amount of 5mCs compared to the number of reads with non-5mC, but not the proportion of methylation at the individual 5mC sites. The average methylation proportion was around 28% (Jeon et al., 2015). In *M. robertsii*, to identify a DMR, a sliding 200-bp window was used, with a threshold of >1.5-fold change in methylation levels were considered to call a DMR. However, again they do not state the methylation proportion of each 5mC site. The authors provide information about the read numbers of 5mCs in the region compared to read numbers of total cytosines in the region (Li et al., 2017b). However, in both of these papers, their bisulphite sequencing was validated by BS-PCR (bisulphite PCR), but not through multiple replicates as seen in this project, which suggests that the individual 5mCs had a higher proportion of methylation than what has occurred here.

4.4.2 Differential methylation occurs mainly in gene bodies

These methylomes presented here show that the majority of the DMCs lie within genes and 1 kb upstream of the gene body between the two strains (251 out of 330 [75%]), with the number within genes and exons themselves are 211 (63%) and 187 (56%) respectively. Although this data is looking at the differential methylation that is occurring, it confirms the conservation of gene body methylation

between eukaryotes (Veluchamy et al., 2013; Zemach et al., 2010). This is interesting from a functional point of view as cytosine methylation has been observed to be enriched in the body of highly transcribed genes in some fungal species, which again will be confirmed in the following chapter by RNA sequencing.

Briefly, studies have shown that fungal DNA methylation displays considerable variation across species, both in genome-wide methylation patterns and the mechanisms of function and role of methylation (Li et al., 2017b; Zemach et al., 2010). In *M. oryzae* (Jeon et al., 2015), as well as *Uncinocarpus reesii* (Zemach et al., 2010), methylation occurring upstream or downstream of the gene has a negative effect on the abundance, whereas gene body methylation has a positive effect (Jeon et al., 2015). In *C. militaris*, the majority of the DMRs were found within the intergenic regions (from a total of DMRs, 141, out of 225, were in the intergenic regions) (Wang et al., 2015). This suggests that the methylation within *C. militaris* in the intergenic regions is responsible for maintenance of genome stability/genome defence. Furthermore, Wang et al. (2015) did not find a correlation between DNA methylation and gene expression. The role of DNA methylation within *M. robertsii* varies even further, with 108 out of the 132 DMRs identified being found within a region 2 kb upstream of a gene or within gene bodies. Within *M. robertsii*, moderate methylation of the promoter and the protein coding region tended to be upregulated (defined as methylation between 33-66%), whereas genes with high or low methylation (<33% or >66%) within these regions were downregulated (Wang et al., 2017).

As mentioned above, the function of gene body methylation is still not entirely known, but it has been suggested that that intragenic cytosine methylation may be directed by spliced mRNA (Maor et al., 2015). The frequency of methylation occurring in the exons compared to introns observed here, and also in other fungi such as *U. reesii* (Zemach et al., 2010), further support this hypothesis, as in some fungi an increase in DNA methylation also leads to transcript abundance. Alternative splicing allows for the increased transcriptome and proteome diversity by producing more mRNA products from a single gene (Maor et al., 2015), leading to increased phenotypic diversity (Wang et al., 2016). It has been shown that in other eukaryotes, such as humans, honey bees, *Arabidopsis* and rice, that there was an increase in methylation in the exons compared to the flanking introns. This notably caused an effect on the splicing of alternative exons and a loss of methylated CpG sites linked with change in the proportion of alternative splicing (Wang et al., 2016).

However, this is not the case in all fungi. In the yeast, *Candida albicans*, Mishra et al. (2011) showed that only six out of the 150 methylation-associated genes contained introns. The methylation they detected did not mark the intron-exon boundaries, therefore would not regulate alternative splicing in *C. albicans*. The majority of their DNA methylation was observed within coding regions which upon further investigation, Mishra et al. (2011) found that the methylation detected was associated with

transcriptional repression of the linked gene. This is in contrast to the data presented here from *Trichoderma*, as out of the DMCs within gene bodies and the proximal genes to the DMRs, only 34 and four did not contain any introns. Additionally, there was not an increase the number of single exon genes that were associated with the DMCs or DMR in either the parent or regenerant.

4.4.3 Functional annotation of differentially methylated associated genes

The functional annotation of differentially methylated associated genes, through both GO and KEGG classifications further revealed that there were no major changes in groups of the hypermethylated genes between the parental strain and the regenerant. It was hypothesised that the regenerant or parent, depending on the function of intragenic methylation, may have more differentially methylated associated genes related to transport, in particular, copper ion transport genes, to explain the tolerance to copper. The GO groups that had the highest frequency of DMC associated genes were very similar between the two, which consisted of lipid metabolism, vesicle-mediated transport, response to stress and microtubule-based movement. Within the KOG classification, the regenerant had more DMC associated genes in the intracellular, trafficking, secretion and vesicular transport group (cellular processing and signalling) with twelve genes compared to only seven in the parent. This could be of interest as these DMC associated genes within this group can be involved in directing movements of proteins in a cell, from one side of a membrane to another, suggesting that there may be a higher frequency of protein transport occurring in either the parent or the regenerant. However, it is important to note that the lack of known genes within this data is not evidence of the absence of DNA methylation for this particular function between the protoplast regenerant and its parent.

4.4.4 Differences between the two analysis types (DMR vs DMC)

The two differential methylation analyses, DMCs (methylKit) and DMRs (DMAP), showed contrasting differences in the calling of differential methylation. One would expect a higher number of DMCs compared to DMRs because each DMR could contain several differentially 5mCs. However, in this dataset, there were only three methylation-associated genes that were shared between the two, and none of the genes that had multiple DMCs were included on that list. This does raise a concern as typically performing different analyses on the same dataset gives similar results. Stockwell et al. (2014) upon publishing DMAP, compared the differential methylation between DMAP, methylKit (version 0.5.7) and BiSeq (version 1.2.4), another differentially methylated region program, between a test dataset on the human chromosome 1 for both a control and diseased sample. They found that DMAP produced 367 DMRs, methylKit 937 DMCs and BiSeq 402 DMRs respectively. Overall 157 sites were found to be shared between the three different programs. In particular, when looking at the individual methylation coordinates, 318 of the 935 DMCs (found within methylKit) overlapped with the CpGs contained in the DMRs that DMAP produced in its output (Stockwell et al., 2014).

There are opposing thoughts on the different analyses type. Stockwell et al. (2014) suggest that the investigation of a large number of CpG sites greatly enhances the false discovery rate. This is as variation at single sites is greater than that of a contig of sites because the relatively lower coverage per site increases the sampling variation (Ehrlich and Lacey, 2013). However, a DMC approach is considered more useful when a smaller number of 5mC sites are analysed (Stockwell et al., 2014). Further, if a small region is variable (differentially methylated) between individuals the use of a 1000 bp or longer window might dilute this variation (Ehrlich and Lacey, 2013). Therefore methylation might be not be detected if a large window size is used. It is important to note that the WGBS analysis workflow that was used for detecting fungal methylation in the parent and regenerant, in the DMAP context is primarily designed for mammalian methylation, which is heavy in CpG and rarely in non-CpG context (~3%). This is different to fungal methylation where 5mC sites are found in all sequencing contexts that vary slightly in preference (CpG, CHG or CHH) between species. Here the DMC data showed there was a preference for non-CpG methylation. Furthermore, *Trichoderma* has a much smaller genome (~36.1 Mb) compared to other higher eukaryotes so subtler differences may have been missed when using the 1000 bp window.

Additionally Darrell Lizamore used both paired-end reads for the methylKit analysis, whereas Peter Stockwell only used the forward-read for DMAP. Paired-end sequencing is known to reduce the error rate and enhance the sensitivity of both read mapping and methylation level estimation, especially in repetitive regions (Tsuji and Weng, 2015). Although *Trichoderma* tend to have a low number of repetitive regions (Kubicek et al., 2011), the extra sensitivity for low differential methylation would be crucial, as fungi in general tend to have low levels of global methylation (0.07-1.5% (Zemach et al., 2010)). This shows how variable different analyses methods can be, as all analyses are composed of many steps, which includes: adapter removal, read quality trimming, read mapping, post-alignment filtering, sample heterogeneity assessment and identification of differentially methylated regions between two conditions. Tsuji and Weng (2015) showed over 192 different combinations between three pre-processing (read quality trimming), five mapping and two post-processing (post-alignment read filtering) methods.

4.4.5 Limitations of this methylome data

It is important to note that 5mC DNA methylation is only one level of multi-layered epigenetic regulation that also includes other forms of DNA modification, histone modifications, chromatin structure and modification and non-coding RNAs (Aramayo and Selker, 2013; Jamieson et al., 2018; Mondo et al., 2017; Strauss and Reyes-Dominguez, 2011). These other forms of modifications could be responsible for the changes seen here in phenotype, despite the lack of any large scale genome recombination. Additional forms of DNA methylation include 5-hydroxymethylcytosine (5hmC) and

N6-methyladenine (6mA), which WGBS does not measure. WGBS cannot distinguish between 5mC and 5hmC DNA methylation. 5hmC is an intermediate in active demethylation, which results from oxidation of 5mC, as well as being a potential stable epigenetic mark (Erdmann et al., 2015). 5hmC is commonly seen in mammalian cells, however it is rarely studied or observed in fungi. Zhang et al. (2014) found three homologues from *Coprinopsis cinerea* of the Ten-Eleven translocation dioxygenases proteins (TET1, 2 and 3), which are responsible for the oxidation of 5mC into 5hmC in mammalian cells. Other fungi, such as *M. robertsii*, *C. militaris* and *Ustilago maydis*, and plants lack genes encoding these TET proteins suggesting some fungi could use other mechanisms to remove 5mC marks (Li et al., 2017b; Wang et al., 2015; Wu and Zhang, 2010; Yaish et al., 2018). This is further supported by the overall changes in 5mC sites seen in these aforementioned fungal methylomes were not simply due to the loss of methylation in pre-existing 5mC sites, but rather a dynamic process in which loss of methylation occurred with the gain of methylation in other sites. This raises the potential that here, along with other fungi, that the mechanism of both *de novo* and reverse methylation may use another mechanism then what has been observed in other organisms.

A lesser studied modification of DNA involves adding a methyl group to base 6 of adenine (6mA) and has been recently reported in the earliest branches of the fungal kingdom. Using single-molecular real-time (SMRT) sequencing from PacBio, Mondo et al. (2017) analysed 16 genomes from across the fungal phylogeny for the presence of both 5mC and 6mA modifications. They showed very high levels of 6mA in these early-diverging fungi, where up to 2.8% of all adenines were methylated. 6mA has been shown to play a crucial role in both gene and transposon regulation, and in these early groups of fungi, this modification was associated with expressed genes. Interestingly, the presence of 5mC and 6mA seemed to be inversely correlated, with 5mC being found in repetitive regions of the genome and 6mA adenine being clustered in dense methylated adenine clusters (MACs) at gene promoters. Greer et al. (2015) identified 6mA in the nematode *Caenorhabditis elegans*, which was assumed that DNA methylation was absent due to lack of detectable 5mC, as well as homologs of the cytosine DNA methyltransferases. 6mA was found to be spread over the genome between promoters, exons, intron, transcriptional termination sites (TTS), and intergenic regions. Another methylation that has been reported, that of the fourth position of the pyrimidine ring in cytosines (4mC). In prokaryotes, 4mC and 6mA are primarily used for distinguishing self from invasive DNA (Iyer et al., 2011). SMRT sequencing can detect modified bases directly and can further distinguish between these different types of methylation including 5mC, 5hmC and 6mA (Flusberg et al., 2010). The ability to detect 5hmC, among these other DNA methylation types would have allowed a more complete picture of the potential effect that methylation and/or the removal of DNA methylation may have on phenotype and alterations that protoplasting may have.

There are additional limitations of this study compared to other methylome studies, notably with the lack of validation of the bisulphite data. The first limitation is the lack of bisulphite PCR validation of the WGBS data. A number of DNA fragments are normally selected for experimental validation to confirm the results of the bisulphite sequencing. Typically, a high percentage of the originally identified 5mCs are validated (between 95-97%). However, due to the lack of both DMRs and DMCs between the parent and regenerant, combined with the low level of methylation, this traditional bisulphite sequencing validation would be ineffective on this data. The low level of methylation occurring at the individual 5mCs within this dataset would make this particularly difficult (Appendices B.3), i.e. if the methylation percentage was only at 15% across the ten plus reads seen in the WGBS at a single 5mC, the chances would be very low that bisulphite PCR and subsequent sequencing would pick up the 5mC. However, compared to other WGBS data sets that tend only to have one replicate of each different strain/condition, this experimental data set had three replicates per strain which would help to decrease the false 5mC rate.

Some studies also use 5-azacytidine (5-AC), which is a methyltransferase inhibitor, as a confirmation of DNA methylation as it reduces the methylation level in genomic DNA (Lin et al., 2013; Mishra et al., 2011). However, this methylome data between the parent and regenerant does not show significant hyper- or hypomethylation in one strain, making it redundant to use 5-AC as a method to confirm the potential effect of methylation on the phenotype. 5-AC also affects gene expression and chromosome structure as it can disturb fungal development, and is also used for studying secondary metabolites in fungi. This means potentially that any change in phenotype seen may not be directly correlated to the methylation levels seen. In *A. flavus*, 5-AC (at 1mM) can induce a "fluffy" phenotype and prevent aflatoxin production (Lin et al., 2013). This is despite *A. flavus* lacking detectable methylation (Liu et al., 2012), so it is unlikely that the role of 5-AC plays in *A. flavus* is as a DNA methylation suppressor, but more as an inhibitor of the genes involved in the aflatoxin biosynthetic pathway cluster. 5-AC can regulate histones, alter chromatin structure or induce DNA mutation as well (Lin et al., 2013). Lange et al. (2016b) further showed when 5-AC was applied to two sister strains of *T*. sp. "*atroviride* B" at a rate of 1×10^{-4} M 5-AC it affected the phenotype. This was both by reducing the growth rate and also causing a change in the colony morphology pattern to one dissimilar to both non-treated plates. Lange et al. (2016b) hypothesised that cytosine methylation may be the cause of the differences observed in the biocontrol abilities of the strains, however a conclusion was not reached.

4.5 Conclusion

The results of this chapter provide an overview of the methylation dynamics for the potential differences between a protoplast regenerant and its parent. It further represents the first WGBS study, to the best of my knowledge, on a *Trichoderma* species. In this work, ~1.1% of the *T*. sp. "*atroviride* B"

genome is methylated which falls into the range of other reported methylomes for fungi, typically range from 0.07%-1.5%. Although there were no significant variations in the methylation patterns or densities between the parent and regenerant, several interesting trends were observed, which showed hypermethylation subtly occurring in the regenerant. Furthermore, as mentioned above, the absence of known/assumed genes in this data set is not evidence of the absence of the potential effect that methylation has resulting from the protoplast process. As the function of intragenic methylation varies greatly between different fungal species, further work is needed to show the functional consequences of the methylation through RNA sequencing, which will be covered in the next chapter.

Chapter 5

The impact of cytosine methylation on the transcriptional activity of a *Trichoderma* sp. "*atroviride* B" parental and protoplast regenerant strains

5.1 Introduction

The use of protoplast regeneration for strain improvement allows for the screening and selection of specific phenotypes in fungal species, such as fungicide tolerance, which makes it a valuable tool for integration of these biological products into an IPM programme. Despite the frequent use of this technology, the underlying mechanisms of what causes this phenotypic plasticity remains unknown. The results from the previous chapter from the whole genome bisulphite sequencing (WGBS) analysis suggest that one reason for the observed phenotypic modifications could be due to cytosine methylation. Cytosine methylation between fungal species is found in the promoter region, transposable elements, repeat sequences and in the transcribed regions of genes, which suggests that it may have a prominent role in the regulation of gene expression (Jeon et al., 2015; Kim et al., 2018). These varying patterns and roles of differential methylation highlights the important of exploring the functional consequences of cytosine methylation through RNA-sequencing (RNA-seq). RNA-seq has previously been used in methylation studies to validate the functional or biological significance of this modification (Jeon et al., 2015; Wang et al., 2015; Yaish et al., 2018).

As discussed in the previous chapter, the function of cytosine methylation in genes has differing effects on the transcript abundance of genes depending on the species. For example, in *Cordyceps militaris*, hypermethylated genes were found to be downregulated (Wang et al., 2015), whereas in *Metarhizium robertsii* (and in contrast to most other eukaryotes) transcription tended to be enhanced in genes with moderate promoter methylation, while gene expression was decreased in genes with high or low promoter methylation (Wang et al., 2017). In *Magnaporthe oryzae* (Jeon et al., 2015), as well as *Uncinocarpus reesii* (Zemach et al., 2010), methylation occurring upstream or downstream of the gene had a negative effect on the transcript abundance, whereas gene body methylation had a positive effect.

In addition to linking the cytosine methylation data, the use of RNA-seq can also be used to investigate differentially expressed genes potentially caused by other regulatory factors that may also be a consequence of the protoplast process. This study has only investigated this one area (cytosine methylation) of the multi-layered epigenetic regulatory system that may cause this phenotypic

plasticity in lieu of large scale genomic differences. However, other epigenetic factors such as histone modifications and various RNA-mediated processes have all been reported to regulate gene expression (Gibney and Nolan, 2010; Holoch and Moazed, 2015; Jaenisch and Bird, 2003; Soyer et al., 2014). This would enable a closer look at any potential off-target consequences from the use of protoplast technology. This possibility has been raised from the use of PEG-mediated protoplast transformations in fungi. Scala et al. (2017) found significant phenotypic diversity in mutants they generated using this method and postulated this may have resulted from protoplasting. It is crucial to investigate if cytosine methylation, or some other regulatory mechanism, may induce changes in gene activity resulting from the process of protoplast regeneration.

In this chapter, the effect of the differential cytosine methylation observed between the two *Trichoderma* sp. "*atroviride* B" strains (parent FCC237 and regenerant FCC237/R5) on transcript activity was investigated. In particular, the objective was to ascertain the response of the parental and regenerant strains to both PDB amended with a sub-lethal level of copper and a non-amended control (plain PDB). This was accomplished in a RNA-seq experiment to determine the genes that were differentially expressed in these two *T.* sp. "*atroviride* B" strains. In the previous chapter, results indicated that although there were no significant differences in differential methylation with both forms of analyse. There were, however, some subtle occurrences of hypermethylation in the regenerant. Based on the varying effect that (intragenic) cytosine methylation has on different fungal species, or indeed even between plants and mammals, functional characterisation of these changes was needed to elucidate the effects that it may have.

5.2 Materials and methods

5.2.1 Fungal growth for RNA extraction and RNA extraction

Biomass was generated for RNA extraction from 3 d mycelium as described in Chapter 2 (section 2.2.1). Three biological replicates, respectively, for each treatment for the regenerant (*T.* sp. "*atroviride* B" FCC237/R5) and parent (*T.* sp. "*atroviride* B" FCC237), were used for the RNA-seq. The two conditions were either PDB amended with a sub-lethal level (1 mM) of copper sulphate ($CuSO_4.5H_2O$) or non-amended PDB (control). For each replicate, six 50 mL Nunc tubes were used to ensure there was enough mycelial mass, and then combined per replicate. The number of tubes had to be increased compared to the mycelium generated for the WGBS as in 1 mM of copper sulphate the parental strain had restricted growth. Total RNA was extracted using the RNeasy Plant Mini Kit (Qiagen) as per the manufacturer's instructions, except RLC buffer was used rather than RTC due to potential of high quantities of secondary metabolites being found in the mycelia of filamentous fungi and that 700 µL of RLC buffer was used instead of 450 µL. The RNA was then treated with TURBO™ DNase (ThermoFisher). The RNA quality was assessed by gel electrophoresis (2% agarose in TAE; 110 V and

500 mA for 50 min) and by electrophoretic analysis via RNA 600 Nano Chip using the 2100 Bioanalyzer (Agilent Technologies) to obtain an RNA integrity number (RIN). DNA contamination and total RNA concentration was measured with the Quibit™ 3.0 Fluorometer high sensitivity RNA assay, as per manufacturer's instructions.

5.2.2 RNA-seq library construction and sequencing

The cDNA libraries preparation was performed by Novogene Co., Ltd (Hong Kong) using a NEBNext® Ultra™ RNA Library Prep kit (New England Biolabs, USA) and sequenced by Novogene Co., Ltd, using the Illumina® HiSeq 2500 sequencing system. The samples were sequenced on a single sequencing lane with 150 paired-end reads being generated for the respective samples.

One of the replicates for the parental strain in control (plain PDB) (par_p3) did not pass quality control upon arrival to Novogene as it had an unexplained low concentration. This meant that only eleven samples were sequenced; three replicates for three of the treatments (parent copper amended PDB, regenerant control PDB, regenerant copper amended PDB), and only two for parent control PDB.

5.2.3 RNA-seq analysis

The NGS data was analysed by bioinformaticians at Novogene Co., Ltd (Hong Kong). The following methods description is a summary based on their report with additional detail (for original report, see Appendices C.1). Anything in *italics* is verbatim from their report.

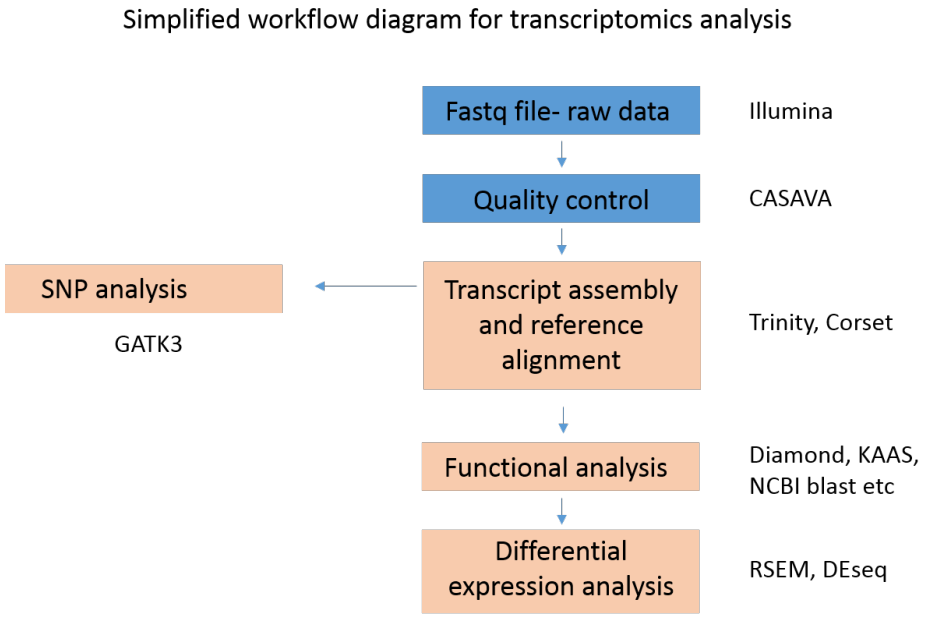

Figure 5.1 A simplified diagrammatic outline of the workflow used in this transcriptomic analysis without a reference sequence by Novogene. Fastq files are the Illumina sequencing output file. Functional analysis used a variety of programs including Diamond, KAAS, NCBI blast among others (see section 5.2.4.3 for full list of the seven databases).

5.2.4 Analysis of Read Data

5.2.4.1 Quality control

Fastq output files were analysed with CASAVA v1.8 software to confirm sequence quality. Briefly, *the raw reads were filtered to remove reads containing adapters or reads of low quality. Reads of low quality are defined as: when uncertain nucleotides constitute more than 10% of either read (N > 10%) or when low quality nucleotides (base quality less than 20) constitute more than 50% of the read.* The error rate (based on the Phred score) and GC content distribution were also analysed.

5.2.4.2 Transcriptome assembly

Clean reads were de novo assembled by Trinity (Grabherr et al., 2011) *to get an assembly transcriptome. The workflow consisted of Inchworm, Chrysalis and Butterfly. Inchworm constructed a k-mer dictionary from all sequenced reads (k=25) and then selected the most frequent seeded k-mer in the dictionary and extended the seed in each direction to form a contig assembly. Chrysalis then clustered minimally overlapping Inchworm contigs into sets of connected components, and constructed a complete de Bruijn graph for each component. Each component defined a collection of Inchworm contigs that are likely to be derived from alternative splice forms or closely relation paralogs. Butterfly then reconstructed plausible, full-length transcripts by reconciling the individual de Bruijn graphs generated by Chrysalis with the original reads and paired ends. It reconstructed distinct transcripts for splice isoforms and paralogous genes, and resolved ambiguities stemming from errors or from sequences >k bases long that are shared between transcripts. Corset v1.05 (-m 10)* (Davidson and Oshlack, 2014) *then performed hierarchical clustering to remove any redundancies. After this, the longest transcript of each cluster was selected as unigenes.*

5.2.4.3 Gene functional annotation

The expressed genes were analysed for matches to known proteins. The seven databases applied by Novogene (Table 5.1) were: Nr (NCBI non-redundant protein sequences), Nt (NCBI nucleotide sequences), Pfam (protein family), KOG (EuKaryotic Orthologous Groups, which are based on NCBI's gene orthologous relationships), Swiss-Prot (a manually annotated and reviewed protein sequence database), KEGG (Kyoto Encyclopedia of Genes and Genomes, which is a database resource for understanding high-level functions and utilities of the biological system) and GO (Gene Ontology, functional annotations of gene products). Any unannotated DEGs were also manually searched in InterPro protein family database (Finn et al., 2016) and had their sequence blasted into the gene models from *Trichoderma atroviride* v2.0 genome (https://genome.jgi.doe.gov/pages/search-for-genes.jsf?organism=Triat2) on JGI.

Table 5.1 Databases used by Novogene Ltd for the gene functional annotation analysis.

Database	Software	Version	Parameter
Nr, KOG, Swiss-Prot	Diamond (Buchfink et al., 2015)	v0.8.22	NR, Swiss-Prot: e-value=1e-5; KOG: e-value 1e-3
KEGG annotation	KAAS (Moriya et al., 2007)	r140224	e-value= 1e-10
Nt annotation	NCBI blast (Altschul et al., 1997)	v2.2.28+	e-value= 1e-5
Pfam annotation	Hmmscan (Finn et al., 2015)	HMMER 3	e-value= 0.01
GO annotation	blast2go (Götz et al., 2008)	b2g4pipe_v2.5	e-value=1.0E-6

5.2.4.4 Single nucleotide polymorphisms (SNPs)

To ensure that single nucleotide polymorphisms (SNPs) were not responsible for the phenotypic variation seen between the parent and regenerant, SNP locations were examined in the RNA sequencing data. Samtools and Picard were used initially to sort the reads according to genome coordinates, followed by screening out repeated reads. GATK3 (Van der Auwera et al., 2013) was then used to carry out SNP calling. After the initial list was produced, the SNPs needed to be validated empirically. The SNPs had to i) be represented by at least eight reads, ii) occur at a position covered by at least eight reads in every other sequenced strain, iii) not have missing data in the reference strain and iv) differ from the reference strain. Additionally, they had to be present in all of the replicates of one treatment and none in the others conditions or treatments. SNP validation is needed as most SNPs will not validate as they occur within microsatellites or homopolymer runs and are therefore unreliable. Others are miscalled insertions, deletions or simple missequencings. As always, it is important to note that strict SNP calling thresholds mean that not all SNPs will have been identified here. Absence of a SNP is not proof of absence.

5.2.4.5 Differential expression analysis

RSEM (Li and Dewey, 2011) was used to map reads back to the reference transcriptome and quantify the expression level. The *de novo* transcriptome filtered by Corset was used as the reference transcriptome. *To calculate the gene expression level, RSEM analysed the mapping reads of Bowtie and gathered the read count per gene for each sample.* The program converted the read counts into a FPKM (fragments per kilobase of transcript sequence per millions of base pairs sequenced) value. Novogene used a threshold of FPKM>0.3 to denote if a gene is expressed. *The FPKM value is a very common*

method of estimating gene expressing levels, as it takes into account the effects of both sequencing depth and gene length when counting the fragments.

The read count value that was obtained from the gene expression analysis was used as the input to do the differential expression analysis. DESeq (Anders and Huber, 2010) was used to do the analysis and is based on the negative binomial distribution. To identify significant differentially expressed genes (DEGs), a $\log_2$ transformation was applied to the fold change (group1/group2- which is all cases in this chapter was the regenerant/the parent). A higher $\log_2$ fold change correlated to larger difference in expression level. The level of significant differences can be detected by the *p* value. To eliminate biological variation, the threshold was set at $p<0.05$. In order to analyse the biological function of the high confidence DEGs provided by Novogene, the data from the transcriptomic comparisons' were divided into multiple gene sets of either upregulated or downregulated DEGs.

5.3 Results

5.3.1 Data quality control, transcript assembly and RNA-seq QC

The number of transcripts produced by both Trinity/Corset and Unigene were very similar, with only thirteen transcripts differing between the two (number of total: transcripts- 25464, unigene- 25451; mean length: transcripts- 1672, unigene- 1673; N50: transcripts- 2513, unigene- 2514 N90: transcripts- 766, unigene- 766). The Unigene assembly was used for any additional analysis as it consists of the longest transcript of each gene. There is a higher level of unigenes as there can be numerous unigenes for a single gene spreading across the exons. These unigenes can include alternative splicing and alleles which accounts for the differences in transcripts.

The sample correlation between the replicates was calculated using the Pearson correlation coefficient. The closer the correlation coefficient is to 1, the greater the similarity of the samples. The square of the Pearson correlation coefficient should be larger than 0.92, however in some replicates, that was not the case. The lowest coefficient was 0.907 between one of the replicates for the regenerant in the control conditions.

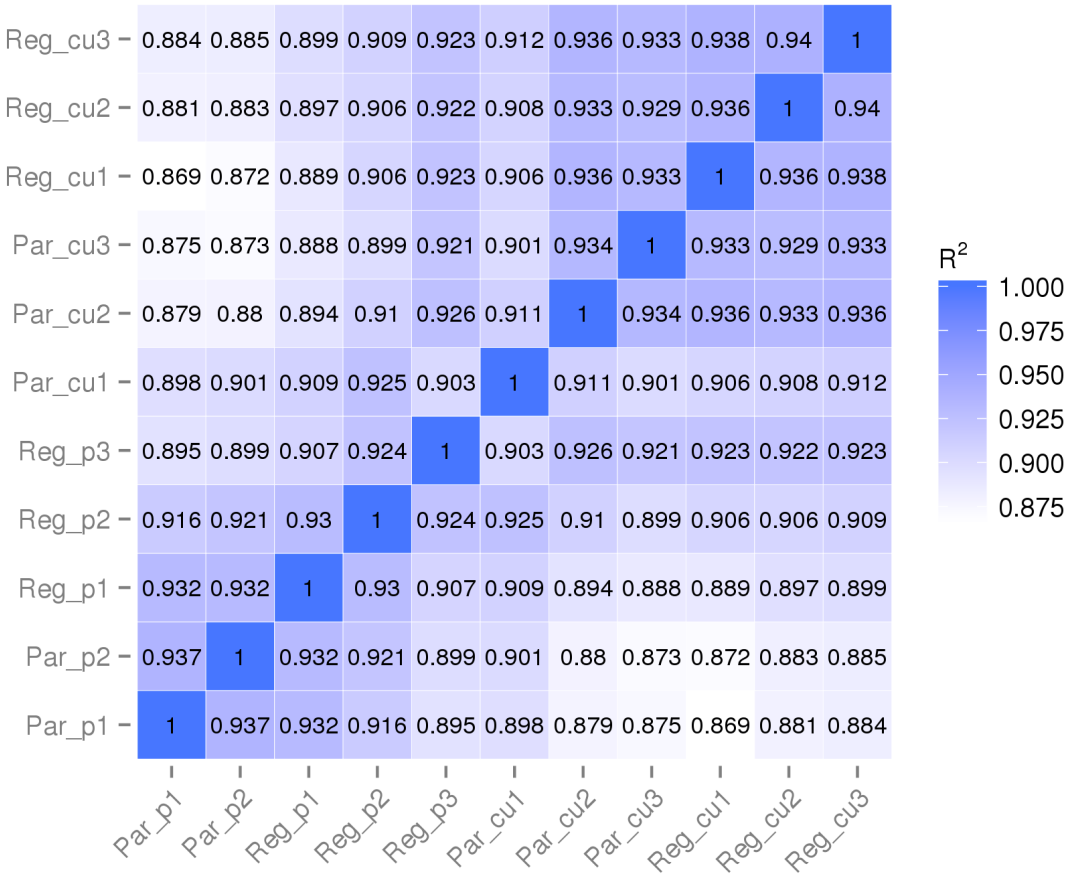

Figure 5.2 The R^2 of the Peason correlation coefficient of the samples for RNA-seq. R^2 is the square of the Pearson coefficient. Figure produced by Novogene.

5.3.2 Differential gene expression and gene ontology analysis

From the comparisons of the read count values from the gene expression analysis, a list of significant (p<0.05; minimum $\log_2$ fold change) DEGs obtained for the respective treatment comparisons were made. Again, to identify significant DEGs, a $\log_2$ transformation was applied to the fold change (group1/group2- which is all cases in the analysis was the regenerant/the parent). For the purpose of this study, the comparisons between reg_cu vs par_cu (copper amended PDB) and reg_p vs par_p (control- plain PDB) were looked at in more detail (see sections 5.3.2.2 and 5.3.2.3 below). For this study, tables listing only known (annotated) transcripts were produced. These tables contain all significant DEGs (high to low confidence, to the 5% level) for upregulated and downregulated transcripts of the regenerant relative to the parent. To reiterate, the comparisons of the transcript levels solely in response to copper were not the focus of this study, but rather the differences (if any) in gene expression in the same condition as a result of protoplast regeneration. Figure 5.3 shows an overview of the significantly DEGs through volcano plots, which are used to infer the overall distribution of the DEGs. Figure 5.4 shows the cluster analysis of DEGs. In this hierarchical clustering, areas of different colours denote different genes, and genes within each cluster may have similar functions. There are varying trends of DEGs spread across the different groups.

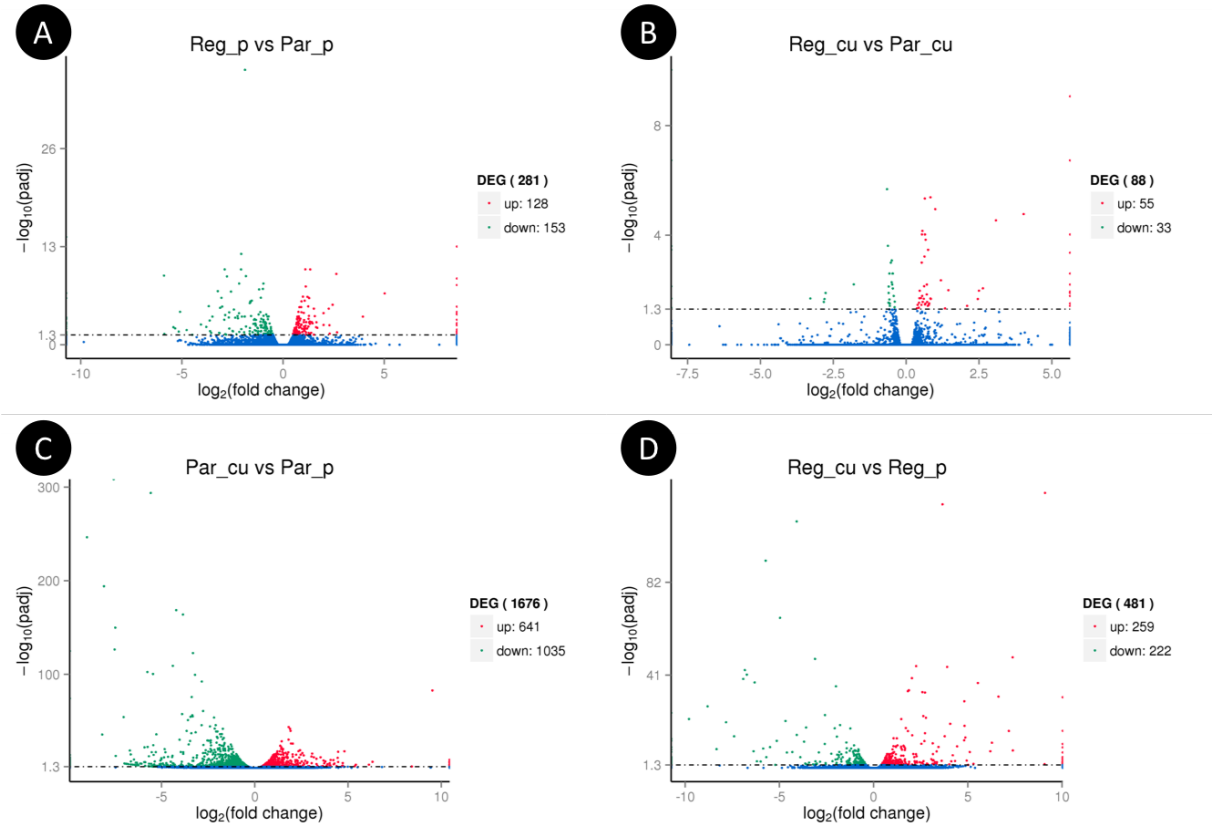

Figure 5.3 **Volcano plots of the differentially expressed genes between the four different comparisons. (A) Regenerant versus parent in plain PDB (control), (B) regenerant versus parent in copper amended PDB, (C) parent in plain PDB (control) versus copper amended PDB, (D) regenerant in plain PDB (control) versus copper amended PDB. Volcano plots show the log_2(fold change) vs the log_{10}(padj), points with more fold change and higher log_{10}(padj) are more reliable. Log counts are the log of the read counts mapping to each gene. Log_2(fold change) indicates the log of the change in expression of the regenerant compared to the parent. The log_2(fold change) [x-axis] represents the gene expression change of the different transcripts. The -log_{10}(padj) [y-axis] is the p-value after normalisation. The greater the -log_{10}(padj) is, the more significant the difference is. The significant differential up regulated genes were represented by red dots, the green dots represented the significant differential down regulated genes and the blue dots were no difference. Figure produced by Novogene.**

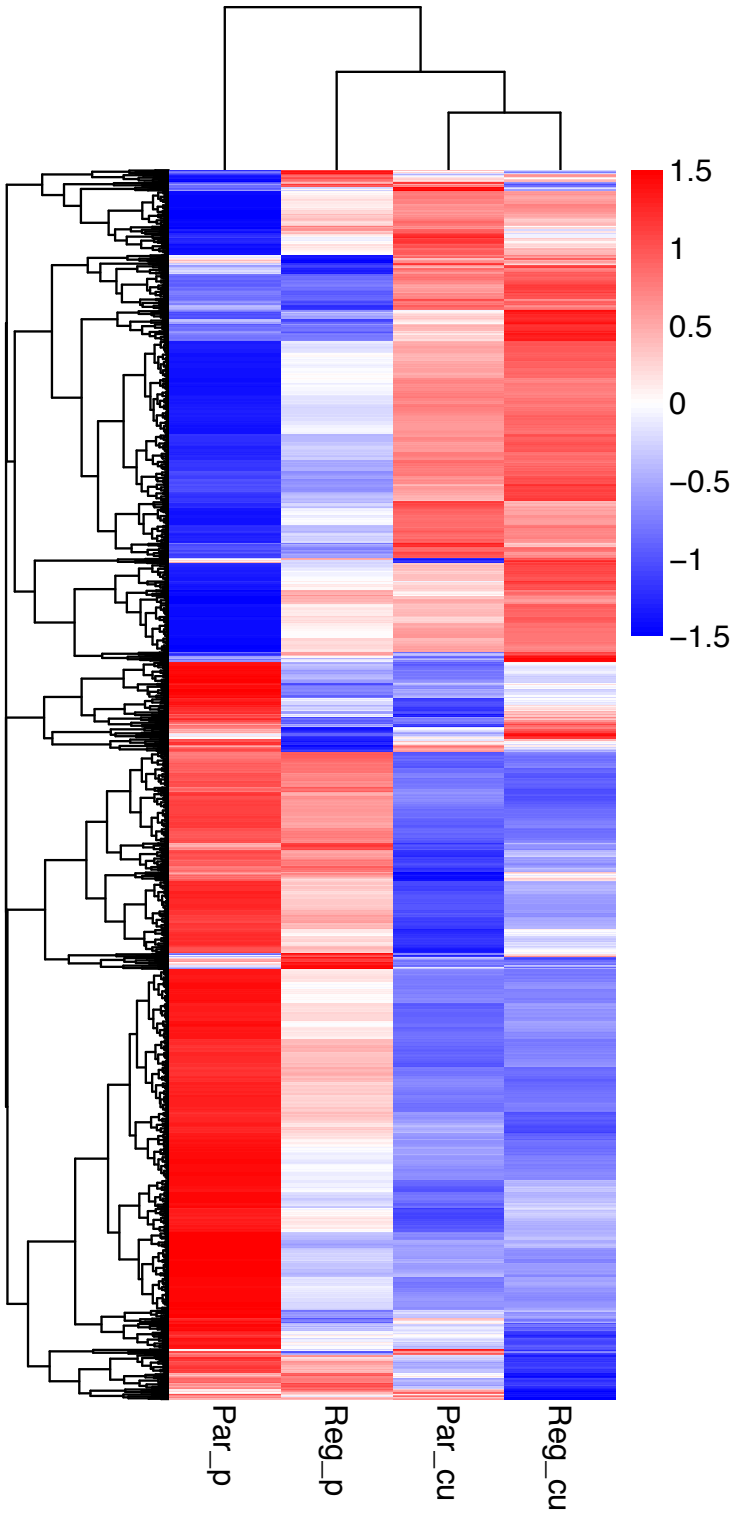

Figure 5.4 **Hierarchical cluster analysis of differentially expressed genes. The overall result of the FPKM (fragments per kilobase of transcript sequence per millions of base pairs sequenced) cluster analysis, clustered using the $\log_{10}$ (FPKM+1) value. Red denotes upregulated genes ad blue denotes downregulated genes. The colour range from red to blue represents the $\log_{10}$ (FPKM+1) value from large to small. Figure produced by Novogene.**

5.3.2.1 Effects of differential methylation on transcription levels

To elucidate the relationship between cytosine methylation and gene expression, the differentially methylated associated genes (from both analysis methods from Chapter 4 [section 4.2.3]) were compared with both up and downregulated genes respectively over two different conditions. The two conditions were sub-lethal levels of copper sulphate in PDB (1 mM) and plain PBD (control). No differentially methylated regions (DMRs) (section 4.3.1, Table 4.1) contained any DEGs compared to both the copper amended broth and the control broth. In the sub-lethal level of copper, two upregulated genes (in relation to the regenerant) were found among the 218 differentially methylated cytosine (DMC)-associated genes, with both DMCs being hypermethylated (increase in cytosine methylation) in the parent. In the control (plain PDB), four upregulated and three downregulated genes were found, with a mix of parental or regenerant hypermethylation occurring. However, the majority of these differentially expressed DMC-associated genes had very low methylation occurring, and no trend occurring in any one treatment were found among these nine differentially expressed genes. Therefore, it is difficult to generate a clear idea about the effect of cytosine methylation on gene expression using the available set of data from this study. This dataset does suggest there is no correlation between the two.

It is important to note that TA_79893 shows up both in the control upregulated dataset and the control downregulated dataset. This is due to two separate transcript clusters being associated with this protein ID from the numerous blast datasets. For the control upregulated transcripts, it is associated with cluster-6987.11652 (read counts regenerant: 146.22, parent: 0) and for the control downregulated transcripts, cluster-6987.11653 (read counts regenerant: 62.83, parent: 223.81). The cluster number above is the equivalent transcript produced from Unigene that Novogene used to identify each transcript. The DMC was found within the gene body at a very low percentage (6.04% hypermethylated in the regenerant).

Table 5.2 Differentially expressed and differentially methylated cytosine's (DMCs)-associated genes in the parent and regenerant strains of *Trichoderma* sp. *"atroviride* B" in sub-lethal levels of copper sulphate (1 mM) amended PBD and the control (plain PDB).

Protein ID[1]	Putative function	DMC location	Differential methylation %[2]	Log_2 fold change[3]	Padj
Copper upregulated					
TA_322377	von Willebrand factor and related coagulation proteins	Gene body	5.77% P	0.50697	0.019892
TA_161203	Hypothetical protein with similarity to Trs120 of the transport protein particle (TRAPP) complex	67 bp upstream	4.89% P	0.78031	0.034597
Control upregulated					
TA_79893	SWR1-complex protein 4	Gene body	6.04% R	Inf	9.53E-14
TA_93282	No putative conserved domains	749 bp upstream	7.42% P	Inf	0.046134
TA_217932	Domain of unknown function (DUF4112)	258 bp downstream	5.35% P	1.0224	6.07E-05
TA_149409	Magnesium transporters: CorA family	719 bp downstream	2.90% P	0.68332	0.028009
Control downregulated					
TA_79893	SWR1-complex protein 4	Gene body	6.04% R	-1.8326	0.0037759
TA_174054	TAP-like protein (ABC transporter)	Gene body	19.61% P	-0.60408	0.0075989
TA_219478	Fasciclin-like (FAS1) domain	Gene body	8.05% R	-1.1869	0.049724

[1] Origin of the protein ID numbers are from *Trichoderma atroviride* v2.0 https://genome.jgi.doe.gov/pages/search-for-genes.jsf?organism=Triat2

[2] P represents hypermethylation in the parental strain, R represents hypermethylation in the regenerant strain

[3] Log_2 fold change is the log fold change in the regenerant as compared to the parent. For the proteins with "Inf" in this column, there was no transcript activity in the one of the strains, meaning the log change is indefinite. Note for the log_2 fold change values that are shown as a negative value it reads as 'how downregulated is the regenerant compared to the parent' i.e. for protein ID TA_174054 the regenerant has –0.6 expression compared to the parent.

5.3.2.2 Differential transcript activity between parent and regenerant in sub-lethal levels of copper sulphate (1 mM)

The list of DEGs obtained between the parent and regenerant in the sub-lethal levels of copper sulphate consisted of 88 transcripts. Of these, 55 were upregulated in the regenerant (62.5%) compared to the parent and 33 (37.5%) transcripts were downregulated in the regenerant, again, compared to the parent. From the putatively 'upregulated' set, three transcripts were unable to be annotated, six transcripts contained no putative conserved domains, and 46 transcripts were encoding conserved proteins. In all conditions, for the transcripts that were unable to be annotated from Novogene, the sequences were manually blasted against the *T. atroviride* IMI206040 genome in JGI from using megablast in Geneious (v10.2.4). From the putatively 'downregulated' set, two transcripts were unable to be annotated, five transcripts contained no putative conserved domains, and the remaining 26 transcripts contained conserved proteins. Table 5.3 lists known and upregulated gene transcripts, Table 5.4 lists known and downregulated gene transcripts. Descriptions of suggested associated putative gene function are included (column 2 of each table) for the comparison. Interestingly, among these, ten (seven upregulated and three downregulated) transcripts were differentially expressed in both the comparisons (copper and control). These DEGs were of particular interest as they were in both conditions with the same activity, suggesting that they may be a direct consequence of protoplasting. Additionally, the read counts from the DEGs can be found in Appendices C.1.

Table 5.3 Significantly upregulated genes in the regenerant strain compared to the parent of *Trichoderma* sp. *"atroviride* B" in sub-lethal levels of copper sulphate (1 mM) amended PDB. Bold entries are also present in the upregulated control dataset.

Protein ID[1]	Putative function	Log_2 fold change[2]	padj
Transcription/DNA metabolism			
TA_321361	**mRNA splicing factor ATP-dependent RNA helicase**	**2.5006**	**0.010684**
TA_295745	Fungal specific transcription factor domain	2.0931	0.038081
TA_46772	DEAD/DEAH box helicase	1.1919	0.0044385
TA_91311	Fibrillarin and related nucleolar RNA-binding protein	1.0002	1.12E-05
TA_90402	Transcriptional activator FOSB/c-Fos and related bZIP transcription factors	0.74641	0.038081
TA_296913	Protein involved in sister chromatid separation and/or segregation	0.60637	0.021046
TA_309419	KEKE-like motif-containing transcription regulator (Rlr1)/suppressor of sin4	0.43241	0.044552
Secondary metabolites			
TA_150983	Acyl-CoA synthetase (related to CoA ligase)	2.6325	0.0087134
TA_295408	Nitronate monooxygenase	2.4581	0.021432

TA_182330	Methyltransferase type 11	1.3328	0.047138
TA_54816	Short chain dehydrogenase	0.83263	0.020454
TA_318290	**Non-ribosomal peptide synthetase/ ferrichrome synthetase**	**0.72358**	**0.027223**
TA_233820	Amidases	0.71028	0.0063435
TA_297716	Uridine 5'- monophosphate synthase/orotate phosphoribosyltransferase	0.56853	0.027386
TA_50326	Coezyme A transferase	0.54868	0.0165
TA_221418	NADH: flavin oxidoreductase	0.54345	9.40E-05
TA_299967	Cys 3 (cystathionine gamma-lyase)	0.53506	0.0010037
TA_38111	Indoleamine 2,3-dioxygenase	0.5259	0.035047
TA_43598	**Cytochrome P450 CYP4/CYP19/CYP26 subfamilies**	**0.45709**	**0.019962**
TA_297703	Putative aminotransferase	0.44115	0.029221
Transporters			
TA_131476	Predicted transporter (major facilitator superfamily)	Inf	1.86E-07
TA_316915	Vacuolar protein sorting-associated protein	Inf	0.031151
TA_262794	OPT oligopeptide transporter protein	Inf	0.031151
TA_152585	Half-sized multidrug resistance protein, ABC superfamily	1.4504	0.010197
TA_201457	Predicted transporter (major facilitator superfamily)	0.79177	0.031151
TA_161203	Hypothetical protein with similarity to Trs120 of the targeting complex (TRAPP) complex	0.78031	0.034597
TA_131960	**Hypothetical ferrioxamine B transporter, major facilitator superfamily**	**0.6316**	**0.00060089**
Stress response/protectors			
TA_315943	PB1 domian (found within NoxR)	Inf	0.012893
TA_53983	FOG: Zn-finger (similarity with Rpn4)	0.83404	4.16E-06
TA_80276	**Rogdi leucine zipper containing protein**	**0.75467**	**0.0003426**
TA_83501	FK506 suppressor Sfk1	0.66783	0.00014656
TA_203336	Molecular chaperone (DnaJ superfamily)	0.64609	9.40E-05
TA_39628	**Glycerol kinase**	**0.64087**	**4.59E-06**
TA_299551	Mannitol dehydrogenase C-terminal domain	0.39793	0.035047
Others			
TA_248609	Glycoside hydrolase family 3 protein	Inf	0.00043822
TA_82772	Glycoside hydrolase family 36 protein	Inf	0.0165
TA_87599	Condensation domain	Inf	0.038081
TA_316153	P-loop NTPase domain superfamily	4.0308	1.70E-05
TA_284709	Uncharacterised conserved protein similar to ATP/GTP-binding protein	3.0802	2.88E-05
TA_47188	WD40 repeat	0.84521	0.021318
TA_173538	Cyclin	0.70703	0.01456
TA_155595	Pal1 cell morphology domain containing protein	0.64552	0.033901
TA_236267	SYLF domain containg protein (DUF500)	0.6183	0.0073444

TA_90885	**Nucleolar GTPase/ATPase p130**	**0.46423**	**0.010684**
TA_302072	C-type lectin	0.36676	0.046663

[1] Origin of the protein ID numbers are from *Trichoderma atroviride* v2.0 https://genome.jgi.doe.gov/pages/search-for-genes.jsf?organism=Triat2

[2] Log_2 fold change is the log fold change in the regenerant as compared to the parent. For the proteins with Inf in this column, there was no transcript activity in the parent, meaning the log change is indefinite.

Table 5.4 Significantly downregulated genes in the regenerant strain compared to the parent of *Trichoderma* sp. *"atroviride* B" in sub-lethal levels of copper sulphate (1 mM) amended PDB. Bold entries are also present in the downregulated control dataset.

Protein ID[1]	Putative function	Log_2 fold change[2]	padj
Stress response/protectors			
TA_152868	Hypothetical histidine kinase HHK6	-Inf	0.0204
TA_161047	Copper chaperone for superoxide dismutase	-0.5747	0.00252
TA_146625	**Stress-response A/B barrel domain**	**-0.574**	**0.02222**
TA_298587	Cytochrome c oxidase assembly protein PET191	-0.4988	0.00525
Ribosome biogenesis/translation			
TA_297753	40S ribosomal protein S10	-0.6579	2.10E-06
TA_298008	60S ribosomal protein L28	-0.626	0.00024
TA_259578	60S ribosomal protein L38	-0.6051	0.02911
TA_298659	60S acidic ribosomal protein P2	-0.6016	0.01289
TA_148397	40S ribosomal protein S13	-0.5243	0.001
TA_300838	40S ribosomal protein S28	-0.4932	0.00084
TA_260382	Ubiquitin-like/40S ribosomal S30 protein fusion	-0.4778	0.00634
TA_254353	40S ribosomal protein S29	-0.4661	0.00252
TA_302500	60S ribosomal protein L31	-0.4561	0.00252
TA_257160	60S ribosomal protein L44	-0.3973	0.04251
Transcription/DNA metabolism			
TA_11002	SNF2 family N-terminal domain	-Inf	0.00034
TA_161417	Sirtuin 5 and related class III sirtuins (SIR2 family)	-Inf	1.86E-07
TA_295745	Fungal specific transcription factor domain	-3.2903	0.02045
TA_297966	Histone H4	-0.4588	0.00888
Other			
TA_231508	Myosin class II heavy chain	-Inf	9.21E-11
TA_214230	Glycoside hydrolase family 79 protein	-Inf	0.00025
TA_133870	Glycoside hydrolase family 18 protein	-Inf	0.04454
TA_161270	Myosin class II heavy chain	-2.8261	0.02739
TA_161159	Glycoside hydrolase family 3 protein	-2.802	0.02143
TA_299415	**YjeF-related domain containing protein**	**-1.7982**	**0.00625**
TA_159580	**Predicted small secreted cysteine-rich protein (killer toxin)**	**-0.5681**	**0.03115**

TA_131179	Acyl-CoA acyltransferase	-0.5635	0.03115

[1] Origin of the protein ID numbers are from *Trichoderma atroviride* v2.0 https://genome.jgi.doe.gov/pages/search-for- genes.jsf?organism=Triat2

[2] Log_2 fold change is the log fold change in the regenerant as compared to the parent. For the proteins with -Inf in this column, there was no transcript activity in the regenerant, meaning the log change is indefinite. Note for the log_2 fold change values that are shown as a negative value it reads as 'how downregulated is the regenerant compared to the parent' i.e. for protein ID TA_295745 the regenerant has –3.2903 expression compared to the parent.

5.3.2.3 Differential transcript activity between parent and regenerant in the control (plain PDB)

The list of DEGs obtained between the parent and regenerant in the control (plain PDB) consisted of 281 transcripts. Of these, 128 were upregulated in the regenerant (45.5%) compared to the parent and 153 (54.5%) transcripts were down regulated in the regenerant again, compared to the parent. From the putatively 'upregulated' set, four transcripts were unable to be annotated, 14 transcripts contained no putative conserved domains, and 111 transcripts contained conserved proteins. From the putatively 'downregulated' set, 23 transcripts were unable to be annotated, 14 transcripts contained no putative conserved domains, and 136 transcripts contained conserved proteins. Table 5.5 lists the top 50 known and upregulated gene transcripts and Table 5.6 lists the top 50 known and downregulated gene transcripts. Descriptions of suggested associated putative gene function are included (column 2 of each table) for the comparison. The full lists are available in Appendices C.2 and C.3, which includes the non-annotated transcripts and transcripts with no putative conserved domains. Additionally, the read counts from the DEGs can be found in Appendices C.1.

Table 5.5 Top 50 most upregulated genes of the regenerant strain compared to the parent of *Trichoderma* sp. *"atroviride* B" in the control (plain PDB). Bold entries are also present in the upregulated sub-lethal levels of copper sulphate dataset.

Protein ID[1]	Putative function	Log_2 fold change[2]	padj
Transcription/DNA metabolism			
TA_79893	SWR1-complex protein 4	Inf	9.53E-14
TA_245214	Structural maintenance of chromosome protein 4 (chromosome condensation complex Condensin, subunit C)	Inf	1.69E-09
TA_175873	Protein involved in sister chromatid separation and/or segregation / WLM domain	Inf	1.22E-08
TA_299841	Transcription factor TCF20	Inf	4.47E-05
TA_12417	Fungal specific transcription factor domain	Inf	0.002077
TA_204552	DNA polymerase theta/eta, DEAD-box superfamily	Inf	0.0097
TA_286297	Predicted histone tail methylase containing SET domain	Inf	0.038263
TA_321361	**mRNA splicing factor ATP-dependent RNA helicase**	**3.9453**	**0.000187**
TA_318116	DEAH-box RNA helicase	2.0016	0.002362

TA_53890	Splicing coactivator SRm160/300, subunit SRm300	1.5191	0.046859
TA_224741	GATA-4/5/6 transcription factors	1.3289	0.001682
TA_219144	tRNA(Ile)-lysidine synthase	1.2505	0.003888
Secondary metabolites			
TA_214849	Phospholipase D	Inf	8.78E-06
TA_138092	FAD dependent oxidoreductase	2.2593	1.65E-05
TA_294099	Predicted AdoMet-dependent methyltransferase	2.2923	0.002566
TA_318290	**Non-ribosomal peptide synthetase/ ferrichrome synthetase**	2.0007	6.52E-05
TA_161189	Ferric reductase NAD binding domain//FAD-binding domain	1.3873	0.026052
TA_37736	Flavin-containing monooxygenase	1.3414	1.04E-10
TA_273644	Acyl transferase domain	1.2648	0.026858
TA_41287	Conserved hypothetical protein similar to ferric/cupric reductases	1.1167	0.003095
TA_43598	**Cytochrome P450 CYP4/CYP19/CYP26 subfamilies**	**1.1439**	**0.001019**
Transporters			
TA_320809	Metal ion transporter CorA-like divalent cation transporter superfamily (Mg^{2+} and Co^{2+} transporter)	Inf	0.048047
TA_80187	Carbohydrate-binding module family 1	5.0182	1.58E-07
TA_39549	Predicted transporter (major facilitator superfamily)- siderophore	1.1863	0.007024
TA_131960	**Hypothetical ferrioxamine B transporter, major facilitator superfamily**	1.2787	0.00015
TA_82465	High-affinity iron permease-like protein	1.6349	0.00477
TA_172844	C_2H_2 Zn-finger protein	1.3295	0.040437
TA_219088	Predicted transporter (major facilitator superfamily)- siderophore	1.2888	6.55E-07
TA_149087	Permease of the major facilitator superfamily	1.2591	0.000363
Stress response/protectors			
TA_39628	**Glycerol kinase**	**1.4545**	**0.001413**
TA_80276	**Rogdi leucine zipper containing protein**	**1.3195**	**0.000837**
TA_39628	**Glycerol kinase**	**1.5705**	**0.000162**
Others			
TA_298699	M6 family metalloprotease domain-containing protein	Inf	0.000478
TA_88959	**Nucleolar GTPase/ATPase p130**	**Inf**	**0.002103**
TA_287118	Protease, Ulp1 family	Inf	0.002659
TA_280742	FOG: Zn-finger	Inf	0.014732
TA_280830	Kinesin light chain	Inf	0.016108
TA_80465	C-type lectin	Inf	0.017361
TA_282906	Predicted starch-binding protein containing an ankyrin repeat	2.6707	0.022994
TA_322497	Predicted alpha/beta hydrolase BEM46	2.6315	4.11E-10
TA_301990	Homeobox protein	2.449	5.02E-06
TA_220486	Ankyrin repeat	2.3069	0.034465
TA_164711	Translocon-associated protein, gamma subunit (TRAP-gamma)/ Sec61 translocon complex//integral component of endoplasmic	1.6953	0.005698

	reticulum membrane/ no putative conserved domains		
TA_41134	Predicted Rho GTPase-activating protein	1.6466	0.001071
TA_286000	Multifunctional pyrimidine synthesis protein CAD (includes carbamoyl-phosphate synthetase, aspartate transcarbamylase, and glutamine amidotransferase)	1.5228	1.65E-05
TA_131025	Putative ankyrin repeat protein	1.415	0.000985
TA_147452	Putative C-14 sterol reductase	1.2864	0.001066
TA_302363	FOG: Zn-finger	1.2031	4.47E-07
TA_255242	SAM-dependent methyltransferases	1.2443	8.32E-06
TA_152707	Long chain fatty acid CoA ligase	1.1312	0.047573

[1] Origin of the protein ID numbers are from *Trichoderma atroviride* v2.0 https://genome.jgi.doe.gov/pages/search-for- genes.jsf?organism=Triat2

[2] Log_2 fold change is the log fold change in the regenerant as compared to the parent. For the proteins with Inf in this column, there was no transcript activity in the parent, meaning the log change is indefinite.

Table 5.6 Top 50 most downregulated genes of the regenerant strain compared to the parent of *Trichoderma* sp. *"atroviride* B" in the control (plain PDB). Bold entries are also present in the downregulated sub-lethal levels of copper sulphate dataset.

Protein ID[1]	Putative function	Log_2 fold change[2]	padj
Transcription/DNA metabolism			
TA_219226	Serine carboxypeptidases	-Inf	0.001047
TA_13549	Fungal specific transcription factor domain	-Inf	0.002077
TA_219427	Fungal specific transcription factor domain	-Inf	0.006891
TA_286610	FOG: RNA recognition motif domain	-Inf	0.037414
TA_211641	Nonsense-mediated mRNA decay 2 protein/ Similarity with Ras GTPase-activating protein domain	-2.1705	7.75E-09
TA_302640	Putative translation initiation inhibitor UK114/IBM1	-2.0784	1.04E-10
TA_79893	SWR1-complex protein 4	-1.8326	0.003776
TA_135674	Splicing factor U2AF, large subunit (RRM superfamily)	-1.4599	0.001708
Secondary metabolites			
TA_89308	Candidate salicylate hydroxylase	-Inf	1.42E-07
TA_302386	Acyl-CoA synthetase	-Inf	0.001413
TA_89308	Candidate salicylate hydroxylase	-5.3314	0.00682
TA_41602	CoA-transferase family III	-5.092	4.43E-05
TA_88456	Flavin-containing monooxygenase	-2.068	9.02E-13
TA_34073	Acyl-CoA acyltransferase	-2.0637	0.008452
TA_43297	Enoyl-CoA hydratase/isomerase	-1.8952	0.000182
TA_40409	Multicopper oxidase	-1.8365	8.00E-10
TA_293815	Cytochrome P450 CYP4/CYP19/CYP26 subfamilies	-1.6484	0.016188
TA_82022	Transcription factor of the Forkhead/HNF3 family	-1.4069	0.000406
TA_38182	Alcohol dehydrogenase, class V	-1.3748	0.042587

Transporters			
TA_29546	Predicted transporter (major facilitator superfamily)	-5.1572	0.018357
TA_320809	Metal ion transporter CorA-like divalent cation transporter superfamily (Mg^{2+} and Co^{2+} transporter)	-4.0603	0.002077
TA_82369	Monocarboxylate transporter/Major Facilitator Superfamily	-2.8545	0.039864
TA_281099	Predicted transporter (major facilitator superfamily)	-2.3619	0.000257
TA_154058	Major Facilitator Superfamily	-1.6183	1.82E-06
TA_281099	Predicted transporter (major facilitator superfamily)	-1.5799	0.000155
Stress response/protectors			
TA_84469	Catalase superfamily domain	-2.7698	8.76E-10
TA_298114	Flavonol reductase/cinnamoyl-CoA reductase	-1.644	3.09E-06
Other			
TA_287118	Protease, Ulp1 family	-Inf	5.11E-15
TA_142959	PHD Zn-finger protein	-Inf	0.000221
TA_280830	Kinesin light chain	-Inf	0.000309
TA_219226	Serine carboxypeptidases	-Inf	0.001047
TA_302386	Acyl-CoA synthetase	-Inf	0.001413
TA_302591	Predicted metal-dependent hydrolase of the TIM-barrel fold/Amidohydrolase	-5.8877	6.89E-10
TA_158569	Methyltransferase domain	-5.4205	0.004628
TA_41510	Catechol dioxygenase N terminus	-3.6724	7.73E-06
TA_134980	Myosin class II heavy chain	-3.6032	0.015621
TA_299543	Fungal hydrophobin	-2.8848	1.04E-10
TA_299415	**YjeF-related domain containing protein**	**-2.6641**	**5.08E-05**
TA_131874	C_2H_2-type Zn-finger protein	-2.4325	2.16E-05
TA_40648	NAD(P)-binding domain superfamily	-2.3034	0.041088
TA_256937	NmrA-like family	-2.1747	6.68E-05
TA_156014	Hypothetical protein, simlar PTH11-type GPCR	-2.1634	0.020054
TA_80187	Carbohydrate-binding module family 1	-2.0351	0.000187
TA_156579	Hypothetical protein, similar to PTH11-type GPCRs	-1.9229	0.02269
TA_132261	NAD(P)-binding domain superfamily	-1.8933	0.04767
TA_258206	Fungal hydrophobin	-1.8834	3.66E-37
TA_317086	Methyltransferase domain containg protein	-1.6533	0.037084
TA_81501	Transmembrane amino acid transporter protein	-1.5473	1.44E-06
TA_302595	Alpha/beta hydrolase fold	-1.504	0.021747
TA_294009	AAA+- type ATPase	-1.4336	0.000502
TA_43454	Putative thioesterase superfamily protein	-1.3936	0.011484

[1] Origin of the protein ID numbers are from *Trichoderma atroviride* v2.0 https://genome.jgi.doe.gov/pages/search-for- genes.jsf?organism=Triat2

[2] Log_2 fold change is the log fold change in the regenerant as compared to the parent. For the proteins with Inf in this column, there were no transcript activity in the parent, meaning the log change is indefinite. Note for the log2FoldChange values that are shown as a negative value it reads as 'how downregulated is the regenerant compared to the parent' i.e. for protein ID TA_38182 the regenerant has –1.3748 expression compared to the parent.

5.3.3 SNPs

The SNPs were validated empirically. The number of total SNPs were 1349, with a total of 316 non-synonymous SNPs and 162 synonymous SNPs. After the filtering with the criteria outlined in section 5.2.4.4, none of the SNPs fit the criteria. Based on these results, the SNPs from the WGBS data were not investigated any further as if they were true SNPs they would have appeared in the RNA-seq data as that is more reliable. This unreliability is based on the programs that were being used to investigate the WGBS SNPs, which are still being developed. Furthermore, calling SNPs from WGBS is complicated due to two primary reasons. The first is as they use only the three bases (A,T and G, as the C's are converted to T's after the bisulphite treatment) to call the SNPs, meaning a true C/T SNP cannot be discerned from the C/T substitutions from the bisulphite treatment. Secondly, the reads from the two genomic strands are not complimentary at methylated loci (Gao et al., 2015). In order to truly validate the WGBS SNPs, more replicates would be needed.

5.4 Discussion

RNA sequencing was used to investigate whether the differential cytosine methylation observed between the parent and protoplast regenerant had a role in regulating transcriptional activity as has been reported in other fungal species. This current study showed that the correlations between the expression level and the changes in methylation are imperceptible. However, changes in transcription levels were detected between the parent and the regenerant in both conditions which suggests that there may be other regulatory factors in place that have an effect on gene expression, putatively resulting from the use of protoplast technology.

5.4.1 Effects of differential methylation on transcriptional levels

Cytosine methylation is often associated with regulating gene expression in fungi. However, these alterations in gene expression levels are influenced by distribution of the 5mC, genotype, tissue, developmental stages and environmental conditions (Yaish et al., 2018), suggesting there are numerous layers involved with this association. Within this dataset, only nine DEGS were observed among the DMC-associated genes, and no association between cytosine methylation and gene expression was found. Therefore, a clear correlation between cytosine methylation and gene expression cannot be made. Although there were various proteins involved in intracellular trafficking and vesicular transport, which hypothetically could be responsible for the increased copper tolerance, the transcript abundance; the level of methylation (being either hypo- or hypermethylated) and even the context of methylation did not trend to in one direction.

In numerous species of fungi, including *Neurospora crassa* and *Magnaporthe oryzae* (Jeon et al., 2015; Rountree and Selker, 2010), cytosine methylation has been reported in regulating transcriptional

activity. However, this potential lack of correlation between transcription activity and changes in cytosine methylation has been documented between the different sexual stages in *Cordyceps militaris* (Wang et al., 2015) and also in the model plant caliph medic (*Medicago truncatula*) in response to salinity stress (Yaish et al., 2018). Gene expression analysis via RT-qPCR did not reveal a constant relationship between the level of cytosine methylation and the transcript abundance of genes that are known to be of importance for salinity tolerance (Yaish et al., 2018). This does however show two things. Firstly, it confirms previous research showing that although cytosine methylation has some common patterns and distribution among the genomes of different fungal species, its action significantly varies among these species. Within rice, cytosine methylation patterns and gene expression activity vary even among the different cultivars of the same species in response to an environmental stimulus (Garg et al., 2015) which shows how context dependent this relationship can be. Secondly, it is likely that other epigenetic regulatory mechanisms may be involved in the phenotypic plasticity resulting from the protoplast process and in this case, the expression level of certain genes in lieu of large scale genomic changes.

Epigenetic mechanisms have been shown to be involved in genome maintenance and integrity but have been increasingly considered to be of importance for regulation of gene expression in various organisms and consequently phenotypic plasticity (Dubey and Jeon, 2017; Holoch and Moazed, 2015; Kronholm et al., 2016; Soyer et al., 2014; Torres-Martínez and Ruiz-Vázquez, 2017). These mechanisms include, but are not limited to, histone modifications (histone methylation and histone deacetylation) and RNA interference (RNAi). In *N. crassa*, different epigenetic mechanisms have varying effects on the phenotypic plasticity of the organism (Kronholm et al., 2016). They showed that, generally, the effects on plasticity were specific to certain environment conditions and the actual mechanism, which indicates that this epigenetic regulation of gene expression is context dependent.

Further examples include RNAi, which is a conserved eukaryotic mechanism that uses small RNA molecules to suppress gene expression through sequence-specific messenger RNA degradation, translational repression or transcriptional inhibition (Torres-Martínez and Ruiz-Vázquez, 2017). In *Mucor circinelloides* phenotypic plasticity has been shown to be mediated by RNAi (Calo et al., 2014). The fungus can become resistant to the antifungal drug FK506 by spontaneously triggering RNAi-mediated silencing of the drug's target gene. This mechanism, however, provides unstable resistance as the 'mutants' revert back to the drug sensitive phenotype when the drug is no longer present in the media (Calo et al., 2014). MicroRNAs (miRNAs) have been shown to be present in *Trichoderma reesei* and further play a regulatory role in *T. atroviride* (Carreras-Villaseñor et al., 2013; Kang et al., 2013; Schmoll et al., 2016). Soyer et al. (2014) moreover showed that chromatin-based transcriptional regulation via histone H3 lysine 9 methylation (H3K9me3) acts on effector gene expression in

Leptosphaeria maculans. Two proteins, HP1 and DIM-5, modulate the expression which can lead to repression of the fungus during growth in axenic culture.

These other epigenetic factors would have to be extensively tested to see if any of them have a role in the regulation of gene expression between these two strains, resulting from the use of protoplast technology. But as there are no large scale changes in the DNA fingerprint, as shown through UP-PCR comparison between the parent and regenerant, identification of the mechanism that is modulating these changes in gene expression remains elusive.

Another possibility to explain these changes in phenotype plasticity, beyond epigenetic regulatory mechanisms, are the subtle changes to the genetic sequence itself such as single nucleotide polymorphisms (SNPs), small deletion/insertion polymorphisms (DIPs) and structural elements. Although SNPs were not observed in this dataset, interestingly, they have been linked to potential changes in phenotype originating in PEG-mediated protoplast transformations previously. Scala et al. (2017) showed that the large scale phenotypic diversity observed in mutants of *Fusarium verticillioides* (generated from a standard PEG-mediated transformation method) could be due to these changes in the genetic sequence. They found over 9000 SNPs and 79 DIPs between the mutant and the wild type parent suggesting these variations could be responsible for the changes in phenotype. They did not look, however, into the gene function and phenotypes of where these changes occurred. They further stated that additional studies are needed to determine which is the main driver of these genome perturbations, being either the transformation event, the presence of a selective agent (in this case hygomycin B) or the disruption cassette. In relation to this dataset from using protoplast technology for strain improvement and the transcriptional and methylation changes that have arisen, one would postulate that it could be the transformation event. The observations of these large off-target rearrangements throughout the genome in the *F. verticillioides* does raise concerns about the need to determine the genetic consequences of using protoplast technology, either for strain improvement or genetic manipulation experiments.

It is important to note however, that the focus of this study was the differential methylation patterns between the parent and regenerant, and it did not focus on the overall methylation pattern or role in *Trichoderma*. At a genome wide, non-differential overview, cytosine methylation may regulate gene expression. The absence of a known correlation in this dataset is not evidence of the absence of the effect that DNA methylation has on gene expression or even the densities and quantity of cytosine methylation of this fungi. Additionally, one major limitation of this study was preforming the WGBS only in the control condition (plain PDB). The 5mC percentage is known to vary based on numerous factors (Jeon et al., 2015; Yaish et al., 2018). There may have been a more pronounced effect of methylation on gene expression activity if the WGBS was also completed in the sub-lethal levels of

copper sulphate as methylation is known to help contribute as a stress adaption to in environmental changes.

5.4.2 Biological function of differentially expressed genes

Despite the lack of correlation between cytosine methylation and the differential gene expression activity, changes in the transcriptional levels were detected between the parent and the regenerant in both conditions. Within this dataset of DEGs there were a few proteins present that are associated with copper acquisition, utilisation and regulation that have been studied in other eukaryotes (Aghcheh and Kubicek, 2015; Fu et al., 2012; Fu et al., 2014; Fu et al., 2010; Smith et al., 2017). There were additionally a number of proteins that were involved in iron transport (siderophores) and oxidative stress that differed between the two.

5.4.2.1 Copper acquisition, utilisation and regulation associated proteins

Within this dataset of DEGs there were only a few proteins present associated with proteins that been studied in other eukaryotes known to be associated with copper acquisition, utilisation and regulation processes. Briefly, to maintain intracellular copper concentrations, copper is first reduced from Cu (II) to Cu (I) by cell surface metalloreducatases (Fre1 and Fre2) and transported across the plasma membrane into the cytoplasm by two dedicated high affinity membrane-associated copper specific transporters (Ctr1 and Ctr3) (Hassett and Kosman, 1995; Smith et al., 2017). Under low copper conditions, transcription of the transporters Ctr1 and Ctr3 is enriched, allowing for copper uptake. In high copper conditions, both Ctr1 and Ctr3 are downregulated to decrease copper uptake (De Freitas et al., 2003). There is an additional low affinity copper uptake system, the Fet4 transporter, which also is a transporter for iron and zinc (Hassett et al., 2000).

Once copper is inside the cytoplasm, from the respective transporters, it is bound by copper chaperones that allow the delivery of copper to either cytoplasmic and mitochondrial enzymes for copper-dependent activation, or subcellular components for storage or loading into secretory copper-dependent enzymes (Harrison et al., 2000; Smith et al., 2017). The copper is delivered to target organelles by copper chaperones which includes Atx1, Ccs and Cos17. These chaperones are regulated by free copper ions. However, if the level of copper increases above homeostasis (which is assumed in the sub-lethal levels of copper at 1 mM in this study), fungi can employ copper detoxification mechanisms such copper sequestration or efflux.

There are numerous other important copper responsive-transcription factors which can activate copper acquisition, buffering or detoxification genes under the respective copper conditions. Under excess copper conditions, the transcription factor, Ace1, is activated to regulate the transcription of cellular copper-detoxifying genes, notably *Cup1, Crs5* and *SOD1* which protect cells by chelating copper

(Fu et al., 2012; Harrison et al., 2000). The *Cup1* gene encodes a metallothionein (MT), which is involved in direct sequestering and prevention of copper toxicity. The Cup1 protein is capable of binding up to eight Cu+ ions. A second MT-like protein, Crs5, also detoxifies excess copper, but it is less effective than Cup1 in copper buffering. Finally, SOD1 (Cu-Zn superoxide dismutase [SOD]) is able to dually protect against oxidative stress, due to disproportionation of oxygen radicals and also acts as a copper-buffering agent (Culotta et al., 1995; Gralla et al., 1991). Conversely in copper limiting conditions, another transcription factor, Mac1, is activated which induces the expression of high affinity copper transporters (Fre1 and Fre2) (Georgatsou et al., 1997).

Naturally occurring copper tolerance is seen throughout the *Trichoderma* genera (Anand et al., 2006; Jovicic-Petrovic et al., 2014). Within these strains, the majority of the copper is present as a layer on the cell walls. The binding of copper on the cell surface immobilises the metal which makes it less available therefore reducing its toxicity which allows the organism to resume its normal growth patterns (Anand et al., 2006). Additionally, a strain of *T. reesei* that had high copper bioaccumulation resulting from *Agrobacterium tumefaciens*-mediated transformation (ATMT) showed that the Tad1 protein (a novel adenine deaminase) was responsible for this homeostasis (Fu et al., 2014). They further showed that once copper concentration increased, a number of copper dependent proteins were also activated to help protect the cell. They included: (i) a ferroxidase like protein (Fet3) which is a multicopper oxidase responsible for the oxidation of Fe2+ to Fe3+ in yeast, (ii) a glutathione transferase, (iii) a c-type cytochrome, (iv) a protein homologous to Ccs1, a copper metallochaperone of SOD1 and (v) Tctr2, which encodes a Ctr2-like protein which may be associated with copper storage (Fu et al., 2014).

Throughout the DEGs over both conditions, there were a few genes that were differentially expressed that were related to these processes, and only one in the presence of copper. One protein that was downregulated in the presence of copper was TA_161047 (Table 5.5). This protein encodes the copper chaperone, Ccs1 for superoxide dismutase, SOD1 within *S. cerevisiae*. SOD1 is activated in response to excess copper (>1 µM) (Gralla et al., 1991; Smith et al., 2017). As mentioned above, in addition to its role in protection against oxidative stress, SOD is also a copper-buffering agent (Culotta et al., 1995; Gralla et al., 1991). In the present study, the fact that it is upregulated in the parent strain suggests the copper excess is observed within this strain, yet not in the regenerant. The regenerant may have a higher threshold for copper than then parent, before copper response transcription factors are activated.

Three other potential copper related DEGs that were interestingly downregulated in the regenerant strain in the control (plain PDB) were TA_300063 (heavy metal domain that is similar to Atx1, a metallochaperone of *S. cerevisiae*), TA_297568 and TA_239015 (both glutathione S-transferases). Atx1

transports copper to Ccc2, for the insertion of the multicopper ferroxidase Fet3, which required for high affinity iron uptake (Lin et al., 1997). Cells lacking Atx1 show reduced Ccc2 mediated activation of Fet3, and resulting in a corresponding iron deficiency. However, this is typically induced under conditions of low iron compared to low copper levels (Lin et al., 1997). Glutathione S-transferases have a significant role in detoxification and protecting from oxidative stress against copper in *Aspergillus niger* (Luna et al., 2015). Similar proteins were also found to be involved in copper homeostasis regulated by Tad1 in *T. reesei*. However, Fu et al. (2014) performed their transcript analysis in the presence of 1 mM of copper sulphate, whereas these were differentially expressed in the control.

In lieu of proteins being involved in solely with copper acquisition and utilisation, there were a number of proteins differentially expressed that were involved in transport, stress response and DNA metabolism. This suggests another mechanism for the copper tolerance that the regenerant strain may use.

5.4.2.2 Differentially expressed genes in copper and the control

Secondary metabolites

There were a number of proteins that are associated with secondary metabolites that were differentially regulated. Secondary metabolites are a broad group that includes hormones, toxins and bioactive compounds all which play an important role in the interactions of *Trichoderma* and other organisms such as bacteria, plants and other fungi. They are an important set of molecules that are important in attack, defensive, mating and potentially in the case of these regenerants communication and nutrient assimilation (Mukherjee et al., 2012; Schmoll et al., 2016). Among the major biosynthetic gene clusters of secondary metabolites are enzymes such as terpenoid synthases/cyclases, polyketide synthases (PKSs), nonribosomal peptide synthases (NRPSs) and accessory enzymes (Mukherjee et al., 2012; Schmoll et al., 2016; Zeilinger et al., 2016). In both the copper and control DEGs list, an intriguing NRPS was upregulated in the regenerant. TA_318290 encoded a candidate NRPS, a putative ferrichrome synthetase and contains similar domains to *Talaromyces marneffei sidC* (Mukherjee et al., 2012). This protein is involved in intracellular siderophore biosynthesis (Eisendle et al., 2006; Pasricha et al., 2016). Eisendle et al. (2006) reported that accumulation of the intracellular siderophore is regulated by intra- and extracellular iron availability as well as oxidative stress in *A. nidulans.* An increase in the number of secondary metabolites associated proteins within the regenerant in the presence of copper could suggest that the regenerant is more tolerant to stresses. This is as one response when filamentous fungi are challenged by different stresses is the production of secondary metabolites (Macheleidt et al., 2016). Their regulation however is incredibly complex and varies from global regulators, to signal transduction pathways such as the mitogen-activated protein kinase (MAPK) pathway and epigenetic controllers such as remodeling of chromatin structures. Additionally, these biosynthetic clusters of secondary metabolites can also include genes for transport and

transcription factors (Mukherjee et al., 2012; Zeilinger et al., 2016). Further investigation is needed to understand the regulation and function of these secondary metabolites within the regenerant.

Transporters

Fungi have numerous transporter families that assist in the uptake and efflux of nutrients and ions. These include the major facilitator super family (MFS) and the ATP-binding cassette (ABC) transporters, both of which are represented in the upregulated DEG list in the regenerant in copper. A number of these encoded transporters as part of the major facilitator super family (MFS). MFS transporters are a large group of transmembrane proteins involved in the transportation of antibiotics, sugars, amino acids, metal ions and various other molecules, namely for nutrient uptake (Chaudhary et al., 2016). ABC transporters are often linked to the secretion of secondary metabolites, resistance to toxic compounds and cell signaling (Schmoll et al., 2016). This increase in expression of transport proteins could imply a more pronounced response in the regenerant to both nutrient uptake and resistance to toxic compounds. However as they were prominent groups in the control DEG list within both the parent and regenerant, it is unclear the role that transporters do play, in particular regarding copper tolerance. This is as numerous ABC transporters were found to be upregulated in the parent strain in the control conditions. However, these ABC transporters have been shown to play an important role during cell-to-cell communication. Putatively in the presence of copper the transporters may be playing a different role compared to the control.

Stress response/protectors

There were a number of genes that were differentially expressed that had varying roles in stress tolerance, in particular with oxidative stress, ranging from NoxR (a key regulator of NADPH oxidases) to domains that are involved in oxidative resistance, such as SOD and glutathione S-transferases (GSTs). However, the regulation differs between the two strains, so further studies are needed to clarify the putative pathways involved.

The regenerant had a higher level of activity in both conditions (copper and the control) of a protein contains a Rogdi leucine zipper domain (TA_80276). This domain is conserved within eukaryotic genomes and includes a region of 30 amino acids with leucine repeats every seven or eight residues and is known to have a regulatory role. Deletion mutants of *FcRav2* (a gene containing this Rogdi leucine zipper domain) in *Fusarium culmorum*, showed significantly decreased growth compared with the parent strains when coping with multiple stresses (Spanu et al., 2018). The mutant further showed significant sensitivity to pH, oxidative and osmotic stresses and also a tebuconazole fungicide. This suggests a putative role of *FcRav2* in stress resistance. As this protein is upregulated in the regenerant in both conditions, it could be inferred that the regenerant has a higher level of stress resistance than then regenerant.

The comparison of DEGs also indicated an indefinite upregulation in copper of a protein which contains a PB1 domain that is present within the *Epichloë festucae* NoxR protein (a key regulator of NADPH oxidase, NoxA) (TA_315943). ROS produced by NoxA has a critical role in regulating hyphal tip growth of the fungal endophyte in the host plant to maintain the mutualist symbiotic interaction through ROS production (Kayano et al., 2013; Scott et al., 2007). Within *T. harzianum,* overexpression and subsequent increased levels of *nox1* (*noxA*) in transformants led to an increase in ROS production during confrontation with a pathogen (Montero-Barrientos et al., 2011). Furthermore, overexpression of NoxR in *E. festucae* increased hyphal branching in culture and reduced the localised production of ROS at the growing hyphal tips, suggesting that NoxR spatially regulates ROS production (Takemoto et al., 2006). However, the role of ROS can vary, as ROS molecules can act either as signal molecules or as free radicals causing cellular damage. The role is dependent on their concentration within the cell. It could be postulated that overexpression of this protein in the regenerant causes hyphal hyperbranching which could led to observed increased biomass compared to the parent in copper.

As mentioned above the copper chaperone Ccs1 for SOD1 and two glutathione S-transferases, which are also associated with oxidative stress, not just in copper were differentially regulated. SOD1, in addition to buffering copper is also involved in protection against oxidative stress (Culotta et al., 1995; Gralla et al., 1991). The GST protein family is thought to function to protect against oxidative damage in cells by removing reactive molecules via conjugation with glutathione (GSH) (Licciardello et al., 2014). The higher concentrations of GSTs are indicative of oxidative stress and are a transcriptional response to higher levels of ROS. A further superoxide dismutase (manganese dependent SOD, SOD2) was also downregulated in the regenerant in the control. Within *Candida albicans*, Li et al. (2015a) showed that in laboratory with excess copper, *C. albicans* expressed Sod1 (the Cu-requiring form of superoxide dismutase) but as Cu levels decline, the cells switched to an alternative manganese-requiring Sod3.

In the present study, a suite of genes associated with stress tolerance were differentially regulated. This change in profile of these oxidative stress associated proteins may therefore indicate a number of potential outcomes in how the two different strains are responding to the oxidative stress produced by the sub-lethal level of copper. The parent has higher activity in proteins that correspond to cellular defence against ROS, suggesting there may be a higher level of ROS in the parent. However, this requires further investigation into different time points, especially earlier in the interaction with copper, and also different concentration levels of the copper.

Transcription factors/DNA metabolism

Transcription factors are major regulatory proteins in fungal species and modulate gene expression control and in turn the function of the cell. Numerous differentially expressed genes over both

conditions were related to transcription factors or DNA metabolism. The mechanism vary between the different groups. Interestingly, two proteins (TA_11002- SNF2 family domain and TA_297966-histone H4) were upregulated in the parent that are related to chromatin remodeling factors. Conversely in the regenerant transcription factors that were upregulated included proteins such as TA_46772 (DEAD/DEAH box helicase) and TA_321361 (mRNA splicing factor ATP-dependent RNA helicase) which are both involved in pre-mRNA splicing. The changes in functions of the transcription factors show further changes in regulation between the parent and regenerant.

Ribosome biogenesis/translation

Additionally in the downregulated copper DEGs list protein synthesis genes, particularly those encoding ribosomal proteins were represented at a high rate. Ten out of the 26 (annotated) downregulated genes contained 40S and 60S ribosomal proteins domains. Ribosomal proteins are no longer considered to be solely involved in ribosomal assembly and protein translation, but have additional roles in differentiation and are involved in various physiological and pathological roles (Zhou et al., 2015). Mendoza-Mendoza et al. (2015) identified 24 different ribosomal proteins that were expressed during germination of *Trichoderma* in a cDNA library. This library was constructed for the investigation of specific growth stage molecular marks in *T*. sp "*atroviride* B" strain (LU132). This suggests a stage-specific expression pattern within the ribosomal proteins that occur solely within germination, rather than in conidia, vegetative growth or conidiophores. Histone H4 (TA_297966), which is involved in chromatin structure and dynamics, was also present in both the germination cDNA library (Mendoza-Mendoza et al., 2015) and the copper downregulated set. Although the biomass generated for RNA was supposed to be in a vegetative stage, this grouping of DEGs that are involved in protein synthesis, suggest that the samples may have been a mix of different developmental stages in the presence of copper.

5.4.2.3 Siderophore transporters and biosynthesis

Another set of differentially expressed proteins were those involved with siderophore transport and biosynthesis. Microorganisms and plants have evolved specific mechanisms to chelate insoluble iron through the release of siderophores. They are low-molecular-mass, ferric-iron specific chelators which are excreted in most fungi in order to solubilise environmental iron (Eisendle et al., 2006; Haas, 2003; Heymann et al., 2002; Oide et al., 2006; Zeilinger et al., 2016).

In both the copper and control DEGs list, two proteins (TA_131960 and TA_318290) in particular were both upregulated in the regenerant involved in siderophore biosynthesis and transport. TA_318290 encoded a candidate NRPS, a putative ferrichrome synthetase. Additionally, TA_131960 encoded a hypothetical ferrioxamine B transporter (major facilitator super family). It shows similarity with *Sit1* of *Saccharomyces cerevisiae* a transporter for ferrichrome-type siderophores (in particular ferrioxamine)

(Heymann et al., 2002). In the absence of iron, the transcription factor, Aft1p, activates genes encoding siderophore transporters such as Sit2 (Heymann et al., 2002). For both of these proteins, there were higher read counts in the copper compared to the control. However, the log_2 fold change was greater in the control. There were a number of proteins that were involved with siderophore transport that were differentially regulated between the two groups. Including TA_41287 and TA_161189, that were upregulated in the control that contain domains that are similar to *S. cerevisiae* Fre2 and Fre3, cell surface metalloreducatases (Georgatsou et al., 1997). Fre2 is both a ferric and cupric reductases, whereas Fre3 is solely a ferric reductase. Between the regenerant and parent DEGs in the control dataset, there were three siderophore transporters present. Proteins TA_39549 and TA_219088, a siderophore transporter similar to mirB in *A. nidulans,* were both upregulated in the regenerant. Additionally, TA_86704 which also contains domains similar to the siderophore transporter mirB was downregulated in the regenerant. The increase in expression of these siderophore related proteins implies that there may be a greater iron deficiency occurring in the regenerant than the parental strain.

Copper and iron are essential metals that are required for their catalytic and structural roles that they play within biomolecules. The fates of these two metals are closely related. Copper is required for iron homeostasis within fungi, plants and mammals and copper deficiency leads to iron deficiency as copper is used as chaperones for high affinity iron transport and can inhibit heme synthesis (De Freitas et al., 2003). Furthermore, excess of these metals is toxic, as they have the capacity to reinforce the production of ROS. The importance of siderophore synthesis and iron uptake systems in the resistance against oxidative stress have been reported in both fungi and bacteria (Li et al., 2015b; Vicente et al., 2016). This relationship between oxidative stress and siderophore synthesis has been reported in *Alternaria alternata* (Chen et al., 2014) and also in *A. nidulans* (Eisendle et al., 2006). Inactivation of *NPS6 (*nonribosomal peptide synthetase 6) gene homologues led to increased sensitivity to oxidative stress in *Cochliobolus heterostrophus* (Lee et al., 2005) and to a variety of plant pathogenic fungi (Oide et al., 2006). Siderophore-mediated iron acquisition is required for resistance to ROS (Chen et al., 2014) in *A. alternata.* For NPS6 in *A. alternata,* transcript profiles revealed that siderophore biosynthesis is regulated by multiple transcription factors implicated in cellular resistance to ROS (Chen et al., 2014). Δnps6 mutant strains displayed increased sensitivity to H_2O_2 and other ROS-generating oxidants. When *NPS6* is impaired, *A. alternata* is likely unable to obtain sufficient iron and displayed elevated sensitivity to oxidants at low-iron conditions. The accumulation of the *NPS6* gene transcript and subsequent biosynthesis of siderophores are regulated by the membrane-bound NADPH oxidase (NOX), the redox responsive transcription factor (YAP1), and the mitogen-activated protein kinase (HOG1). Chen et al. (2014) postulated that the production of H_2O_2 by NOX may play a role in signaling and facilitating nuclear localisation of YAP1 and HOG1, which consequently activate the genes involved in siderophore biosynthesis for iron acquisition.

This study does need to be validated and explored further to explore the differing hypothesis of the cause of the tolerance of the regenerants to copper. Four genes that would be of interest are listed in Table 5.7.

Table 5.7 List of differentially expressed genes for potential future validation from this RNA-seq dataset across both conditions (control and copper).

Protein ID[1]	Putative function
TA_321361	mRNA splicing factor ATP-dependent RNA helicase
TA_258206	Fungal hydrophobin
TA_318290	Non-ribosomal peptide synthetase/ferrichrome synthetaste
TA_161047	Copper chaperone for superoxide dismutase (SOD1)

[1] Origin of the protein ID numbers are from *Trichoderma atroviride* v2.0 https://genome.jgi.doe.gov/pages/search-for- genes.jsf?organism=Triat2

Two of these genes (TA_321361 and TA_318290) were included as they were present in both conditions datasets and differentially regulated in the same strain over the conditions. For TA_321361 (mRNA splicing factor ATP-dependent RNA helicase), it also had a high $\log_2$ fold change ratio of 2.50 in the presence of copper and 3.95 in the control. It was upregulated in both conditions, suggesting that the change in phenotype has led to this differential expression. TA_318290 putatively encodes a non-ribosomal peptide synthetase (NRPS)/ferrichrome synthetaste. This upregulation of the regenerant across both conditions suggests that another pathway of stress tolerance may be responsible for the change in phenotype. The role of NRPS' during stress have been reported in some organisms, for example the inactivation of NSP6 led to an increase in sensitivity to oxidative stress *C. heterostrophus* (Lee et al., 2005). These two genes, as they were upregulated in both strains, suggest a permanent change in phenotype in the regenerant opposed only being differentiated in certain conditions. As there were only ten DEGs shared across the two conditions respectively by each strain, these genes warrant further investigation as the changes here appears to be as a result of the protoplasting process.

TA_258206, a fungal hydrophobin (which was down regulated in the regenerant in the control dataset) was also included as it had a particularly high read count compared to the other DEGs. In the control dataset, the regenerant had a read count of 7,037, whereas the parent had 25,950 ($\log_2$ fold change of -1.88). Fungal hydrophobins are generally found on the outer surface of conidia and hyphal walls, and may be involved in mediating contact and communication between the fungus and its environment (Whiteford and Spanu, 2001). Additionally, they have the ability to form a hydrophobic coating on surfaces of objects. Higher read counts of a differentially expressed gene are associated with higher levels of activity. The high read counts here suggest that this could be an important DEG for the parent in the control (plain PDB) dataset.

Finally, TA_161047 (copper chaperone for superoxide dismutase [SOD1]) has been shown to be important for protecting cells by chelating copper. SOD1 has been shown to be activated in response to excess copper (>1 µM), and is further able to protect against oxidative stress, due to disproportionation of oxygen radicals (Gralla et al., 1991; Smith et al., 2017). Being upregulated in the parent strain suggests the copper excess is observed within this strain, yet not in the regenerant. The regenerant may have a higher threshold for copper than then parent, before copper response transcription factors are activated. As this is the only DEG that has been directly linked to copper tolerance and acquisition, further investigation including transcription levels at higher copper amounts (above 1 µM) could help explain the phenotypic differences observed here.

The combination of differentially expressed genes suggest a hypothesis that the regenerant may induce a general oxidative stress response for the copper, rather than the specific pathway for copper tolerance being activated. Exposing the regenerant to other stresses, including osmotic and oxidative, would allow this to be investigated in more detail. Additionally, further studies into the transport of iron in the regenerant and parent would also be of interest, as the relationship between siderophore synthesis and oxidative stress has been shown previously in other fungi.

5.5 Conclusion

RNA-seq was used to investigate if the observed differential cytosine methylation between the two strains had a role in regulating transcriptional activity as it has been reported in some other fungal species. This current study showed that the correlations between the differential expression level and the changes in methylation are imperceptible between the parental and regenerant strain. However, changes in transcription levels were detected between the parent and the regenerant in both sub-lethal copper and also the plain PDB control, suggesting that there may be other regulatory factors in place that have an effect on gene expression resulting from protoplasting. The number of DEGs, in particular, within the control dataset is evidence that the act of removing the cell wall during protoplasting does have a non-specific effect on the transcription of the genome of this *Trichoderma* sp. "*atroviride* B" strain. The significance of this needs to be elucidated further, as it could have a large effect for the use of protoplast technology both in genetic manipulation experiments and for the use of stain improvement. Although this study requires further validation by means of reverse-transcription quantitative PCR (RT-qPCR) experimentation to confirm differential gene expression, putatively it does show changes in gene expression that potentially could have resulted from the use of protoplast technology.

As there was no correlation between cytosine methylation and the level of transcriptional activity, this data does call into question the biological significance of cytosine methylation in this context. There were changes in differentially methylated cytosines between the parent and regenerant, and cytosine

methylation has been shown in other fungal species to have a role in transcriptional regulation. Cytosine methylation takes energy and has specific proteins that are conserved between eukaryotic species that are involved with the process, however as it occurred at such low levels in this dataset, is it just a redundant mechanism? Understanding the role of cytosine methylation in a biologically significant context and exploring other epigenetic regulatory factors resulting from the use of protoplast technology does require further, intensive elucidation.

Chapter 6

General discussion

This study aimed to i) produce improved biocontrol agents with the use of protoplast technology and to ii) investigate the molecular mechanisms responsible for the phenotypic changes that were induced. Consequently, numerous protoplast regenerants were produced from bioactive *Trichoderma* strains selected from BPRC research programmes targeted at kiwifruit health for protection against the bacterium that causes kiwifruit canker*, Pseudomonas syringae* pv. *actinidiae* (Psa). These regenerants were screened and selected for pesticide tolerance to either copper sulphate or Chief® (a.i. 500 g/L carbendazim). Despite the use of fungal protoplast technology for strain improvement very little is known of the underlying genetic changes responsible for the modified phenotypes. An understanding of the basic genetic events that occur during protoplasting in *Trichoderma* may allow for greater advances in not only strain enhancement, but also in genetic modification experiments, not only in *Trichoderma* but other filamentous fungi.

This study was the first to examine the consequences of protoplast regeneration through a multi-layered, integrative 'omics approach. This was accomplished by a number of approaches using a copper tolerant *Trichoderma* sp. "*atroviride* B" (FCC237/R5) as a model system to examine these molecular consequences. By i) producing protoplast regenerant strains and characterising the resultant regenerants including their bioactivity against Psa; by ii) examining the cytosine methylation profile of the parent and regenerant strains genome via WGBS as this methylation was hypothesised to be responsible for the phenotypic plasticity observed in the regenerants in lieu of large scale genome arrangements or recombination; and by iii) performing RNA-seq to examine the impact of cytosine methylation on the transcriptional activity of these strains.

For the purpose of this study, protoplast regeneration and fusion was employed to enhance selected *Trichoderma* strains, notably to make them pesticide tolerant. This pesticide tolerance would potentially enable strains with improved characteristics to be more suited to incorporation into an IPM programme or function in the event of high levels of fungicide residues in soil. Protoplast regeneration in particular was shown to be an effective tool. In this study, various strains of *Trichoderma* that are currently being investigated for use against Psa in kiwifruit orchards were used to produce protoplast regenerants that were tolerant to pesticides used in these orchards: copper and Chief®. The use of protoplast fusion (both intra-strain and inter-strain) is a common technique used to enhance biocontrol agents, however it has been have found that by regenerating protoplasts on selection media allows for selection for rare genetic variants at a rate that far exceeds that within the parental population. This highlights the potential for the usage of protoplast regeneration in place of traditional

mutant forming methods such as UV or chemical mutagenesis. Additionally, the UP-PCR (universally primed PCR) patterns were identical between both the parent strains and the respective progeny suggesting no major DNA rearrangements had occurred. Others have postulated that it may be possible that the observed phenotypic variation may be further due to subtle changes in gene sequence Scala et al. (2017). However, previous work within our group on other protoplast progeny using MSAP analysis detected remodelling of the methylation profile, suggesting that gene expression through methylation changes could be the cause of the enhanced phenotypic plasticity observed in the regenerant variants produced.

Due to the aforementioned changes in phenotype of the protoplast regenerants that were produced, the biocontrol potential of these strains were assessed to ensure there was no reduction. Across the three trials, there was no decrease in the biocontrol potential of the protoplast regenerants. Although there was a bias in the screening and selection of the protoplast progeny on the pesticide amended plates (i.e. was not selecting for bioactivity initially) the selected strains do not appear to have lost their biocontrol abilities in the Biotron seedling trials. The ability to enhance desired traits however, is not guaranteed as an outcome from producing protoplast progeny with numerous papers finding a high degree of variability in the progenies abilities (Migheli et al., 1995), which highlights the importance of further testing.

Although the scoring method was changed after the results from Trial 1 to ensure it was more quantitative and followed the spread of the disease within the plant, there is still room for improvement for this bioassay. However as mentioned previously, no pathogenicity assay and respective scoring that reflects the whole range of pathogenic capabilities of Psa as the progression of the disease appears differently depending on the age of the plants and inoculation method (Vanneste, 2017). Further research into the mode of action of these selective bioactive *Trichoderma* strains would help to characterise the resulting changes from protoplasting. Some of the DEGs that were associated with oxidative stress resistance could help the *Trichoderma* regenerant in its interaction with the plant and pathogen respectively. The relationship between *Trichoderma* and plants is very complex. Nogueira-Lopez et al. (2018) showed the secreted proteins of *T. virens* under interaction with maize roots were mainly involved in cell wall hydrolysis, scavenging of reactive oxygen species and secondary metabolism. Numerous ROS and secondary metabolites associated genes were both found to be differentially expressed between the parent and regenerant across both conditions which could potentially aid in this interaction. However, without understanding of the interaction of the fungi with the host plant, the full potential may not be realised.

Chapter 4 describes the first genome wide differential cytosine methylation mapping at a single base resolution with deep bisulphite sequencing of a *Trichoderma* species and additionally between a

protoplast regenerant and its parent. Although it showed sparse differential methylation between the two strains, the majority of this differential methylation did occur within genes bodies or within 1 kb upstream of the gene. The low levels of methylation at each individual 5mC (averaging only 6.8% per 5mC) was unexpected compared to previous fungal methylomes. The only other paper that mentioned low individual 5mC levels in fungi was Liu et al. (2012) with *Aspergillus flavus.* Only a very small fraction of the 5mCs were higher than 5% and few were higher than 15% between their two replicates. These 5mCs in turn were non-converted unmethylated cytosines opposed to true methylcytosines. Although the overlap filter was applied which ensured that each 5mC must be present in at least two of the replicates, the purpose of these low methylation levels still require further explanation. One other possibility is that *de novo* cytosine methylation may occur transiently during the different life stages of this fungus and respective time point and conditions of this bisulphite sequencing may not have detected this. The transient nature of methylation has been shown in other fungi including the reduced virulence of *Botrytis cinerea* in *in vitro* culture over a period of time (Breen et al., 2016). They suggested that virulence was a non-essential plastic character that was regulated by cytosine methylation.

These observations call into question the actual role of cytosine methylation within these strains and the biological significance of this change as it did not modulate gene expression levels (from Chapter 5) or appear to be involved in the copper tolerance abilities of the *Trichoderma* regenerant strain. There are a few limitations to note regarding the methylome and conclusions that can be drawn from this data set. Firstly, it is important to note that this methylation analysis only looked at differential methylation between the two strains. Focusing solely on the methylation levels in the parent alone would allow for baseline level of methylation to be observed in *Trichoderma.* Additionally functional analysis on the genes with the highest levels of methylation would allow for further clarification on the role of the differential methylation. In plants, it has been shown that there is an interplay between cytosine methylation, gene expression and small RNA abundances, particularly in the hypermethylated CHH context of cytosine methylation in stress inducing conditions (Garg et al., 2015; Yaish et al., 2018). This suggests a more complex regulatory interaction may be in place. This has been shown within *Neurospora crassa*, as different epigenetic mechanisms have been reported to affect phenotypic plasticity over several key physiological processes (Kronholm et al., 2016). Cytosine methylation, different histone methylation (at both H3K36 and H3K4), histone deactylation and RNA interference pathways were all shown to have different responses over the varying environmental conditions that were exposed to (Kronholm et al., 2016). One of these other forms of heritable epigenetic mechanisms could play a role in the phenotypic plasticity observed in the protoplast regenerant.

Finally, WGBS cannot distinguish between 5mC, 5hmC (which is an intermediate in active demethylation, resulting from oxidation of 5mC), or 6mA (addition of a methyl group to base 6 of adenine), therefore sequencing via single-molecular real-time (SMRT) sequencing from PacBio would

allow for a more in-depth analysis of the sequencing. Future NGS studies on this *T*. sp. "*atroviride* B" regenerant stain would further benefit from an annotated genome of *T*. sp. "*atroviride* B". The available *T. atroviride* IMI206040 genome from JGI that was used as the reference genome was a limiting factor in both of these 'omics analyses. A comprehensive genome assembly and annotation of *T*. sp. "*atroviride* B", a recently described sister species to *T*. *atroviride* s.s. (Braithwaite et al., 2017) would allow investigation into potential novel genomic arrangements or genes, and would have allowed a better comparison between the parent and regenerant. There is a potential that some differential cytosine methylation may have been missed with approximately 65% mapping efficiency being achieved, as the alignment is only as good as the reference genome.

The effect of the differential cytosine methylation observed between the parental and regenerant strain on regulating transcript activity was further investigated. As intragenic cytosine methylation has a varying effect on different fungal species, functional characterisation of these changes was needed to elucidate the effects that it may have. However, there was no significant correlation between the differential expression level and the observed changes in methylation from Chapter 4. There were changes in transcription levels between the parent and regenerant in both sub-lethal levels of copper (88 DEGs) and also in the control of the plain PDB (281 DEGs). The changes in DEGs profiles, especially regarding proteins involved in oxidative stress, such as NoxR and SOD1, secondary metabolites and transporters could suggest that the regenerant may induce a general stress response as opposed to specific pathway for copper tolerance. The number of DEGs, in particular within the control dataset is evidence that the act of removing the cell wall during protoplasting does have an off-target effect on the transcription of the genome of this *Trichoderma* sp. "*atroviride* B" strain. The significance of this needs to be elucidated further, as it could have a large effect for the use of protoplast technology both in genetic manipulation and for the use of strain improvement. In other fungal methylomes that did not show a clear correlation between cytosine methylation levels and activity levels of genes of interest it has been suggested that cytosine methylation may be a fine-tuner rather than an on-off switch of transcriptional activity (Jeon et al., 2015). Other epigenetic factors, including histone and chromatin modifications, are likely to play an important in regulating gene expression states. Although other epigenetic modifications have not been tested here, they would be expected to be present due to the interconnectedness of the epigenome. Importantly, the absence of a known correlation in this dataset is not evidence of the absence of the effect that cytosine methylation may have on the gene expression in *Trichoderma* species. Again, this transcriptome was only performed in one time point and the expression levels of genes is a dynamic process. Performing the WGBS in sub-lethal levels of copper would allow for further investigation as methylation has been shown to be involved in stress conditions.

As previously stated in Chapter 5, the transcriptome study does requires further validation by means of RT-qPCR experimentation to confirm differential gene expression levels for the selected genes of interest. Possible genes of interest for further investigation in expression levels and functional analysis include those involved in oxidative stress response, ribosome biogenesis and transporters. Further elucidation about the potential relationship between the siderophore synthesis and oxidative stress in *Trichoderma,* as seen in other fungi and bacteria (Eisendle et al., 2006; Lee et al., 2005; Li et al., 2015b; Vicente et al., 2016), could help to explain alternative mechanisms for copper tolerance as observed in the regenerant.

6.1 Future directions

Overall, future work building on this thesis would be separated into two main categories. The first being to investigate other regulatory features responsible for the observed phenotypic plasticity, these as previously mentioned, could include changes in the DNA sequence (e.g. SNPs), extrachromosomal elements and other epigenetic factors. However, based on Scala et al.,'s work on *Fusarium* and the relative ease of investigation SNPs compared to other more complicated epigenetic methods such as ChIP analysis for histone modification and interactions, potential SNPs in the promoter regions of these DEGs could be responsible for the plasticity observed.

Additionally the biological significance of cystosine DNA methylation also would be interesting to further investigate. This would include qRT-PCR on DNA methyltransferases (DNMTases) orthologues found within the *T. atroviride* genome and Pac-Bio re-sequencing on *T.* sp. "*atroviride* B". Being able to investigate the transcriptional abundance of DNMTases such as Dim-2 which is responsible for maintenance and *de novo* methylation in other fungi, over different time periods or fungal growth stages, would allow a more precise view of this mechanism. Pac-Bio sequencing would further allow for re-mapping of methylation, not just 5mC but other kinds and also allow investigations into subtle changes in the DNA sequence. This would dually help to look at other regulatory features as well.

Importantly this study has raised two main future discussion points. Firstly, these observations call into question the actual role of cytosine methylation alterations in modulating gene expression in *Trichoderma* species. However, precise identification of this role requires further intensive investigation, which may eventually aid in the understanding of the complexity of this epigenetic mechanism. This current study showed subtle changes in differential methylation patterns between the parent and regenerant strain, putatively due to protoplasting, but the correlation between the expression levels and these differentially methylated cytosines are imperceptible via this integrated analysis of WGBS and RNA-seq. Other whole genome methylation studies have shown differential methylation between two samples, yet a lack of correlation with gene expression levels (Wang et al., 2015; Yaish et al., 2018).There are multiple, subtle changes in the differential methylation profiles

between the two strains here, additionally *T. atroviride* has orthologues of DNA methyltransferase genes involved in DNA methylation. However understanding the biological significance of cytosine methylation in this example resulting from protoplast regeneration requires further clarification.

Secondly, it also questions the potential implications about the underlying molecular mechanisms and off-target changes from the use of protoplast technology. Protoplast technology is used extensively in both strain improvement and genetic manipulation through PEG-mediated protoplast transformation, in both plant and fungal systems. Concerns have previously been stated about PEG-mediated protoplast transformations in other filamentous fungi such *as Fusarium verticillioides* (Scala et al., 2017) and *Aspergillus giganteus* (Meyer et al., 2003). Meyer et al. (2003) compared different transformation methods and showed that *Agrobacterium tumefaciens*-mediated transformation (ATMT) produced the most stable, integrative transformants compared with PEG-mediated protoplast transformation, electroporation and biolistic transformation. Additionally, even from the initial usage of protoplast-based transformation in *Mycosphaerella graminicola*, concerns about the significant variations in successful protoplast generation were observed (Idnurm et al., 2017; Payne et al., 1998). Different hybridisation profiles between the four transformants that were produced indicated that DNA was inserted into different sites in the *M. graminicola* genome. Scala et al. (2017) suggested that transformation practices "commonly used in the reverse genetics of fungi, may potentially be responsible for unexpected, stochastic and henceforth off-target rearrangements throughout the genome" (p. 1). Based on the current results being inconclusive about the mechanism behind the phenotypic plasticity resulting from protoplasting and other author's hesitations, I think caution should be used when employing protoplast technology without further research. These differences in gene expression particularly in the control (plain PDB) between the parent and regenerant (281 DEGs) show changes that should not be there. Even between the transcript activity of the each strain solely in response to copper, which was not the focus of this study, showed a difference between the parent and regenerant in the number of DEGS (parent: 1676 DEGs between copper and control, regenerant: 481 DEGs between copper and control).

To conclude, this study has demonstrated the fundamental importance for exploring and characterising the effects of protoplast regeneration and shows the need for further research into these mechanisms and elucidating any potential off target changes that may arise from the use of protoplast technology for both strain improvement and genetic manipulation. A variety of other epigenetic factors could be responsible for the phenotypic plasticity that has been observed, this hypothesis will need further testing.

Appendix A

Access to Raw Data from Bioactivity Trials

The raw data from Chapter 3's bioactivity data of selected *Trichoderma* sp. "*atroviride* B" parental and regenerant strains for their biocontrol potential against *Pseudomonas syringae* pv. *actinidiae* has been made available on the open access database Figshare. To access please see: https://figshare.com/s/3249c3c0cac39bb417bc

Appendix B

Access to Methylation Reports and Data

B.1 WGBS differentially methylated regions (Peter Stockwell)

Peter Stockwell's report on his DMAP run on *Trichoderma atroviride* mapping for Chapter 4 has been made available on the open access database Figshare. To access please see: https://figshare.com/s/375bd259de8cf97e99d0

B.2 WGBS differentially methylated cytosines (Darrell Lizamore)

Darrell Lizamore's report on his analysis on the WGBS data for Chapter 4 has been made available on the open access database Figshare. To access please see: https://figshare.com/s/2c652fcd03d3cab1284d

B.3 Full list of differentially methylated cytosines (DMCs)

Table B.1 (Full list of the 330 differentially methylated cytosines [DMCs] between the parent and regenerant strains through methylKit analysis completed by Darrell Lizamore) has been available on the open access database Figshare. To access please see: https://figshare.com/s/6d86c8e256484b0f189f

The table contains 335 methylation points opposed to 330 due to five of the individual 5mCs being within overlapping or overprinting genes. The five individual 5mCs are: contig 24: 1,840,368, contig 25: 929,609, contig 25: 1,428,802, contig 25: 2,397,592 and contig 26: 3,760,038. These five 5mCs have two genes associated with them.

Appendix C

Access to RNA-seq Reports and full DEGs lists

C.1 Novogene RNA-seq report, QC data and read counts

Novogene's report on the bioinformatics analysis of the RNA-seq data for Chapter 5 has been made available on the open access database Figshare. To access please see: https://figshare.com/s/99efe1cdf3491a55ae8c

Additionally, the original list from Novogene containing their annotations and read counts have also been made available on the open access database Figshare. To access please see: https://figshare.com/s/cbba40b0bd898e71a28c

C.2 Complete list of all upregulated genes of the regenerant strain compared to the parent of *Trichoderma* sp. *"atroviride* B" in the control (plain PDB)

Table C.1 **All upregulated differentially expressed genes in the regenerant strain compared to the parent of *Trichoderma* sp. *"atroviride* B" in the control (plain PDB). Bold entries are also present in the upregulated sub-lethal levels of copper sulphate dataset.**

Protein ID[1]	Putative function	Log_2 fold change[2]	padj
TA_79893	SWR1-complex protein 4	Inf	9.53E-14
TA_245214	Structural maintenance of chromosome protein 4 (chromosome condensation complex Condensin, subunit C)	Inf	1.69E-09
TA_175873	Protein involved in sister chromatid separation and/or segregation / WLM domain	Inf	1.22E-08
TA_214849	Phospholipase D	Inf	8.78E-06
TA_299841	Transcription factor TCF20	Inf	4.47E-05
N/a	-	Inf	7.20E-05
N/a	-	Inf	9.26E-05
TA_298699	M6 family metalloprotease domain-containing protein	Inf	0.00047803
N/a	-	Inf	0.0014127
TA_12417	Fungal specific transcription factor domain	Inf	0.0020767
TA_88959	Nucleolar GTPase/ATPase p130	Inf	0.0021029
TA_287118	Protease, Ulp1 family	Inf	0.0026591
TA_204552	DNA polymerase theta/eta, DEAD-box superfamily	Inf	0.0097003
TA_280742	FOG: Zn-finger	Inf	0.014732
TA_280830	Kinesin light chain	Inf	0.016108
TA_80465	C-type lectin	Inf	0.017361
TA_311969	No putative conserved domains	Inf	0.02269
TA_297571	No putative conserved domains	Inf	0.026728

TA_302783	No putative conserved domains	Inf	0.038047
TA_286297	Predicted histone tail methylase containing SET domain	Inf	0.038263
TA_93282	No putative conserved domains	Inf	0.046134
TA_320809	Metal ion transporter CorA-like divalent cation transporter superfamily (Mg^{2+} and Co^{2+} transporter)	Inf	0.048047
TA_80187	Carbohydrate-binding module family 1	5.0182	1.58E-07
TA_321361	**mRNA splicing factor ATP-dependent RNA helicase**	**3.9453**	**0.00018726**
TA_282906	Predicted starch-binding protein containing an ankyrin repeat	2.6707	0.022994
TA_322497	Predicted alpha/beta hydrolase BEM46	2.6315	4.11E-10
TA_301990	Homeobox protein	2.449	5.02E-06
TA_220486	Ankyrin repeat	2.3069	0.034465
TA_294099	Predicted AdoMet-dependent methyltransferase	2.2923	0.0025662
TA_138092	FAD dependent oxidoreductase	2.2593	1.65E-05
TA_318116	DEAH-box RNA helicase	2.0016	0.0023615
TA_318290	**Non-ribosomal peptide synthetase/ ferrichrome synthetase**	**2.0007**	**6.52E-05**
TA_164711	Translocon-associated protein, gamma subunit (TRAP-gamma)/ Sec61 translocon complex//integral component of endoplasmic reticulum membrane/ no putative conserved domains	1.6953	0.0056976
TA_41134	Predicted Rho GTPase-activating protein	1.6466	0.0010714
TA_82465	High-affinity iron permease-like protein	1.6349	0.0047698
TA_39628	**Glycerol kinase**	**1.5705**	**0.00016232**
TA_286000	Multifunctional pyrimidine synthesis protein CAD (includes carbamoyl-phophate synthetase, aspartate transcarbamylase, and glutamine amidotransferase)	1.5228	1.65E-05
TA_53890	Splicing coactivator SRm160/300, subunit SRm300	1.5191	0.046859
TA_39628	**Glycerol kinase**	**1.4545**	**0.0014127**
TA_131025	Putative ankyrin repeat protein	1.415	0.00098516
TA_161189	Ferric reductase NAD binding domain//FAD-binding domain	1.3873	0.026052
TA_37736	Flavin-containing monooxygenase	1.3414	1.04E-10
TA_172844	C2H2 Zn-finger protein	1.3295	0.040437
TA_224741	GATA-4/5/6 transcription factors	1.3289	0.0016818
TA_80276	**Rogdi leucine zipper containing protein**	**1.3195**	**0.00083746**
TA_219088	Predicted transporter (major facilitator superfamily)-siderophore	1.2888	6.55E-07
TA_147452	Putative C-14 sterol reductase	1.2864	0.0010661
TA_131960	**Hypothetical ferrioxamine B transporter, major facilitator superfamily**	**1.2787**	**0.00015048**
TA_273644	Acyl transferase domain	1.2648	0.026858
TA_149087	Permease of the major facilitator superfamily	1.2591	0.00036279
TA_219144	tRNA(Ile)-lysidine synthase	1.2505	0.0038876
TA_255242	SAM-dependent methyltransferases	1.2443	8.32E-06
TA_302363	FOG: Zn-finger	1.2031	4.47E-07

TA_39549	Predicted transporter (major facilitator superfamily)-siderophore	1.1863	0.007024
TA_43598	**Cytochrome P450 CYP4/CYP19/CYP26 subfamilies**	**1.1439**	**0.0010185**
TA_297186	No putative conserved domains	1.1334	0.022994
TA_152707	Long chain fatty acid CoA ligase	1.1312	0.047573
TA_136201	No putative conserved domains	1.1185	1.87E-08
TA_41287	Conserved hypothetical protein similar to ferric/cupric reductases	1.1167	0.0030951
TA_161084	Multidrug/pheromone exporter, ABC superfamily	1.116	0.0071073
TA_79977	Glycerol-3-phosphate dehydrogenase	1.099	1.00E-10
TA_216039	Arrestin domain-containing protein	1.0684	0.014717
TA_302230	Dihydrodipicolinate synthetase family	1.0673	1.48E-06
TA_77838	Thiamine pyrophosphate-requiring enzyme	1.0608	0.005967
TA_44659	Hypothetical protein, similar to PTH11-type GPCRs	1.04	0.0084958
TA_184804	Isoprenoid synthase domain	1.0392	0.00053167
TA_53935	No putative conserved domains	1.0369	0.013187
TA_228383	Putative flavoprotein monooxygenase	1.0351	0.0037077
TA_321537	O-methyltransferase	1.0239	0.0010185
TA_217932	Domain of unknown function (DUF4112)	1.0224	6.07E-05
TA_322580	Fungal specific transcription factor domain	1.0165	0.047573
TA_299986	Molecular chaperone (small heat-shock protein Hsp26/Hsp42)	1.0009	0.044117
TA_32165	Galactonate dehydratase	0.98227	4.22E-07
TA_152848	Predicted transporter (major facilitator superfamily)	0.95419	0.020226
TA_33258	RNA polymerase II transcription mediator	0.93922	0.0075668
TA_317673	Metallopeptidase	0.91303	1.81E-06
TA_29973	Aromatic amino acid aminotransferase and related proteins	0.91142	4.94E-05
TA_88379	Catalase-peroxidase	0.9068	0.0020157
TA_85736	DUFF1774 domain-containing protein	0.89724	1.04E-05
TA_156888	NADP/FAD dependent oxidoreductase	0.89309	0.0025662
TA_82663	Proline oxidase	0.8571	0.00036144
TA_151976	UDP-glucose 6-dehydrogenase	0.85005	0.0049098
TA_300082	Succinyl-CoA synthetase, beta subunit	0.84579	0.0045315
TA_256509	RNA polymerase II, large subunit	0.83548	0.026728
TA_283039	N-acetylglucosaminyl phosphatidylinositol de-N-acetylase	0.82288	0.00060344
TA_130416	5-aminolevulinate synthase	0.81254	1.05E-05
TA_152437	Choline kinase	0.79738	0.00029312
TA_259021	CCAAT-binding factor, subunit B (HAP2)	0.79552	0.01752
TA_39628	Glycerol kinase	0.78817	0.0054934
TA_302229	Oxidoreductase family, NAD-binding Rossmann fold	0.78667	0.0014892
TA_161626	Transcription factor MEIS1 and related HOX domain proteins	0.77501	0.00017525
TA_302863	Alpha/beta hydrolase fold	0.76998	0.040444
TA_259095	No putative conserved domains	0.76757	0.044366
TA_303080	Acetyl-CoA acetyltransferase	0.76223	4.43E-05
TA_290150	Tyrosyl-DNA phosphodiesterase	0.76147	0.01752
TA_229715	RTK signaling protein MASK/UNC-44	0.76069	0.0014127

TA_154210	Hypothetical short chain dehydrogenase/reductase	0.75329	0.0026837
TA_301285	3-isopropylmalate dehydratase (aconitase superfamily)	0.75011	0.00080695
TA_298756	Amidases	0.73506	0.023275
TA_201537	Squalene monooxygenase	0.73097	0.00033846
TA_302946	No putative conserved domains	0.70803	0.00040602
TA_255394	Molecular chaperone (small heat-shock protein Hsp26/Hsp42)	0.70591	0.00018703
TA_301901	No putative conserved domains	0.69443	0.00043522
TA_300080	No putative conserved domains	0.68541	0.00036144
TA_149409	Magnesium transporters: CorA family	0.68332	0.028009
TA_214839	Arrestin domain-containing protein	0.6793	0.0011673
TA_317519	Na+/H+ antiporter	0.67109	0.010621
TA_136201	No putative conserved domains	0.66864	0.001515
TA_281797	Predicted esterase of the alpha-beta hydrolase superfamily	0.66297	0.016108
TA_90885	**Nucleolar GTPase/ATPase p130**	**0.66176**	**0.013422**
TA_151594	Putative ERG4/ERG24 ergosterol biosynthesis protein	0.66146	0.0044688
TA_79473	Glycosyl hydrolases family 16	0.65333	0.0019907
TA_151822	SPX domain	0.64599	0.0075549
TA_88066	DNA directed RNA polymerase, 7 kDa subunit	0.64356	0.029705
TA_300540	Serine/threonine protein kinase	0.59815	0.038159
TA_302802	NADPH oxidase (similar to NoxA)	0.59408	0.03734
TA_297700	Ribonucleotide reductase, alpha subunit	0.59258	0.025696
TA_300107	Coproporphyrinogen III oxidase	0.57899	0.013195
TA_141213	Glutamate synthase	0.57874	0.0060683
TA_302057	RNA polymerase II subunit 9	0.57528	0.028785
TA_301188	Candidate acyl-CoA desaturase 1	0.57528	0.029705
TA_254651	Cytochrome P450, E-class, group IV	0.57291	0.0083381
TA_154508	Ribonucleotide reductase, beta subunit	0.56312	0.044187
TA_133007	Candidate norsolorinic acid reductase	0.54885	0.011484
TA_130709	Hydroxymethylglutaryl-CoA synthase	0.54273	0.017361
TA_301217	C-4 sterol methyl oxidase	0.53317	0.016573
TA_298259	Monooxygenase involved in coenzyme Q (ubiquinone) biosynthesis	0.50478	0.043264
N/a	-	0.49294	0.033823

[1] Origin of the protein ID numbers are from *Trichoderma atroviride* v2.0 https://genome.jgi.doe.gov/pages/search-for- genes.jsf?organism=Triat2

[2] Log_2 fold change is the log fold change in the regenerant as compared to the parent. For the proteins with Inf in this column, there was no transcript activity in the parent, meaning the log change is indefinite.

N/a= non-annotated transcript

C.3 Complete list of all downregulated genes of the regenerant strain compared to the parent of *Trichoderma* sp. *"atroviride* B" in the control (plain PDB)

Table C.2 **All downregulated differentially expressed genes in the regenerant strain compared to the parent of *Trichoderma* sp. *"atroviride* B" in the control (plain PDB). Bold entries are also present in the downregulated sub-lethal levels of copper sulphate dataset.**

Protein ID[1]	Putative function	Log_2 fold change[2]	padj
TA_287118	Protease, Ulp1 family	-Inf	5.11E-15
TA_89308	Candidate salicylate hydroxylase	-Inf	1.42E-07
TA_256565	No putative conserved domains	-Inf	6.35E-07
TA_142959	PHD Zn-finger protein	-Inf	0.00022081
TA_280830	Kinesin light chain	-Inf	0.00030867
TA_320247	No putative conserved domains	-Inf	0.00040602
TA_219226	Serine carboxypeptidases	-Inf	0.001047
TA_302386	Acyl-CoA synthetase	-Inf	0.0014127
TA_13549	Fungal specific transcription factor domain	-Inf	0.0020767
N/a	-	-Inf	0.0037759
N/a	-	-Inf	0.0037759
TA_219427	Fungal specific transcription factor domain	-Inf	0.0068914
TA_310443	No putative conserved domains	-Inf	0.019994
N/a	-	-Inf	0.020346
N/a	-	-Inf	0.031542
TA_286610	FOG: RNA recognition motif domain	-Inf	0.037414
N/a	-	-Inf	0.041515
TA_302591	Predicted metal-dependent hydrolase of the TIM-barrel fold/Amidohydrolase	-5.8877	6.89E-10
TA_278852	No putative conserved domains	-5.8664	0.037414
TA_158569	Methyltransferase domain	-5.4205	0.0046283
TA_89308	Candidate salicylate hydroxylase	-5.3314	0.0068202
TA_29546	Predicted transporter (major facilitator superfamily)	-5.1572	0.018357
TA_41602	CoA-transferase family III	-5.092	4.43E-05
N/a	-	-4.7619	0.01139
N/a	-	-4.4849	0.048047
TA_320809	Metal ion transporter CorA-like divalent cation transporter superfamily (Mg^{2+} and Co^{2+} transporter)	-4.0603	0.0020767
N/a	-	-3.7949	0.0043478
TA_41510	Catechol dioxygenase N terminus	-3.6724	7.73E-06
N/a	-	-3.6255	0.0006192
TA_134980	Myosin class II heavy chain	-3.6032	0.015621
N/a	-	-3.5517	0.026469
N/a	-	-3.4922	0.00018617

N/a	-	-3.2277	7.88E-08
N/a	-	-3.1587	0.026858
TA_26612	No putative conserved domains	-3.139	0.028894
N/a	-	-3.1104	1.29E-05
N/a	-	-3.0483	6.06E-07
N/a	-	-3.0108	8.67E-06
N/a	-	-2.9047	0.00048292
TA_299543	Fungal hydrophobin	-2.8848	1.04E-10
N/a	-	-2.8582	0.00011567
TA_82369	Monocarboxylate transporter/Major Facilitator Superfamily	-2.8545	0.039864
N/a	-	-2.8182	0.046134
TA_84469	Catalase superfamily domain	-2.7698	8.76E-10
TA_246657	No putative conserved domains	-2.6837	0.00023974
TA_299415	**YjeF-related domain containing protein**	**-2.6641**	**5.08E-05**
N/a	-	-2.6559	0.0071073
TA_319293	No putative conserved domains	-2.5737	9.07E-08
N/a	-	-2.4997	0.0152
N/a	-	-2.4733	0.016564
TA_131874	C2H2-type Zn-finger protein	-2.4325	2.16E-05
TA_281099	Predicted transporter (major facilitator superfamily)	-2.3619	0.00025705
TA_40648	NAD(P)-binding domain superfamily	-2.3034	0.041088
TA_133343	No putative conserved domains	-2.2446	0.00015672
TA_298895	No putative conserved domains	-2.2324	0.00031598
TA_256937	NmrA-like family	-2.1747	6.68E-05
TA_211641	Nonsense-mediated mRNA decay 2 protein/ Similarity with Ras GTPase-activating protein domain	-2.1705	7.75E-09
TA_156014	Hypothetical protein, simlar PTH11-type GPCR	-2.1634	0.020054
TA_302640	Putative translation initiation inhibitor UK114/IBM1	-2.0784	1.04E-10
TA_88456	Flavin-containing monooxygenase	-2.068	9.02E-13
TA_34073	Acyl-CoA acyltransferase	-2.0637	0.008452
TA_80187	Carbohydrate-binding module family 1	-2.0351	0.00018703
TA_156579	Hypothetical protein, similar to PTH11-type GPCRs	-1.9229	0.02269
TA_43297	Enoyl-CoA hydratase/isomerase	-1.8952	0.00018233
TA_132261	NAD(P)-binding domain superfamily	-1.8933	0.04767
TA_258206	Fungal hydrophobin	-1.8834	3.66E-37
TA_40409	Multicopper oxidase	-1.8365	8.00E-10
TA_79893	SWR1-complex protein 4	-1.8326	0.0037759
TA_317086	Methyltransferase domain containg protein	-1.6533	0.037084
TA_293815	Cytochrome P450 CYP4/CYP19/CYP26 subfamilies	-1.6484	0.016188
TA_298114	Flavonol reductase/cinnamoyl-CoA reductase	-1.644	3.09E-06

TA_294283	Multidrug resistance-associated protein/mitoxantrone resistance protein, ABC superfamily	-1.638	0.0060473
TA_154058	Major Facilitator Superfamily	-1.6183	1.82E-06
TA_139480	No putative conserved domains	-1.6115	2.37E-06
TA_281099	Predicted transporter (major facilitator superfamily)	-1.5799	0.00015511
TA_81501	Transmembrane amino acid transporter protein	-1.5473	1.44E-06
TA_302595	Alpha/beta hydrolase fold	-1.504	0.021747
TA_135674	Splicing factor U2AF, large subunit (RRM superfamily)	-1.4599	0.0017082
TA_294009	AAA+- type ATPase	-1.4336	0.00050159
TA_82022	Transcription factor of the Forkhead/HNF3 family	-1.4069	0.00040602
TA_43454	Putative thioesterase superfamily protein	-1.3936	0.011484
TA_38182	Alcohol dehydrogenase, class V	-1.3748	0.042587
TA_299585	Kinase-like domain superfamily	-1.3683	0.0015279
TA_159395	Putative transcriptional regulator DJ-1	-1.3536	0.0020527
TA_294283	Multidrug resistance-associated protein/mitoxantrone resistance protein, ABC superfamily	-1.3463	0.0030338
TA_156579	Hypothetical protein, similar to PTH11-type GPCRs	-1.3403	0.00051645
TA_316156	1-aminocyclopropane-1-carboxylate synthase	-1.3362	0.014057
TA_348134	Glycoside hydrolase family 18 protein (TAC2)	-1.2649	0.0055398
TA_38111	Indoleamine 2,3-dioxygenase	-1.246	0.0065234
TA_298879	Predicted transporter (major facilitator superfamily)	-1.2447	0.025756
TA_159580	**Predicted small secreted cysteine-rich protein (killer toxin)**	**-1.2217**	**0.040038**
TA_152486	Permease of the major facilitator superfamily	-1.2182	0.016108
TA_298879	Predicted transporter (major facilitator superfamily)	-1.2085	9.71E-05
TA_219478	Fasciclin-like (FAS1) domain	-1.1869	0.049724
TA_293429	Protein of unknown function (DUF1479)	-1.1832	4.63E-08
TA_31787	Predicted exosome subunit	-1.1232	4.64E-05
TA_297166	Alcohol dehydrogenase, class V	-1.1206	0.002671
TA_299404	Amino acid transporters	-1.1155	0.00088027
TA_33989	Acyl-CoA acyltransferase	-1.0975	0.017383
TA_48521	Major Facilitator Superfamily	-1.0962	5.96E-07
TA_302820	Acyl transferase domain	-1.0859	0.005024
TA_87384	Arylacetamide deacetylase	-1.0824	0.015049
TA_256835	No putative conserved domains	-1.0752	0.00036881
TA_292554	L-kynyrenine hydrolase	-1.0454	0.0025517
TA_41568	Mitogen-activated protein kinase kinase (MAP2K)	-0.99562	3.98E-08

TA_243287	Tetratricopeptide repeat protein domain	-0.98335	0.0010185
TA_134048	B-block binding subunit of transcription factor C subunit 3	-0.97559	0.0058313
TA_299189	Berberine and berberine like//FAD binding domain	-0.97335	7.89E-09
TA_46050	Acyl-CoA acyltransferase	-0.96939	0.00048031
TA_286000	Multifunctional pyrimidine synthesis protein CAD (includes carbamoyl-phophate synthetase, aspartate transcarbamylase, and glutamine amidotransferase)	-0.96836	0.00071174
TA_301229	Predicted hydrolase related to dienelactone hydrolase	-0.96473	0.00014218
TA_300344	Glutathione-dependent formaldehyde-activating enzyme	-0.9539	0.033799
TA_302080	Tetrahydrofolate dehydrogenase/cyclohydrolase, catalytic domain	-0.91164	0.0044772
TA_288955	A/G-specific adenine DNA glycosylase	-0.89775	0.012736
TA_146625	**Stress-response A/B barrel domain**	**-0.89588**	**0.0017634**
TA_132911	Cytochrome P450 CYP2 subfamily	-0.89014	0.039736
TA_302717	Peroxisomal membrane protein MPV17 and related proteins	-0.88989	0.012172
TA_297871	HD domain containing protein	-0.88953	0.0025172
TA_298882	N-methyltransferase	-0.88828	0.00098516
TA_297568	Glutathione S-transferase	-0.88132	0.0014312
TA_239015	Predicted glutathione S-transferase	-0.8768	0.0020157
TA_299063	Flavonol reductase/cinnamoyl-CoA reductase	-0.86619	0.0061739
TA_280821	Growth factor receptor-bound proteins (GRB7, GRB10, GRB14)	-0.86501	0.032286
TA_298990	LisH motif-containing protein	-0.86226	0.0020767
TA_50385	No putative conserved domains	-0.85397	0.0012414
TA_297051	Predicted membrane protein	-0.85321	0.0057311
TA_242764	Activating signal cointegrator 1	-0.85099	0.003603
TA_300299	Cytochrome P450 CYP11/CYP12/CYP24/CPY27 subfamilies	-0.8508	0.0033371
TA_259945	Basic region leucine zipper transcription factor	-0.84564	0.013195
N/a		-0.84334	0.001468
TA_320431	HpcH/HpaI aldolase/citrate lyase family	-0.84092	0.036796
TA_299725	H+/oligopeptide symporter	-0.83421	9.71E-05
TA_302097	Protein of unknown function (DUF1348)	-0.81747	0.0045315
TA_88870	Multidrug resistance-associated protein, ABC superfamily	-0.79319	0.048047
TA_86704	Hypothetical siderophore iron transporter, major facilitator superfamily	-0.77831	0.007527
TA_184981	GPR1/FUN34/yaaH family	-0.77605	0.00018726
TA_302346	Glutathione-dependent formaldehyde-activating enzyme	-0.75819	0.026728

TA_214328	Permease of the major facilitator superfamily	-0.74824	0.00041764
TA_300455	MIOREX complex component 7 (Mrx7)	-0.74749	0.02269
TA_82820	Manganese superoxide dismutase (like SOD2)	-0.71196	0.00017525
TA_300063	Copper chaperone (similar to Atx1)	-0.70219	0.015179
TA_157299	NAD(P)-binding domain	-0.69826	0.038832
TA_139373	Fungal specific transcription factor domain	-0.66321	0.0015223
TA_299214	Homeobox-like domian superfamily	-0.62427	0.025291
TA_292963	H+/oligopeptide symporter	-0.61001	0.026858
TA_299224	No putative conserved domains	-0.60486	0.00463
TA_174054	TAP-like protein (ABC transporter)	-0.60408	0.0075989
TA_140468	Nucleolar GTPase	-0.60079	0.0045209
TA_301756	Histidine phosphatase superfamily (branch 2)	-0.59076	0.013362
TA_220620	FOG: Ankyrin repeat	-0.58897	0.044366
TA_298232	Nucleolar GTPase/ATPase p130	-0.57438	0.037777
TA_182407	No putative conserved domains	-0.5696	0.015049
TA_297946	Aldehyde dehydrogenase	-0.51273	0.032163

[1] Origin of the protein ID numbers are from *Trichoderma atroviride* v2.0 https://genome.jgi.doe.gov/pages/search-for- genes.jsf?organism=Triat2

[2] Log_2 fold change is the log fold change in the regenerant as compared to the parent. For the proteins with Inf in this column, there were no transcript activity in the parent, meaning the log change is indefinite. Note for the log_2 fold change values that are shown as a negative value it reads as 'how downregulated is the regenerant compared to the parent' i.e. for protein ID TA_38182 the regenerant has –1.3748 expression compared to the parent.

N/a= non-annotated transcript

References

Aghcheh, R. K., Kubicek, C. P., 2015. Epigenetics as an emerging tool for improvement of fungal strains used in biotechnology. Applied Microbiology and Biotechnology. 99**,** 6167-6181.

Ahmed, M., Fatma, N. T., 2007. Intra-strain crossing in *Trichoderma harzianum* via protoplast fusion to enhance chitinase productivity and biocontrol activity. Arab Journal of Biotechnology 10**,** 233-240.

Aiuchi, D., Inami, K., Sugimoto, M., Shinya, R., Tani, M., Kuramochi, K., Koike, M., 2008. A new method for producing hybrid strains of the entomopathogenic fungus *Verticillium lecanii* (*Lecanicillium* spp.) through protoplast fusion by using nitrate non-utilizing (*nit*) mutants. Micologia Aplicada International. 20**,** 1-16.

Akalin, A., Kormaksson, M., Li, S., Garrett-Bakelman, F. E., Figueroa, M. E., Melnick, A., Mason, C. E., 2012. methylKit: a comprehensive R package for the analysis of genome-wide DNA methylation profiles. Genome Biology. 13**,** R87.

Altschul, S. F., Madden, T. L., Schäffer, A. A., Zhang, J., Zhang, Z., Miller, W., Lipman, D. J., 1997. Gapped BLAST and PSI-BLAST: a new generation of protein database search programs. Nucleic Acids Research. 25**,** 3389-3402.

Anand, P., Isar, J., Saran, S., Saxena, R. K., 2006. Bioaccumulation of copper by *Trichoderma viride*. Bioresource Technology. 97**,** 1018-1025.

Anders, S., Huber, W., 2010. Differential expression analysis for sequence count data. Genome Biology. 11**,** R106.

Anné, J., 1982. Comparison of penicillins produced by inter-species hybrids from *Penicillium chrysogenum*. Applied Microbiology and Biotechnology. 15**,** 41-46.

Aramayo, R., Selker, E. U., 2013. *Neurospora crassa*, a model system for epigenetics research. Cold Spring Harbor Perspectives in Biology. 5**,** a017921.

Atanasova, L., Druzhinina, I. S., Jaklitsch, W. M., Mukherjee, P., Horwitz, B., Singh, U., Two hundred *Trichoderma* species recognized on the basis of molecular phylogeny. In: P. Mukherjee, et al., Eds.), *Trichoderma*: biology and applications. CABI, Wallingford, 2013, pp. 10-42.

Avivi, Y., Morad, V., Ben-Meir, H., Zhao, J., Kashkush, K., Tzfira, T., Citovsky, V., Grafi, G., 2004. Reorganization of specific chromosomal domains and activation of silent genes in plant cells acquiring pluripotentiality. Developmental Dynamics. 230**,** 12-22.

Balasubramanian, N., Lalithakumari, D., 2008. Characteristics of protoplast inter, intra-fusant and regeneration of antagonistic fungi *Trichoderma harzianum* and *Trichoderma viride*. African Journal of Biotechnology. 7**,** 3235-3243.

Bewick, A. J., Ji, L., Niederhuth, C. E., Willing, E.-M., Hofmeister, B. T., Shi, X., Wang, L., Lu, Z., Rohr, N. A., Hartwig, B., 2016. On the origin and evolutionary consequences of gene body DNA methylation. Proceedings of the National Academy of Sciences. 113**,** 9111-9116.

Bird, A., 2002. DNA methylation patterns and epigenetic memory. Genes & Development. 16**,** 6-21.

Braithwaite, M., Johnston, P., Ball, S., Nourozi, F., Hay, A., Shoukouhi, P., Chomic, A., Lange, C., Ohkura, M., Nieto-Jacobo, M., Cummings, N., Bienkowski, D., Mendoza-Mendoza, A., Hill, R., McLean, K., Stewart, A., Steyaert, J., Bissett, J., 2017. *Trichoderma* down under: species diversity and occurrence of *Trichoderma* in New Zealand. Australasian Plant Pathology. 46**,** 11-30.

Braithwaite, M., Kandula, J., Steyaert, J., Hay, A., Stewart, A., Development of a *Trichoderma atroviride* LU132 variant active at lower temperatures for control of *Botrytis cinerea* on grapes using protoplast technology. 19th Australasian Plant Pathology Conference Auckland, New Zealand, 2013, pp. 72.

Breen, J., Mur, L., Sivakumaran, A., Akinyemi, A., Wilkinson, M., Lopez, C. R., 2016. DNA methylation plays a role on in vitro culture induced loss of virulence in *Botrytis cinerea*. bioRxiv. 059477.

Brotman, Y., Landau, U., Cuadros-Inostroza, Á., Takayuki, T., Fernie, A. R., Chet, I., Viterbo, A., Willmitzer, L., 2013. *Trichoderma*-plant root colonization: escaping early plant defense responses and activation of the antioxidant machinery for saline stress tolerance. PLoS Pathogens. 9**,** e1003221.

Buchfink, B., Xie, C., Huson, D. H., 2015. Fast and sensitive protein alignment using DIAMOND. Nature Methods. 12**,** 59.

Bulat, S. A., Lübeck, M., Mironenko, N., Jensen, D. F., Lübeck, P. S., 1998. UP-PCR analysis and ITS1 ribotyping of strains of *Trichoderma* and *Gliocladium*. Mycological Research. 102**,** 933-943.

Calo, S., Shertz-Wall, C., Lee, S. C., Bastidas, R. J., Nicolás, F. E., Granek, J. A., Mieczkowski, P., Torres-Martínez, S., Ruiz-Vázquez, R. M., Cardenas, M. E., 2014. Antifungal drug resistance evoked via RNAi-dependent epimutations. Nature. 513**,** 555.

Cameron, A., Sarojini, V., 2014. *Pseudomonas syringae* pv. *actinidiae*: chemical control, resistance mechanisms and possible alternatives. Plant Pathology. 63**,** 1-11.

Card, S., Walter, M., Jaspers, M., Sztejnberg, A., Stewart, A., 2009. Targeted selection of antagonistic microorganisms for control of *Botrytis cinerea* of strawberry in New Zealand. Australasian Plant Pathology. 38**,** 183-192.

Carreras-Villaseñor, N., Esquivel-Naranjo, E. U., Villalobos-Escobedo, J. M., Abreu-Goodger, C., Herrera-Estrella, A., 2013. The RNAi machinery regulates growth and development in the filamentous fungus *Trichoderma atroviride*. Molecular Microbiology. 89**,** 96-112.

Chatterjee, A., Ozaki, Y., Stockwell, P. A., Horsfield, J. A., Morison, I. M., Nakagawa, S., 2013. Mapping the zebrafish brain methylome using reduced representation bisulfite sequencing. Epigenetics. 8**,** 979-989.

Chatterjee, A., Stockwell, P. A., Rodger, E. J., Morison, I. M., 2012. Comparison of alignment software for genome-wide bisulphite sequence data. Nucleic Acids Research. 40**,** e79-e79.

Chaudhary, N., Kumari, I., Sandhu, P., Ahmed, M., Akhter, Y., 2016. Proteome scale census of major facilitator superfamily transporters in *Trichoderma reesei* using protein sequence and structure based classification enhanced ranking. Gene. 585**,** 166-176.

Chen, L.-H., Yang, S. L., Chung, K.-R., 2014. Resistance to oxidative stress via regulating siderophore-mediated iron acquisition by the citrus fungal pathogen *Alternaria alternata*. Microbiology. 160**,** 970-979.

Chen, Z. J., 2007. Genetic and epigenetic mechanisms for gene expression and phenotypic variation in plant polyploids. Annual Review of Plant Biology. 58**,** 377-406.

Clarke, J., Wynn, S., Twining, S., 2011. Impact of changing pesticide availability. Aspects of Applied Biology. 263-267.

Colombi, E., Straub, C., Künzel, S., Templeton, M. D., McCann, H. C., Rainey, P. B., 2017. Evolution of copper resistance in the kiwifruit pathogen *Pseudomonas syringae* pv. *actinidiae* through acquisition of integrative conjugative elements and plasmids. Environmental Microbiology. 819-832.

Couteaudier, Y., Viaud, M., Riba, G., 1996. Genetic nature, stability, and improved virulence of hybrids from protoplast fusion in *Beauveria*. Microbial Ecology. 32**,** 1-10.

Cox, M. P., Dong, T., Shen, G., Dalvi, Y., Scott, D. B., Ganley, A. R. D., 2014. An interspecific fungal hybrid reveals cross-kingdom rules for allopolyploid gene expression patterns. PLOS Genetics. 10.

Culotta, V. C., Joh, H.-D., Lin, S.-J., Slekar, K. H., Strain, J., 1995. A physiological role for *Saccharomyces cerevisiae* copper/zinc superoxide dismutase in copper buffering. Journal of Biological Chemistry. 270**,** 29991-29997.

Daskalov, A., Heller, J., Herzog, S., Fleissner, A., Glass, N. L., 2017. Molecular mechanisms regulating cell fusion and heterokaryon formation in filamentous fungi. Microbiology Spectrum. 5.

Davidson, N. M., Oshlack, A., 2014. Corset: enabling differential gene expression analysis for de novo assembled transcriptomes. Genome Biology. 15**,** 410.

Davière, J.-M., Langin, T., Daboussi, M.-J., 2001. Potential role of transposable elements in the rapid reorganization of the *Fusarium oxysporum* genome. Fungal Genetics and Biology. 34**,** 177-192.

De Freitas, J., Wintz, H., Kim, J. H., Poynton, H., Fox, T., Vulpe, C., 2003. Yeast, a model organism for iron and copper metabolism studies. Biometals. 16**,** 185-197.

De Meyer, G., Bigirimana, J., Elad, Y., Höfte, M., 1998. Induced systemic resistance in *Trichoderma harzianum* T39 biocontrol of *Botrytis cinerea*. European Journal of Plant Pathology. 104**,** 279-286.

Dillon, A. J. P., Camassola, M., Henriques, J. A. P., Fungaro, M. H. P., Azevedo, A. C. S., Velho, T. A. F., Laguna, S. E., 2008. Generation of recombinants strains to cellulases production by protoplast

fusion between *Penicillium echinulatum* and *Trichoderma harzianum*. Enzyme and Microbial Technology. 43**,** 403-409.

Dolzhenko, E., Smith, A. D., 2014. Using beta-binomial regression for high-precision differential methylation analysis in multifactor whole-genome bisulfite sequencing experiments. BMC Bioinformatics. 15**,** 215-233.

Dubey, A., Jeon, J., 2017. Epigenetic regulation of development and pathogenesis in fungal plant pathogens. Molecular Plant Pathology. 18**,** 887-898.

Eeckhaut, T., Lakshmanan, P. S., Deryckere, D., Van Bockstaele, E., Van Huylenbroeck, J., 2013. Progress in plant protoplast research. Planta. 238**,** 991-1003.

Ehrlich, M., Lacey, M., 2013. DNA methylation and differentiation: silencing, upregulation and modulation of gene expression. Epigenomics. 5**,** 553-568.

Eisendle, M., Schrettl, M., Kragl, C., Müller, D., Illmer, P., Haas, H., 2006. The intracellular siderophore ferricrocin is involved in iron storage, oxidative-stress resistance, germination, and sexual development in *Aspergillus nidulans*. Eukaryotic Cell. 5**,** 1596-1603.

Erdmann, R. M., Souza, A. L., Clish, C. B., Gehring, M., 2015. 5-Hydroxymethylcytosine is not present in appreciable quantities in *Arabidopsis* DNA. G3: Genes, Genomes, Genetics. 5**,** 1-8.

Everett, K. R., Taylor, R. K., Romberg, M. K., Rees-George, J., Fullerton, R. A., Vanneste, J. L., Manning, M. A., 2011. First report of *Pseudomonas syringae* pv. *actinidiae* causing kiwifruit bacterial canker in New Zealand. Australasian Plant Disease Notes. 6**,** 67-71.

Feng, S., Cokus, S. J., Zhang, X., Chen, P.-Y., Bostick, M., Goll, M. G., Hetzel, J., Jain, J., Strauss, S. H., Halpern, M. E., 2010. Conservation and divergence of methylation patterning in plants and animals. Proceedings of the National Academy of Sciences. 107**,** 8689-8694.

Finn, R. D., Attwood, T. K., Babbitt, P. C., Bateman, A., Bork, P., Bridge, A. J., Chang, H.-Y., Dosztányi, Z., El-Gebali, S., Fraser, M., 2016. InterPro in 2017—beyond protein family and domain annotations. Nucleic Acids Research. 45**,** D190-D199.

Finn, R. D., Coggill, P., Eberhardt, R. Y., Eddy, S. R., Mistry, J., Mitchell, A. L., Potter, S. C., Punta, M., Qureshi, M., Sangrador-Vegas, A., 2015. The Pfam protein families database: towards a more sustainable future. Nucleic Acids Research. 44**,** D279-D285.

Flusberg, B. A., Webster, D. R., Lee, J. H., Travers, K. J., Olivares, E. C., Clark, T. A., Korlach, J., Turner, S. W., 2010. Direct detection of DNA methylation during single-molecule, real-time sequencing. Nature Methods. 7**,** 461-465.

Fournier, P., Provost, A., Bourguignon, C., Heslot, H., 1977. Recombination after protoplast fusion in the yeast *Candida tropicalis*. Archives of Microbiology. 115**,** 143-149.

Fu, K., Fan, L., Li, Y., Gao, S., Chen, J., 2012. *Tmac1*, a transcription factor which regulated high affinity copper transport in *Trichoderma reesei*. Microbiological Research. 167**,** 536-543.

Fu, K., Fan, L., Yu, C., Li, Y., Gao, S., Li, Y., Chen, J., 2014. Adenine deaminase is encoded by *Tad1* and participates in copper accumulation in *Trichoderma reesei*. Fungal Genetics and Biology. 63**,** 17-23.

Fu, K., Liu, L., Fan, L., Liu, T., Chen, J., 2010. Accumulation of copper in *Trichoderma reesei* transformants, constructed with the modified *Agrobacterium tumefaciens*-mediated transformation technique. Biotechnology Letters. 32**,** 1815-1820.

Gao, S., Zou, D., Mao, L., Liu, H., Song, P., Chen, Y., Zhao, S., Gao, C., Li, X., Gao, Z., 2015. BS-SNPer: SNP calling in bisulfite-seq data. Bioinformatics. 31**,** 4006-4008.

Garg, R., Chevala, V. N., Shankar, R., Jain, M., 2015. Divergent DNA methylation patterns associated with gene expression in rice cultivars with contrasting drought and salinity stress response. Scientific Reports. 5**,** 14922.

Georgatsou, E., Mavrogiannis, L. A., Fragiadakis, G. S., Alexandraki, D., 1997. The yeast Fre1p/Fre2p cupric reductases facilitate copper uptake and are regulated by the copper-modulated Mac1p activator. Journal of Biological Chemistry. 272**,** 13786-13792.

Ghabrial, S. A., Castón, J. R., Jiang, D., Nibert, M. L., Suzuki, N., 2015. 50-plus years of fungal viruses. Virology. 479**,** 356-368.

Gibney, E., Nolan, C., 2010. Epigenetics and gene expression. Heredity. 105**,** 4.

Goto, M., Hikota, T., Nakajima, M., Takikawa, Y., Tsuyumu, S., 1994. Occurrence and properties of copper-resistance in plant pathogenic bacteria. Annals of the Phytopathological Society of Japan (Japan). 147-153.

Götz, S., García-Gómez, J. M., Terol, J., Williams, T. D., Nagaraj, S. H., Nueda, M. J., Robles, M., Talón, M., Dopazo, J., Conesa, A., 2008. High-throughput functional annotation and data mining with the Blast2GO suite. Nucleic Acids Research. 36**,** 3420-3435.

Grabherr, M. G., Haas, B. J., Yassour, M., Levin, J. Z., Thompson, D. A., Amit, I., Adiconis, X., Fan, L., Raychowdhury, R., Zeng, Q., 2011. Full-length transcriptome assembly from RNA-Seq data without a reference genome. Nature Biotechnology. 29**,** 644.

Gralla, E. B., Thiele, D. J., Silar, P., Valentine, J. S., 1991. ACE1, a copper-dependent transcription factor, activates expression of the yeast copper, zinc superoxide dismutase gene. Proceedings of the National Academy of Sciences. 88**,** 8558-8562.

Greer, E. L., Blanco, M. A., Gu, L., Sendinc, E., Liu, J., Aristizábal-Corrales, D., Hsu, C.-H., Aravind, L., He, C., Shi, Y., 2015. DNA methylation on N 6-adenine in *C. elegans*. Cell. 161**,** 868-878.

Greer, G., Saunders, C., The costs of Psa-V to the New Zealand kiwifruit industry and the wider community In: A. a. E. R. Unit, (Ed.), 2012.

Gruber, F., Visser, J., Kubicek, C., De Graaff, L., 1990. The development of a heterologous transformation system for the cellulolytic fungus *Trichoderma reesei* based on a *pyrG*-negative mutant strain. Current Genetics. 18**,** 71-76.

Guetsky, R., Shtienberg, D., Elad, Y., Dinoor, A., 2001. Combining biocontrol agents to reduce the variability of biological control. Phytopathology. 91**,** 621-627.

Guo, W., Fiziev, P., Yan, W., Cokus, S., Sun, X., Zhang, M. Q., Chen, P.-Y., Pellegrini, M., 2013. BS-Seeker2: a versatile aligning pipeline for bisulfite sequencing data. BMC Genomics. 14**,** 774.

Guo, W., Zhu, P., Pellegrini, M., Zhang, M. Q., Wang, X., Ni, Z., 2017. CGmapTools improves the precision of heterozygous SNV calls and supports allele-specific methylation detection and visualization in bisulfite-sequencing data. Bioinformatics.

Haas, H., 2003. Molecular genetics of fungal siderophore biosynthesis and uptake: the role of siderophores in iron uptake and storage. Applied Microbiology and Biotechnology. 62**,** 316-330.

Hanson, L. E., Howell, C. R., 2002. Biocontrol efficacy and other characteristics of protoplast fusants between *Trichoderma koningii* and *T. virens*. Mycological Research. 106**,** 321-328.

Harman, G., Lorito, M., Lynch, J., 2004a. Uses of *Trichoderma* spp. to alleviate or remediate soil and water pollution. Advances in Applied Microbiology. 56**,** 313-330.

Harman, G. E., 2000. Myths and dogmas of biocontrol: Changes in perceptions derived from research on *Trichoderma harzianum* T-22. Plant Disease. 84**,** 377-393.

Harman, G. E., 2006. Overview of mechanisms and uses of *Trichoderma* spp. Phytopathology. 96**,** 190-194.

Harman, G. E., Hayes, C., The genetic nature and biocontrol ability of progeny from protoplast fusion in *Trichoderma*. In: I. Chet, (Ed.), Biotechnology in Plant Disease Control. Wiley-Liss, New York, 1993, pp. 237-255.

Harman, G. E., Hayes, C., Ondik, K., Asexual genetics in *Trichoderma* and *Gliocladium*: Mechanisms and implications. In: C. Kubicek, G. E. Harman, Eds.), *Trichoderma* and *Gliocladium*: Basic biology, taxonomy and genetics. Taylor & Francis Ltd, London, United Kingdom, 1998, pp. 243-270.

Harman, G. E., Herrera-Estrella, A. H., Horwitz, B. A., Lorito, M., 2012. Special issue: *Trichoderma*–from basic biology to biotechnology. Microbiology. 158**,** 1-2.

Harman, G. E., Howell, C. R., Viterbo, A., Chet, I., Lorito, M., 2004b. *Trichoderma* species - Opportunistic, avirulent plant symbionts. Nature Reviews Microbiology. 2**,** 43-56.

Harman, G. E., Stasz, T. E., Protoplast fusion for the production of superior biocontrol fungi. In: D. TeBeest, (Ed.), Microbial Control of Weeds. Springer US, 1991, pp. 171-186.

Harrison, M. D., Jones, C. E., Solioz, M., Dameron, C. T., 2000. Intracellular copper routing: the role of copper chaperones. Trends in Biochemical Sciences. 25**,** 29-32.

Hassan, M. M., 2014. Influence of protoplast fusion between two *Trichoderma* spp. on extracellular enzymes production and antagonistic activity. Biotechnology & Biotechnological Equipment. 28**,** 1014-1023.

Hassan, M. M., El-Awady, M. A., Lakhani, H. K., El-Tarras, A. E., 2013. Improvement of biological control activity in *Trichoderma* against some grapevine pathogens using protoplast fusion. Life Science Journal. 10**,** 2275-2283.

Hassan, M. M., Ragaa, A. E., Hamza, H. A., 2011. Molecular characterization of intraspecific protoplast fusion in *Trichoderma harzianum*. New York Science Journal. 4**,** 48-53.

Hassett, R., Dix, D. R., Eide, D. J., Kosman, D. J., 2000. The Fe (II) permease Fet4p functions as a low affinity copper transporter and supports normal copper trafficking in *Saccharomyces cerevisiae*. Biochemical Journal. 351**,** 477.

Hassett, R., Kosman, D. J., 1995. Evidence for Cu (II) reduction as a component of copper uptake by *Saccharomyces cerevisiae*. Journal of Biological Chemistry. 270**,** 128-134.

Hatvani, L., Manczinger, L., Kredics, L., Szekeres, A., Antal, Z., Vagvolgyi, C., 2006. Production of *Trichoderma* strains with pesticide-polyresistance by mutagenesis and protoplast fusion. Antonie Van Leeuwenhoek. 89**,** 387-93.

Hermosa, R., Viterbo, A., Chet, I., Monte, E., 2012. Plant-beneficial effects of *Trichoderma* and of its genes. Microbiology. 158**,** 17-25.

Herrero, N., Márquez, S. S., Zabalgogeazcoa, I., 2009. Mycoviruses are common among different species of endophytic fungi of grasses. Archives of Virology. 154**,** 327-330.

Heymann, P., Gerads, M., Schaller, M., Dromer, F., Winkelmann, G., Ernst, J. F., 2002. The siderophore iron transporter of *Candida albicans* (Sit1p/Arn1p) mediates uptake of ferrichrome-type siderophores and is required for epithelial invasion. Infection and Immunity. 70**,** 5246-5255.

Hill, R., Stark, C., Cummings, N., Elmer, P., Hoyte, S., 2015. Use of Beneficial Microorganisms and Elicitors for Control of *Pseudomonas syringae* pv. *actinidiae* in Kiwifruit (*Actinidia* spp.). Acta Horticulturae.

Holoch, D., Moazed, D., 2015. RNA-mediated epigenetic regulation of gene expression. Nature Reviews Genetics. 16**,** 71.

Howell, C., 2002. Cotton seedling preemergence damping-off incited by *Rhizopus oryzae* and *Pythium* spp. and its biological control with *Trichoderma* spp. Phytopathology. 92**,** 177-180.

Howell, C., 2003. Mechanisms employed by *Trichoderma* species in the biological control of plant diseases: the history and evolution of current concepts. Plant Disease. 87**,** 4-10.

Hoyte, S., Reglinski, T., Elmer, P., Mauchline, N., Stannard, K., Casonato, S., Ah Chee, A., Parry, F., Taylor, J., Wurms, K., Yu, J., Cornish, D. A., Parry, J., Developing and Using Bioassays to Screen for Psa Resistance in New Zealand Kiwifruit. International Symposium on Bacterial Canker of Kiwifruit, 2013, pp. 171-180.

Hua, S., Qi, B., Fu, Y.-P., Li, Y., 2017. DNA Methylation Changes in *Pleurotus eryngii* Subsp. *tuoliensis* (Bailinggu) in Response to Low Temperature Stress. International Journal of Agriculture & Biology. 19.

Hyakumachi, M., Takahashi, H., Matsubara, Y., Someya, N., Shimizu, M., Kobayashi, K., Nishiguchi, M., 2014. Recent studies on biological control of plant diseases in Japan. Journal of General Plant Pathology. 1-16.

Idnurm, A., Bailey, A. M., Cairns, T. C., Elliott, C. E., Foster, G. D., Ianiri, G., Jeon, J., 2017. A silver bullet in a golden age of functional genomics: the impact of *Agrobacterium*-mediated transformation of fungi. Fungal Biology and Biotechnology. 4**,** 6.

Iyer, L. M., Abhiman, S., Aravind, L., 2011. Natural history of eukaryotic DNA methylation systems. Progress in Molecular Biology and Translational Science. 101**,** 25-104.

Jaenisch, R., Bird, A., 2003. Epigenetic regulation of gene expression: how the genome integrates intrinsic and environmental signals. Nature Genetics. 33**,** 245-254.

Jamieson, K., McNaught, K. J., Ormsby, T., Leggett, N. A., Honda, S., Selker, E. U., 2018. Telomere repeats induce domains of H3K27 methylation in *Neurospora*. eLife. 7.

Jang, H. S., Shin, W. J., Lee, J. E., Do, J. T., 2017. CpG and non-CpG methylation in epigenetic gene regulation and brain function. Genes. 8**,** 148.

Jeon, J., Choi, J., Lee, G.-W., Park, S.-Y., Huh, A., Dean, R. A., Lee, Y.-H., 2015. Genome-wide profiling of DNA methylation provides insights into epigenetic regulation of fungal development in a plant pathogenic fungus, *Magnaporthe oryzae*. Scientific Reports. 5.

Jovicic-Petrovic, J., Danilovic, G., Curcic, N., Milinkovic, M., Stosic, N., Pankovic, D., Raicevic, V., 2014. Copper tolerance of *Trichoderma* species. Archives of Biological Sciences. 66**,** 137-142.

Kandula, J., Braithwaite, M., Steyaert, J., Hay, A., Stewart, A., Development of a cold tolerant *Trichoderma atroviride* LU132 variant for control of *Botrytis cinerea* on grapes using protoplast technology. 12th International *Trichoderma* and *Gliocladium* Workshop, Lincoln, New Zealand, 2012.

Kang, K., Zhong, J., Jiang, L., Liu, G., Gou, C. Y., Wu, Q., Wang, Y., Luo, J., Gou, D., 2013. Identification of microRNA-Like RNAs in the filamentous fungus *Trichoderma reesei* by solexa sequencing. PloS One. 8**,** e76288.

Katoh, K., Standley, D. M., 2016. A simple method to control over-alignment in the MAFFT multiple sequence alignment program. Bioinformatics. 1933-1942.

Kayano, Y., Tanaka, A., Akano, F., Scott, B., Takemoto, D., 2013. Differential roles of NADPH oxidases and associated regulators in polarized growth, conidiation and hyphal fusion in the symbiotic fungus *Epichloë festucae*. Fungal Genetics and Biology. 56**,** 87-97.

Kearse, M., Moir, R., Wilson, A., Stones-Havas, S., Cheung, M., Sturrock, S., Buxton, S., Cooper, A., Markowitz, S., Duran, C., 2012. Geneious Basic: an integrated and extendable desktop software platform for the organization and analysis of sequence data. Bioinformatics. 28**,** 1647-1649.

Kim, D.-H., So, K.-K., Ko, Y.-H., Chun, J., Bal, J., Jeon, J., Kim, J.-M., Choi, J., Lee, Y.-H., Huh, J. H., 2018. Global DNA methylation in the Chestnut Blight Fungus *Cryphonectria parasitica* and genome-wide changes in DNA methylation accompanied with sectorization. Frontiers in Plant Science. 9**,** 103.

Kim, J. S., Skinner, M., Gouli, S., Parker, B. L., 2011. Generating thermotolerant colonies by pairing *Beauveria bassiana* isolates. FEMS Microbiology Letters. 324**,** 165-172.

Kistler, H. C., Miao, V. P., 1992. New modes of genetic change in filamentous fungi. Annual Review of Phytopathology. 30**,** 131-153.

Komárek, M., Čadková, E., Chrastný, V., Bordas, F., Bollinger, J.-C., 2010. Contamination of vineyard soils with fungicides: a review of environmental and toxicological aspects. Environment International. 36**,** 138-151.

Kouzminova, E., Selker, E. U., 2001. *dim-2* encodes a DNA methyltransferase responsible for all known cytosine methylation in *Neurospora*. The EMBO Journal. 20**,** 4309-4323.

Kronholm, I., Johannesson, H., Ketola, T., 2016. Epigenetic control of phenotypic plasticity in the filamentous fungus *Neurospora crassa*. G3: Genes, Genomes, Genetics. 6**,** 4009-4022.

Krueger, F., Andrews, S. R., 2011. Bismark: a flexible aligner and methylation caller for Bisulfite-Seq applications. Bioinformatics. 27**,** 1571-1572.

Krueger, F., Kreck, B., Franke, A., Andrews, S. R., 2012. DNA methylome analysis using short bisulfite sequencing data. Nature Methods. 9**,** 145-151.

Kubicek, C. P., Herrera-Estrella, A., Seidl-Seiboth, V., Martinez, D. A., Druzhinina, I. S., Thon, M., Zeilinger, S., Casas-Flores, S., Horwitz, B. A., Mukherjee, P. K., 2011. Comparative genome sequence analysis underscores mycoparasitism as the ancestral life style of *Trichoderma*. Genome Biology. 12**,** R40.

Kumar, M., Ashraf, S., Role of *Trichoderma* spp. as a biocontrol agent of fungal plant pathogens. Probiotics and Plant Health. Springer, 2017, pp. 497-506.

Kunde-Ramamoorthy, G., Coarfa, C., Laritsky, E., Kessler, N. J., Harris, R. A., Xu, M., Chen, R., Shen, L., Milosavljevic, A., Waterland, R. A., 2014. Comparison and quantitative verification of mapping algorithms for whole-genome bisulfite sequencing. Nucleic Acids Research. 42**,** e43-e43.

Kungolos, A., Emmanouil, C., Tsiridis, V., Tsiropoulos, N., 2009. Evaluation of toxic and interactive toxic effects of three agrochemicals and copper using a battery of microbiotests. Science of the Total Environment. 407**,** 4610-4615.

Künkel, W., Berger, D., Risch, S., Wittmann-Bresinsky, B., 1992. Genetic instability of industrial strains of *Penicillium chrysogenum*. Applied Microbiology and Biotechnology. 36**,** 499-502.

Lakhani, H. N., Vakharia, D. N., Hassan, M. M., Eissa, R. A., 2016. Fingerprinting and molecular comparison among two parental strains of *Trichoderma* spp. and their corresponding fusants produced by protoplast fusion. Biotechnology & Biotechnological Equipment. 30**,** 1065-1074.

Lalithakumari, D., Mrinalini, C., Chamola, A. B., Annamali, P., 1996. Strain improvement by protoplast fusion for enchancement of biocontrol potential integrated with fungicide tolerance in *Trichoderma* spp. Zeitschrift fur Pflanzenkraukeiten und Pfanzenschutz. 103**,** 206-212.

Lange, C., The genome and beyond: Phenotypic determinants of two *Trichoderma cf. atroviride* sister strains. . Bio-Protection Reserach Centre, Vol. Doctor of Philosophy Lincoln University, Lincoln, 2015.

Lange, C., Weld, R. J., Cox, M. P., Bradshaw, R. E., McLean, K. L., Stewart, A., Steyaert, J. M., 2016a. Genome-scale investigation of phenotypically distinct but nearly clonal *Trichoderma* strains. PeerJ. 4**,** e2023.

Lange, C., Weld, R. J., Cox, M. P., Bradshaw, R. E., Stewart, A., Mendoza-Mendoza, A., Rostás, M., Steyaert, J., Considering genomic, epigenetic and extra-chromosomal features affecting *Trichoderma* phenotypes. 13th European Conference on Fungal Genetics, Paris, France 2016b.

Langmead, B., Trapnell, C., Pop, M., Salzberg, S. L., 2009. Ultrafast and memory-efficient alignment of short DNA sequences to the human genome. Genome Biology. 10**,** R25.

Law, J. A., Jacobsen, S. E., 2010. Establishing, maintaining and modifying DNA methylation patterns in plants and animals. Nature Reviews Genetics. 11**,** 204.

Lawry, R., Cross-communication between *Trichoderma* and plants during root colonisation. Bio-Protection Reserach Centre, Vol. Doctor of Philosophy. Lincoln University, Lincoln, 2016.

Lee, B.-N., Kroken, S., Chou, D. Y., Robbertse, B., Yoder, O., Turgeon, B. G., 2005. Functional analysis of all nonribosomal peptide synthetases in *Cochliobolus heterostrophus* reveals a factor, NPS6, involved in virulence and resistance to oxidative stress. Eukaryotic Cell. 4**,** 545-555.

Lee, S., Yap, M., Behringer, G., Hung, R., Bennett, J. W., 2016. Volatile organic compounds emitted by *Trichoderma* species mediate plant growth. Fungal Biology and Biotechnology. 3**,** 7.

Li, B., Dewey, C. N., 2011. RSEM: accurate transcript quantification from RNA-Seq data with or without a reference genome. BMC Bioinformatics. 12**,** 323.

Li, C. X., Gleason, J. E., Zhang, S. X., Bruno, V. M., Cormack, B. P., Culotta, V. C., 2015a. *Candida albicans* adapts to host copper during infection by swapping metal cofactors for superoxide dismutase. Proceedings of the National Academy of Sciences. 112**,** E5336-E5342.

Li, W.-C., Chen, C.-L., Wang, T.-F., 2018. Repeat-induced point (RIP) mutation in the industrial workhorse fungus *Trichoderma reesei*. Applied Microbiology and Biotechnology. 1-8.

Li, W.-C., Huang, C.-H., Chen, C.-L., Chuang, Y.-C., Tung, S.-Y., Wang, T.-F., 2017a. *Trichoderma reesei* complete genome sequence, repeat-induced point mutation, and partitioning of CAZyme gene clusters. Biotechnology for Biofuels. 10**,** 170.

Li, W., Wang, Y., Zhu, J., Wang, Z., Tang, G., Huang, B., 2017b. Differential DNA methylation may contribute to temporal and spatial regulation of gene expression and the development of mycelia and conidia in entomopathogenic fungus *Metarhizium robertsii*. Fungal Biology. 121**,** 293-303.

Li, Y., Liu, Y., Chew, S. C., Tay, M., Salido, M. M. S., Teo, J., Lauro, F. M., Givskov, M., Yang, L., 2015b. Complete genome sequence and transcriptomic analysis of the novel pathogen *Elizabethkingia anophelis* in response to oxidative stress. Genome Biology and Evolution. 7**,** 1676-1685.

Licciardello, C., D'Agostino, N., Traini, A., Recupero, G. R., Frusciante, L., Chiusano, M. L., 2014. Characterization of the glutathione S-transferase gene family through ESTs and expression analyses within common and pigmented cultivars of *Citrus sinensis* (L.) Osbeck. BMC Plant Biology. 14**,** 39.

Lin, J.-Q., Zhao, X.-X., Zhi, Q.-Q., Zhao, M., He, Z.-M., 2013. Transcriptomic profiling of *Aspergillus flavus* in response to 5-azacytidine. Fungal Genetics and Biology. 56**,** 78-86.

Lin, S.-J., Pufahl, R. A., Dancis, A., O'Halloran, T. V., Culotta, V. C., 1997. A role for the *Saccharomyces cerevisiae ATX1* gene in copper trafficking and iron transport. Journal of Biological Chemistry. 272**,** 9215-9220.

Liu, S.-Y., Lin, J.-Q., Wu, H.-L., Wang, C.-C., Huang, S.-J., Luo, Y.-F., Sun, J.-H., Zhou, J.-X., Yan, S.-J., He, J.-G., 2012. Bisulfite sequencing reveals that *Aspergillus flavus* holds a hollow in DNA methylation. PloS One. 7**,** e30349.

Lubeck, M., Bulat, S. A., Lubeck, P. S., Mironenko, N., Jensen, D. F., Identification and characterization of isolates of *Trichoderma* and *Gliocladium* by PCR-based methods. In: D. F. Jensen, et al., Eds.),

Monitoring Antagonistic Fungi Deliberately Released into the Environment, Developments in Plant Pathology. Kluwer Academic Publishers, Dordrecht, The Netherlands, 1996.

Luna, C., Marcos, A., Rodrigues Vieira, E., Okada, K., Campos-Takaki, G. M., do Nascimento, A. E., 2015. Copper-induced adaptation, oxidative stress and its tolerance in *Aspergillus niger* UCP1261. Electronic Journal of Biotechnology. 18**,** 418-427.

Macheleidt, J., Mattern, D. J., Fischer, J., Netzker, T., Weber, J., Schroeckh, V., Valiante, V., Brakhage, A. A., 2016. Regulation and role of fungal secondary metabolites. Annual Review of Genetics. 50**,** 371-392.

Madlung, A., 2013. Polyploidy and its effect on evolutionary success: old questions revisited with new tools. Heredity. 110**,** 99-104.

Manczinger, L., Ferenczy, L., 1985. Somatic cell fusion of *Trichoderma reesei* resulting in new genetic combinations. Applied Microbiology and Biotechnology. 22**,** 72-76.

Maor, G. L., Yearim, A., Ast, G., 2015. The alternative role of DNA methylation in splicing regulation. Trends in Genetics. 31**,** 274-280.

Martienssen, R. A., Colot, V., 2001. DNA methylation and epigenetic inheritance in plants and filamentous fungi. Science. 293**,** 1070-1074.

Mastouri, F., Björkman, T., Harman, G. E., 2010. Seed treatment with *Trichoderma harzianum* alleviates biotic, abiotic, and physiological stresses in germinating seeds and seedlings. Phytopathology. 100**,** 1213-1221.

McCann, H. C., Rikkerink, E. H., Bertels, F., Fiers, M., Lu, A., Rees-George, J., Andersen, M. T., Gleave, A. P., Haubold, B., Wohlers, M. W., 2013. Genomic analysis of the kiwifruit pathogen *Pseudomonas syringae* pv. *actinidiae* provides insight into the origins of an emergent plant disease. PLoS Pathogens. 9**,** e1003503.

McLean, K., Stewart, A., 2000. Application strategies for control of onion white rot by fungal antagonists. New Zealand Journal of Crop and Horticultural Science. 28**,** 115-122.

Mendoza-Mendoza, A., Nogueira-López, G., Padilla-Arizmendi, F., Cripps-Guazzone, N., Nieto-Jacobo, M., Kandula, D., Salazar-Badillo, F., Salas-Muñoz, S., Mauricio-Castillo, J., Hill, R., Stewart, A., Steyaert, J., Mechanisms of growth promotion by members of the rhizosphere fungal genus *Trichoderma*. In: H. Singh, et al., Eds.), Advances in PGPR Research. CABI, United Kingdom, 2017, pp. 1-15.

Mendoza-Mendoza, A., Steyaert, J., Nieto-Jacobo, M. F., Holyoake, A., Braithwaite, M., Stewart, A., 2015. Identification of growth stage molecular markers in *Trichoderma* sp.'*atroviride* type B'and their potential application in monitoring fungal growth and development in soil. Microbiology. 161**,** 2110-2126.

Meyer, V., Mueller, D., Strowig, T., Stahl, U., 2003. Comparison of different transformation methods for *Aspergillus giganteus*. Current Genetics. 43**,** 371-377.

Migheli, Q., Whipps, J., Budge, S., Lynch, J., 1995. Production of inter-and intra-strain hybrids of *Trichoderma* spp. by protoplast fusion and evaluation of their biocontrol activity against soil-borne and foliar pathogens. Journal of Phytopathology. 143**,** 91-97.

Mishra, P. K., Baum, M., Carbon, J., 2011. DNA methylation regulates phenotype-dependent transcriptional activity in *Candida albicans*. Proceedings of the National Academy of Sciences. 108**,** 11965-11970.

Mohamed, H., Haggag, W., 2010. Mutagenesis and inter-specific protoplast fusion between *Trichoderma koningii* and *Trichoderma reesei* for biocontrol improvement. American Journal of Scientific and Industrial Research. 1**,** 504-515.

Mondo, S. J., Dannebaum, R. O., Kuo, R. C., Louie, K. B., Bewick, A. J., LaButti, K., Haridas, S., Kuo, A., Salamov, A., Ahrendt, S. R., 2017. Widespread adenine N6-methylation of active genes in fungi. Nature Genetics.

Montanini, B., Chen, P.-Y., Morselli, M., Jaroszewicz, A., Lopez, D., Martin, F., Ottonello, S., Pellegrini, M., 2014. Non-exhaustive DNA methylation-mediated transposon silencing in the black truffle genome, a complex fungal genome with massive repeat element content. Genome Biology. 15**,** 1.

Monte, E., 2010. Understanding *Trichoderma*: between biotechnology and microbial ecology. International Microbiology. 4**,** 1-4.

Montero-Barrientos, M., Hermosa, R., Cardoza, R., Gutiérrez, S., Monte, E., 2011. Functional analysis of the *Trichoderma harzianum nox1* gene, encoding an NADPH oxidase, relates production of reactive oxygen species to specific biocontrol activity against *Pythium ultimum*. Applied and Environmental Microbiology. 77**,** 3009-3016.

Moriya, Y., Itoh, M., Okuda, S., Yoshizawa, A. C., Kanehisa, M., 2007. KAAS: an automatic genome annotation and pathway reconstruction server. Nucleic Acids Research. 35**,** W182-W185.

Mrinalini, C., Lalithakumari, D., 1998. Integration of enhanced biocontrol efficacy and fungicide tolerance in *Trichoderma* spp. by electrofusion/Integration einer verbesserten Wirksamkeit der biologischen Bekämpfung und der Flungizidtoleranz in *Trichoderma* spp. durch Elektrofusion. Zeitschrift für Pflanzenkrankheiten und Pflanzenschutz/Journal of Plant Diseases and Protection. 34-40.

Mukherjee, P. K., Buensanteai, N., Moran-Diez, M. E., Druzhinina, I. S., Kenerley, C. M., 2012. Functional analysis of non-ribosomal peptide synthetases (NRPSs) in *Trichoderma virens* reveals a polyketide synthase (PKS)/NRPS hybrid enzyme involved in the induced systemic resistance response in maize. Microbiology. 158**,** 155-165.

Nakajima, M., Tadaaki, H., 2002. Similarity between copper resistance genes from *Pseudomonas syringae* pv. *actinidiae* and *P. syringae* pv. tomato. Journal of General Plant Pathology. 68**,** 68-74.

Narayanasamy, P., Genetic engineering for improving the performance of biotic biological control agents. Biological Management of Diseases of Crops. Springer, 2013, pp. 471-509.

Nicolás, C., Hermosa, R., Rubio, B., Mukherjee, P. K., Monte, E., 2014. *Trichoderma* genes in plants for stress tolerance-status and prospects. Plant Science. 228**,** 71-78.

Nieto-Jacobo, M. F., Steyaert, J. M., Salazar-Badillo, F. B., Nguyen, D. V., Rostás, M., Braithwaite, M., De Souza, J. T., Jimenez-Bremont, J. F., Ohkura, M., Stewart, A., 2017. Environmental growth conditions of *Trichoderma* spp. affects indole acetic acid derivatives, volatile organic compounds, and plant growth promotion. Frontiers in Plant Science. 8.

Nogueira-Lopez, G., Greenwood, D. R., Middleditch, M., Winefield, C., Eaton, C., Steyaert, J. M., Mendoza-Mendoza, A., 2018. The apoplastic secretome of *Trichoderma virens* during interaction with maize roots shows an inhibition of plant defence and scavenging oxidative stress secreted proteins. Frontiers in Plant Science. 9**,** 409.

Nuskern, L., Ježić, M., Liber, Z., Mlinarec, J., Ćurković-Perica, M., 2017. *Cryphonectria* hypovirus 1-induced epigenetic changes in infected phytopathogenic fungus *Cryphonectria parasitica*. Microbial Ecology. 1-9.

Nuss, D. L., 2005. Hypovirulence: mycoviruses at the fungal–plant interface. Nature Reviews Microbiology. 3**,** 632-642.

Nuss, D. L., Koltin, Y., 1990. Significance of dsRNA genetic elements in plant pathogenic fungi. Annual Review of Phytopathology. 28**,** 37-58.

Oide, S., Moeder, W., Krasnoff, S., Gibson, D., Haas, H., Yoshioka, K., Turgeon, B. G., 2006. *NPS6*, encoding a nonribosomal peptide synthetase involved in siderophore-mediated iron metabolism, is a conserved virulence determinant of plant pathogenic ascomycetes. The Plant Cell. 18**,** 2836-2853.

Ou, X., Zhang, Y., Xu, C., Lin, X., Zang, Q., Zhuang, T., Jiang, L., von Wettstein, D., Liu, B., 2012. Transgenerational inheritance of modified DNA methylation patterns and enhanced tolerance induced by heavy metal stress in rice (*Oryza sativa* L.). PloS One. 7**,** e41143.

Papavizas, G., Lewis, J., Moity, T., 1982. Evaluation of new biotypes of *Trichoderma harzianum* for tolerance to benomyl and enhanced biocontrol capabilities. Phytopathology. 72**,** 126-132.

Pasricha, S., Schafferer, L., Lindner, H., Joanne Boyce, K., Haas, H., Andrianopoulos, A., 2016. Differentially regulated high-affinity iron assimilation systems support growth of the various cell types in the dimorphic pathogen *Talaromyces marneffei*. Molecular Microbiology. 102**,** 715-737.

Paszkowski, J., Peterhans, A., Schlüpmann, H., Basse, C., Lebel, E. G., Masson, J., 1992. Protoplasts as tools for plant genome modifications. Physiologia Plantarum. 85**,** 352-356.

Patil, N., Patil, S., Govindwar, S., Jadhav, J., 2015. Molecular characterization of intergeneric hybrid between *Aspergillus oryzae* and *Trichoderma harzianum* by protoplast fusion. Journal of Applied Microbiology. 118**,** 390-398.

Payne, A. C., Grosjean-Cournoyer, M.-C., Hollomon, D. W., 1998. Transformation of the phytopathogen *Mycosphaerella graminicola* to carbendazim and hygromycin B resistance. Current Genetics. 34**,** 100-104.

Pe'er, S., Chet, I., 1990. *Trichoderma* protoplast fusion: a tool for improving biocontrol agents. Canadian Journal of Microbiology. 36**,** 6-9.

Porciuncula, J. d. O., Furukawa, T., Mori, K., Shida, Y., Hirakawa, H., Tashiro, K., Kuhara, S., Nakagawa, S., Morikawa, Y., Ogasawara, W., 2013. Single nucleotide polymorphism analysis of a *Trichoderma reesei* hyper-cellulolytic mutant developed in Japan. Bioscience, Biotechnology, and Biochemistry. 77**,** 534-543.

Prabavathy, V., Mathivanan, N., Sagadevan, E., Murugesan, K., Lalithakumari, D., 2006a. Intra-strain protoplast fusion enhances carboxymethyl cellulase activity in *Trichoderma reesei*. Enzyme and Microbial Technology. 38**,** 719-723.

Prabavathy, V., Mathivanan, N., Sagadevan, E., Murugesan, K., Lalithakumari, D., 2006b. Self-fusion of protoplasts enhances chitinase production and biocontrol activity in *Trichoderma harzianum*. Bioresource Technology. 97**,** 2330-2334.

Pradhan, P., Fischer, G., van Velthuizen, H., Reusser, D. E., Kropp, J. P., 2015. Closing yield gaps: How sustainable can we be? PloS One. 10**,** e0129487.

Robinson, J. T., Thorvaldsdóttir, H., Winckler, W., Guttman, M., Lander, E. S., Getz, G., Mesirov, J. P., 2011. Integrative genomics viewer. Nature Biotechnology. 29**,** 24-26.

Rodriguez-Iglesias, A., Schmoll, M., Protoplast transformation for genome manipulation in fungi. Genetic Transformation Systems in Fungi, Volume 1. Springer, 2015, pp. 21-40.

Rountree, M., Selker, E., 2010. DNA methylation and the formation of heterochromatin in *Neurospora crassa*. Heredity. 105**,** 38-44.

Samac, D. A., Leong, S. A., 1989. Mitochondrial plasmids of filamentous fungi: characteristics and use in transformation vectors. Molecular Plant-Microbe Interactions. 2**,** 155-159.

Samuels, G. J., 1996. *Trichoderma*: a review of biology and systematics of the genus. Mycological Research. 100**,** 923-935.

Sarrocco, S., Guidi, L., Fambrini, S., Degl'Innocenti, E., Vannacci, G., 2009. Competition for cellulose exploitation between *Rhizoctonia solani* and two *Trichoderma* isolates in the decomposition of wheat straw. Journal of Plant Pathology. 331-338.

Savitha, S., Sadhasivam, S., Swaminathan, K., 2010. Regeneration and molecular characterization of an intergeneric hybrid between *Graphium putredinis* and *Trichoderma harzianum* by protoplasmic fusion. Biotechnology Advances. 28**,** 285-292.

Scala, V., Grottoli, A., Aiese Cigliano, R., Anzar, I., Beccaccioli, M., Fanelli, C., Dall'Asta, C., Battilani, P., Reverberi, M., Sanseverino, W., 2017. Careful with that axe, gene, genome perturbation after a PEG-mediated protoplast transformation in *Fusarium verticillioides*. Toxins. 9**,** 183.

Schardl, C., Craven, K., 2003. Interspecific hybridization in plant-associated fungi and oomycetes: a review. Molecular Ecology. 12**,** 2861-2873.

Schmoll, M., Dattenböck, C., Carreras-Villaseñor, N., Mendoza-Mendoza, A., Tisch, D., Alemán, M. I., Baker, S. E., Brown, C., Cervantes-Badillo, M. G., Cetz-Chel, J., 2016. The genomes of three uneven siblings: footprints of the lifestyles of three *Trichoderma* species. Microbiology and Molecular Biology Reviews. 80**,** 205-327.

Schübeler, D., 2015. Function and information content of DNA methylation. Nature. 517**,** 321-326.

Schuster, E., Schroeder, D., 1990. Side-effects of sequentially-and simultaneously-applied pesticides on non-target soil microorganisms: laboratory experiments. Soil Biology and Biochemistry. 22**,** 375-383.

Scortichini, M., Marcelletti, S., Ferrante, P., Petriccione, M., Firrao, G., 2012. *Pseudomonas syringae* pv. *actinidiae*: a re-emerging, multi-faceted, pandemic pathogen. Molecular Plant Pathology. 13**,** 631-40.

Scott, B., Takemoto, D., Tanaka, A., 2007. Fungal endophyte production of reactive oxygen species is critical for maintaining the mutualistic symbiotic interaction between *Epichloë festucae* and perennial ryegrass. Plant Signaling & Behavior. 2**,** 171-173.

Selker, E. U., Tountas, N. A., Cross, S. H., Margolin, B. S., Murphy, J. G., Bird, A. P., Freitag, M., 2003. The methylated component of the *Neurospora crassa* genome. Nature. 422**,** 893-897.

Sharma, M., Sharma, P., Singh, R., Raja, M., Sharma, P., 2016. Fast isolation and regeneration method for protoplast production in *Trichoderma harzianum*. Internatinal Journal of Current Microbiology and Applied Sciences. 5**,** 891-897.

Sharma, P., Kumar, V., Ramesh, R., Saravanan, K., Deep, S., Sharma, M., Mahesh, S., Dinesh, S., 2014. Biocontrol genes from *Trichoderma* species: a review. African Journal of Biotechnology. 10**,** 19898-19907.

Sharma, P. K., Gothalwal, R., *Trichoderma*: A potent fungus as biological control agent. In: J. S. Singh, G. Seneviratne, Eds.), Agro-Environmental Sustainability: Volume 1: Managing Crop Health. Springer International Publishing, Cham, 2017, pp. 113-125.

Sharon, E., Chet, I., Viterbo, A., Bar-Eyal, M., Nagan, H., Samuels, G. J., Spiegel, Y., 2007. Parasitism of *Trichoderma* on *Meloidogyne javanica* and role of the gelatinous matrix. European Journal of Plant Pathology. 118**,** 247-258.

Shoji, J.-y., Charlton, N. D., Yi, M., Young, C. A., Craven, K. D., 2015. Vegetative hyphal fusion and subsequent nuclear behavior in *Epichloë* grass endophytes. PloS One. 10**,** e0121875.

Sivan, A., Chet, I., 1986. Biological control of *Fusarium* spp. in cotton, wheat and muskmelon by *Trichoderma harzianum*. Journal of Phytopathology. 116**,** 39-47.

Sivan, A., Harman, G., 1991. Improved rhizosphere competence in a protoplast fusion progeny of *Trichoderma harzianum*. Microbiology. 137**,** 23-29.

Smith, A. D., Logeman, B. L., Thiele, D. J., 2017. Copper Acquisition and Utilization in Fungi. Annual Review of Microbiology. 71**,** 597-623.

Soyer, J. L., El Ghalid, M., Glaser, N., Ollivier, B., Linglin, J., Grandaubert, J., Balesdent, M.-H., Connolly, L. R., Freitag, M., Rouxel, T., 2014. Epigenetic control of effector gene expression in the plant pathogenic fungus *Leptosphaeria maculans*. PLoS Genetics. 10**,** e1004227.

Spanu, F., Scherm, B., Camboni, I., Balmas, V., Pani, G., Oufensou, S., Macciotta, N., Pasquali, M., Migheli, Q., 2018. *FcRav2*, a gene with a ROGDI domain involved in Fusarium head blight and crown rot on durum wheat caused by *Fusarium culmorum*. Molecular Plant Pathology. 19**,** 677-688.

Stark, C. H., Hill, R. A., Cummings, N. J., Li, J.-H., 2018. Amendment with biocontrol strains increases *Trichoderma* numbers in mature kiwifruit (*Actinidia chinensis*) orchard soils for up to six months after application. Archives of Phytopathology and Plant Protection. 1-16.

Stasz, T., Harman, G., Weeden, N., 1988. Protoplast preparation and fusion in two biocontrol strains of *Trichoderma harzianum*. Mycologia. 141-150.

Stasz, T. E., Harman, G. E., 1990. Nonparental progeny resulting from protoplast fusion in *Trichoderma* in the absence of parasexuality. Experimental Mycology. 14**,** 145-159.

Stasz, T. E., Harman, G. E., Gullino, M. L., 1989. Limited vegetative compatibility following intra-and interspecific protoplast fusion in *Trichoderma*. Experimental Mycology. 13**,** 364-371.

Stockwell, P. A., Chatterjee, A., Rodger, E. J., Morison, I. M., 2014. DMAP: differential methylation analysis package for RRBS and WGBS data. Bioinformatics. btu126.

Strauss, J., Reyes-Dominguez, Y., 2011. Regulation of secondary metabolism by chromatin structure and epigenetic codes. Fungal Genetics and Biology. 48**,** 62-69.

Strom, N. B., Bushley, K. E., 2016. Two genomes are better than one: history, genetics, and biotechnological applications of fungal heterokaryons. Fungal Biology and Biotechnology. 3**,** 1.

Sumeet, Mukerji, K. G., Exploitation of protoplast fusion technology in improving biocontrol potential. In: R. K. Upadhyay, et al., Eds.), Biocontrol potentila and its exploitation in sustainable agriculture. Volume 1: Crop diseases, weeds, and nematodes. Kluwer Academics/Plenum Publishers, New York, 2000.

Sundh, I., Goettel, M. S., 2013. Regulating biocontrol agents: a historical perspective and a critical examination comparing microbial and macrobial agents. BioControl. 58**,** 575-593.

Supek, F., Bošnjak, M., Škunca, N., Šmuc, T., 2011. REVIGO summarizes and visualizes long lists of gene ontology terms. PloS One. 6**,** e21800.

Tahoun, M., 1993. Gene manipulation by protoplast fusion and penicillin production by *Penicillium chrysogenum*. Applied Biochemistry and Biotechnology. 39**,** 445-453.

Takemoto, D., Tanaka, A., Scott, B., 2006. A $p67^{Phox}$-like regulator is recruited to control hyphal branching in a fungal–grass mutualistic symbiosis. The Plant Cell. 18**,** 2807-2821.

Tatusov, R. L., Fedorova, N. D., Jackson, J. D., Jacobs, A. R., Kiryutin, B., Koonin, E. V., Krylov, D. M., Mazumder, R., Mekhedov, S. L., Nikolskaya, A. N., 2003. The COG database: an updated version includes eukaryotes. BMC Bioinformatics. 4**,** 41.

Thorvaldsdóttir, H., Robinson, J. T., Mesirov, J. P., 2013. Integrative Genomics Viewer (IGV): high-performance genomics data visualization and exploration. Briefings in Bioinformatics. 14**,** 178-192.

Torres-Martínez, S., Ruiz-Vázquez, R. M., 2017. The RNAi universe in fungi: a varied landscape of small RNAs and biological functions. Annual Review of Microbiology. 71**,** 371-391.

Tripathi, A., Sharma, N., Tripathi, N., Biological control of plant diseases: An overview and the *Trichoderma* system as biocontrol agents. In: A. Arya, A. E. Perelló, Eds.), Management of Fungal Plant Pathogens. CAB International Cambridge, 2010.

Tschen, J. S.-M., Li, I.-F., 1994. Optimization of formation and regeneration of protoplasts from biocontrol agents of *Trichoderma* species. Mycoscience. 35**,** 257-263.

Tsiridis, V., Petala, M., Samaras, P., Hadjispyrou, S., Sakellaropoulos, G., Kungolos, A., 2006. Interactive toxic effects of heavy metals and humic acids on *Vibrio fischeri*. Ecotoxicology and Environmental Safety. 63**,** 158-167.

Tsuji, J., Weng, Z., 2015. Evaluation of preprocessing, mapping and postprocessing algorithms for analyzing whole genome bisulfite sequencing data. Briefings in Bioinformatics. 17**,** 938-952.

Tyson, J., Horner, I., Curtis, C., Blackmore, A., Manning, M., 2015. Influence of leaf age on infection of *Actinidia* species by *Pseudomonas syringae* pv. *actinidiae*. New Zealand Plant Protection. 68**,** 328-331.

Ushijima, S., Nakadai, T., Uchida, K., 1990. Breeding of new koji-molds through interspecific hybridization between *Aspergillus oryzae* and *Aspergillus sojae* by protoplast fusion. Agricultural and Biological Chemistry. 54**,** 1667-1676.

Van der Auwera, G. A., Carneiro, M. O., Hartl, C., Poplin, R., Del Angel, G., Levy-Moonshine, A., Jordan, T., Shakir, K., Roazen, D., Thibault, J., 2013. From FastQ data to high-confidence variant calls: the genome analysis toolkit best practices pipeline. Current Protocols in Bioinformatics. 11.10. 1-11.10. 33.

Vanneste, J., 2017. The scientific, economic, and social impacts of the New Zealand outbreak of bacterial canker of kiwifruit (*Pseudomonas syringae* pv. *actinidiae*). Annual Review of Phytopathology. 55**,** 377-399.

Veluchamy, A., Lin, X., Maumus, F., Rivarola, M., Bhavsar, J., Creasy, T., O'Brien, K., Sengamalay, N. A., Tallon, L. J., Smith, A. D., 2013. Insights into the role of DNA methylation in diatoms by genome-wide profiling in *Phaeodactylum tricornutum*. Nature Communications. 4**,** 2091.

Verhoeven, K. J., Jansen, J. J., Van Dijk, P. J., Biere, A., 2010. Stress-induced DNA methylation changes and their heritability in asexual dandelions. New Phytologist. 185**,** 1108-1118.

Vicente, C. S., Nascimento, F. X., Ikuyo, Y., Cock, P. J., Mota, M., Hasegawa, K., 2016. The genome and genetics of a high oxidative stress tolerant *Serratia* sp. LCN16 isolated from the plant parasitic nematode *Bursaphelenchus xylophilus*. BMC Genomics. 17**,** 301.

Wang, M., Liu, S., Li, Y., Xu, R., Lu, C., Shen, Y., 2010. Protoplast mutation and genome shuffling induce the endophytic fungus *Tubercularia* sp. TF5 to produce new compounds. Current Microbiology. 61**,** 254-260.

Wang, X., Hu, L., Wang, X., Li, N., Xu, C., Gong, L., Liu, B., 2016. DNA methylation affects gene alternative splicing in plants: an example from rice. Molecular Plant. 9**,** 305-307.

Wang, Y.-l., Wang, Z.-x., Liu, C., Wang, S.-b., Huang, B., 2015. Genome-wide analysis of DNA methylation in the sexual stage of the insect pathogenic fungus *Cordyceps militaris*. Fungal Biology. 119**,** 1246-1254.

Wang, Y., Wang, T., Qiao, L., Zhu, J., Fan, J., Zhang, T., Wang, Z.-x., Li, W., Chen, A., Huang, B., 2017. DNA methyltransferases contribute to the fungal development, stress tolerance and virulence of the entomopathogenic fungus *Metarhizium robertsii*. Applied Microbiology and Biotechnology. 101**,** 4215-4226.

Wilson, C. L., 1997. Biological control and plant diseases- A new paradigm. Journal of Industrial Microbiology and Biotechnology. 19**,** 158-159.

Woo, S. L., Ruocco, M., Vinale, F., Nigro, M., Marra, R., Lombardi, N., Pascale, A., Lanzuise, S., Manganiello, G., Lorito, M., 2014. *Trichoderma*-based products and their widespread use in agriculture. Open Mycological Journal. 8**,** 71-126.

Wu, S. C., Zhang, Y., 2010. Active DNA demethylation: many roads lead to Rome. Nature Reviews Molecular Cell Biology. 11**,** 607.

Xi, Y., Li, W., 2009. BSMAP: whole genome bisulfite sequence MAPping program. BMC Bioinformatics. 10**,** 232.

Xiang, H., Zhu, J., Chen, Q., Dai, F., Li, X., Li, M., Zhang, H., Zhang, G., Li, D., Dong, Y., 2010. Single base-resolution methylome of the silkworm reveals a sparse epigenomic map. Nature Biotechnology. 28**,** 516-520.

Xu, F., Jin, H., Li, H., Tao, L., Wang, J., Lv, J., Chen, S., 2012. Genome shuffling of *Trichoderma viride* for enhanced cellulase production. Annals of Microbiology. 62**,** 509-515.

Yaish, M. W., Al-Lawati, A., Al-Harrasi, I., Patankar, H. V., 2018. Genome-wide DNA Methylation analysis in response to salinity in the model plant caliph medic (*Medicago truncatula*). BMC Genomics. 19**,** 78.

Yong-Villalobos, L., González-Morales, S. I., Wrobel, K., Gutiérrez-Alanis, D., Cervantes-Peréz, S. A., Hayano-Kanashiro, C., Oropeza-Aburto, A., Cruz-Ramírez, A., Martínez, O., Herrera-Estrella, L., 2015. Methylome analysis reveals an important role for epigenetic changes in the regulation of the *Arabidopsis* response to phosphate starvation. Proceedings of the National Academy of Sciences. 112**,** E7293-E7302.

Yoo, M., Szadkowski, E., Wendel, J., 2013. Homoeolog expression bias and expression level dominance in allopolyploid cotton. Heredity. 110**,** 171-180.

Zeilinger, S., Gruber, S., Bansal, R., Mukherjee, P. K., 2016. Secondary metabolism in *Trichoderma*–Chemistry meets genomics. Fungal Biology Reviews. 30**,** 74-90.

Zemach, A., McDaniel, I. E., Silva, P., Zilberman, D., 2010. Genome-wide evolutionary analysis of eukaryotic DNA methylation. Science. 328**,** 916-919.

Zhang, H., Zhang, Q., Zhou, Q., Zhang, C., 2003. Binary-joint effects of acetochlor, methamidophos, and copper on soil microbial population. Bulletin of Environmental Contamination and Toxicology. 71**,** 746-754.

Zhang, L., Chen, W., Iyer, L. M., Hu, J., Wang, G., Fu, Y., Yu, M., Dai, Q., Aravind, L., He, C., 2014. A TET homologue protein from *Coprinopsis cinerea* (CcTET) that biochemically converts 5-methylcytosine to 5-hydroxymethylcytosine, 5-formylcytosine, and 5-carboxylcytosine. Journal of the American Chemical Society. 136**,** 4801-4804.

Zhou, W., 2016. BISCUIT-0.1.3. 10.5281/zenodo.48262.

Zhou, X., Liao, W.-J., Liao, J.-M., Liao, P., Lu, H., 2015. Ribosomal proteins: functions beyond the ribosome. Journal of Molecular Cell Biology. 7**,** 92-104.

Zhou, X., Wei, Y., Zhu, H., Wang, Z., Lin, J., Liu, L., Tang, K., 2008. Protoplast formation, regeneration and transformation from the taxol-producing fungus *Ozonium* sp. African Journal of Biotechnology. 7.